Université Gustave Eiffel

Impact of a fire-retardant treatment on the acoustic properties of bio-based insulation wools: from laboratory to pilot-scale production

Thèse de doctorat de l'Université Gustave Eiffel

École doctorale n° 531, Sciences, Ingénierie et Environnement (ED-SIE)
Spécialité de doctorat: Science des Materiaux
Unité de recherche : MAST/CPDM

Thèse présentée et soutenue à l'Université Gustave Eiffel, le 21/11/2025, par :

Thomas SCHATZMAYR WELP SÁ

Composition du Jury

Rodolphe SONNIER Professeur, IMT Mines Alès	Rapporteur
Nicolas DAUCHEZ Professeur des Universités, UTC, Compiègne	Rapporteur
Céline PERLOT BASCOULES Professeur des Universités, Université de Pau et des Pays de l'Adour	Présidente et Examinatrice
Lily DEBORDE Docteure, Cavac Biomatériaux	Examinatrice
M'hamed Yassin Rajiv da GLORIA Docteur, Federal University of Rio de Janeiro (Brésil)	Examinateur
Sandrine MARCEAU Directrice de Recherche, Université Gustave Eiffel	Directrice de thèse
Clément PIEGAY Docteur, UMRAE, Cerema, Université Gustave Eiffel	Co-Encadrant de thèse
Fouad LAOUTID Docteur, HDR, Materia Nova (Belgique)	Co-Encadrant de thèse

Acknowledgment

Firstly, I would like to express my gratitude to my supervisors that contributed extensively to the success of this work. Every meeting, every discussion, every visit were always pleasant, enriching and memorable. In special, Sandrine and Clément, that made these three years very special to me, professionally and personally.

Huge thanks to the institution that welcomed me during the PhD, Université Gustave Eiffel, Cerema, Materia Nova and Cetelor. Thanks to the MAST department and especially to every member of the CPDM laboratory, that not only contributed to the success of this thesis but also made it much lighter and enjoyable. To the direction to the administration, technicians and students of the CPDM laboratory, I appreciate all the moments that I have lived here and I will miss them.

To the my friends that accompanied me during these three years and supported me in every way, day after day, many thanks. A special thanks to Ana, Natalia, Janette and Coralie, that were with me since the beginning and helped me integrate, learn french and to personally grow during those years. Thank you very much.

To my family and friends in Brazil that I have missed very much, thank you for every heartwarming messages. Being away from my home country was not easy, but I always knew that they were there for me, in person or not.

Finally, to my wife Gabriela, my mother Betina, my father Guilherme and my sister Ursula. I love you all, and I appreciate everything that you have done for me. Thank you so much.

Abstract

Vegetal wools have very interesting multi-functional properties that reinforce their use as a building insulation alternative to traditional insulation materials, such as excellent acoustic absorption properties, high thermal insulation, and a hygroscopic nature for humidity regulation. However, their high flammability imposes limitations on their application in constructions, requiring the use of flame-retardants. For vegetal wools, the flame-retardants need to be in agreement with the bio-based nature of the material and comply with the manufacturing process. Furthermore, the fireproof treatment should not cause changes in the structure of the fibers and in their properties, since the acoustic and thermal performances of the material depends on them. Therefore, the goal of this thesis is to reduce the flammability of vegetal wools while taking into account their manufacture, application processes, and bio-based nature, as well as to evaluate their performance as acoustic and thermal insulators.

The study was conducted on different scales of the hemp wool panels development, starting from bulk hemp fibers, passing to hemp wool prototypes and ending with hemp wool panels produced on a pilot scale. In the first step, phytic acid and urea were chosen as flame retardants, due to their bio-based origin and accessibility, respectively. Then, two different application methods were tested, immersion and pulverization, aiming for an efficient and scalable treatment. The treatment was able to graft phosphorus molecules on the hemp fibers, which significantly reduced their flammability. A slight reduction in the fiber stacks' sound absorption capacity was observed, linked to a small increase in the estimated fiber radius from the Tarnow model. No significant changes were observed in the thermal conductivity of these samples.

At the prototype scale, small hemp wool panels, containing hemp and synthetic fibers as binder, were produced using a simplified method. Four different concentrations of flame retardants and two treatment methods were tested: by treating all fibers before the panel's fabrication, or only their surfaces after the panel's fabrication. It was observed that the surface treatment was not enough to significantly reduce the flammability of the hemp wools, as their interior still burned intensely. Therefore, the chosen treatment method consisted of hemp wools treated before panel production with 5% phytic acid and 15% urea, which were used in the production of a fireproof treated hemp wool at an industrial scale. On the acoustic side, the characteristic parameters of the pore network of the hemp wools were obtained by direct measurements or by inversion of the JCAL model. A reduction in porosity, airflow resistivity, and slight changes in other characteristic parameters of the pore geometry led to a reduction in their sound absorption performance.

The chosen treatment formulation was used to treated hemp wool panels produced by airlay method, which is commonly used in the industry. The fire reaction characterization indicated a significant improvement in the flammability of the treated hemp wools when compared to a reference panel, which proves that the treatment method and formulation chosen was adapted to the material. Treated and untreated samples presented similar sound absorption performance, when produced using the same parameters, despite the porosity reduction in the treated samples. This can be attributed to an increase in airflow resistivity associated with a better fiber distribution.

In conclusion, this study establishes the feasibility of producing flame-retardant hemp wools through an optimized treatment process specifically developed in this work. The proposed method represents a novel approach that enhances the fire resistance of hemp fibers while maintaining their excellent acoustic absorption and thermal insulation properties.

Résumé

Les laines végétales présentent des propriétés multifonctionnelles remarquables qui en font une alternative prometteuse aux isolants traditionnels dans le secteur de la construction. Elles se distinguent notamment par leurs excellentes capacités d'absorption acoustique, leur performance thermique élevée et leur nature hygroscopique favorable à la régulation de l'humidité. Cependant, leur haute inflammabilité impose des limites à leur application dans les constructions, nécessitant l'utilisation de retardateurs de flamme. Pour les laines végétales, les retardateurs de flamme doivent respecter la nature biosourcée du matériau et leur utilisation doit être compatible avec leur process de fabrication. De plus, le traitement ignifuge ne doit pas entraîner de modifications de la structure des fibres et de leurs propriétés, car les performances acoustiques et thermiques du matériau en dépendent. L'objectif de cette thèse est donc de réduire l'inflammabilité des laines végétales tout en tenant compte de leur fabrication, de leurs processus d'application et de leur nature biosourcée, ainsi que l'évaluation de leurs performances en tant qu'isolants acoustiques et thermiques.

L'étude a été menée à différentes échelles du développement de panneaux en laine de chanvre, en partant des fibres de chanvre en vrac, en passant par des prototypes en laine de chanvre et en terminant par des panneaux en laine de chanvre produits à l'échelle pilote. Dans un premier temps, l'acide phytique et l'urée ont été choisis comme retardateurs de flamme, respectivement en raison de leur origine biosourcée et de leur accessibilité. Ensuite, deux méthodes d'application différentes ont été testées, l'immersion et la pulvérisation, dans le but d'obtenir un traitement efficace et adaptable. Le traitement a permis de greffer des molécules de phosphore sur les fibres de chanvre, ce qui a considérablement réduit leur inflammabilité. Une légère réduction de la capacité d'absorption acoustique des amas de fibres a été observée, liée à une légère augmentation du rayon estimé des fibres selon le modèle de Tarnow. Aucun changement significatif n'a été observé dans la conductivité thermique de ces échantillons.

À l'échelle du prototype, de petits panneaux en laine de chanvre, contenant du chanvre et des fibres synthétiques liantes, ont été produits à l'aide d'une méthode simplifiée. Quatre concentrations différentes de retardateurs de flamme et deux méthodes de traitement ont été testées : en traitant toutes les fibres avant la fabrication du panneau, ou seulement leurs surfaces après la fabrication du panneau. Il a été observé que le traitement de surface n'était pas suffisant pour réduire de manière significative l'inflammabilité des laines de chanvre, dont le coeur brûlait toujours intensément. Par conséquent, c'est la méthode consistant à traiter les laines de chanvre avant la production des panneaux avec 5% d'acide phytique et 15% d'urée, qui a été retenue et utilisée pour la production à l'échelle industrielle d'une laine de chanvre ignifugée. Sur le plan acoustique, les paramètres caractéristiques du réseau de pores des laines de chanvre ont été obtenus par des mesures directes ou par l'inversion du modèle JCAL. Une réduction de la porosité, de la résistivité à l'écoulement de l'air et de légères modifications d'autres paramètres caractéristiques de la géométrie des pores ont entraîné une réduction de leurs performances d'absorption acoustique.

En conclusion, cette recherche établit la faisabilité de la production de laines de chanvre ignifugées au moyen d'un procédé de traitement optimisé spécifiquement développé dans cette thèse. Le traitement proposé constitue une approche innovante qui améliore la résistance au feu du matériau sans compromettre ses performances acoustiques et thermiques.

Contents

List of Acronyms **9**

Publications **11**

Introduction **13**

1 State of the art **18**
1.1 Vegetal wools: base fiber and binder 18
1.2 Hemp fibers: the heart of the hemp wools 19
1.2.1 Chemical constitution 21
1.2.2 Description of the hemp fibers microstructure 22
1.3 Vegetal wools manufacturing 23
1.3.1 The binder 23
1.3.2 Fabrication of insulation vegetal wool panels 24
1.3.3 Microstructure of vegetal wools 26
1.4 Acoustic performance and modeling 29
1.4.1 Acoustics of vegetal wools 30
1.4.2 Modeling of acoustic performance of vegetal wools 31
1.4.3 Compression model 34
1.4.4 Homogenization modeling methods 35
1.5 Thermal performance 36
1.5.1 Thermal conductivity of vegetal wools 37
1.5.2 Hygrothermal performance 40
1.6 Enhancement of fire behavior from lignocellulosic fibers 43
1.6.1 Combustion reaction 43
1.6.2 Thermal degradation of lignocellulosic materials 43
1.6.3 Fire reaction assessment 45
1.6.4 Flame retardants: types and modes of action 48
1.6.5 Application methods and identified solutions 50
1.6.6 Flame retardants for lignocellulosic fibers 54
1.7 Thermal degradation and fire reaction of thermoplastic fibers 57
1.8 Effects of the treatment on the acoustic and thermal performances of vegetal wools 58
1.9 Fungi development on vegetal wools 60
1.9.1 Environmental conditions for fungi development 60
1.9.2 Substrate conditions for fungi development 61
1.10 Literature review conclusions 63
1.10.1 Coupling fireproof treatment with acoustics and thermal performances of hemp wools 63
1.10.2 Objectives of the thesis 65

2 Materials and methods **66**
2.1 Formulation of vegetal wools . . . 67
2.1.1 Hemp fibers . . . 67
2.1.2 Thermoplastic fibers . . . 67
2.1.3 Flame retardants: phytic acid and urea . . . 67
2.2 Morphology and physico-chemical characterizations . . . 68
2.2.1 Homogeneity test . . . 68
2.2.2 Weight and solid skeleton density variation . . . 68
2.2.3 Fiber morphology observation . . . 69
2.2.4 Fiber diameter . . . 70
2.2.5 Airflow resistivity . . . 70
2.2.6 Tortuosity . . . 71
2.2.7 Quantification of phosphorus content . . . 71
2.2.8 Chemical characterization of hemp fibers . . . 72
2.2.9 Mass loss through thermogravimetric analysis . . . 73
2.3 Flammability characterization . . . 74
2.3.1 Ignitability of hemp fibers and hemp wools . . . 74
2.3.2 Fire reaction characterization . . . 74
2.3.3 Smoke density . . . 76
2.4 Acoustic characterization . . . 76
2.5 Thermal characterization . . . 78
2.5.1 Thermal conductivity, diffusivity, and specific heat capacity on a transient state heat flux . . . 78
2.5.2 Thermal conductivity on a steady-state heat flux . . . 79
2.6 Sensibility to fungal development tests . . . 79
2.6.1 Fungal growth . . . 80
2.6.2 Fungal extraction . . . 80
2.6.3 Fungal impregnation . . . 81

3 Raw materials scale: Hemp fibers **84**
3.1 Article: Comparison of two flame-retardant treatment methods on bulk hemp fibers: towards a large-scale viability as a raw material for building insulation . . . 85
3.1.1 Introduction . . . 86
3.1.2 Materials and methods . . . 88
3.1.3 Results and discussion . . . 90
3.1.4 Conclusion . . . 100
3.2 Article: Impact of a phosphorus-based fireproof treatment on the acoustic performances of bulk hemp fibers . . . 101
3.2.1 Introduction . . . 101
3.2.2 Materials and methods . . . 103
3.2.3 Results and discussion . . . 108
3.2.4 Conclusion . . . 114
3.4 Thermal properties of fireproof treated hemp fibers . . . 115
3.4.1 Apparent density . . . 115
3.4.2 Thermal conductivity, diffusivity and specific heat . . . 115
3.5 Fungal development on hemp fibers . . . 116
3.6 Conclusion . . . 118

4 Simplified production scale: Hemp wool prototypes 120
4.1 Article: Investigation on the sound absorption performance of fireproof treated hemp wools . . . 121
4.1.1 Introduction . . . 122
4.1.2 Materials and methods . . . 123
4.1.3 Modeling . . . 128
4.1.4 Results and discussion . . . 130
4.1.5 Conclusion . . . 136
4.2 Thermal properties of fireproof treated hemp wool prototypes . . . 137
4.2.1 Thermal conductivity . . . 137
4.2.2 Thermal diffusivity and specific heat . . . 139
4.3 Fireproof treatment and flame retardancy of hemp wool prototypes . . . 140
4.3.1 Fire reaction assessment . . . 140
4.3.2 Relationship with phosphorus content . . . 144
4.3.3 Flame-retardant hemp wool prototypes . . . 147
4.4 Fungal development on fireproof treated hemp wools . . . 147
4.4.1 Development of fungi in hemp wool prototypes in favorable conditions 148
4.4.2 Development of fungi in contaminated hemp wool prototypes . . . 150
4.5 Conclusion . . . 152

5 Industrial production scale: Hemp wool airlay panels 154
5.1 Hemp wools manufacturing by airlay . . . 155
5.1.1 Fireproof treatment . . . 155
5.1.2 Airlay production . . . 156
5.1.3 Panels heating . . . 158
5.2 Physico-chemical properties of airlay hemp wool panels . . . 159
5.2.1 Solid skeleton density, apparent density and porosity . . . 159
5.2.2 Phosphorus content . . . 160
5.3 Fire reaction of fireproof treated hemp wool airlay panels . . . 161
5.3.1 Single-flame source test . . . 161
5.3.2 Mass loss cone calorimeter . . . 162
5.3.3 Smoke density test . . . 165
5.4 Acoustic performance of fireproof treated hemp wool airlay panels . . . 166
5.4.1 Sound absorption coefficient . . . 166
5.4.2 Characteristic parameters of the pore geometry . . . 168
5.5 Thermal properties of fireproof treated hemp wool airlay panels . . . 172
5.5.1 Thermal conductivity of airlay hemp wools . . . 172
5.5.2 Thermal diffusivity and specific heat . . . 173
5.6 Fungal development of fireproof treated hemp wool airlay panels . . . 175
5.7 Conclusion . . . 176

Conclusion and Perspectives 179

Bibliography 185

List of Acronyms

AL	Airlay
AP	Aluminum phosphinate
APP	Ammonium polyphosphate
APTES	3-Aminopropyl triethoxysilane
ASTM	American Society for Testing and Materials
ATH	Aluminum trihydroxide
ATR	Attenuated total reflection
BiCo	Bi-component
coPE	Copolyethylene
DAP	Dihydrogen ammonium phosphate
DMF	Dimethylformamide
DOPO	9,10-Dihydro-9-oxa-10-phosphaphenanthrene-10-oxid
DTG	Derivative thermogravimetry
EDS	Energy dispersive x-ray spectroscopy
EGMP	Ethylene glycol methacrylate phosphate
EHC	Effective heat of combustion
EPD	Environmental product declaration
EPS	Expanded polystyrene
FR	Flame retardant
FTIR	Fourier transform infrared spectroscopy
GHG	Greenhouse gases
GHP	Guarded hot plate
GPTES	(3-Glycidyloxypropyl) triethoxysilane
HDPE	High-density Polyethylene
HEDP	1-Hydroxyethylidene-1,1-diphosphonic acid
HF	Hemp fiber
HFM	Heat flow meter
HRR	Heat release rate
HW	Hemp wool
HWC	Hemp wool core
HWS	Hemp wool surface
ICP-AES	Inductively coupled plasma atomic emission spectroscopy
ICPTES	3-isocyanatopropyltriethoxysilane
IFRS	Intumescent flame retardant systems
IMM	Immersion
IPCC	Intergovernmental Panel on Climate Change
ISO	International Organization for Standardization
JCAL	Johnson-Champoux-Allard-Lafarge
LCA	Life cycle assessment
LCCA	Life cycle cost analysis

LDPE	Low-density Polyethylene
LOI	Loss on ignition
MCC	Microscale combustion calorimeter
MDH	Magnesium di-hydroxide
MLC	Mass loss cone calorimeter
MVP	Dimethylvinyl phosphonate
PA	Phytic acid
PBAT	Poly(butylene adipate-co-terephthalate)
PBDE	Polybromodiphenylether
PBS	Poly(butylene succinate)
PCFC	Pyrolysis-combustion flow calorimetry
PCP	Pyrovatex CP
PE	Polyethylene
PES	Poly(ether-sulfone)
PET	Polyethylene terephthalate
PHA	Poly(hydroxyl alcanoate)
pHRR	Peak heat release rate
PLA	Polylactic acid
PMIDA	N-(Phosphonomethyl iminodiacetic acid hydrate
PP	Polypropylene
PS	Polystyrene
PUL	Pulverization
PVC	Poly(vinyl chloride)
REF	Reference
REV	Representative elementary volume
RH	Relative humidity
SBI	Single burning item
SEM	Scanning electron microscopy
TAP	Triallyl phosphate
TBP	Tributyl phosphate
TBBPA	Tetrabromobisphenol A
TEOS	Tetraethoxysilane
TESPI	3-triethoxysilyl propyl isocyanate
TGA	Thermogravimetric analysis
THEIC	1,3,5-tris(2-hydroxyethyl)isocyanurate
THR	Total heat released
TL	Transmission loss
TMOS	Tetramethoxysilane
TOF	Time of combustion
TPS	Transient plane source
TPT	Triallyl phosphoric triamide
TRIAMO	(3-trimethoxysilylpropyl)diethylenetriamine
TTI	Time to ignition
VPA	Vinyl phosphonic acid
VTES	Vinyltriethoxysilane
VW	Vegetal wool
XPS	Extruded polystyrene
ZB	Zinc borate

Publications

Journals

1. Sá, T. S. W., Marceau, S., Piégay, C., Glé, P. Laoutid, F., Segovia, C., and Gourlay, E., "Comparison of two flame-retardant treatment methods on bulk hemp fibers: Towards a large-scale viability as a raw material for building insulation", Industrial Crops & Products, 2025, 228, 120903.

2. Sá, T. S. W., Marceau, S., Piégay, C., Glé, P. Laoutid, F., Segovia, C., and Gourlay, E., "Impact of a phosphorus-based fireproof treatment on the acoustic performances of bulk hemp fibers", Applied Acoustics, under review.

International Conferences

1. Sá, T. S. W., Marceau, S., Piégay, C., Glé, P. Laoutid, F., Segovia, C., Gourlay, E., and Gourdon, E., "Optimized vegetal wools for indoor comfort: coupling fire treatment with acoustic and hygrothermal performances", International Conference on Bio-Based Building Materials (ICBBM), 2023, Vienna, Austria.

2. Sá, T. S. W., Marceau, S., Piégay, C., Glé, P., Laoutid, F., Segovia, C., Gourlay, E., and Gourdon, E., "Acoustical Characterization and Modelling of the Effects of an Eco-Friendly Flame Retardant Treatment on Hemp Fiber Stacks", 53rd International Congress and Exposition on Noise Control Engineering (INTERNOISE), 2024, Nantes, France.

3. Sá, T. S. W., Marceau, S., Piégay, C., Glé, P., Laoutid, F., Segovia, C., Gourlay, E., and Gourdon, E., "Optimized vegetal wools for indoor comfort: coupling fire treatment with acoustic and hygrothermal performances", 78th Rilem Week & Rilem Conference on Smart Materials and Structures: Meeting the Major Challenges of the 21st Century, 2024, Toulouse, France.

4. Sá, T. S. W., Marceau, S., Piégay, C., Glé, P., Laoutid, F., Segovia, C., and Gourlay, E., "Evaluation of an Eco-Friendly Fireproof Treatment for Vegetal Wools", International Conference on Bio-Based Building Materials (ICBBM), 2025, Rio de Janeiro, Brazil.

5. Sá, T. S. W., Piégay, C., Mutel L., Bossert H., Marceau S., Glé, P., Segovia C., "Evaluation of methods for modelling the impact of flame-retardant treatments on the acoustic performance of hemp wools", Forum Acusticum Euronoise, 2025, Malaga, Spain.

National Conferences

1. Sá, T. S. W., Marceau, S., Piégay, C., Glé, P., Laoutid, F., Segovia, C., Gourlay, E., and Gourdon, E., "Optimized vegetal wools for indoor comfort: coupling fire

treatment with acoustic and hygrothermal performances", Congrès Français du Génie Civil (CFGC): Ville du futur et changement climatique, 2023, Gif-sur-Yvette, France.

2. Sá, T. S. W., Marceau, S., Piégay, C., Glé, P., Laoutid, F., Segovia, C., Gourlay, E., and Gourdon, E., "Influence du Traitement au Feu sur les Performances Acoustiques des Fibres de Chanvre", 42èmes Rencontres Universitaires du Génie Civil (RUGC): le Génie Civil en territoires maritimes et portuaires, adaptation au changement climatique et transition énergétique, 2024, Le Havre, France.

3. Sá, T. S. W., Marceau, S., Piégay, C., Glé, P., Laoutid, F., Segovia, C., Gourlay, E., and Gourdon, E., "Influence du Traitement au Feu sur les Performances Acoustiques des Fibres de Chanvre", Journées Techniques Acoustique et Vibrations (JTAV), 2024, Autun, France.

4. Sá, T. S. W., Piégay, C., Marceau S., Glé, P., Laoutid F., Segovia C., "Caractérisation et modélisation des effets des traitements ignifuges biosourcés sur les performances acoustiques de laines végétales", Congrès Français d'Acoustique (CFA), 2025, Paris, France

5. Sá, T. S. W., Piégay, C., Marceau S., Glé, P., Laoutid F., Segovia C., "Caractérisation et modélisation des effets des traitements ignifuges biosourcés sur les performances acoustiques de laines végétales", Journées Techniques Acoustique et Vibration (JTAV), 2025, Videoconference.

Introduction

General context and motivation

Bio-based materials: combining sustainable development with high performance functional properties in buildings

It is unquestionable that human activities have a significant impact on all terrestrial ecosystems, causing global warming, rising sea levels and its acidification, as well as increasing the disappearance or endangerment of all living organisms. One of the main causes of that is the huge amount of greenhouse gases (GHG) that are emitted yearly by human activities, which includes the areas of industries, energy production, transportation, agriculture, buildings... In the Intergovernmental Panel on Climate Change (IPCC) report from 2023 (IPC23), different scenarios for the future are designed, depending on the measures that are taken to control and limit humans' activities' impact on the environment. Five scenarios have been considered: two of them if the GHG emissions are doubled by 2050 or 2100; a scenario where the emissions remain at current levels; and two scenarios where the emissions decline to net zero by 2050 or 2070. At current levels of emission, an increase up to 3°C in the average global temperature is expected, and if it continues to grow, the global temperature increase can surpass 4°C. Therefore, it is clear that measures to reduce GHG emissions need to be urgently taken.

One of the main sectors responsible for a large proportion of CO_2 emissions, as well as energy consumption, is the construction. The United Nations (UN) report from 2020 (UNE20) shows that, in 2019, about 35% of global energy consumption and 38% of global carbon emissions were associated directly or indirectly with the building and construction industry, as shown in Figure 1. In 2020, a slight reduction in energy demand and carbon emission from the building industry was observed, due to the COVID-19 pandemic year, but in 2021, more recent data shows that these parameters surpass the values of 2019, which shows that we are stepping further away from the net zero goal (UNE22).

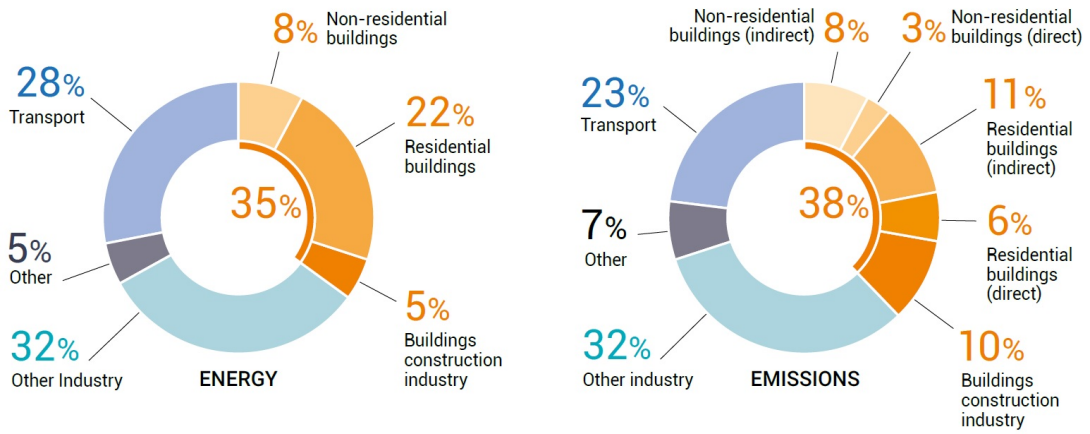

Figure 1: Global share of energy and CO_2 emissions from the building sector (UNE20)

The International Energy Agency (IEA) states on its website whether the sectors and its components are in the right pathway to achieve net zero emissions by 2050 (https://www.iea.org /reports/tracking-clean-energy-progress-2023). Regarding the building sector, it is divided into six components: heating; space cooling; lighting; appliances and equipment; building envelopes; and heat pumps. Among those components, only lighting is considered to be on track. Heating, space cooling, appliances and equipment, and heat pumps need more effort to be in the desired pace, and building envelopes are considered to be not on track at all. This means that there is a large margin of improvement that can be made, especially with regard to the building envelope.

The insulation system is a key component of the building envelope, helping to protect the interior from heat gain in summer, heat loss in winter and noise pollution, for example. It also plays a role in the regulation of humidity between the exterior and the interior. Therefore, building insulation refers to thermal, acoustic and hygric insulation. An efficient insulation of the building would reduce energy consumption, reduce costs, and improve comfort (GAL22).

On the acoustic side, building insulation is not only associated with indoor comfort, but also health. The World Health Organization (WHO) states that exposure to noise can lead to auditory effects on health such as hearing loss and tinnitus (WHO18). It can also have other effects for example, sleep disturbance, annoyance, learning impairment, heart disease and even premature deaths (WHO18; ENV20). Therefore, recommendations for traffic, railway, aircraft, and industry noise have been made, limiting the noise pressure to levels that would not harm people (WHO18; ENV20). So, it is essential for building envelopes to offer high-performance insulation to guarantee indoor comfort and the well-being of occupants.

All these factors lead to the conclusion that building insulation is one of the key elements that can contribute to the fight against environmental problems currently faced by humanity. To meet these huge and urgent challenges, the use of bio-based materials is an alternative to traditional solutions, which consume a lot of energy and have a significant environmental impact (FUC22; ZIE20). For this thesis, work will be carried out on a specific type of bio-based insulating material belonging to the vegetal wools family: the hemp wool.

Overcoming the vegetal wools limitations: the development of fireproof treated hemp wools

Vegetal wools have interesting characteristics that validate them as sustainable building insulators. First of all, it is mainly composed of plant fibers, which is a renewable resource, highly available, that require low energy for processing and can be obtained as a co-product from agricultural activities (GRA21; ZAM13). Furthermore, plants have the capacity to sequester carbon and store in its composition through photosynthesis, known as biogenic carbon, reducing carbon levels in the atmosphere (PIT21; ZAM13). Therefore, by opting for a bio-based solution, one would not only exploit these advantages but also avoid the impacts associated with non-sustainable alternatives.

Besides environmental benefits, vegetal wools are also excellent acoustic and thermal insulators, comparable to well established alternatives in the market, such as mineral and glass wools. Due to their physico-chemical composition, and their fibrous and porous structure, the vegetal wools offer good levels of sound absorption and low thermal conductivity (CHA16; KOR11; OLD11; VOL15). In addition to that, vegetal wools can easily exchange humidity with the environment, which reduces condensation of water vapor and contributes to the humidity regulation inside the building (AMZ17; PAL18).

In social aspects, the vegetal wools promote the comfort and health of the users inside

the building, through the absorption of the sound waves energy and attenuation of the extreme temperatures and humidity, which translates to economical benefits by reducing the energy consumption needed for heating and cooling (FUC22; GAL22).

Despite all the environmental, technical, economical and social advantages presented by hemp wools, their high flammability remains as the main limitation that hinders the applicability of the bio-based materials (KIM18; LIA23; MUL25). Based on the data sheet of vegetal wool manufacturers and sellers, they are classified as Euroclass E or F, which are the two worst classifications possible for a material (HEM25; IND25; TEC25).

The high flammability limits the application possibilities of bio-based materials because they need to be inserted into a building system that offers fire protection for the bio-based material. In the case of vegetal wools, for example, it is usually recommended by the manufacturers to be associated with a plaster or mortar layer. The use of the material alone, or in conjunction with a wooden panel would probably not meet the fire safety standards, which limits their application possibilities.

Research problem and objectives

To expand the applications possibilities of the vegetal wools, they need to be fireproof treated. However, with that, two problems and motivations of this study arise: The first one is regarding which type of fireproof treatment to use. Historically, multiple flame retardants have been banned in different countries because they were associated with environmental and health issues for the people. In addition, many flame-retardants originate from non-sustainable or non-renewable sources, which do not fit the sustainable nature and purpose of the vegetal wools. Therefore, an environmental- and health-friendly solution for flame retardants needs to be found.

The second point is the up-scaling of the production of fireproof treated vegetal wools. In the context of insulation building material, a large amount of materials are used, even for a low-density material like the vegetal wools. So, not only must the fireproof treatment be compatible with the nature of the vegetal wools, but also its application method needs to be scalable to a large-scale production.

As a result, the main question to be answered is: how can we produce flame-retarded hemp wool panels for building insulation, considering their large-scale application, bio-based nature and functional performances?

This thesis aims to address this question through the following objectives:

- Define a flame retardant that is environmentally friendly and suitable for vegetal wools fireproof treatment.
- Determine the flame retardants application method suitable for the development of fireproof treated vegetal wools.
- Optimize the fireproof treatment at the scale of vegetal wools.
- Evaluate the acoustic and thermal performances of fireproof treated vegetal wools.
- Validate the chosen methodology at an industrial level.

Context

The Ph.D. work presented in this thesis is funded by the CLEAR-Doc (City Lab Education And Research Doctoral Programme) project, which is part of the European Union's Horizon 2020 research and innovation program under the Marie Skłodowska-Curie CO-FUND grant agreement No 101034248. It also received funding from the French Agence Nationale de la Recherche (ANR) under grant ANR-23-CE22-0012 (BIOMETA).

Due to the multidisciplinary context of this thesis, it involved the Université Gustave Eiffel and three partners, whose roles are presented in the following:

- **Université Gustave Eiffel**: This thesis was developed in the facilities of the department Matériaux et Structures (MAST) and the laboratory Comportement Physico-Chimique et Durabilité des Matériaux (CPDM). The CPDM laboratory provided the main office for this thesis and the equipments for physico-chemical characterization of the material.

- **Cerema**: The Cerema's agency of Strasbourg provided the means for acoustic and thermal characterization as well as for the modeling of the materials' performance, as part of the Unité Mixte de Recherche en Acoustique Environnementale (UMRAE), and the Pôle BioGéo - Groupe Bâtiment Construction Immobilier.

- **Materia Nova**: The Materia Nova's laboratory is a center of research and development of materials, associated with the Univeristé de Mons (UMONS), at Mons, in Belgium. It provided the infrastructure needed for the reaction to fire tests.

- **Cetelor**: The Cetelor is a center of technology for textiles and fibers, linked to the Université de Lorraine, located in Epinal, in France. It is equipped with a line of production of vegetal wools equivalent to one in industrial level. Cetelor was responsible for the manufacturing of the hemp wools.

Outline

The thesis consists of 5 chapters. From Chapter 3 to Chapter 5, the material studied evolves from the raw material until the final product, as illustrated in Figure 2.

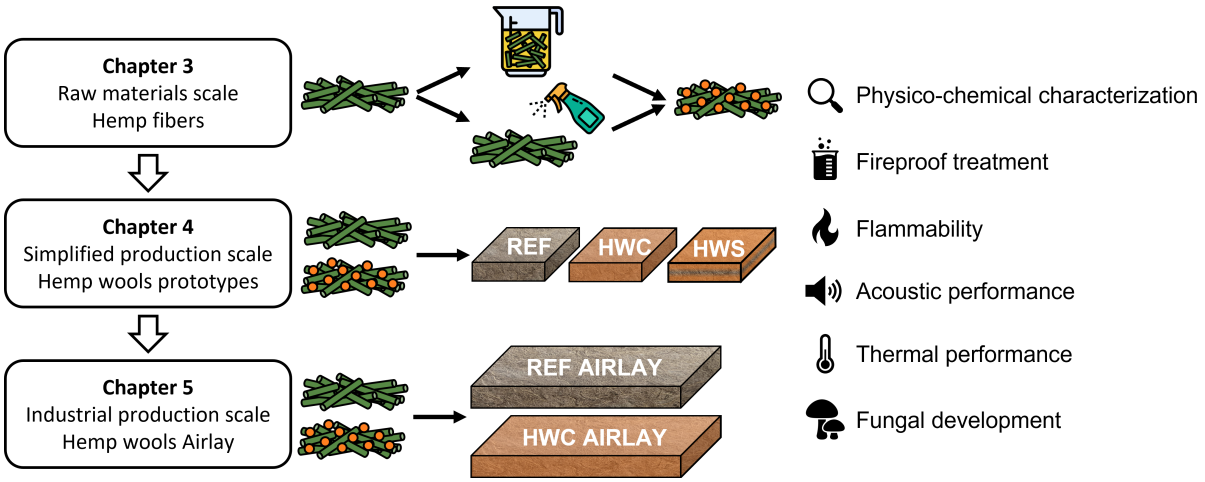

Figure 2: Schematic representation of the thesis organization

- **Chapter 1** presents the state of the art of fireproof treatment, flame retardants, reaction to fire, acoustic and thermal characterization and performances, and fungal development of vegetal wools.

- **Chapter 2** details the materials and methods used in this work to characterize the physico-chemical properties of the materials, as well as their fire reaction and their acoustic and thermal performances. In this Chapter, the hemp wool prototypes production and the airlay method production are detailed.

- **Chapter 3** tackles the investigation of the eco-friendly flame-retardant and the application method that is adaptable to be used at an industrial level, by investigating the hemp fiber's fire reaction. It also presents the effect of the treatment on the acoustic and thermal performances, and on the fungal development of the hemp fibers.
- **Chapter 4** presents the characterization of the fire reaction, acoustic and thermal performances and fungal development of hemp wool prototypes.
- **Chapter 5** presents the same characterizations but done with hemp wools produced by the airlay method, following an industrial-scale production.

Chapter 1

State of the art

In this chapter, a literature review that covers the main topics of this thesis is presented. Section 1.1 introduces the vegetal wools, their definition, main characteristics and advantages. Then, Section 1.2 presents the hemp fibers, the main constituent of hemp wools, including their chemical composition, morphology and microstructural aspects. In the following, Section 1.3 describes the vegetal wools manufacturing processes and the microstructure of the final product.

After that, Section 1.4 presents the definition of key parameters related to the acoustic performance of vegetal wools, and addresses modeling methods that are used to simulate and predict the acoustic performance of fibrous materials. The following Section 1.5 covers the thermal performances of the vegetal wools and the main parameters that influence it.

In Section 1.6, the main points related to the combustion and thermal degradation of lignocellulosic fibers are presented, as well as the types of flame retardants and their mechanisms of action. This section also covers the fire reaction of vegetal wools and its components. After that in Section 1.7, the thermal degradation and fire reaction of thermoplastic fibers are presented. The flammability part concludes with the presentation of the effects of the fireproof treatment on the acoustic and thermal performances of vegetal wools, in Section 1.8.

In the last part of this Chapter (Section 1.9), a review of the developments of fungi in vegetal wools and the influence of the environmental conditions and the substrate is presented. Finally, the main conclusions obtained after the literature review are presented in Section 1.10.

1.1 Vegetal wools: base fiber and binder

Vegetal wools are part of the group of bio-based materials, which are defined as materials that are fully or partially composed by elements derived from renewable organic matter (biomass) of plant or animal origin. Some examples are the natural fibers, cellulose fibers, cork boards, sheep wool, wood fiber, cotton, straw bales and, last but not least, vegetal wools.

The composition of the vegetal wools involves a base fiber and usually a binder. The base fiber can be only one type of plant fiber, such as hemp, flax or wood, or a mix of multiple fibers (Figure 1.1). The company Cavac Biomatériaux commercializes a vegetal wool composed of hemp, flax and cotton, for example (biofib.com/gamme-biofib/biofib-trio/). The base fibers are the main constituent of the vegetal wools and account for the majority of the final product's weight, usually at about 85% to 92%.

The remaining weight refers to the binder. For this function, thermoplastic fibers are used. These fibers partially melt during the manufacturing process and ensure bonding with the base fibers, adding cohesion and stability to the vegetal wools. These thermo-

plastic fibers can be synthetic or bio-based. Some vegetal wools do not use any type of binder, being 100% composed of base fibers. However, they have format of a mat, with an aspect and application completely different from the vegetal wool panels used for building insulation.

In this thesis, the vegetal wools developed are composed of hemp fibers, as the base fiber, and a synthetic thermoplastic fiber, as the binder. Therefore, in the following Section, the main characteristics of the hemp fibers will be explored, including definitions, morphology and physico-chemical properties. Then, thermoplastic fiber main characteristics will be detailed along with the manufacturing process of the vegetal wools, in Section 1.3.



(a) (b)

Figure 1.1: Commercial vegetal wools with different base fibers (biofib.com): (a) Hemp; (b) Hemp, flax and cotton

1.2 Hemp fibers: the heart of the hemp wools

The vegetal wool development process starts with the cultivation of the vegetal fiber. Among the multiple possibilities, hemp was chosen to be used in this thesis. It is a widely available and accessible resource in many continents, including Europe, where France leads the production with 22000 hectares (pole-europeen-chanvre.eu). Other types of vegetal wools will have similar development process, but with certain specificities for the processing of other plant species.

Furthermore, hemp is considered one the main bio-based products for a sustainable development in a large-scale, due to multiple characteristics that are presented by the European Hemp Center (pole-europeen-chanvre.eu). It resists long periods of drought with its long and deep roots; it is very resistant to pests, avoiding the use of pesticides; it grows rapidly, taking about 4 months between sowing and harvesting; it is an excellent CO_2 sink, where 1 ha of hemp cultivation absorbs 15 tons of CO_2. Hemp is also considered to integrate perfectly into the rotation of crops, due to the short cultivation cycle time, improvements in soil quality, and a source of nitrates for the soil (ABO10; TER20). These interesting aspects of the hemp cultivation are highlighted in Figure 1.2.

Another interesting aspect, is that hemp is fully exploited. The grains are used in the animal and human food industry and in the chemical and cosmetic industry. The hemp shives can be used for the production of hempcretes, the fibers for insulation, woven and non-woven products, and the remaining powder can be used to produce energy. These advantages solidify hemp as a strong sustainable alternative to a mineral- and oil-based solution in multiple fields.

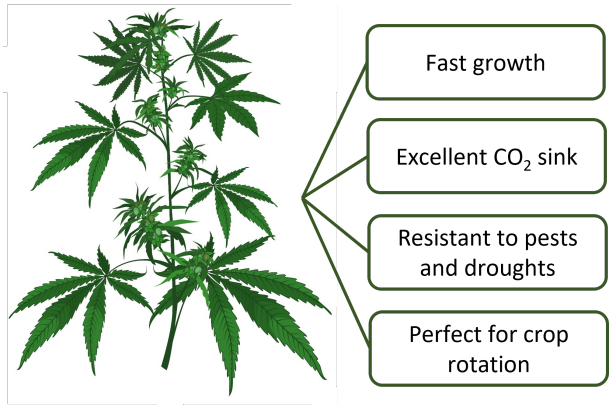

Figure 1.2: Advantages of hemp cultivation

In France, hemp is seeded in the second half of April and in the beginning of May, and is harvested in the middle of August and the beginning of September (TER20; VAN02). While still in the field, the hemp is submitted to the retting process, which is a biological and chemical process where the harvested plant is left in the field under the sun and rain for 10 to 20 days (TER20). During this time, microorganisms will start to decompose the hemp facilitating their extraction from the woody part of the plant (TER20; PAN14; THY06). During the August and September period, favorable conditions for the natural retting process to be done in the field are found, as the weather is warm and sunny, with rainfall spaced out over time. Periods of low temperature and high precipitation lead to plant degradation (TER20). Retting is an important and controlled process that impacts the quality of the fibers and their properties (LEC21).

After that, mechanical processes of scutching and hackling can be used to clean and improve the quality of the fibers, depending on their use (THY06). Scutching process breaks and removes the woody parts of the hemp stem, while hackling refines this process by removing short fibers and residual shives (PAN14). Following these processes, hemp fibers can be considered ready as a raw material for production of building insulation.

However, before looking at vegetal wool panels, it seems relevant to focus more specifically on the internal structure of hemp fibers and their specific characteristics. Hemp fibers have a complex structure that can be analyzed in multiple scales, as shown in Figure 1.3 (DES22). It goes from the cross-section of a fiber's stem, to fiber bundles (technical fiber), to individual fibers (elementary fiber), and finally to the main constituents of the lignocellulosic fibers, which are cellulose, hemi-cellulose and lignin. Throughout this literature review, these different fiber scales will be addressed, either through their processing or their physical and chemical properties.

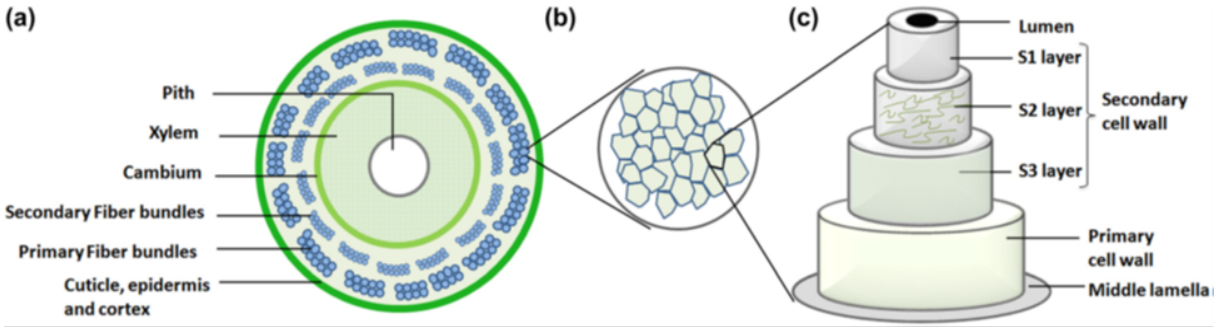

Figure 1.3: Multi-scale structure of hemp fibers (DES22): (a) cross-section of hemp stem; (b) hemp fiber bundle; (c) elementary hemp fiber

As seen in Figure 1.2 (DES22), the hemp fibers are organized in bundles and are located in the region beneath the epidermis and cortex, in a region called phloem. Each

elementary hemp fiber is composed of layers of cell wall and a hollow center located in the middle, which is the lumen.

Hemp fibers are mainly commercialized as technical fibers. However, their size can vary considerably as a function of the number of fibers in the bundle, which results in a heterogeneous material. In addition, the presence of individual elementary fibers further contributes to the heterogeneity of the fiber properties. Through Figures 1.4a and 1.4b, this heterogeneity can be observed (SAU18). This creates a challenge and an opportunity for the exploitation of this heterogeneity for the development of high performing insulators.

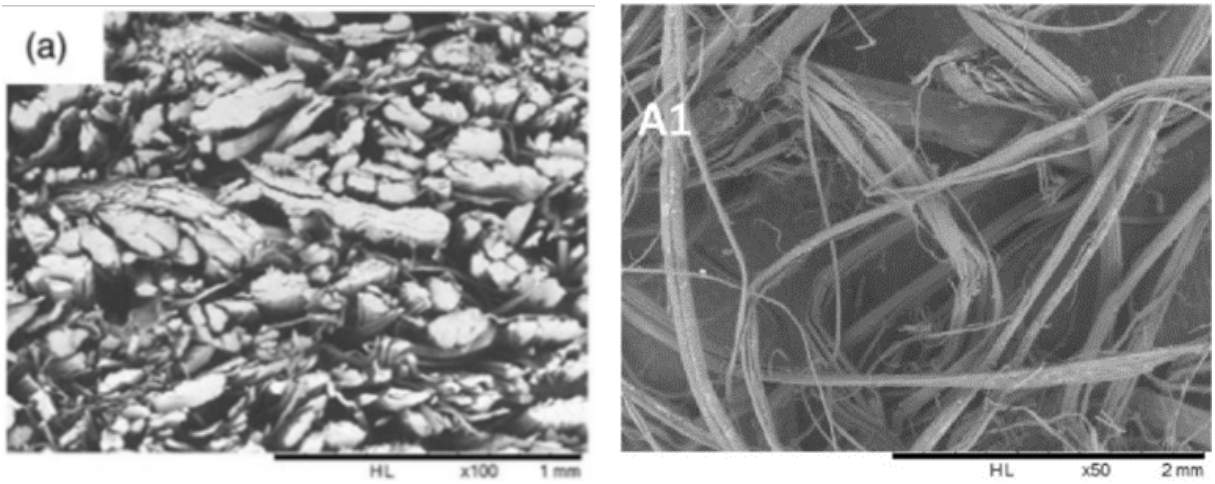

(a) (b)

Figure 1.4: Scanning electron microscope images of hemp fibers (SAU18): (a) cross-section view; (b) Longitudinal view

1.2.1 Chemical constitution

Vegetal fibers can be considered as natural composites and are mainly composed by cellulose, hemicellulose and lignin (BER21). The main component is cellulose, which is a fibrous component that provides stiffness and strength to the fiber. Moreover, it is a semi-crystalline polyssacharide, formed by chains of glucose units, with a large amount of hydroxyl groups (COS17; YAN14). Hemicellulose can be found in cell walls where it acts as cross-linking material between cellulose micro-fibrils. It differs from cellulose by being amorphous, with a branched chemical structure of different sugars and a lower molecular weight (COS17; YAN14). Lignin, on the other hand, acts mainly as a bonding agent in plant fibers, and has an amorphous and highly complex chemical structure, mainly aromatic (YAN14).

The amount of each component varies not only between plant species, but also between plant samples of the same species due to growth conditions (BER21; SUM10). Some range of values of the chemical composition of each bio-based material is presented in Table 1.1. In this thesis, the chemical composition will be mostly relevant for thermal degradation and fire reaction of the hemp fibers, which will be presented in Section 1.6.

Table 1.1: Chemical composition of bio-based materials

Material	Cellulose (%)	Hemicellulose (%)	Lignin (%)	References
Hemp fiber	60-85	10-23	2.5-6	PER15 KOZ08 BER21 DES22
Flax fiber	60-85	11-21	1-3	PAN14 PER15 MOU19 MEL22
Sisal fiber	53-78	6-26	7-14	PER15 KOZ08 BER21 DES22
Miscanthus fiber	33-45	30	20-25	HAJ20
Jute fiber	58-73	12-24	12-16	BER21 DES22
Bamboo	26-65	11-30	2-31	KOZ08 BER21
Soft Wood	30-60	20-30	21-37	PER15
Hard Wood	31-64	25-40	14-34	PER15

1.2.2 Description of the hemp fibers microstructure

The microstructure of vegetal fibers plays an important role in their functional performance. To characterize this microstructure, several key parameters are commonly used to describe it, such as the apparent density, solid skeleton density, porosity and fiber diameter.

The apparent density (ρ_{ap}) is defined as the ratio between the mass of the material and its total volume occupied, including open and closed pores. For insulation materials, it is an important parameter that influences their acoustic and thermal performance. On the other hand, the solid skeleton density (ρ_s) considers the ratio between the mass of the material and only the volume occupied by its solid skeleton (V_s) and its closed pores. The Equation that describes these parameters are presented by Equations 1.1 and 1.2.

A relationship between these two parameters allows the description of the amount of pores present in a material, given by the porosity (ϕ) parameter. It is defined as the ratio between the volume occupied by the voids (V_v) and the total volume (V_t) occupied by the material and can be rewritten as a function of the apparent density and the solid skeleton density, as shown in Equation 1.3.

$$\rho_{ap} = \frac{m_s}{V_t} \tag{1.1}$$

$$\rho_s = \frac{m_s}{V_s} \tag{1.2}$$

$$\phi = \frac{V_v}{V_t} = 1 - \frac{\rho_{ap}}{\rho_s} \tag{1.3}$$

1.3 Vegetal wools manufacturing

As mentioned previously, the manufacture of vegetal wools requires the use of vegetal fibers combined with a binder composed of thermoplastic fibers. Even if it accounts for a small percentage of the weight, the binder is responsible for the consolidation of the panel, providing cohesion between fibers and stability. In this section, the characteristics, options and selection criteria for the binder are presented in Section 1.3.1 and the methods of fabrication of insulation vegetal wool panels are described in Section 1.3.2.

1.3.1 The binder

Thermoplastic fibers are synthetic fibers made from polymers that soften and become moldable when heated and solidify again upon cooling. This reversible behavior allows them to act as binders in nonwoven products, such as vegetal wools, where they melt to form bonds with the natural fibers and then resolidify to provide structural stability. This process is called thermal-bonding process. The temperature used in this process will depend on the polymer and if the fiber is mono- or bi-component.

The polymers that constitute the fibers can originate from oil-based or bio-based sources. The oil-based are typically polyolefins, such as polyethylene (PE) or polypropylene (PP), polystyrene (PS), polyethylene terephthalate (PET) and poly(vinyl chloride) (PVC) (BER21). Bio-based polymers are obtained from fermentation of sugars and starch, and some examples are poly(lactid acid) (PLA), poly(butylene succinate) (PBS), poly(hydroxyl alcanoate) (PHA) and poly(butylene adipate-co-terephthalate) (PBAT) (BER21; SIG09).

Thermoplastic fibers may be either mono-component, consisting of a single polymer, or bi-component, composed of two polymers. During the thermal-bonding process these fibers need to melt, in order to create bonds with the natural fibers, therefore a mono component fiber melts entirely during this process. A bi-component fiber can be composed of a high melting point polymer at the core, and a low melting point polymer at the sheath, allowing a partial melting of the fibers. The temperature used during the thermal-bonding process depends on the melting point of the polymers that compose the thermoplastic fibers. However, this temperature cannot exceed 200°C to avoid thermal degradation of hemicellulose present in the natural fibers (BER21; COS17; DOR14).

Table 1.2: Melting point of thermoplastic materials

Polymer	Melting temperature	References
PVC	200-215°C	ROY11
PET	245-265°C	ROY11
PP	160-175°C	TOM10 ROY11
LDPE	113-115°C	TOM10 ROY11
PLA	150-171°C	JOM13 FAR16
PBS	113-120°C	THE15 XUM19
PBAT	115-125	JOM13 JIA20

The melting point of some of the polymers mentioned above are indicated in Table 1.2. It can be observed that some of them start to melt at high temperatures, which

prevents their use in vegetal wools as a mono-component fiber. Yet, they can still be used at the core of a bi-component fiber, in association with a low melting point polymer at the sheath. Two examples of bi-component fibers are a synthetic option with PET core and LDPE sheath, and a bio-based option with PLA core and PBS sheath, from the company Trevira.

As opposed to vegetal fibers, thermoplastic fibers have homogeneous dimensions and a round cross-section with a uniform diameter. A cross-section of a bi-component thermoplastic fiber (PLA-PBS) is shown in Figure 1.5.

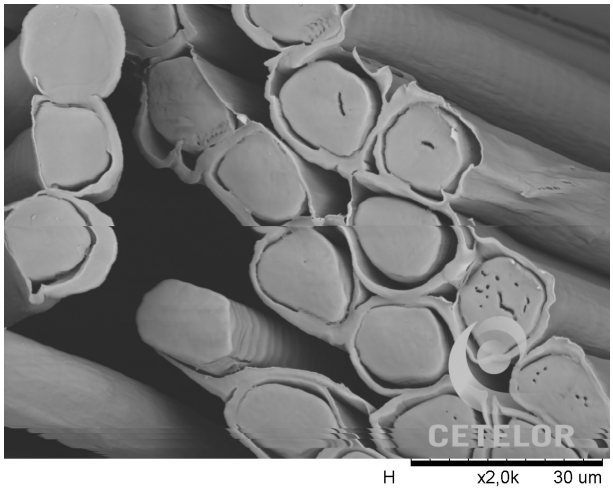

Figure 1.5: Cross-section of PLA-PBS fiber (Cetelor)

1.3.2 Fabrication of insulation vegetal wool panels

Prior to the fabrication of vegetal wools, technical vegetal fibers often undergo a process called fiber opening. In this process, the fibers pass through a fiber-opening machine equipped with metallic cylinders, equipped with spikes and lining teeth with different densities per cm^2, as presented in Figure 1.6 (AYA23). These cylinders untangle the fibers, separate them from their bundles, remove unwanted woody parts that may be present, and break the fibers into smaller pieces (HYS16).

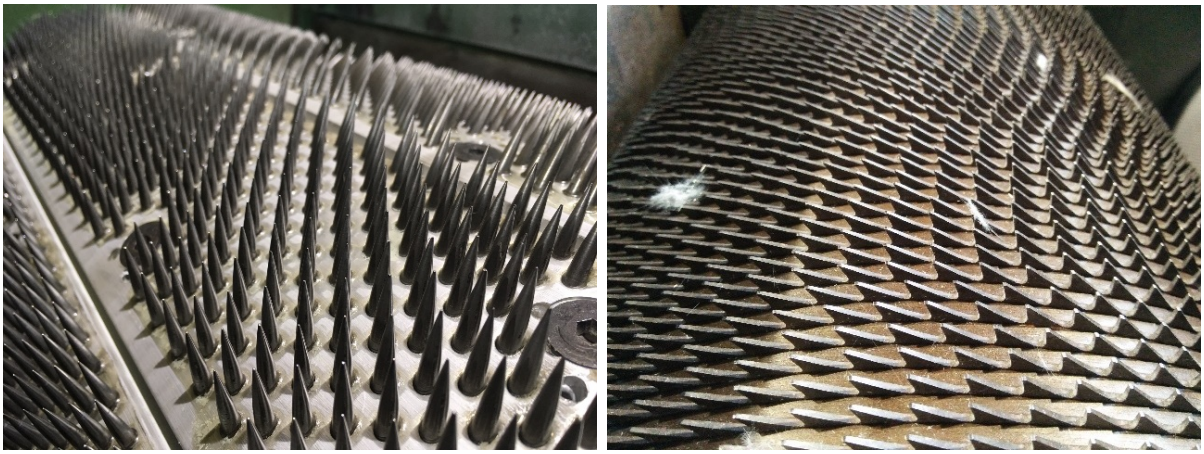

(a) (b)

Figure 1.6: Metallic cylinders responsible for fiber opening step (AYA23)

There are three methods commonly used for the manufacturing of vegetal wools, that

produce materials with different characteristics and applications. Therefore, it is important to define them and contextualize their differences. These methods are known as needle-punching (FRE11; HYS16; PAU22), hydro-entanglement (FRE12; FRE14; GUL18) and air-laying (AYA23; HYS16).

In the needle-punching process, mechanical bonding between the fibers is created. The fibers are punched multiple times with needles that entangle them, forming an interlocked fiber mat. This can be observed in the side view of a needle-punched hemp mat, in Figure 1.7 (HYS16). Several parameters can affect the final product, such as the punching rate, feeding speed, needle shape, and punch depth (HYS16). In this case, the use of thermoplastic fibers is optional. The vegetal wools produced through this method are often used as geotextiles, for applications requiring cushioning, drainage, and regularization of surfaces (KEL16).



Figure 1.7: Needle-punched mat (HYS16)

The hydro-entanglement process consists of creating a web of fibers and exposing it to a curtain of high-velocity jets that interlock and entangle the fibers (GUL18). This curtain is created using a porous belt or a perforated patterned screen and at the end of the process, the vegetal wool is dried. The size of the pores in the porous belt, the water pressure, and the conveyor speed are parameters that influence the final product's properties and quality. The vegetal wools produced through hydro-entanglement process often used as fabrics, mats or geotextiles, with application with applications ranging from clothing to soil reinforcement. An example of a hemp wool produced by hydro-entanglement is shown in Figure 1.8 (FRE14).



Figure 1.8: Hemp wool produced by hydro-entanglement (FRE14)

In the air-laying process, the fibers are moved into a chamber, where with the use of pressurized air, they are air-laid and form a fiber web layer in a dry process (HYS16). This fiber layer is then moved to an oven for the thermo-bonding process. The fibers are heated with hot air at a temperature that partially melts the thermoplastic fibers,

forming bonds with the natural fibers after they are cooled down (ROY11). The product's thickness can be controlled, and at the end, it is cut to the desired length in the form of panels. This processing method allows for high production rates (ROY11). Figures 1.9a and 1.9b present the fibers distribution throughout the thickness of two air-laid hemp wools made of flax and hemp, respectively.



(a) (b)

Figure 1.9: Air-laying vegetal wools (HYS16): (a) Flax; (b) Hemp

In summary, for the development of vegetal wool panels for building insulation, the air-lay method associated with the thermal-bonding process is a suitable production method, since it is a dry process and allows the formation of panels with controlled thickness. The whole process can be divided into four steps: fiber opening, fiber mixing, panel formation through air-laying, and thermal-bonding.

1.3.3 Microstructure of vegetal wools

The properties and performance of vegetal wools result from the physical and chemical characteristics of the raw materials combined with the interactions formed between them during production. The result is a material with a particular microstructure, which will be detailed in this Section.

For vegetal wools, their apparent density ranges between 25 to 100 kg.m^{-3}, based in information found in the literature (COL11; FRE14; KOR11; KOR16; PIE19; PIE18) and in the Environmental Product Declaration (EPD) of commercial hemp wools (HEM25; IND25; TEC25). This parameter can be controlled during the vegetal wools production, but it can also vary as a function of the type of vegetal fiber or polymer and formulation, since they have different values of solid skeleton density.

Regarding vegetal fibers that can be used in vegetal wools, they share the same order of magnitude of solid skeleton density at about 1400 and 1500 kg.m^{-3}, with little variety between plants, as shown in Table 1.3 for hemp, flax, sisal and jute fibers. Thermoplastic fibers are generally lighter with values close to 1000 kg.m^{-3} (Table 1.3). The solid skeleton density values of glass and mineral fibers are also presented for comparison purposes. It can be seen that vegetal fibers present a significantly lower solid skeleton density than glass and mineral fibers, which benefits the production of lightweight products.

Another important parameter in describing the microstructure of the fiber is their diameter. The vegetal fibers and the thermoplastic fibers have very different fiber diameter distributions. The vegetal fibers have irregular shapes, and an overall heterogenic fiber diameter not only between fibers but also the same fiber can have thicker or thinner parts. Furthermore, the fibers can be found as an elementary fiber, or grouped as a bundle as technical fibers, which drastically increases the effective fiber radius. This depends mainly on the processing of the fiber after harvesting them, mentioned in Section 1.1.

Therefore, their characterization are not simple. The most reliable method is by measuring multiple fibers using an optical or digital microscope, or even by scanning

electron microscopy (SEM) and creating a histogram of fiber diameter (KER15; LUU17; PIE19; SIN12). In contrary, the thermoplastic fibers have uniform cross-section and circular shape, without changes in diameter throughout the fiber. An example of a SEM image of a hemp wool, and the identification of a hemp fiber and a bi-component fiber (BiCo) is represented by Figure 1.10.

Table 1.3: Density of vegetal, thermoplastic, glass and mineral fibers

Material	Density (kg.m^{-3})	Reference
Hemp	1480-1560	FRE11 PER15 SUM10 THY06
Flax	1500	OLD11 PER15
Sisal	1410-1500	OLD11 PER15
Jute	1370-1520	OLD11 SUM10
Low-density Polyethylene	910-940	plasticseurope.org
High-density Polyethylene	930-970	plasticseurope.org
Polypropylene	895-920	plasticseurope.org
Polystyrene	1060	physics.nist.gov
Polylactic acid	1240	Polyfluor plastics
Glass	2480-2620	RUD00 BRA09
Mineral	2700-2800	textilelearner.net HUS23

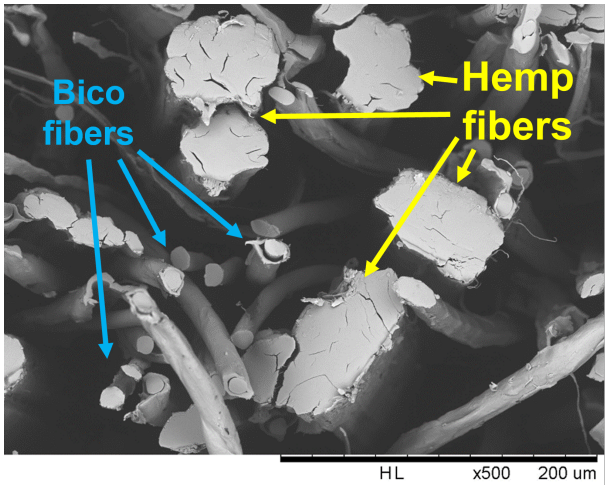

Figure 1.10: Identification of hemp and bicomponant fibers in hemp wool (Source: Cetelor)

It is possible to model the distribution of the fiber diameter with a distribution law. Some options can be considered. The lognormal distribution is generally used and can well describe the distribution of fibrous materials (KER15; PIE19; SIN12). Another possible approach is using a gamma distribution (LUU17). Unweighted arithmetic mean and median values can also be useful to characterize the fiber diameter sizes. Figure

1.11 illustrates the fiber diameter distribution of glass fibers, with the measurements represented by the histogram in blue, a normal-log distribution represented in green and a cumulative distribution in red (KER15).

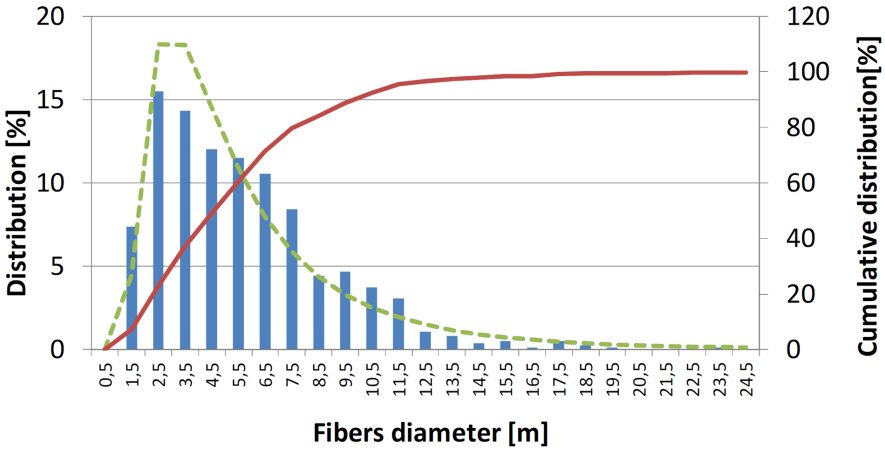

Figure 1.11: Fiber diameter distribution of glass fibers (KER15)

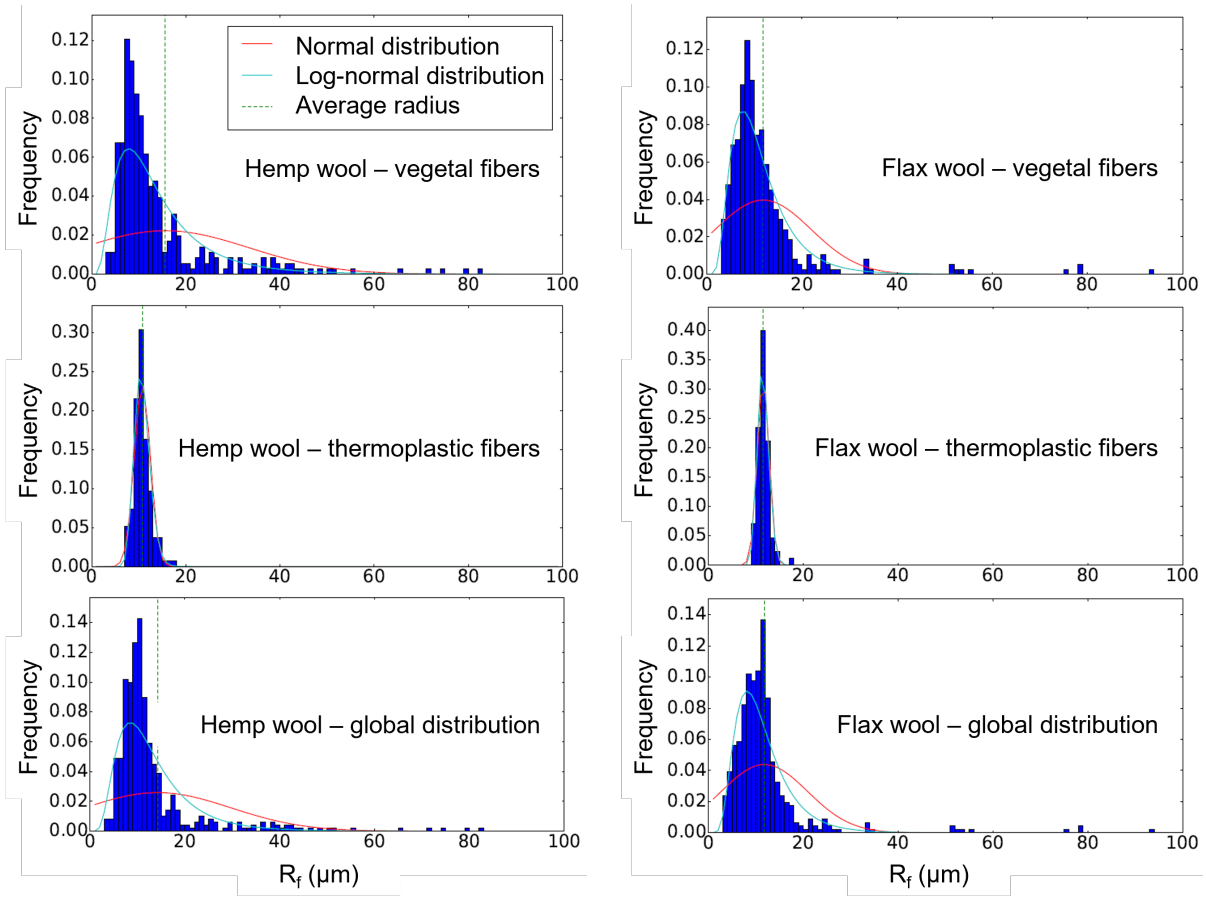

(a) (b)

Figure 1.12: Vegetal wools fiber radius distribution: (a) Hemp fibers, thermoplastic fibers and global distribution; (b) Flax wools vegetal fibers, thermoplastic fibers and global distribution (PIE19)

Luu et al. (LUU17) have measured the diameter of 744 Asclepias fibers and 184 bi-component thermoplastic fibers, considering the hypothesis of circular cross-section. A mean diameter of $25 \pm 6.6\ \mu m$ and $14.7 \pm 1.7\ \mu m$ were obtained for the vegetal fibers and

thermoplastic fibers, respectively. Noticeably, the standard deviation of the thermoplastic fibers is significantly lower than the one obtained for the vegetal fibers, indicating their greater homogeneity in terms of diameter size.

Piégay (PIE19) measured the fiber radius of hemp and flax wools, using the same hypothesis of circular cross-section. The results were reported through fiber distribution histograms, which are shown in Figure 1.12. It includes the fiber radius distribution of only the vegetal fibers, only the thermoplastic fibers and the global distribution. From them, it is observed that both vegetal fibers have a wider variation of fiber radius, with most of them smaller than 20 μm, but reaching almost 100 μm. The thermoplastic fibers present a concentrated peak, indicating a homogeneous radius.

1.4 Acoustic performance and modeling

For acoustic studies, vegetal wools can be considered as a porous material, constituted by two phases: a solid phase, represented by the solid skeleton of the fibers, and a fluid phase, represented by the air that saturates the pores between fibers. It is assumed that the material is homogeneous and isotropic. In general, the solid phase would be assumed to be elastic, to account for the effects of the two compression waves and one sheer wave that could propagate in the fluid and in the solid phases of the material (BIO56; BIO6A). However, previous works have shown that, in the case of vegetal wools, the analysis can be simplified to consider the frame as a rigid body (PIE19).

Another hypothesis made is that the pores of the vegetal wools are open and connected, with a size large enough to be permeable to acoustic waves in the audible domain (> 10 μm) (PIE19). Also, the hypothesis of linear acoustic is considered, neglecting second-order variables (BRU06).

The acoustic behavior of insulation materials is fundamentally related to their ability to absorb and isolate sound. These two functions correspond, respectively, to acoustics correction and acoustics insulation.

Acoustics correction characterizes the capacity to regulate the sound level within an environment. This occurs through the control of reverberation effects that happen with the reflection of sound waves at the room's surfaces, such as walls, ceilings and floor. Through acoustics correction, the main objective is to ensure sound quality and comfort for the users.

Acoustic insulation characterizes the capacity of a material or building system to attenuate the transmission of acoustic energy between one side of the wall and the other. The main goal is to reduce the sound levels that are transmitted to an adjacent room, ensuring comfort and privacy for the users.

A proper acoustic correction and effective acoustic insulation require an understanding of how incident sound waves interact with the material. An incident sound wave that hits the material will form a reflected wave and a transmitted wave, as demonstrated in Figure 1.13 (TIE20). From these waves, two acoustic parameters can be defined: the sound absorption coefficient (α) and the transmission loss (TL).

The sound absorption coefficient describes the capacity of the material in absorbing the sound wave energy, as opposed to reflecting it, therefore, it depends on the incident and reflected sound wave pressure. With that, considering a material with a rigid end at its back, the reflection coefficient (R) can be defined as the ratio between the pressure of the reflected sound wave (p_r) and the incident sound wave (p_i) (Equation 1.4).

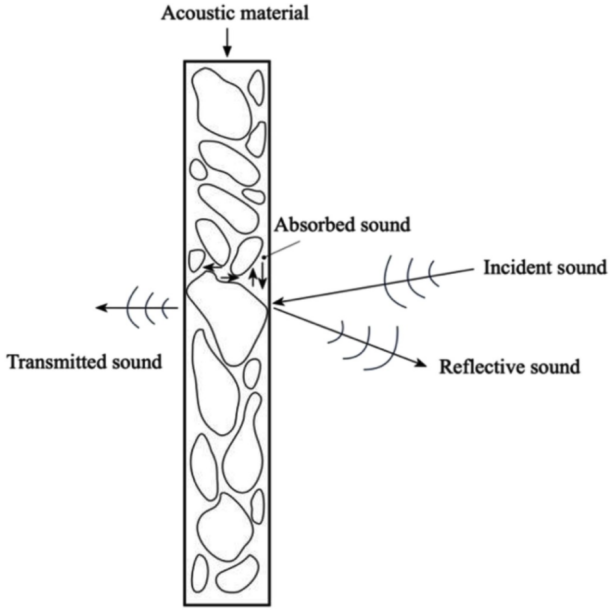

Figure 1.13: Incident, absorbed, reflected and transmitted sound waves (TIE20)

$$R = \frac{p_r}{p_i} \tag{1.4}$$

Then, the sound absorption coefficient is given by Equation 1.5. It varies between 0 and 1, where 0 is for a totally reflective material ($R = 1$), and 1 for a completely absorbent material ($R = 0$).

$$\alpha = 1 - |R|^2 \tag{1.5}$$

Transmission loss measures how much sound energy is stopped from reaching the opposite side of a material or building system. It is a function of the incident and transmitted sound wave pressure, given by the transmission factor (τ) presented in Equation 1.6. The transmission loss is measured in decibels (dB) and is given by Equation 1.7.

$$\tau = \left| \frac{p_t}{p_i} \right|^2 \tag{1.6}$$

$$TL = -10log(\tau) \tag{1.7}$$

1.4.1 Acoustics of vegetal wools

In this thesis, the study of the acoustic performance of vegetal wools is limited to the scale of the material. Therefore, the characterization of acoustic performance will focus on the sound absorption properties of the hemp wools. Moreover, vegetal wools are not good insulators when used alone, outside of a wall system, and characterization of their transmission loss does not provide relevant results.

Previous studies have characterized the sound absorption coefficient of vegetal wools. In the studies from Glé (GLE13), the acoustic performance of multiple vegetal wools was characterized, including hemp, flax, jute wools, varying thicknesses and production methods. Figure 1.14 presents a comparison between the sound absorption coefficient of the samples studied and their respective thickness between parentheses.

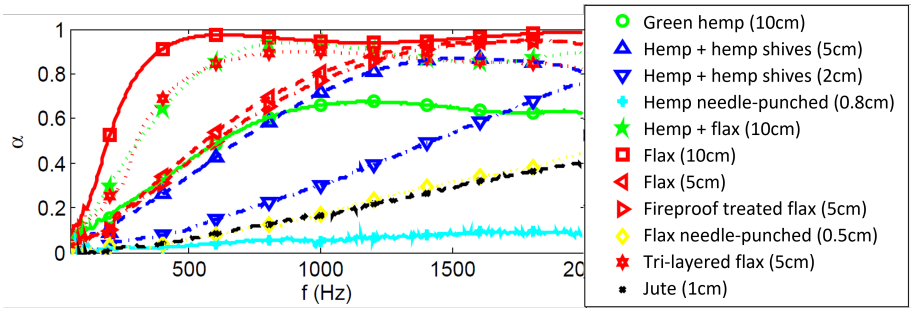

Figure 1.14: Sound absorption curves of vegetal wools (GLE13)

From these results, it can be observed that a large variety of sound absorption profiles can be obtained from vegetal wools, depending on the materials used, their thickness, and also their production method. The author highlights that a high performance can be obtained from flax, hemp or mixed formulations.

Ayadi (AYA23) also studied vegetal wools composed of different vegetal fibers. The author obtained the sound absorption coefficient of posidonia, alfa and hemp wools, with different thickness, apparent density and compression rates.

In another study, Piégay (PIE19) also characterizes the sound absorption coefficient of different vegetal wools. Figures 1.15a and 1.15b present the curves obtained from hemp and flax wools, respectively, with varying thickness and apparent density.

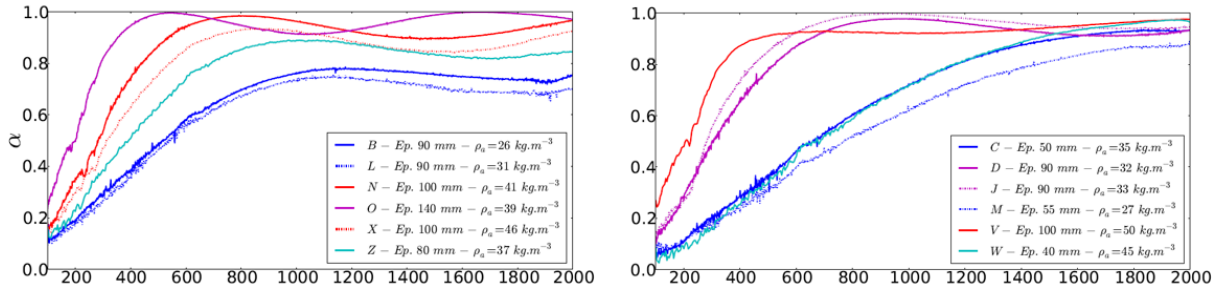

(a) (b)

Figure 1.15: Sound absorption coefficient (PIE19): (a) Hemp wools; (b) Flax wools

It can be observed once again that the thickness plays an important role in the sound absorption performance of vegetal wools, since the thicker samples presented a shift of the peak absorption towards the lower frequencies, and maintained a higher absorption in the whole range of frequencies presented. Furthermore, an influence of the apparent density is also observed.

Therefore, as seen in Section 1.2.2, there is a link between the microstructure and the acoustic performance of vegetal wools, and this microstructure present a high variability due to the heterogeneity of formulations, morphologies and dimensions.

1.4.2 Modeling of acoustic performance of vegetal wools

Aiming to understand, predict or simulate the acoustic behavior of fibrous and porous materials, two modeling approaches have been developed along the years: based on the equivalent fluid theory or on homogenization methods. The former will be detailed in this Section, whereas the latter will be presented in Section 1.4.4.

The acoustic wave that penetrates the structure of the materials sets the air saturating the pores in motion. The equivalent fluid theory assumes the solid phase of the materials as a rigid body, thus eliminating mechanical dissipation phenomena. As a result, the

dissipation of the acoustic wave's energy is based on visco-thermal dissipation phenomena corresponding to the friction of the fluid on the material's skeleton (solid phase), as well as heat exchange between the fluid phase and the solid phase. Modeling approaches based on equivalent fluid theory introduce parameters that describe these viscous and thermal dissipation effects that occur in the pores, such as the dynamic density (ρ) and the dynamic bulk modulus (K), respectively. Both parameters are considered to be intrinsic to the material.

During the time, to refine the models and increase accuracy, the number of parameters used to describe the equivalent fluid increased. Figure 1.16 presents the evolution of these models, and the number of parameters required (JAO25).

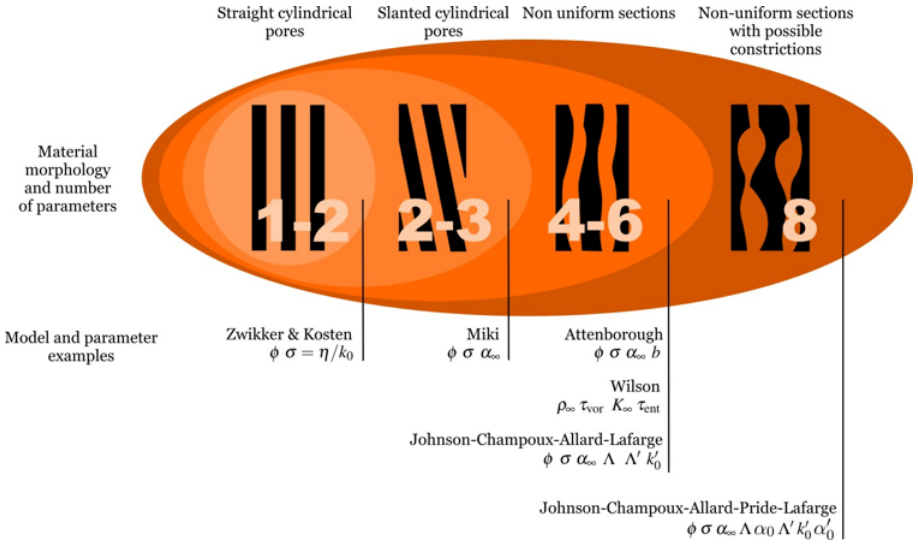

Figure 1.16: Pore geometry models evolution over time (JAO25)

Previous studies have shown that the Johnson–Champoux–Allard–Lafarge (JCAL) (ALL94; CHA91; JOH87; LAF97) model can describe well the sound absorption performance of vegetal wools, using a reasonable amount of parameters that can be obtained through direct characterization (AYA23; GLE13; PIE19). These parameters are described in the following.

- Porosity (ϕ): Presents the relationship between the volume of voids and the total volume of a sample, as shown in Section 1.2.2
- Airflow resistivity (σ): It describes the resistance provided by the material to the air passage through it. It can be measured experimentally using an air resistivity-meter, or by an approximation of the imaginary part of the dynamic density at low frequencies, as shown in Equation 2.

$$\sigma = \lim_{\omega \to 0} -\omega Im(\rho) \tag{1.8}$$

- Tortuosity (α_∞): It defines the disorder of the system and can be represented by the path that the sound waves need to percolate through the material, instead of passing in a straight line through it. The minimum value of this parameter is 1.00. It can be measured directly with an ultrasonic tortuosity-meter or determined using Equation 3.

$$\alpha_\infty = \frac{\phi}{\rho_0}\left(Re(\rho) - \sqrt{Im(\rho)^2 - \frac{\sigma^2}{\omega^2}}\right) \tag{1.9}$$

- Characteristic viscous length (Λ): It describes the viscous effects that occur in porous materials, at medium and high frequencies. This length is expressed in meters and is considered to be approximately the size of the radius of the pore constrictions. It can be schematically represented by Figure 1.17 and calculated using Equation 4.

$$\Lambda = \frac{\alpha_\infty}{\phi}\sqrt{\frac{2\eta\rho_0}{\omega Im(\rho)}\left[\frac{\alpha_\infty\rho}{\phi} - Re(\rho)\right]} \tag{1.10}$$

- Characteristic thermal length (Λ'): This parameter characterizes the thermal effects in the material at medium and high frequencies and can be schematically represented by the radius of the larger pores (Figure 1.17). It is therefore larger than Λ. It is calculated using Equation 5.

$$\Lambda' = 2\sqrt{\frac{\kappa}{C_p\rho_0\omega}\left[-Im\left[\left(\frac{\gamma P_0 - \phi K}{\gamma P_0 - \gamma\phi K}\right)^2\right]\right]^{-1}} \tag{1.11}$$

- Thermal permeability (k_0'): It describes the thermal exchanges between the frame and the fluid at low frequencies. It can be assimilated to how easily the material is penetrated by a thermal flux. It can be calculated using Equation 6.

$$k_0' = \frac{\phi\kappa}{C_p\rho_0\omega}\Big/\sqrt{-Re\left[\left(\frac{\gamma P_0 - \phi K}{\gamma P_0 - \gamma\phi K}\right)^2\right]} \tag{1.12}$$

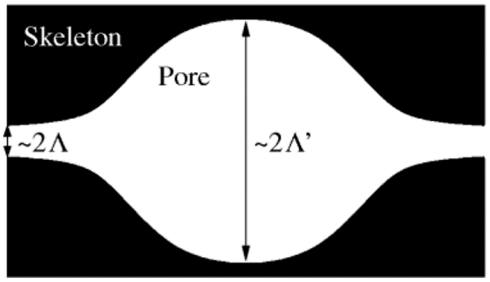

Figure 1.17: Schematic representation of the characteristic viscous and thermal lengths (apmr.matelys.com)

The equations presented for α_∞, Λ, Λ' and k_0' constitute an indirect characterization approach and are obtained by the analytical inversion of ρ and K given by the JCAL model (JAO20), which are given by Equations 7 and 1.14.

$$\rho = \frac{\rho_0\alpha_\infty}{\phi}\left[1 - j\frac{\sigma\phi}{\rho_0\alpha_\infty\omega}\sqrt{1 + j\frac{4\eta\alpha_\infty^2\rho_0\omega}{\Lambda^2\sigma^2\phi^2}}\right] \tag{1.13}$$

$$K = \frac{\gamma P_0}{\phi}\left[\gamma - (\gamma-1)\left(1 - j\frac{\phi\kappa}{\Theta_0 C_p\rho_0\omega}\sqrt{1 + j\frac{4\Theta_0^2 C_p\rho_0\omega}{\kappa\phi^2\Lambda'^2}}\right)^{-1}\right]^{-1} \tag{1.14}$$

From the values of ρ and K, the characteristic impedance (Z_c) and the wave number (k) of the material are calculated using Equations 1.15 and 1.16. With them, the surface

impedance (Z_s) and the reflection coefficient (R) are calculated, as shown in Equations 1.17 and 1.4, respectively.

$$Z_c = \sqrt{\rho K} \tag{1.15}$$

$$k = \omega \sqrt{\frac{\rho}{K}} \tag{1.16}$$

$$Z_s = -jZ_c \tan(ke)^{-1} \tag{1.17}$$

$$R = \frac{(Z_s - Z_0)}{(Z_s + Z_0)} \tag{1.18}$$

With the value of the reflection coefficient, the sound absorption coefficient is calculated as presented by Equation 1.5 in Section 1.4.

In summary, with the parameters that describe visco-inertial (ρ) and thermal (K) dissipation effects in the equivalent fluid, obtained experimentally through the impedance tube test, it is possible to calculate the characteristic parameters that describe the pore network of the material. With these characteristic parameters, the dynamic density and the bulk modulus given by Equations 7 and 1.14 can be calculated and used to obtain the sound absorption coefficient, which can be validated by comparing it with experimental values.

1.4.3 Compression model

The sound absorption is sensible to the apparent density of the materials. Frequently during the manufacturing of products, variations in apparent density may occur. This is especially relevant for insulation materials, since many of their functional properties depend on the apparent density, including their sound absorption. To overcome this problem, a compression model can be used to standardize all samples to the same apparent density.

This model was presented by Castagnède (CAS00). It consists of determining five of the six parameters used in the JCAL model (porosity, air resistivity, tortuosity, characteristic viscous and thermal lengths), while considering a 1D or a 2D compression of the samples. The factor (n) is used to define the compression rate of the material, as the ratio between the thickness of the material before (h_i) and after (h_n) being compressed (Equation 1.19).

Considering a 1D compression, the parameters can be calculated as shown in Equation 1.20 to 1.24. The sixth parameter used in the JCAL model (static thermal permeability) can be approximated by Equation 1.25 (LEI18).

$$n = \frac{h_i}{h_n} \tag{1.19}$$

$$\phi_n = 1 - n(1 - \phi) \tag{1.20}$$

$$\sigma_n = n\sigma \tag{1.21}$$

$$\alpha_{\infty n} = 1 - n(1 - \alpha_\infty) \tag{1.22}$$

$$\Lambda_n = \frac{\Lambda}{\sqrt{n}} + \frac{r}{2}\left(\frac{1}{\sqrt{n}} - 1\right) \tag{1.23}$$

$$\Lambda'_n = \frac{\Lambda'}{\sqrt{n}} + \frac{r}{2}\left(\frac{1}{\sqrt{n}} - 1\right) \tag{1.24}$$

$$k'_0 = \frac{\phi \Lambda'^2}{8} \tag{1.25}$$

In these Equations, the term r is the fiber radius, that is estimated by the Tarnow model, which will be presented in Section 1.4.4.

Castagnède et al. (CAS00) presented measurements for the sound absorption coefficient of compressed and uncompressed fibrous materials for the automotive industry. They noted that when a fibrous material is compressed, the absorption coefficient has a strong decrease, which was attributed to the reduction in thickness over changes in the acoustic parameters. In a subsequent study, Castagnède et al. (CAS01) indicate that the agreement between the experimental and numerical results is good for porosity and characteristic lengths, approximate for tortuosity and poor for the air resistivity.

Campolina et al. (CAM12) have shown that this compression model has higher error with higher compression rates. They have measured the transmission loss of glass wool associated with an isotropic plate, in the condition of uncompressed and compressed glass wool, using a compression rate of 1.25 and 2.0. They observed a maximum error of 3 dB between the experimental and theoretical values when the compression rate was 1.25 and an error of 5 dB when the compression rate was 2.0.

Ayadi et al. (AYA23) used the compression model to correct and compare the density of vegetal wools, with a compression rate between 1.0 and 2.17. The authors found a general good agreement between the model and the experimental results for porosity and airflow resistivity.

In another study (LEI18), glass wool and melamine foam were compressed with compression rates of up to 9.0. Based on this, the authors proposed new relationships for the acoustic parameters of the compressed material, considering the influence of the fiber orientation. They compare the results obtained experimentally, numerically with their model, and numerically with the Castagnède model. Their model presented a good agreement in all ranges of compression rates, while the Castagnède model diverges at high compression rates (especially above 2.0).

1.4.4 Homogenization modeling methods

The modeling of the acoustic performances of vegetal wools using the fluid equivalent approach has been proven to provide satisfactory results, especially through the JCAL model. However, this approach is limited to the description of the pore geometry, and information about the solid frame is not exploited.

An alternative approach is to use a micro–macro strategy based on homogenization methods. Instead of replacing the pore medium with an equivalent fluid that describes the viscous and thermal dissipation effects on the material, the micro-macro homogenization methods define a homogeneous medium at a microscopic scale that is equivalent to the heterogeneous medium at the macroscopic scale. This technique allows for the link between micro-scale properties with macro-scale performances of the material (PER06; PIE19).

To do this, the creation of a representative elementary volume (REV) is needed. This element is used for the reconstruction of the material and has the same global mechanical behavior and the same limit conditions as the macroscopic heterogeneous medium (CER05). For modeling the properties of porous insulation materials, the homogenization method of periodical structures is frequently used (BEN78). This method allows for

the description of the laws that govern the acoustic dissipation phenomena at the macroscopic scale, based on the equations governing viscous flows and heat transfer in the fluid at the pore scale (the Navier-Stokes and heat equations, respectively) (PIE19).

However, while homogenization methods offer a detailed micro–macro description, this level of complexity typically requires numerical simulations. Therefore, other homogenization approaches have been developed based on the simplification of the homogenization method of periodical structures, proposing analytical relationships between the macro properties of materials and microstructural parameters. Specifically for fibrous materials, two models that follow these approaches can be highlighted, which are the Tarnow (TAR96) and Umnova (UMN09) models.

The Tarnow model proposes an analytical relationship between airflow resistivity (a macrostructure parameter), fiber radius and porosity (microstructure parameters). The assumptions of rigid, cylindrical, parallel fibers with a uniform radius r, placed uniformly or randomly in the space, with the flux parallel or perpendicular to the fibers are made. The application of this model in vegetal wools has been validated by Piégay et al. (PIE18).

These hypothesis create 4 scenarios, 2 different fiber disposal (uniform or random) and 2 flux (parallel or perpendicular). Each scenario was studied by Glé (GLE13) for the case of vegetal wools. The author shows that the configuration of random fibers with flux perpendicular to the fibers is ideal for vegetal wools. The relationship between the fiber radius (R_f), airflow resistivity and the material's porosity is given by Equation 1.26.

$$R_f = \sqrt{\frac{4\eta(1-\phi)}{\sigma[0.64ln(\frac{1}{1-\phi}) - 0.737 + (1-\phi)]}} \tag{1.26}$$

The value of fiber radius obtained through this approach is, however, an estimation, and does not correspond exactly to the fiber's real radius. Furthermore, hemp fibers do not have uniform cross-sections, but rather a distribution of fiber radius, as shown in Section 1.2.2. In spite of that, the fiber radius estimation can be used for comparison between formulations to identify changes in the material's microstructure.

The Umnova model also provides an analytical relationship between the airflow resistivity, the fiber radius and the porosity of the fibrous material. However, this model takes into consideration the slip effects that occur on the pore surfaces when the characteristic pore size becomes comparable to a saturating gas molecular mean free path (l_{mean}). This parameter depends on the fluid viscosity, density and temperature. For air at normal conditions, it is about 60 nm. Since the pore size in hemp wools are significantly higher than 60 nm, the air is in the continuum regime, and the slip effects can be neglected.

In this case, assuming an airflow perpendicular to the fibers, the Umnova model provides a relationship between the fiber radius, airflow resistivity and air viscosity, given by Equation 1.27.

$$R_f = \sqrt{\frac{16\eta(1-\phi)}{\sigma(-2ln(1-\phi) - 2\phi - \phi^2)}} \tag{1.27}$$

1.5 Thermal performance

The thermal properties of materials play a crucial role in their performance as insulation. These properties determine how the material exchanges heat with its surroundings, particularly under conditions where the system is not in thermodynamic equilibrium. Understanding these behaviors is essential to evaluate the efficiency of vegetal wools in regulating temperature, contributing to energy savings, and ensuring comfort in built environments.

The three types of heat transfer are the radiation, convection and conduction. Radiation is defined by the heat transfer through electromagnetic waves and it depends on the material's emissivity and the surface's temperature. Convection is the transfer of heat caused by the movement of a fluid, such as air or water. Conduction is the heat transfer phenomenon that occurs within a solid or between solids due to a temperature difference. Since the object of study in this thesis is the vegetal wools in the material scale, it is the properties related to the thermal insulation of materials that will be taken into account.

Based on previous studies (LAN97; MOJ25), each mode of heat transfer can be represented as a specific thermal conductivity (λ_{cond}, λ_{conv}, λ_{rad}), and the sum of the three contributions gives an equivalent thermal conductivity (λ_{eq}) of the material, as shown in Equation 1.28.

$$\lambda_{eq} = \lambda_{cond} + \lambda_{conv} + \lambda_{rad} \tag{1.28}$$

Effectively, the experimental characterization of materials determine their equivalent thermal conductivity. There are two main families of techniques used to assess this property: those based on steady-state conditions and those relying on transient heat flux. In the steady-state case, both the temperature distribution and the heat flux remain constant over time, which requires longer measurement times since thermal equilibrium must first be reached. In contrast, in transient methods the heat flux and temperature vary over time following a thermal disturbance, and the rate of temperature change is analyzed.

1.5.1 Thermal conductivity of vegetal wools

In previous studies, the effective thermal conductivity of vegetal wools has been assessed. Some examples have been extracted from the literature and are reported in Table 1.4.

Table 1.4: Thermal conductivity of vegetal and mineral wools

Base material	Apparent density ($kg.m^{-3}$)	Heat flux state	Thermal conductivity ($W.m^{-1}.K^{-1}$)	Reference
Hemp	30.2	Steady	0.049	KOR11
	33.1	Steady	0.044	KOR16
	45.4	Transient	0.044	PIE20
	67.2	Transient	0.055	PIE20
	25-40	-	0.038-0.043	LEK15
Flax	32.1	Steady	0.043	KOR11
	32.1	Steady	0.044	KOR16
	35.0	Transient	0.040	PIE20
	66.3	Transient	0.050	PIE20
Mineral	14.9	Transient	0.039	VOL15
	70-170	Transient	0.036-0.041	JER12
	40-200	-	0.033-0.040	SCH16
Glass	15-75	-	0.031-0.037	SCH16

Overall, for hemp and flax wools, the values are found to be around 0.04 to 0.05 $W.m^{-1}.K^{-1}$ (KOR11; KOR16; PIE20). These thermal conductivities are very low, fitting one of the main purposes of the material as a thermal insulator. These values depend on a series of factors such as the materials they are made of, the apparent density of the samples, the method of characterization, and the conditions of testing.

Since the vegetal wools are composed of vegetal and thermoplastic fibers, their thermal performance are directly linked to the nature of these materials. For instance, the solid phase of hemp has a thermal conductivity of 0.72 $W.m^{-1}.K^{-1}$, and the flax 0.66 $W.m^{-1}.K^{-1}$ (PIE20). Authors have also shown that the thermal conductivity of the solid phase can vary if the fiber is placed longitudinally or transversely to the heat flux (EL-16), which can be explained by the anisotropy structure of the skeleton of the fibers, with the presence of the lumen (air) inside the fiber.

Thermoplastic fibers present even lower values of thermal conductivity, varying between 0.11 and 0.22 $W.m^{-1}.K^{-1}$ for PP, 0.25 and 0.32 $W.m^{-1}.K^{-1}$ for LDPE, 0.35 and 0.39 $W.m^{-1}.K^{-1}$ for HDPE and about 0.111 $W.m^{-1}.K^{-1}$ for PLA (CHA20; FAR16; PAT20). A summary of the material and their solid skeleton thermal conductivity is shown in Table 1.5.

Table 1.5: Solid skeleton thermal conductivity of bio-based materials and polymers

Material	Solid skeleton thermal conductivity ($W.m^{-1}.K^{-1}$)	Reference
Hemp	0.72	PIE20
Hemp (transversal)	0.44	EL-16
Hemp (longitudinal)	0.88	EL-16
Flax	0.66	PIE20
PP	0.11-0.22	PAT20
LDPE	0.25-0.32	CHA20
HDPE	0.35-0.39	CHA20
PLA	0.111	FAR16

Regarding the role of apparent density, it presents a particular behavior in the heat exchange of highly porous materials. This effect can be observed in Figure 1.18 (LAN04). In this example, the thermal conductivity of a mineral wool is shown as a function of the material's apparent density. It can be observed that, as density decreases, the thermal conductivity also decreases, reaching a minimal point. Beyond this point, further reductions in density lead to a rapid increase in thermal conductivity.

In fact, if we account for both the conduction and the radiation effect, the effective thermal conductivity of porous materials can be divided into two distinct regimes. At densities above the minimum point, heat transfer is predominantly governed by conduction through the solid phase. As the density of the material decreases, the proportion of solid matter is reduced, leading to a corresponding decrease in the effective thermal conductivity. However, below this minimum point, further reductions in density result in increasingly open pores, which reduces the material's ability to block thermal radiation. As a consequence, the effective thermal conductivity increases drastically. Thus, to optimize this effective thermal conductivity of vegetal wools, their performance as a function of the apparent density of the material needs to be studied.

The same effect is observed in vegetal wools. Piégay (PIE19) determined experimentally the effective thermal conductivity of vegetal wools composed of different vegetal fibers and apparent densities. Then, the relationship between thermal conductivity and apparent density was modeled using a modeling method considering the effects of heat transfer through conduction and radiation using the approaches of Bankvall (BAN73) and Rosseland-Deissler (DEI64). These results are presented in Figure 1.19.

Depending on the nature of the material, the minimum value was observed in samples with porosity close to 97% to 98%. At lower porosities, the effective thermal conductivity increases linearly with the increase in thermal conductivity. At higher porosities, the

radiation effect increase and the effective thermal conductivity also increases. Therefore, the range of porosity observed in these results are a good indicator of the optimal apparent density for the vegetal wools.

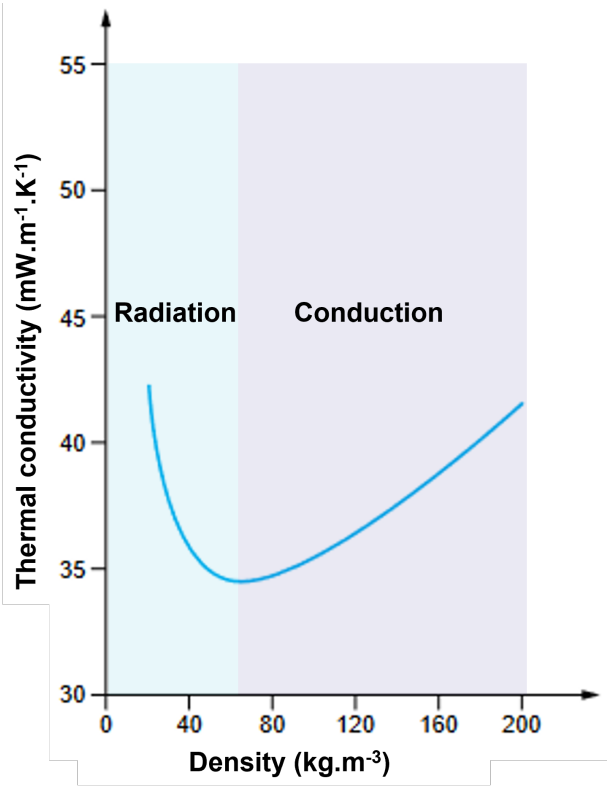

Figure 1.18: Typical curve of effective thermal conductivity at low density (LAN04)

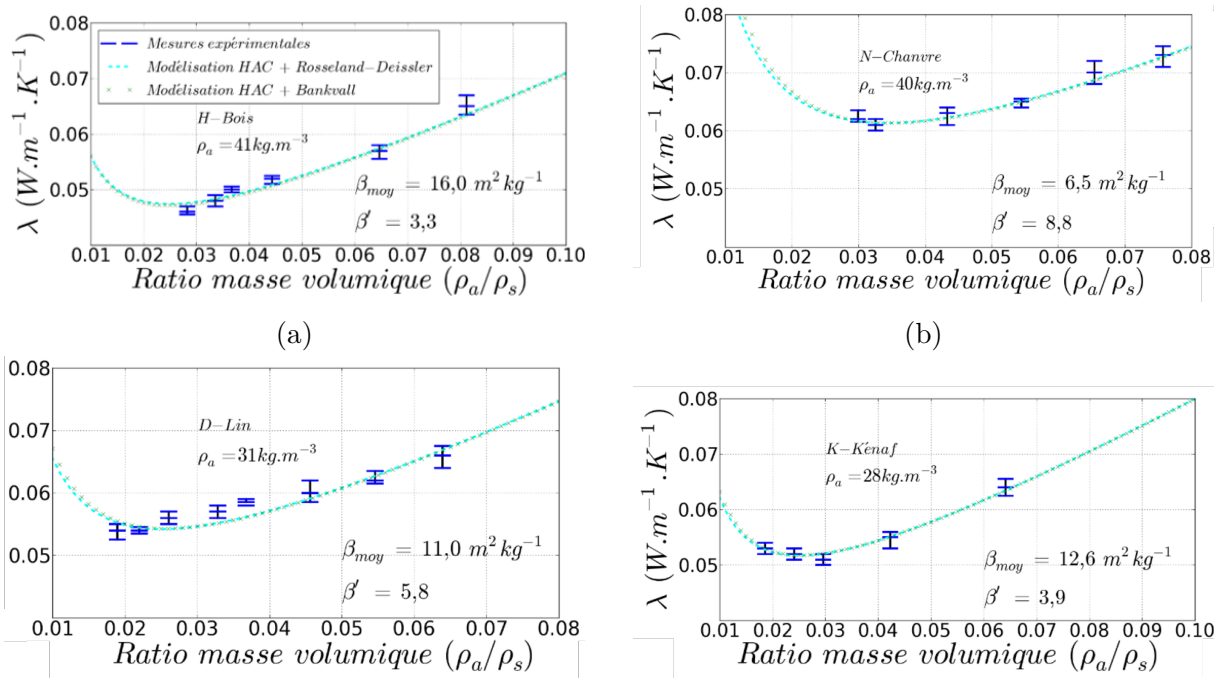

Figure 1.19: Thermal conductivity of vegetal wools as a function of the apparent density (PIE19): (a) Wood; (b) Hemp; (c) Flax; (d) Kenaf

.

1.5.2 Hygrothermal performance

Another factor that has to be considered when evaluating heat transfer in materials, is their water content. The thermal conductivity of a material can increase significantly if its pores are saturated with water, instead of air (JER12). In the case of bio-based materials, their hygroscopic nature is attributed to their chemical composition and porous microstructure. Cellulose and hemicellulose have a high amount of hydroxyl groups that easily bond with water, particularly in their amorphous regions (ISL25; MOU19). The water molecules enter and break inter-molecular hydrogen bonds, increasing the inter-molecular distance of the cellulose chains, causing fiber swelling (ISL25; MOU19). This allows the formation of nano or multilayers of water molecules in this space.

The structure of the fiber wall favors the water molecules adsorption by the pores, which then penetrates into the fibers. The open and high porosity, creates low vapor resistance, which means that the water molecules can easily travel through the material, and help with the regulation of the interior's humidity (COL11; VOL15).

Depending on the relative humidity (RH) of the air, a certain amount of water vapor will be adsorbed by the fiber's surface. At low RH, typically between 5% and 35-40%, water molecules are adsorbed as monomolecular layer. As RH increases, a multimolecular water layer is formed, and at high RH, capillary condensation occurs (COL11). This process is illustrated in Figure 1.20.

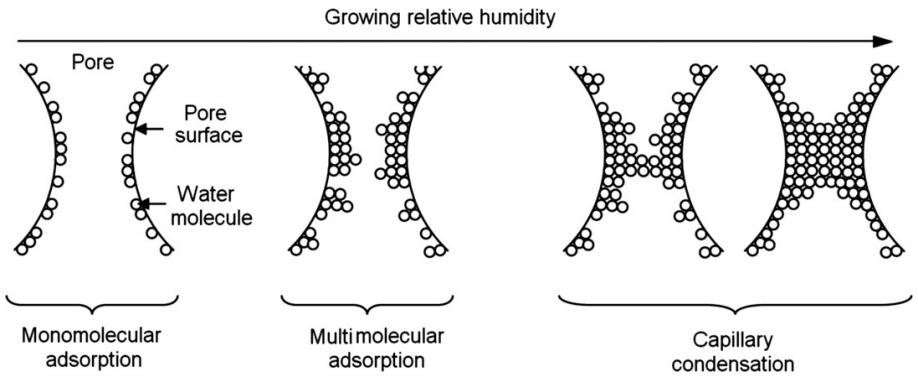

Figure 1.20: Water adsorption process, as the relative humidity increases (COL11)

In general, the equilibrium moisture content of hemp and flax fibers is around 5-10%, but depends on the environment humidity (ISL25; MOU19). Stamboulis et al. (STA00; STA01) reported a water content on flax fibers of 3%, 15%, and 24% when exposed to 20%, 66%, and 93% RH environments, respectively. Moudood et al. (MOU19) reported a moisture content of approximately 2.3%, 3.5%, 6.2%, 7.9% and 14.3%, for flax fiber in environments of 10%, 30%, 50%, 70% and 90% RH, and that only one hour is needed to achieve an equilibrium of water content, independently of the RH of the environment (MOU19).

The relationship between the relative humidity of the environment and the water content of a material is usually analyzed through curves of water sorption. Volf et al. (VOL15) presented these curves for multiple natural fibers and for a mineral wool sample as a reference (Figure 1.21). Noticeably, the moisture content inside the fibers depends on the nature of the fiber. Among the bio-based samples, straw bale, untreated sheep wool and wood fibers presented the highest absorption of water, whereas flax and hemp presented lower values. However, all of them presented significantly higher absorption than the mineral material, which highlights how the material interacts with the environment for humidity regulation, but also the necessary attention to small variations in ambient humidity during experimental analyses, which can lead to significant changes in the amount of water absorbed by natural fibers.

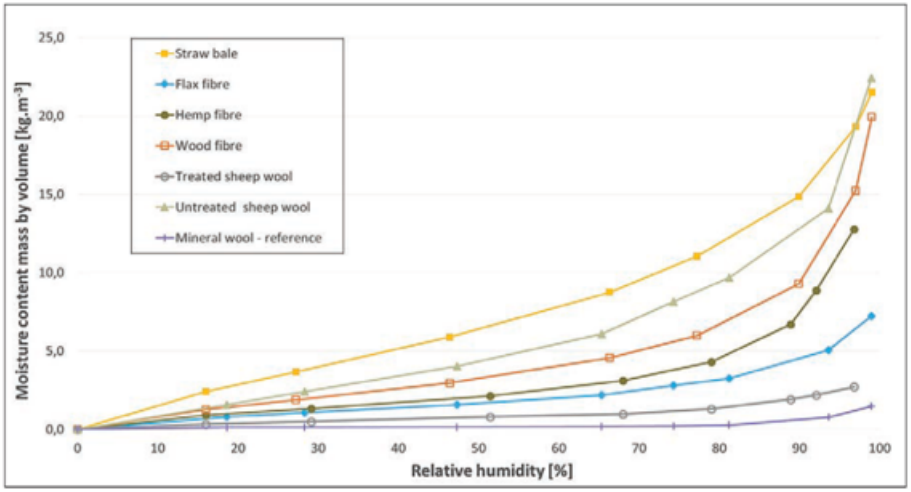

Figure 1.21: Sorption curve of bio-based fibers and mineral wool (VOL15)

Korjenic et al. (KOR11; KOR16) presented the influence of water content on the thermal conductivity of jute (sample 1), flax (sample 2) and hemp wools (samples 3 to 9). Figure 1.22 presents the sorption curves of these samples. Figures 1.23 and 1.24 present the relationship between thermal conductivity of vegetal wools, moisture and temperature, respectively. From the sorption curves, it is seen that the hemp wool samples were those with lower water content absorbed. At a moisture level below 5%, the thermal conductivity values are constant. With higher water content, the thermal conductivity increases significantly. The role of temperature is also highlighted, since higher temperatures led to an increase in the thermal conductivity. This reinforces the need to ensure stable environment conditions during experimental testing.

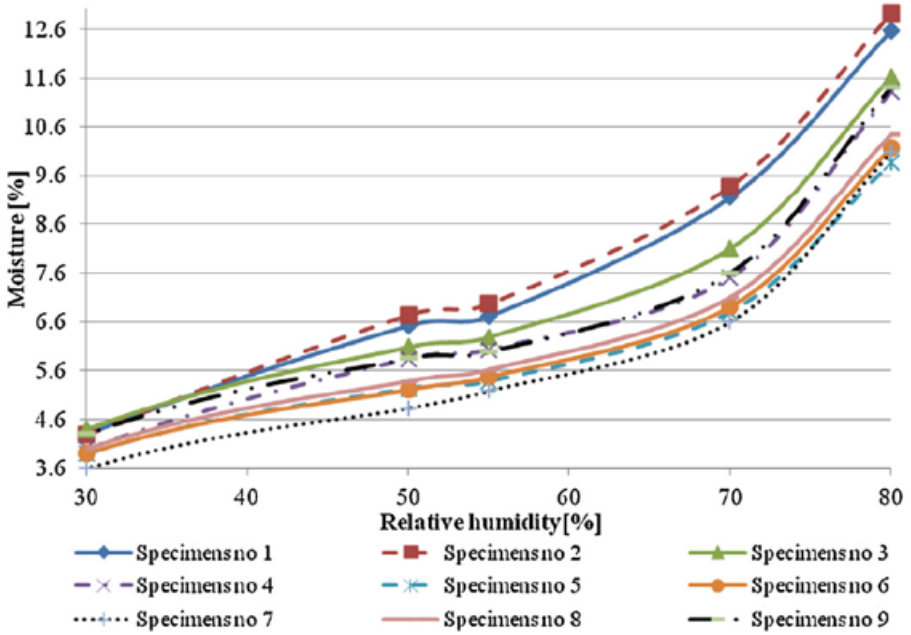

Figure 1.22: Sorption curves of vegetal wools (KOR16)

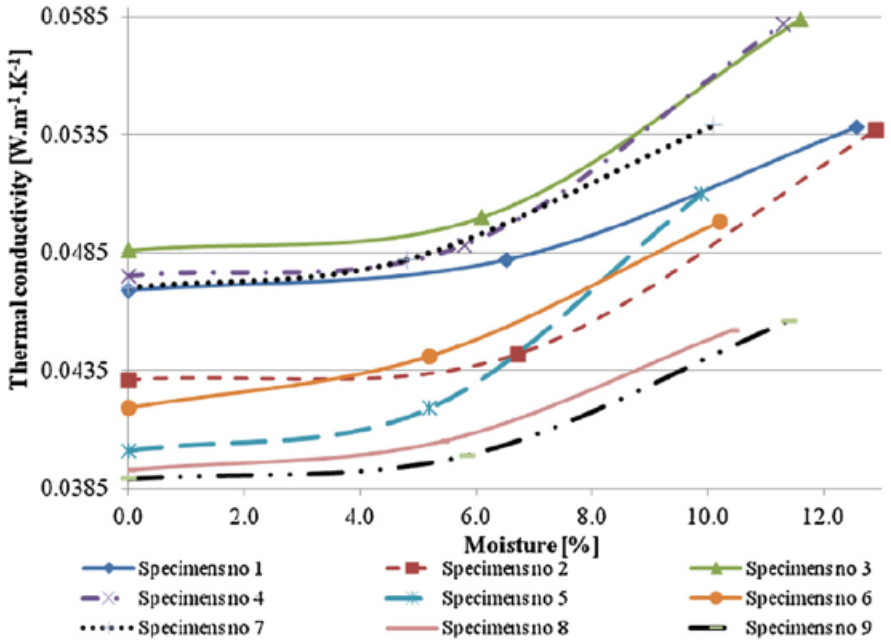

Figure 1.23: Relationship between thermal conductivity and water content of vegetal wools (KOR16)

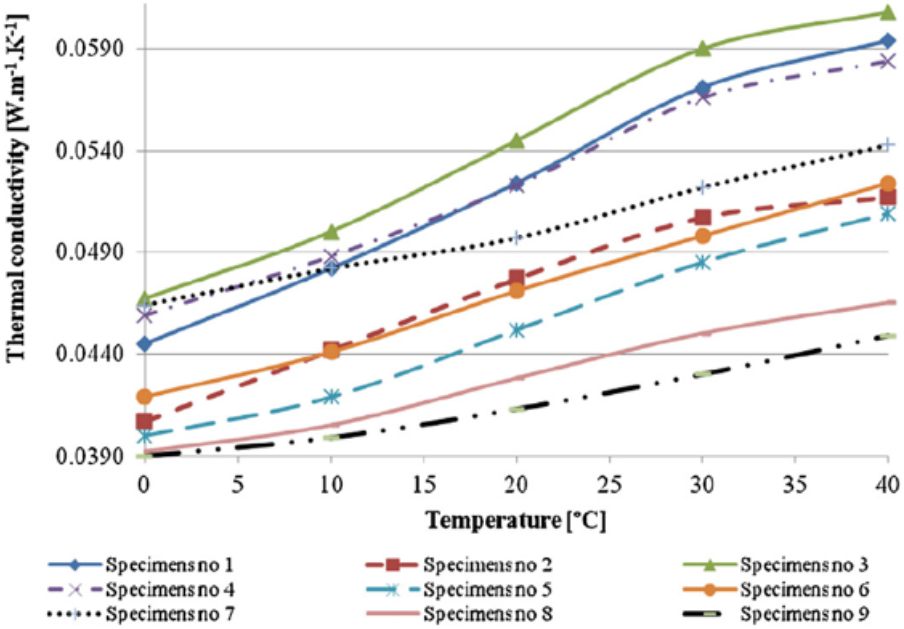

Figure 1.24: Relationship between thermal conductivity and temperature of vegetal wools (KOR16)

1.6 Enhancement of fire behavior from lignocellulosic fibers

Despite the excellent capacity of the vegetal wool in absorbing sound and isolating heat, this material faces a major challenge, which is their fire behavior. As a bio-based material, the vegetal wools are flammable, and their use can be limited if the fire safety requirements are not met. Therefore, in this section, the key concepts of combustion and thermal degradation of lignocellulosic fibers are described. In addition, the types of flame retardants and their mechanisms of flame retardancy to reduce the flammability of lignocellulosic fibers are presented.

1.6.1 Combustion reaction

Combustion is a chemical reaction between a fuel, usually referred to as the reducing agent, and an oxidant, also known as the oxidizing agent, which is usually the oxygen present in the air. For this reaction to happen, it needs heat. If the temperature of the fuel reaches the auto-ignition temperature, it ignites spontaneously and the combustion reaction starts. Alternatively, the fuel can also ignite at a lower temperature, known as flash point, when exposed to an external source of intense energy, e.g. spark (LAO09). The combustion reaction can be visually described by the fire triangle, demonstrated in Figure 1.25.

The triangle illustrates the three essential elements required for a combustion reaction: a heat source, a fuel, and the air. As long as these three elements are present in the system, the reaction continues. The heat source can be external to the system, transferred by radiation, convection or conduction, or internal if originated from the exothermic reactions caused by the combustion. In this thesis, the fuel will be considered, and often referred to, the lignocellulosic fibers or thermoplastic polymers.

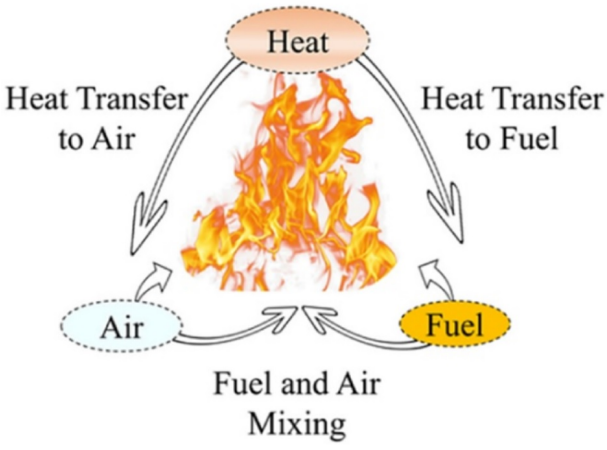

Figure 1.25: Representation of fire triangle (TAI22)

1.6.2 Thermal degradation of lignocellulosic materials

Combustion of solid fuels is not a single reaction but a combination of processes. As the material is heated, pyrolysis produces gases, vapors, and char, which are then oxidized in the presence of oxygen. These steps of thermal decomposition will be defined and explored in this Section, with a focus on lignocellulosic materials.

Thermal degradation of lignocellulosic materials can occur in the presence and absence of the oxidizing agent. The process of pyrolysis occurs in the absence of oxygen. During

pyrolysis of bio-based materials, the chemical bonds break down, releasing volatiles (i.e. CO and CO_2) and leaving char, which is a carbon-rich residue. In contrast, oxidation occurs when the fuel reacts with oxygen in the air. Depending on the temperature of the thermal decomposition, the rate of pyrolysis is very high, and oxidation occurs only in the gas phase (LAO09).

The thermal degradation of bio-based materials can be evaluated by thermogravimetric analysis (TGA), in both inert (pyrolysis exclusive) and reactive (pyrolysis and oxidation) atmospheres. In inert atmospheres, decomposition occurs in a single step, between 250°C and 400°C, as shown in Figure 1.26. At the end of the test, the remaining mass is referred as residue, consisting of a carbon-rich structure known as char. In the presence of oxygen during TGA analysis a second decomposition step is observed at higher temperatures, corresponding to the oxidation of char (DOR14; KAC11). Figure 1.27 shows the thermal degradation curve for hemp fiber (black straight lines) from a TGA test performed in an oxidative environment.

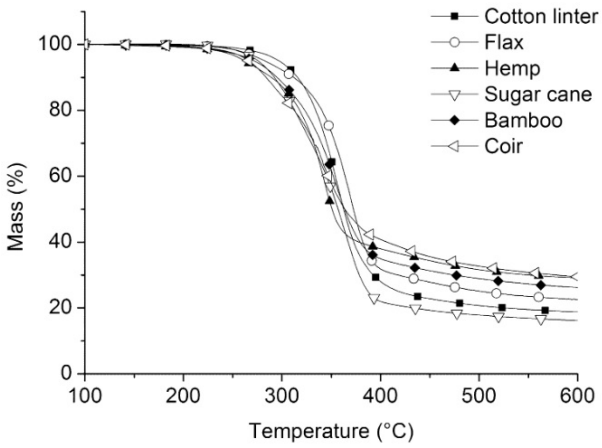

Figure 1.26: Mass loss result of different biomasses in inert atmosphere (DOR14)

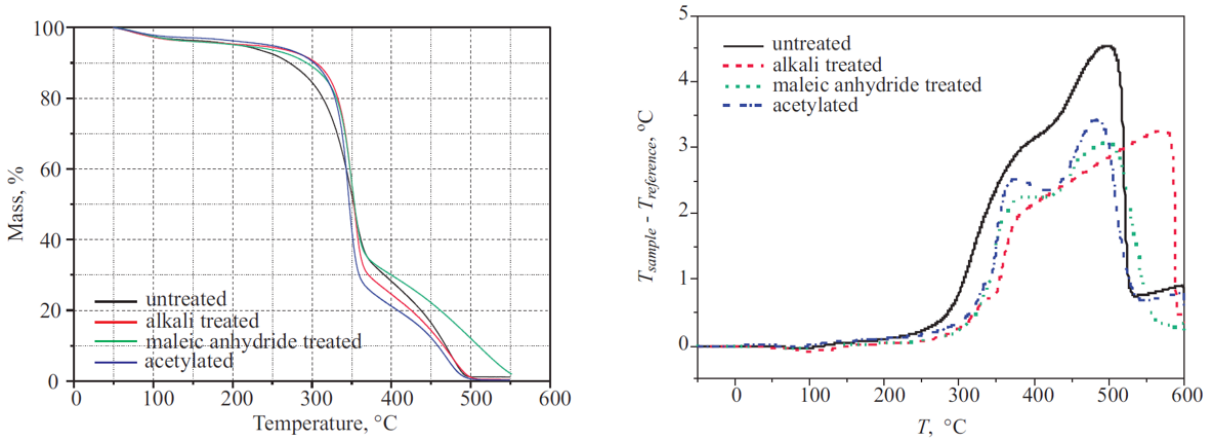

(a) (b)

Figure 1.27: Thermal degradation of hemp fibers in oxidative environment (KAC11): (a) TGA; (b) DTG

.

Thermal degradation is related to the chemical composition of bio-based materials, so mainly from cellulose, hemicellulose and lignin (Section 1.2.1). Their mass loss and Derivative Thermogravimetry (DTG) curve is presented in Figure 1.28.

During thermal degradation, cellulose exhibits a rapid mass loss within a narrow temperature range (typically between 315°C and 400°C), characterized by a sharp peak in the Derivative Thermogravimetry (DTG) curve (DOR14; PAS12; YAN07). At 600°C in a non-oxidative atmosphere, the amount of remaining charred residue is low, typically around 10% of the initial mass (CHE12; DOR14).

Compared to cellulose, hemicellulose undergoes thermal degradation at lower temperatures (between 220°C and 315°C), due to its amorphous and branched structure and lower molecular weight (COS17; DOR14; YAN14; YAN07). The mass of charred residue found at 600°C in an inert atmosphere represents approximately 30% of the initial mass (CHE12; DOR14).

Lignin, on the other hand, has an amorphous and highly complex chemical structure that is mainly aromatic (YAN14). Its thermal degradation occurs over a broader temperature range, from 150°C to 700°C, in several steps (COS17; DOR14; ZHA14).

Since hemp is mainly composed of cellulose and hemicellulose (Table 1.1 in Section 1.2.1), its thermal degradation will be mainly influenced by their behavior.

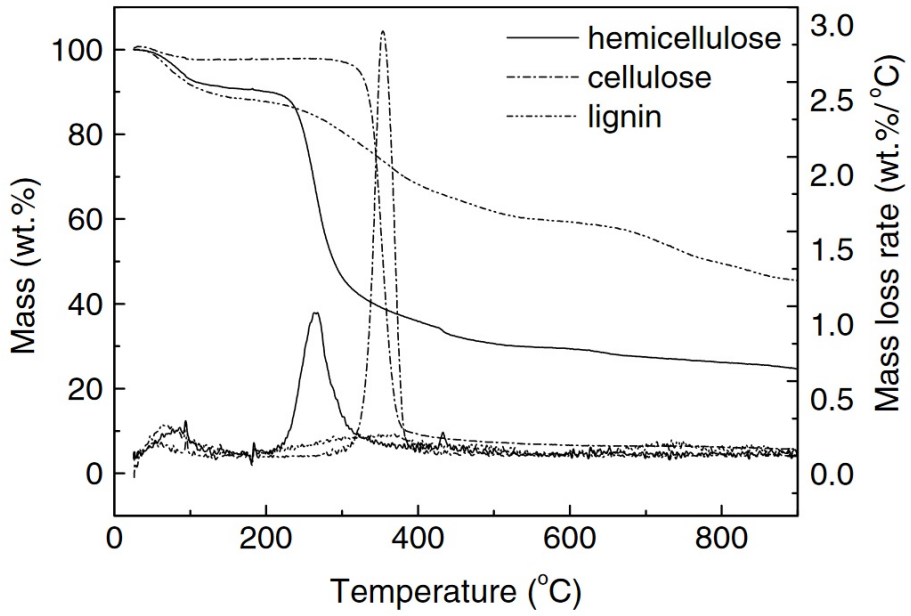

Figure 1.28: Pyrolysis of cellulose, hemicellulose and lignin (YAN07)

Overall, thermogravimetric analysis of bio-based materials provides insight into the temperature range over which thermal degradation occurs and quantifies the amount of residual char formed. Moreover, it is a tool for the evaluation of the mode of action of flame retardant treatments, which will be presented in Section 1.6.6.

1.6.3 Fire reaction assessment

The fire behavior of building materials is classified according to the European Euroclass system, as defined by the standard EN 13501-1 (AFN18). Depending on the material's fire reaction, it is classified from A1 and A2 (non combustible) to E (highly flammable and flame-spreading) or F (not classified or tested). It also classifies the smoke production (s1, s2, s3), the presence of flaming droplets (d0, d1, d2) and the acidity of released gas (a1, a2, a3). The Euroclass classification is summarized in Table 1.6.

Table 1.6: Fire reaction classification according to Euroclass

Classification	Description
A1	Non combustible
A2	Non combustible
B	Slightly flammable
C	Flammable
D	Highly flammable
E	Highly flammable and flame-spreading
F	Not classified or tested
s1	Visibility guaranteed
s2	Lower visibility
s3	No or low visibility
d0	No dripping
d1	Persistent dripping for a short time
d2	Persistent dripping for a long time
a1	Non-acidic, non-corrosive gases and smoke
a2	Slightly acidic but corrosive gases and smoke
a3	Acidic and corrosive fumes and gases

The tests used for the Euroclass classification are the single flame source test, single burning item (SBI) test, non-combustibility test, and the determination of the gross heat of combustion (calorific value). The single flame source, or the ignitability test, (ISO 11925-2:2020 (ISO20)) is a simple test that applies a flame at a 45° angle to a 250 mm high sample for 15 or 30 seconds, illustrated in Figure 1.29. The height of the burning is measured and is part of the classification from E to B, depending on the burning zone height and the duration of the flame application.



Figure 1.29: Single flame source test (cstb.fr)

The SBI test (EN 13823:2022 (AFN22)) is an object-scale test where a sandbox burner with propane is placed in a corner of a frame beneath an exhaust system (Figure 1.30).

The reaction of the specimen to the burner is monitored instrumentally and visually, with measurements of heat and smoke release rates. These results enable the classification from D to A2. The non-combustible test (ISO 1182:2020 (ISO20)) and the determination of the gross heat of combustion (ISO 1716:2018 (ISO18)) are tests conducted on a room scale that determines whether a material qualifies for classification A1 or A2.



Figure 1.30: Single burning item test (cstb.fr)

However, most of these tests have limitations. Apart from the single flame source test, they tend to be expensive and can only be carried out in specialized facilities. If the goal is to study the fire reaction of a building material rather than obtain an official classification, alternative fire reaction tests can be performed to obtain parameters similar to those from the SBI test, for example. These alternative tests are conducted at the material scale and are more cost-effective. For assessing the fire reaction of lignocellulosic fibers and vegetal wools, the most representative test would be the mass loss cone calorimeter (MLC) test. Standardized by ISO 5660:2015 (ISO15), this test provides the heat release rate (HRR) over time, and with that multiple parameters related to the material's fire behavior is obtained, such as peak heat release rate (pHRR); the time to ignition (TTI); from the integration of the curve, total heat released (THR) and effective heat of combustion (EHC). These parameters are equivalent, but not comparable, to those obtained in the SBI test. An example of HRR curve of hemp fiber is presented in Figure 1.31.

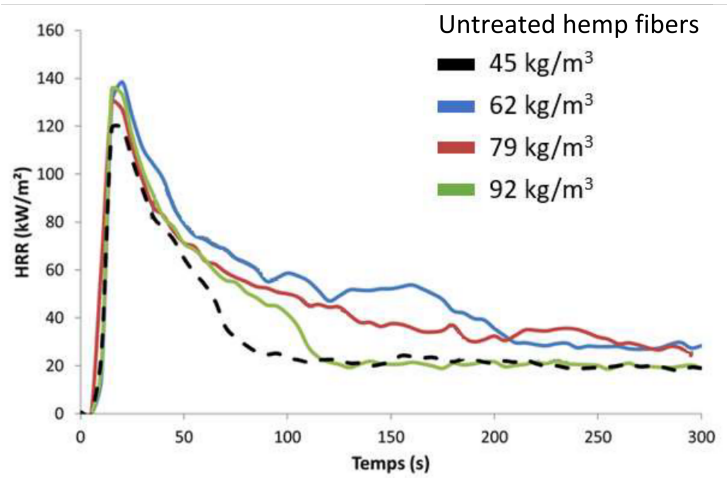

Figure 1.31: Heat release rate curve obtained from cone calorimeter test (DEB23)

1.6.4 Flame retardants: types and modes of action

In order to improve the fire behavior of bio-based materials, the use of flame retardants (FR) are needed. They are a group of materials that can act physically or chemically, to improve the overall fire properties of materials, and in the case of this thesis, lignocellulosic materials. In particular, FRs can act in three different ways to improve the flame retardancy of these bio-based materials (LAO09; TAI22):

- The first method is in the gas phase, by the release of specific radicals that react with H^+ and OH^-, to form less reactive or inert molecules, reducing the exothermicity of the combustion reaction and diluting the gas mixture.
- The second method is by acting in the solid or condensed phase with char formation.
- The third method involves the use of hydrated compounds that decompose endothermically when exposed to fire, thereby acting as a "heat sink".

The main products that can be used to enhance the fire behavior of lignocellulosic materials include mineral-based, halogenated, phosphorus-based, nitrogen-based and silicon-based flame retardants (LAO09).

Mineral-based flame retardants are very efficient and widely used. They act as a filler material, which reduces the content of combustible products, reducing the flammability. Also, some minerals, like aluminum trihydroxide (ATH), magnesium di-hydroxide (MDH), zinc borate (ZB), decompose endothermically when degrading at high temperatures, absorbing energy from the system. Furthermore, they release non-flammable molecules, such as H_2O and CO_2, which dilute combustible gases. However, depending on the material and the desired improvement in flame retardancy, the quantity of mineral added may be high, which can negatively affect the material's mechanical properties, thermal conductivity and viscosity (COS17; HUL11; LAO09).

Halogenated flame retardants are compounds that contain halogen elements, namely fluorine (F), chlorine (Cl), bromine (Br) and iodine (I), which belong to Group 17 of the periodic table. This type of FRs have been used since the 1930s, and act in the gas phase by releasing halogen radicals that scavenge the free radicals released and form stable molecules (COS17). Due to their low bonding energy, bromine and chlorine can easily release radicals, being, therefore, very effective (LAO09; TAI22). Some common halogenated FRs are Tetrabromobisphenol A (TBBPA) and Polybromodiphenylether (PBDE). Despite being very effective, the use of halogenated FRs has been increasingly avoided and restricted in various countries due to environmental and health concerns. They release toxic and corrosive gases during burning, causing diseases and polluting the environment (COS17; HAJ18; TAI22).

In the timeline sequence, phosphorus-based flame retardants have been increasingly studied as alternatives to halogenated ones, since they emit low smoke during combustion and there is the possibility of using non-toxic products (HAJ18; TAI22; TAI22). Phosphorus FRs can act in the condensed and gas phases, as their thermal decomposition leads to the production of phosphoric acid, which condensates and liberates water (LAO09; YUM24). When used with bio-based materials, phosphorus FRs lower the temperature of decomposition and increase the char formation, which is a physical protective layer that blocks external heat, oxygen penetration and flame spread (TAI22). The lower thermal stability is related to changes in the decomposition of cellulose, due to phosphorus substances, which reduces levoglucosan production and favors char formation (HAJ20), as shown in 1.32.

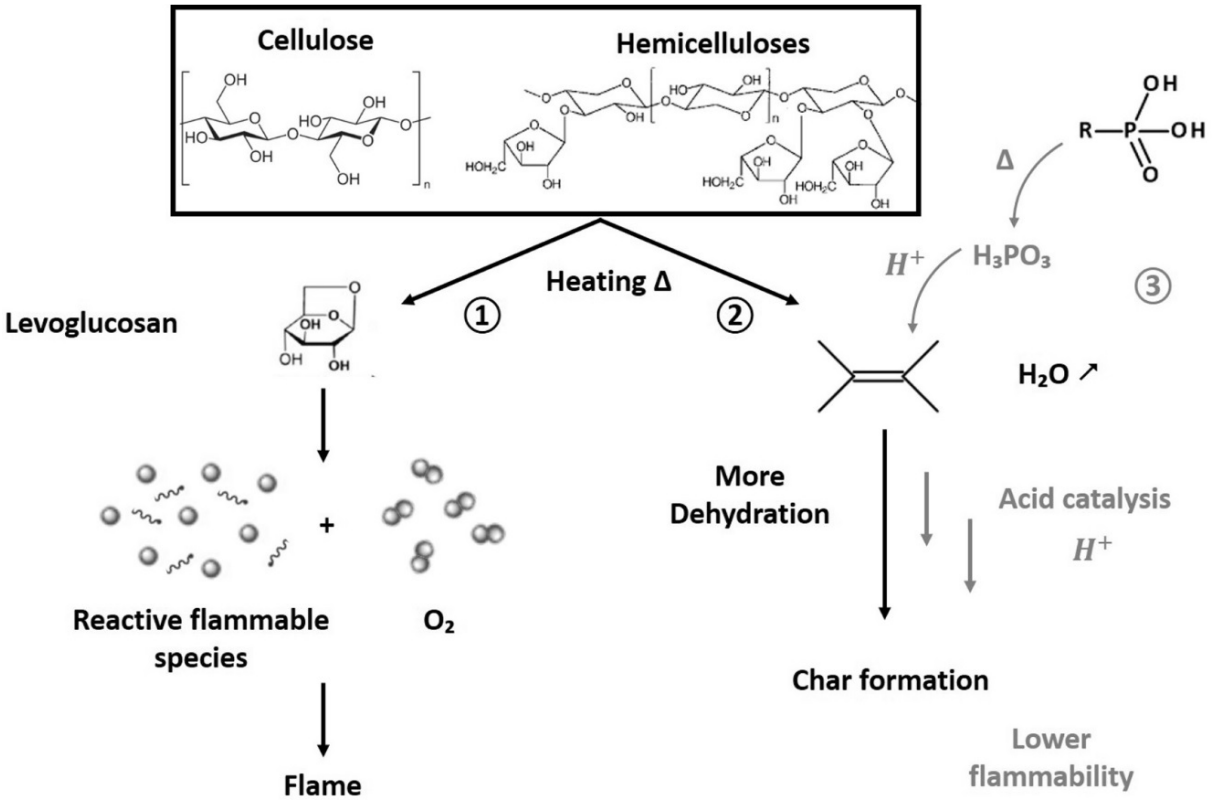

Figure 1.32: Mechanisms of thermal degradation of cellulosic material. Path 1: depolymerization, with formation of levoglugosan; Path 2: dehydration and increased char formation, in presence of phosphorus-based FR (HAJ20)

An interesting phenomenon, associated to the use of phosphorus-based FRs, nitrogen sources, and bio-based materials, is the formation of intumescent flame retardant systems (IFRS). The concept of IFRS is related to the formation of an expanded carbonized layer (char) during thermal degradation, which acts as an insulating barrier, reducing heat transfer between the heat source and the material's surface, and limiting fuel transfer and oxygen diffusion (LAO09). For the formation of a IFRS, three components are required:

- An acid source: this is where the phosphorus-based product can take action, simply by the use on phosphorus-containing acids (phosphoric acid, phosphonic acid, phytic acid...), or as part of the thermal decomposition of phosphorus groups into phosphoric acid (CHA10; GAA07; LAO09). A side effect from the use of phosphoric acid in lignocellulosic materials is the changes in the decomposition path of cellulose, favoring dehydration instead of the formation of levoglugosan, and increasing char formation, as presented in Figure 1.32 (CHA10; COL19; HAJ20).

- A carbonizing agent: a carbohydrate that is dehydrated by the acid to form a char (LAO09). Bio-based materials fits this purpose, as their chemical composition is mainly carbohydrates.

- A blowing agent: can be obtained by nitrogen products, which decompose and release gas, causing expansion and swelling of the cellular layer, forming the char (COS17; LAO09; MOU20). To form an expanded carbonized layer, the gas must be released during the thermal decomposition of the carbonizing agent (LAO09).

The schematic illustration presented in Figure 1.33 (YUM24) demonstrates in detail the mechanisms of flame retardancy of phosphorus- and nitrogen-based flame retardants. In the gas phase, chain reactions involving hydroxyls, oxygen, carbon monoxide, hydrogen

ions, and methane gas are inhibited by phosphorus-derived ions. The formation of water, ammonia and nitrogen gas also helps the dilution of flammable gases and oxygen. In the condensed phase, the flame retardants promote a dense char formation, developed by the intumescent effect of the phosphorus and nitrogen flame retardants.

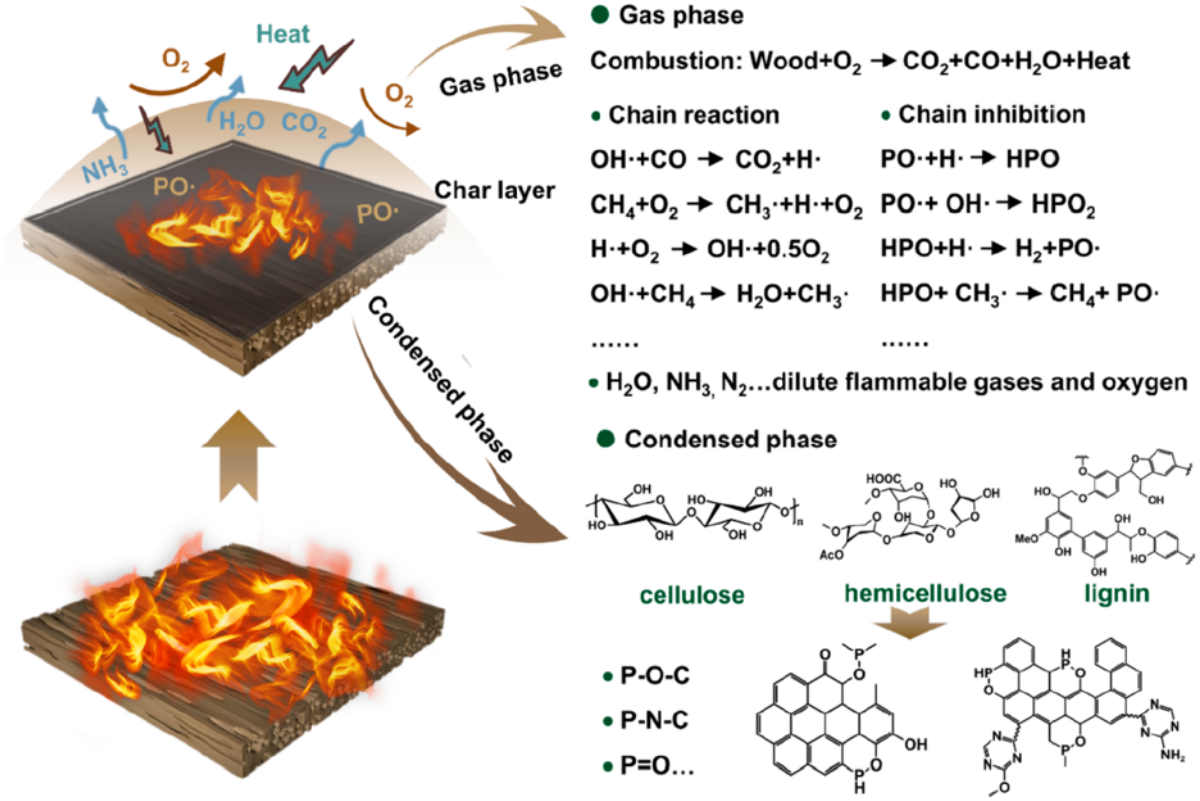

Figure 1.33: Phosphorus-based flame retardant mechanism (YUM24)

Other families of flame retardants exist, such as silane coatings, proteins, DNA, bio-based (cellulose, lignin, starch, chitosan, among others) and nanometric particles. However, they will not be further discussed in this work, as they still present limitations that make them unattractive for improving the flame retardancy of an application such as vegetal wools. Nonetheless, future advancements may overcome these challenges, potentially broadening the range of applicable flame retardant solutions.

1.6.5 Application methods and identified solutions

One of the possible approaches to enhance the flame retardancy of lignocellulosic materials with phosphorus- and nitrogen-based compounds, is by chemically reacting them, in a process called grafting. To accomplish that, different methods of application are possible. However, for the treatment of vegetal wool in industrial scale, this method needs to not only be efficient and effective but also scalable to large scale application.

Some of the methods used for the grafting of phosphorus and nitrogen molecules into the lignocellulosic material composition are gamma or e-beam radiation and chemical grafting (HAJ20; SON15; TAI22).

Radiation grafting acts by generating free radicals on the surface of the fibers, allowing the formation of covalent bonds between the phosphorus- and/or nitrogen-containing molecules with the cellulose, hemicellulose and lignin (TAI22). This method have been used in multiple studies, and it is effective in grafting the flame retardants into lignocellulosic materials (HAJ18; HAJ20; SON15; TAI22; TEI18). In the literature, when specified,

the radiation grafting method has been used to treat 2 g of fibers (HAJ18; HAJ20), or a fabric with dimensions of 3x3 cm^2 (TAI22).

Modification of vegetal fibers can also be achieved through chemical grafting. Depending on how much energy, and how aggressive the treatment is, different chemical reactions may occur. Under mild conditions, the main reaction will be the condensation between the phosphorus compound with the aromatic hydroxyl groups, which are found in the lignin. In that condition, the lignocellulosic fibers are treated in solutions with temperatures ranging between 70°C and 160°C (HAJ18). Under severe conditions, the phosphorylation of cellulose occurs, meaning the phosphorus compound form a covalent bond with the cellulose. This reaction requires a treatment temperature between 150°C and 160°C (ANT22; HAJ18; MOU20). For lignin-poor fibers, treatments under severe conditions appear to be more effective in enhancing flame retardancy (HAJ20). Both reactions, as well as the radiation reaction previously presented, are shown in Figure 1.34. For the chemical grafting method, a wider range of amount of fibers treated is observed in the literature, starting from 0.25 g (HAJ18; HAJ20) up to 100 g (DEB23).

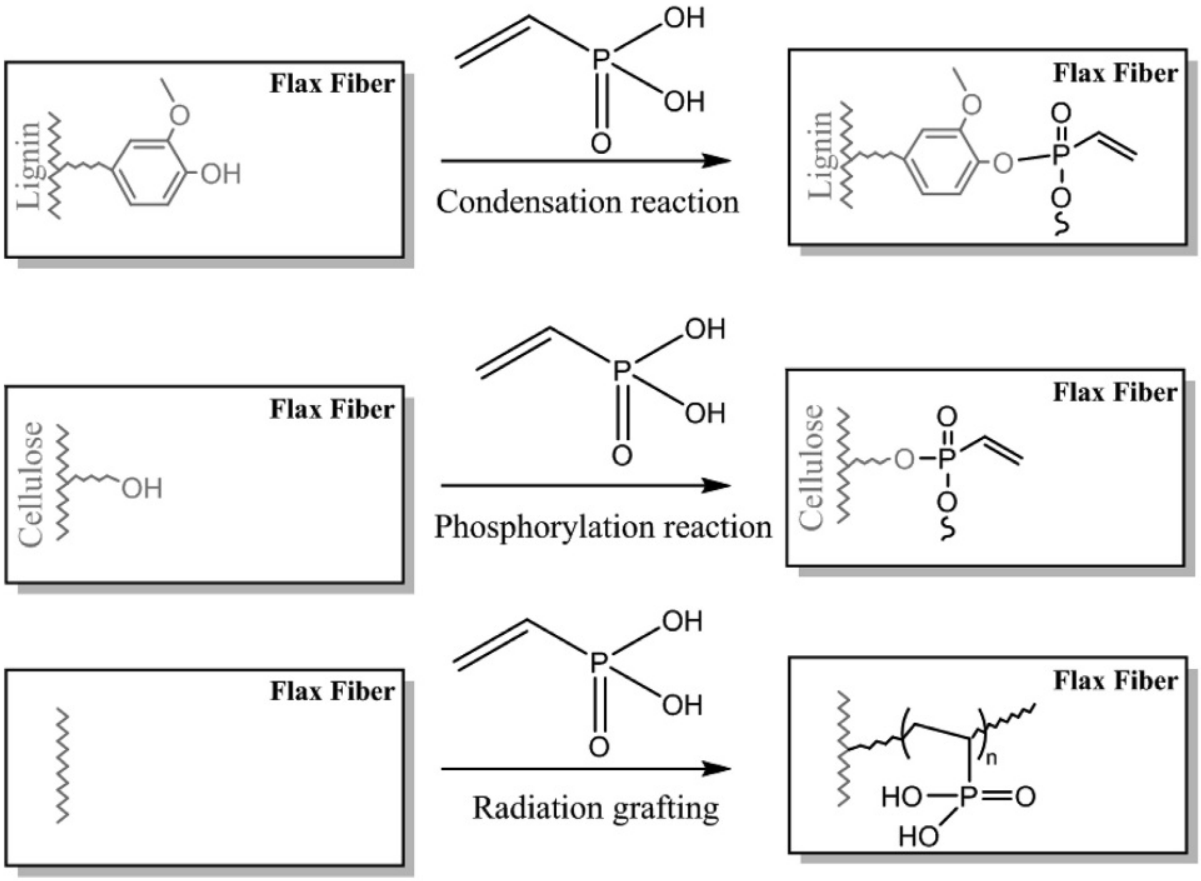

Figure 1.34: Upper: Chemical modification in mild conditions (condensation reaction); Middle: Chemical modification in severe conditions (phosphorylation reaction); Lower: Radiation grafting (HAJ18)

Considering the application of vegetal wools and the volumes of treated material required, the chemical grafting method offers several advantages over radiation grafting. It is more accessible, as it does not require specialized equipment, and it allows treatment of larger quantities of fibers per batch.

For chemical grafting, two application methods have been identified in the literature. The most common is the immersion method, in which the fibers are dipped in a solution containing flame retardants. This is followed by heating to initiate the chemical reaction,

washing to remove unreacted molecules, and drying the fibers. This approach has been shown to successfully graft phosphorus molecules onto lignocellulosic fibers, resulting in a reduction in their flammability (ANT22; DOR14; HAJ20; MOU20).

However, this method has shown limitations in terms of time and energy efficiency, mainly due to the washing and drying steps required after immersion. Additionally, the amount of fibers that can be treated per batch is relatively low, often requiring a high solution-to-fiber mass ratio, which reduces the overall process efficiency for large-scale applications. This ratio is usually around 10-20 (ANT22; DOR14; MOU20), but can go up to 80 (HAJ18; HAJ20). These studies treated 0.25 g to 50 g of fibers, which, added to the previous problems, questions the scalability of the procedure.

Another possible method is the application of the treatment solution by pulverization. This approach, which is not yet well explored in the literature, involves spraying the solution directly onto the fibers without soaking them. Deborde et al. (DEB23) used this approach and treated 100 g of lignocellulosic fibers with 100 g of solution containing flame retardants, representing a solution to fiber mass ratio of 1. Concerning other materials, Lee et al. (LEE23) applied flame retardants by spraying them onto the surface of low-density wood fiberboards, using a certain amount per m^2, as specified by the flame retardant company. In recycled technical textiles, Danihelová et al. (DAN21) used both approaches, by immersion and by pulverization of the surface, following the specifications of the flame retardant products.

Regardless of the method employed, a key parameter for evaluating the effectiveness of phosphorus grafting is the quantification of the phosphorus content in the treated material, frequently performed by ICP-AES. Numerous studies highlight that the higher the phosphorus content, the better the flame retardancy observed (ANT22; HAJ20; MOU20; SON15; TAI22; TEI18). In Figure 1.35, this relationship becomes more evident, by presenting how the increase in phosphorus content affects two key parameters obtained from calorimeter tests: the peak heat release rate and the total heat released. Both graphs show a significant decrease in pHRR and THR as the phosphorus content increases from 0% to 1%. Beyond 1%, these parameters continue to decrease but at a slower rate. Therefore, quantifying the phosphorus content serves as an indirect measure of the flame retardancy of lignocellulosic fibers.

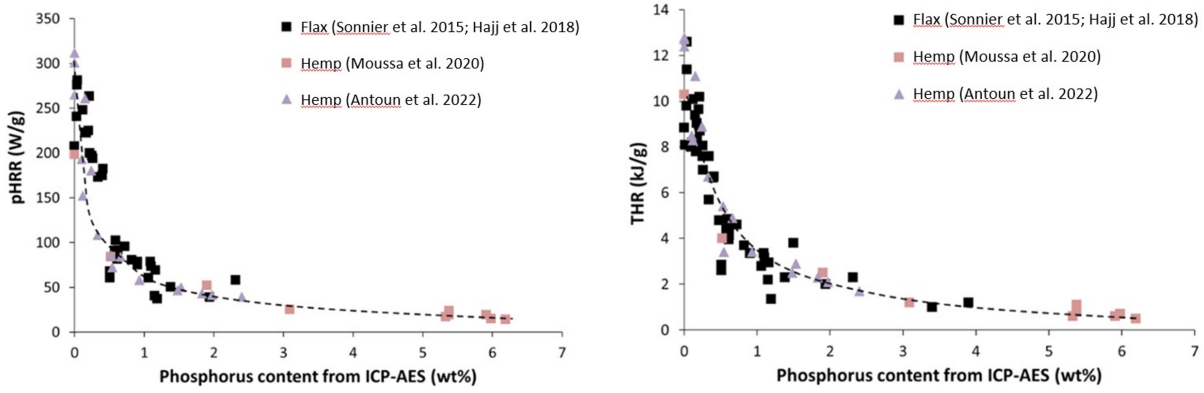

(a) (b)

Figure 1.35: Relationship between fire reaction parameters and the phosphorus content in lignocellulosic fibers: (a) pHRR x P content; (b) THR x P content

In Table 1.7, a compilation of the amount of phosphorus grafted, in wt.%, needed to achieve self-extinguishing behavior is presented. Notably, some studies related that a small amount of 0.5% was enough to achieve that performance. In fact, it is worth to mention that, two of these studies used an intumescent flame retardant system (ANT22;

MOU20), which could explain the low amount of phosphorus content required for self-extinguishment behavior.

Table 1.7: Phosphorus content needed for achieving self-extinguishing behavior

Base fiber	FR	Grafting method	P (%)	Reference
Flax	MVP	Radiation	1.5	SON15
Flax	EGMP	Radiation	0.5	TEI18
Flax	VPA	Chemical	0.5 - 1.0	HAJ18
Hemp	HEDP + Urea	Chemical	0.5	MOU20
Hemp	PA + Urea	Chemical	0.5	ANT22

An interesting aspect of the chemical grafting can be observed by scanning electron microscopy, coupled with energy dispersive x-ray spectroscopy (SEM-EDS). Through this technique it is possible to evaluate if the compounds grafted are spread within the whole fiber, including its core, or limited to certain regions, such as its surface. Figures 1.36 and 1.37 present the phosphorus mapping of the transversal section of flax and hemp fibers, treated with mild and severe conditions, respectively. Indeed, through chemical grafting, it is possible to graft phosphorus on the fiber's surface and on its core. This enables a higher amount of phosphorus to be grafted and better flame retardancy behavior.

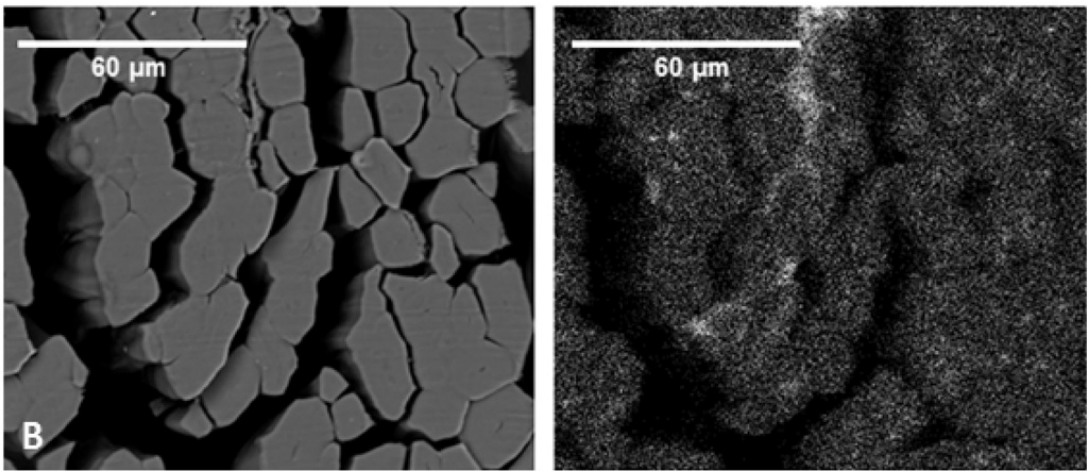

Figure 1.36: Left: SEM image from flax fibers; Right: EDS mapping of phosphorus grafted on the flax fibers (HAJ20)

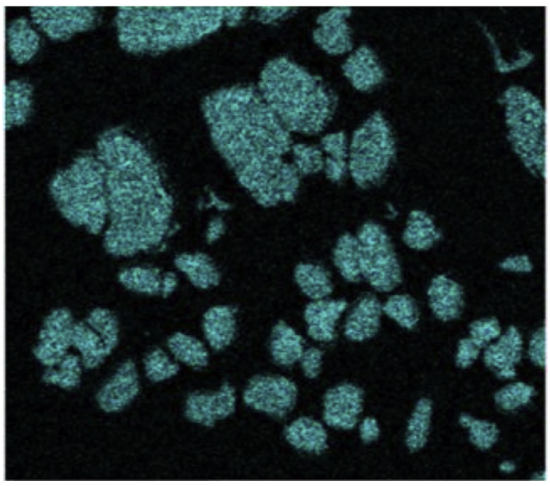

Figure 1.37: SEM-EDS phosphorus mapping of treated hemp fibers (MOU20)

1.6.6 Flame retardants for lignocellulosic fibers

The aforementioned treatments can be achieved by many different products. For an efficient phosphorus grafting, it was essential to analyze the characteristics, advantages, limitations, and the effectiveness as a flame retardant of each possible material. Therefore, this section provides a more detailed overview of studies that have applied the phosphorus chemical grafting approach to lignocellulosic and thermoplastic fibers.

As previously mentioned, the chemical phosphorus grafting can be done in mild or severe conditions. In part of the studies from Hajj et al. (HAJ18), the authors treated flax fabrics under both conditions, plus intermediate conditions, using different solutions and treatment temperatures:

- Mild condition: Flax fabrics were treated in a solution composed of 90% ethanol, 10% water, with 5% of vinyl phosphonic acid (VPA). The mixture was heated under reflux at 70°C for 2h.

- Intermediate condition 1: The solution was composed of water and the mixture was heated at 100°C for 2h. The VPA content in solution was 5%.

- Intermediate condition 2: The solvent used was dimethylformamide (DMF), as it has higher boiling point. The treatment temperature was 100°C, and the VPA content in solution was 5%.

- Severe condition: This condition is similar to the previous one, despite the temperature which becomes 160°C.

The mild and intermediate conditions achieved a phosphorus content in the flax fabrics of less than 0.5% in weight, as flax fibers contains low amount of lignin (around 2.7% in the article). In contrast, the severe condition grafting reached a phosphorus content of 2.3%, which shows that, for lignocellulosic materials with low lignin content, a more severe condition is needed for efficient phosphorus grafting, through phosphorylation of the cellulose. The phosphorus content reflected directly in the flammability of the fibers, where those treated at severe conditions presented a bigger reduction in their fire reaction parameters.

In a subsequently study (HAJ20), the authors confirmed the role of the chemical composition of the fibers, by testing the chemical grafting of phosphonic acids in mild condition in flax, poor in lignin content (about 3%), and miscanthus fibers, rich in lignin content (about 20%). With C6 biphosphonic acid, miscanthus fibers achieved a phosphorus content of 1.4% in weight, whereas flax fabrics only reached 0.3%. This study also highlighted that not only the phosphorus content is important for an effective improvement of fire behavior from lignocellulosic fibers, but also the thermal degradation of the flame retardant itself. The authors stated that when the flame retardant is more thermally stable than the fiber, which means that it degrades at a higher temperature range, the phosphorus that is grafted does not have the same effect, as when a FR degrades earlier or within the same temperature range as the base fiber. Therefore, a understanding of the thermal stability, which can be assessed by TGA, is necessary for a successful improvement of the fire behavior of bio-based materials.

Dorez et al. (DOR14) also tried to graft phosphorus onto flax fibers under mild conditions. The authors varied the treatment agent concentrations in ethanol solution between 2.5% and 10%. Two phosphorus compounds were used: dihydrogen ammonium phosphate (DAP) and phosphoric acid. The maximum amount of phosphorus grafted with DAP was 1.13% and 0.52% with phosphoric acid, in weight. In this case, the use of

DAP showed an interesting result, as it was possible to surpass 1% of phosphorus grafting under mild conditions.

DAP was also tested, among other phosphorus FRs, such as Pyrovatex CP (PCP), phosphoric acid (PA), triallyl phosphate (TAP), tributyl phosphate (TBP), and triallyl phosphoric triamide (TPT), to improve the fire resistance of cotton fabrics (GAA07). Thermogravimetric analysis under air, which is presented in Figure 1.38, showed a similar behavior between cotton fabrics treated with PA, DAP, PCP and TPT. These flame retardants caused an earlier thermal degradation and a higher final residue of 20-25% in weight. TAP and TBP samples showed a 2 stages decomposition and no improvement in the final residue, at 500°C.

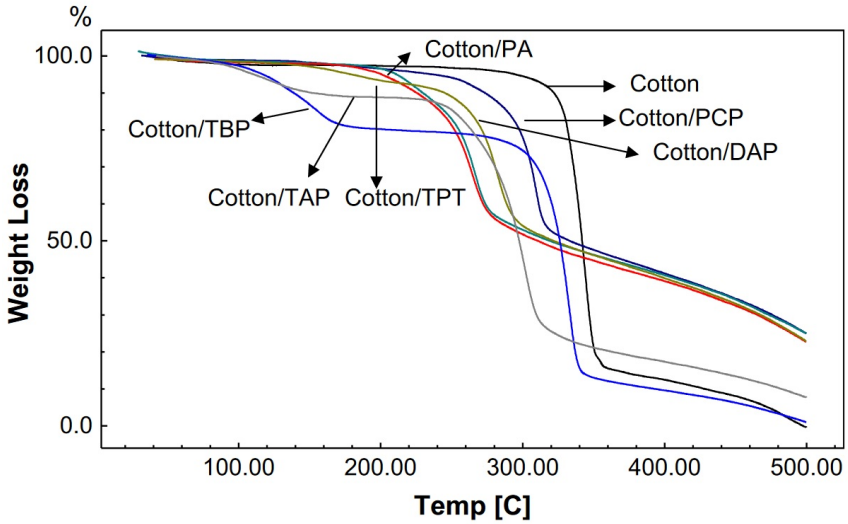

Figure 1.38: TGA results for cotton fabrics treated with various phosphorus-based FR (about 2% of phosphorus grafted) (GAA07)

Using the phosphorylation approach, Moussa et al. (MOU20) treated hemp fibers, which also have a low lignin content, with 1-hydroxyethylidene-1,1-diphosphonic acid (HEDP) and urea, in aqueous solution. The fibers were mixed in the solution with the phosphorus and nitrogen compounds for 1 hour, then dried in an oven under vacuum. After that, the fibers went through a cooking step at 150°C for 2h. The phosphorus and nitrogen content achieved was of 5.4% and 3.3%, respectively. Consequently, a significant improvement in fire properties was observed. From TGA, it was observed that the residue at 750°C increased from 21.2 wt.% to 40 wt.%, for the reference and the treated hemp fiber respectively. The fire reaction was assessed with the Pyrolysis-combustion flow calorimetry (PCFC) test (LYO04), where a small sample is first decomposed under pyrolytic conditions and then burned in O_2/N_2 atmosphere. In this test, the heat release rate is obtained as a function of the temperature, and the fire reaction parameters are given per unit of mass of the sample. The PCFC test showed a reduction in pHRR from 103 $W.g^{-1}$ to 24 $W.g^{-1}$, and a reduction in THR from 6.8 $kJ.g^{-1}$ to 1.1 $kJ.g^{-1}$.

Antoun et al. (ANT22) used the same methodology to graft phosphorus and nitrogen into hemp fibers, however, in this case, phytic acid (PA) was employed as the phosphorus source. Phytic acid is a bio-based source of phosphorus, obtainable from grains, beans and seeds, and shows great potential as a flame retardant due to its high phosphorus content (about 28%) (MOK22; WAN22). Different concentrations of urea (between 1% and 20%) and phytic acid (between 0.32% and 6.26%) were evaluated. The results showed that increasing the concentrations led to a higher amount of phosphorus and nitrogen being grafted onto the fibers (see samples 1 to 6 in Table 1.8). Using a non-standardized fire test, the authors evaluated qualitatively if the treated hemp fibers were

flammable, non-flammable, or if they became self-extinguishable. Samples 1 and 2 were still flammable, due to the low phosphorus grafted onto them. Sample 3 was classified as self-extinguishable, and samples 4, 5 and 6 were classified as non-flammable. This highlights the importance of the phosphorus content for the flammability behavior of treated lignocellulosic fibers.

Table 1.8: Phosphorus and nitrogen grafted (adapted fromANT22)

Sample	Phytic acid (%)	Urea (%)	P (%)	N (%)
1	0.32	1	0.15	0.05
2	0.63	2	0.24	0.31
3	1.57	5	0.53	0.66
4	3.31	10	0.93	0.78
5	4.70	15	1.48	1.07
6	6.26	20	1.83	1.40
7	-	20	-	0.54
8	6.26	-	1.10	-
9	6.26	20	0.10	0.05

Samples 7 and 8 were used to evaluate the fire behavior of fibers treated solely of phytic acid or urea. These samples showed a synergetic effect between a phosphorus-based and nitrogen-based products. The aforementioned samples had significantly less amount of phosphorus and nitrogen grafted when compared to samples 6, which used the same concentration of phytic acid and urea in solution. The authors stated that urea promotes swelling of the fibers, which contributes to a higher grafting of phytic acid. The synergetic effect as a flame retardant was measured by PCFC, and it is shown in Figure 1.39. In the Figure, a significant reduction in the heat release rate (HRR) can be observed when both compounds are incorporated into the chemical composition of the hemp fibers. Finally, sample 9 was prepared under mild conditions without the cooking step, evidencing that even with large amount of phytic acid and urea, phosphorus and nitrogen cannot be effectively grafted onto the fibers.

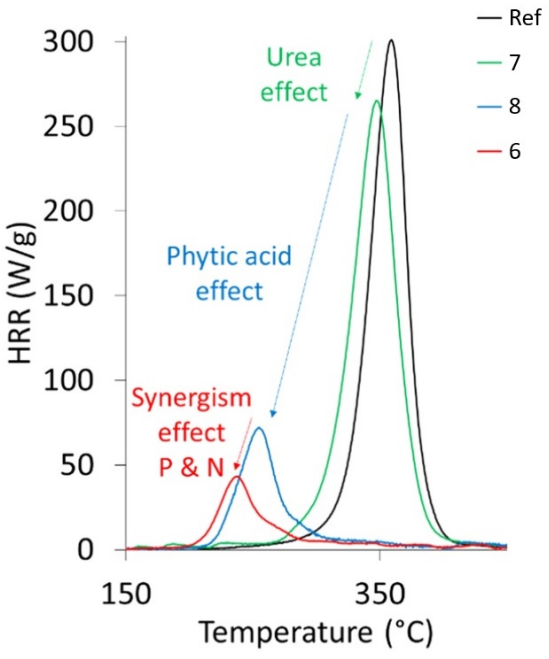

Figure 1.39: PCFC results from samples treat only with urea (7), only with phytic acid (8) and with both (6) (ANT22)

1.7 Thermal degradation and fire reaction of thermoplastic fibers

Given that vegetal wools consist not only of lignocellulosic fibers but also of thermoplastic components, a thorough understanding of their fire behavior is essential. Therefore, in this section, the flame retardancy and thermal degradation of thermoplastic fibers will be detailed.

As shown in Section 1.1, an important parameter of thermoplastic fibers is their melting temperature (Table 1.2). The melting point determines the consolidation temperature of the panels and depends on the polymer used, typically ranging from about 115 °C for PBS and LDPE up to 265 °C for PET.

It is also relevant to verify whether these polymers would be susceptible to thermal degradation in this range of temperature. For LDPE, the thermal degradation occurs between 370°C and 510°C (TOM10), for PP it ranges from 345°C and 493°C (TOM10), for PBS it starts at about 360°C (BAU15), and for PLA it is from 309°C and 365°C (CHE16). Therefore, in a normal scenario of hemp wool production, these temperatures would not be reached, preserving the chemical composition of the polymers. Furthermore, these temperatures are higher than the temperatures observed for the lignocellulosic fibers constituents, which can start at about 150°C for the lignin, as shown in Section 1.6.2.

The thermogravimetric analysis (TGA) of LDPE and PP in argon gas is illustrated in Figure 1.40 (TOM10). It can be observed that there is one single mass loss step in both cases, that occurs due to chain scission or depolymerization. Moreover, after this mass loss step, the residual mass is equal to zero, which corresponds to full decomposition into volatiles and no char formation.

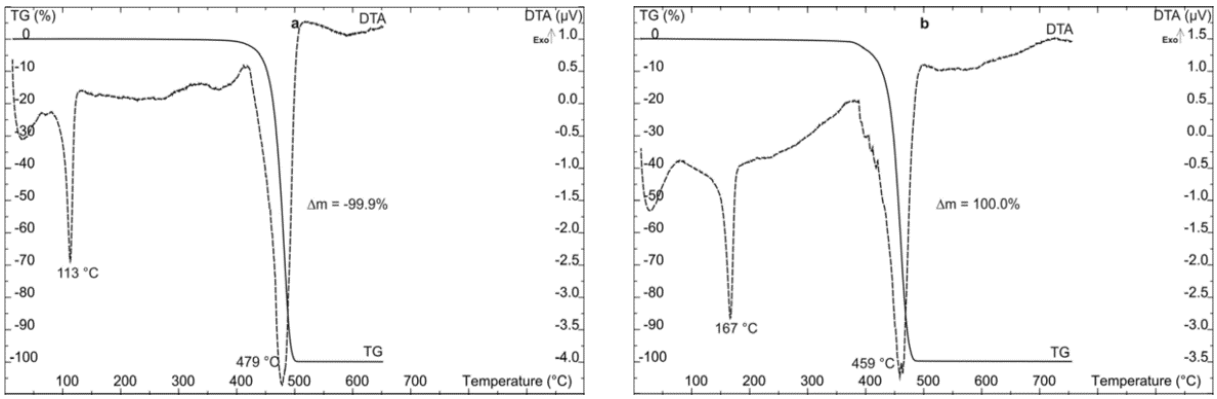

(a) (b)

Figure 1.40: Thermal degradation of polymers - TGA (straight line) DTG (dashed line): (a) LDPE; (b) PP

The improvement in the flame retardancy of thermoplastic fibers is usually done by an addictive or reactive route (LIU22). The former is the simpler method, where the flame retardants are blended with the polymers, resulting in a physical interaction between them (LIU22). Surface treatments can also be considered as an additive to the polymers. In the reactive route, the chemical composition of the polymers is altered by co-polymerization, in order to incorporate the flame retardants into the polymeric chain. This approach creates a more stable and durable bond (LIU22; SZO13).

1.8 Effects of the treatment on the acoustic and thermal performances of vegetal wools

In the literature, studies addressing the impact of flame-retardant treatments on the other functional properties of materials, such as the acoustic and thermal insulation, particularly in bio-based materials, are scarce. This underscores the need to understand the potential effects of the flame retardants on these properties. In this Section, some studies presenting the use of flame retardants and the assessment of the acoustic or thermal performances of materials, that are relevant to this thesis, will be discussed in detail.

Four different flame retardants, based on phosphorus and boron, solely phosphorus or ceramic powder were tested in low-density wood fiberboards for building applications (LEE23). The application methods were done either in the resin used in the fabrication of the fiberboards (samples C and E), or through liquid solutions sprayed onto the surface of the material (samples A, B, D and E). The flame-retardancy was evaluated with 45° Meckel burner test, that follows a Korean standard, and the sound absorption coefficient of the fiberboards was evaluated with an impedance tube test. The thermal conductivity was measured according to ISO 8302:1991 using a guarded hot plate apparatus, with a temperature difference of 15°C between the upper and lower plates.

The authors reported a preference, in terms of flame retardancy, for the application of phosphorus in the resin, due to a uniform distribution of the flame retardants in all fiberboards body, or by spraying a phosphorus solution onto the surface. For the acoustic assessment, the treatments applied led to an increase in the sound absorption coefficient, especially at frequencies above 1000 Hz (Figure 1.41). This effect was associated with the destruction of the adhesive layer on the surface and to the surface swelling caused by moisture absorption. Regarding thermal conductivity, a slight reduction was observed with the treatment, from 0.043 to 0.041 $W.m^{-1}.K^{-1}$, but no standard deviation was reported to evaluate whether this difference is statistically significant.

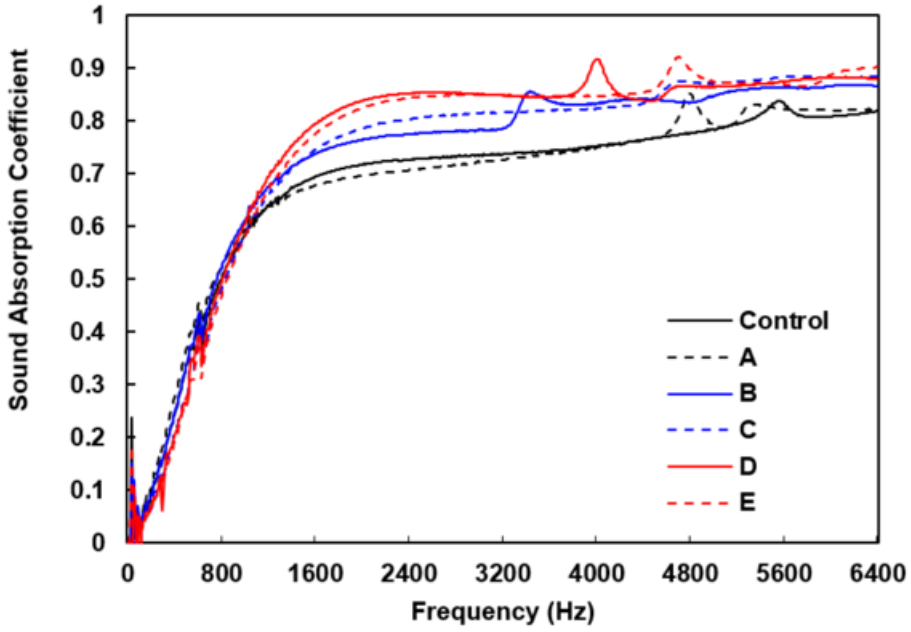

Figure 1.41: Sound absorption curve of fireproof treated wood fiberboards (LEE23)

In a material that can be considered closer to the vegetal wools, the study of Danihelová et al. (DAN21) evaluated the flame retardant impregnation in the acoustic and thermal properties of recycled technical textiles, using an impedance tube and extended dynamic plane source method, respectively. Three commercial flame retardants were

tested by spraying or by immersion of the samples. The sound absorption coefficient did not change with the treatments, besides a small reduction between 200 and 400 Hz (Figure 1.42). The authors stated that the flame retardants cover the surface of the fibers, but there are no significant changes in the volume of air between them. However, this affirmation was not proved. A flame retardant applied by immersion led to a small reduction in sound absorption, which was associated with a small reduction in the porosity of the sample.

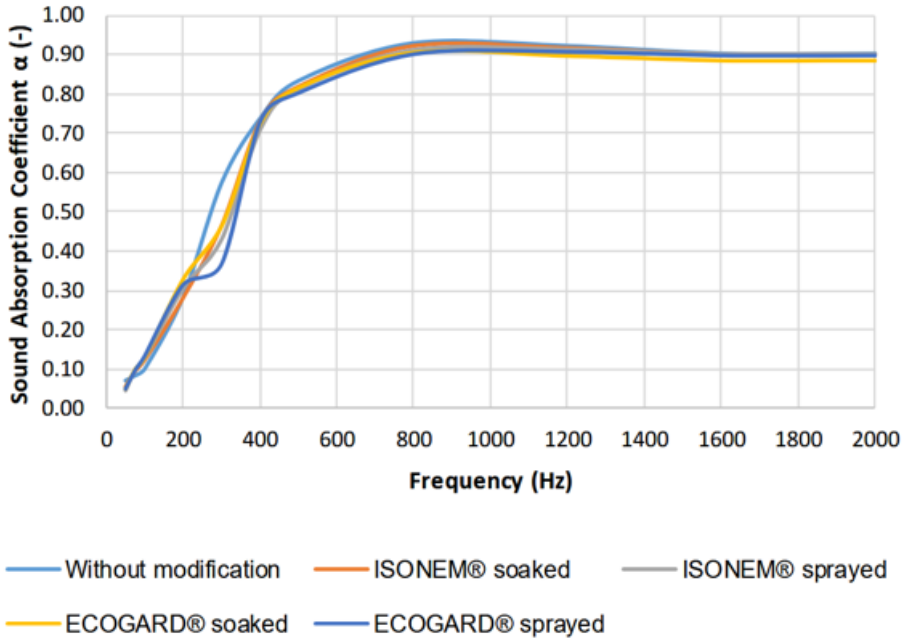

Figure 1.42: Sound absorption curve of fireproof treated recycled technical textiles (DAN21)

The treatments led to a slight increase in the apparent density for the samples treated by spraying and a significant increase (almost double) for the samples treated by immersion. The thermal conductivity also increased, proportionally to the increase in apparent density, except for one flame retardant that presented a less important impact on the thermal conductivity, despite the significant increase in apparent density (Figure 1.43). Even though this study applied flame retardants, the flammability of the samples was not assessed before or after treatment.

In the study by Fatima and Mohanty (FAT11), the flammability and acoustic performance of the jute composites were assessed. The authors evaluated the flammability using a flame spread test from Federal Motor Vehicle Safety System (FMVSS) standard and smoke production using a smoke density test. The sound absorption was measured using an impedance tube, and characteristic parameters of the pore geometry were measured directly (for porosity and airflow resistivity) and indirectly with empirical formulas (for tortuosity) and with the Allard model (for the characteristic viscous and thermal lengths).

The sound absorption of untreated jute fibers was assessed as well as jute fibers treated with 1%, 2% and 3% alkali treatment, in order to remove the hemi-cellulose and separate the fibers. This treatment did not lead to significant changes in sound absorption. The jute fibers were then used to produce composites with natural rubber latex. These samples had their acoustic performance and their flammability assessed, but the sample that was flame-retarded with sodium phosphate had only its flammability tested. Therefore, an exploration of the influence of the treatment on the sound absorption and on the characteristic parameters of the pore geometry was missing.

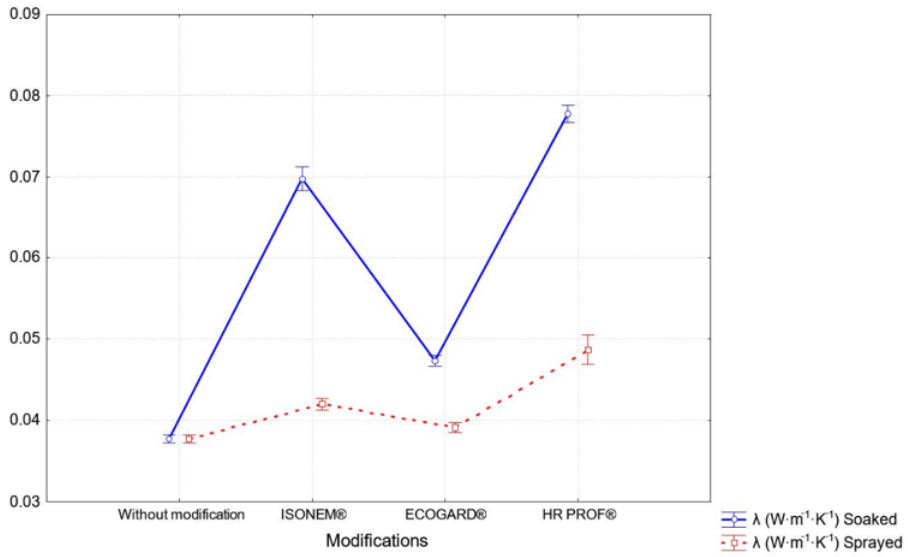

Figure 1.43: Thermal conductivity as a function of the apparent density of fireproof treated recycled technical textiles (DAN21)

Flame-retarded bamboo pulp foam was evaluated for flammability, using cone calorimeter and limiting oxygen index (LOI) tests, and for acoustic performance using an impedance tube test (YUE24). The thermal conductivity was also assessed using a hot disc test. The treatment consisted of applying chitosan, phytic acid, and halloysite nanotubes, using a layer-by-layer technique. The fire reaction parameters significantly improved with the application of two or four layers of flame retardants. The sound absorption was positively affected by the use of flame retardants. The authors attributed this increase to the increase in foam density, which led to higher energy loss due to surface friction between the sound waves and the fibers. The thermal conductivity decreases slightly with treatment, going from 42.9 $mW.m^{-1}.K^{-1}$ to 40.3 $mW.m^{-1}.K^{-1}$ and 41.8 $mW.m^{-1}.K^{-1}$ for samples treated with two and four layers, respectively. However, without any statistical dispersion, it was inconclusive if this result is significant or not.

1.9 Fungi development on vegetal wools

In the context of vegetal wools for building insulation, the term durability can be defined as the retention of the characteristics of the material and the preservation of its performance over time. Bio-based materials are frequently questioned regarding their susceptibility to fungal growth and, therefore, their durability. Indeed, plants naturally contain microorganisms, and their presence is even exploited during the retting step, for the deterioration of cell walls and pectin (AMZ17; TER20; THY06). However, the proliferation of these microorganisms can modify the intrinsic properties of materials and affect the indoor air quality, causing allergies and infections (AMZ17). Therefore, it is important to understand the key factors that lead to the proliferation of fungi.

1.9.1 Environmental conditions for fungi development

In short, fungi are organisms that obtain nutrients by absorbing organic matter and reproduce through spores. Molds, in particular, are a subset of fungi that grows by spreading a filamentous structure, forming a visible network called mycelium, and reproduce through the emission of spores into the air. Naturally, multiple spores are present in the air, but in large quantities some species can cause health problems to humans and animals (TUP24;

VAS22). If the spores find favorable conditions for their development, including temperature and relative humidity, they germinate and start to grow. If not, the spores can remain in a latent state for multiple years, waiting for favorable conditions to germinate (AMZ17; DEB25; TUP24).

During their growth, the fungi consume organic matter, as long as it is available. This includes the organic composition of the bio-based materials. Indeed, cellulose, hemicellulose and lignin can be metabolized by fungi (GOU19), and are a real treat for the biological durability of bio-based insulation products. The main factors that contribute to mold growth are temperature and relative humidity. The minimum value of relative humidity of the material for fungal growth is between 70% and 90% (GRA89; NYK06).

Grant et al. (GRA89) divided the molds into three groups, depending on the relative humidity available for microorganisms development, called water activity (A_w). The primary group included molds that required a water activity lower than 0.8. This group included *Penicillium spp.* and *Aspergillus*, for example. The second group needed water activity between 0.8 and 0.9, and the third group needed more than 0.9. The temperature usually reduces the water activity needed for fungal growth. For example, the fungi *Aspergillus versicolor* needed a water activity of 0.87 to grow at the surface of a emulsion-painted wood-chip paper at 12°C, and a A_w of 0.79 on the same surface at 25°C.

Extreme temperatures also affect fungal development. Nykter (NYK06) observed the same number naturally present fungi colonies in hemp fibers at relative humidity between 30% and 80 %, but higher quantities when relative humidity increased to 90%. Low temperatures (< 10°C), cause most molds to be metabolically inactive, stopping their growth and reproduction. High temperatures (> 40°C) also inhibits mold growth, or even kills them (DEA06; DEB25; GRA89)

1.9.2 Substrate conditions for fungi development

The nutrients present at the substrate that the mold is growing also influences their development. The main nutrient is carbon-rich organic compounds such as mono- and polysaccharides, triglycerides and proteins. Other important nutrients are phosphorus-rich and nitrogen-rich structures, used in the synthesis of nucleic acids, proteins and enzymes (DEA06; DEB25). Therefore, it is hypothesized that the use of phosphorus-based and nitrogen-based flame retardants, such as phytic acid and urea, can promote the fungi development and compromise the durability of the hemp wools.

This was observed in flame-retarded hemp shives and corn starch composites. The use of a commercial flame retardant with phosphorus and nitrogen in the composites, promoted the development of a bacteria *P. putida* and a fungi *Rh. oryzae*, when compared to a control sample (VAS22). These microorganisms were impregnated in the composite, and were incubated up to 6 months. They were selected because they are known to be good cellulose degraders. The microstructure of these samples was damaged, with more pores and voids than the reference, and a decrease in the apparent density was observed (Figure 1.44). The degradation came from the fungal activity, since no bacteria development was observed. The authors stated that, besides the phosphorus and nitrogen composition, the acidic pH of the flame retardant could have contributed to the development of the fungi.

However, recent studies have shown that phytic acid has antifungal activity and can be used as a fungicide, inhibiting the growth of certain fungi (LIP23; LIA24). The mechanism of action of phytic acid as a fungicide relies on the destruction of the cell membrane, increasing its permeability causing the cell contents to spill out and impairing fungal growth (LIP23). Moreover, phytic acid reduced the activity of enzymes produced by the fungi, blocking the degradation of the plant components (LIP23). Li et al. observed that the growth of *F. oxysporum*, *V. mali*, *A. alternata* and *B. cinerea* was reduced or

inhibited as a function of the phytic acid concentration, as presented by the graphics in Figure 1.45.

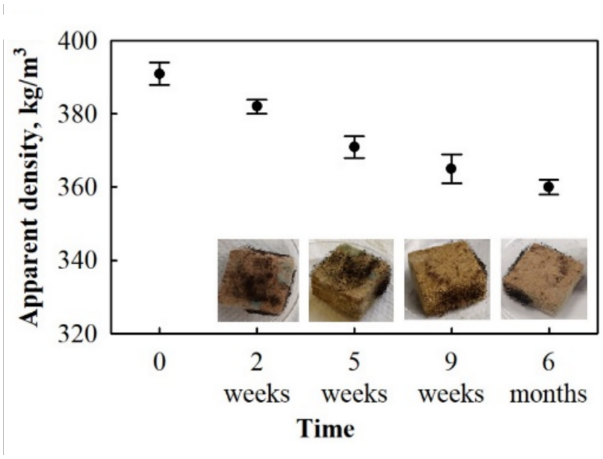

Figure 1.44: Apparent density of hemp shives and corn starch composites after incubation of *P. putida* and *Rh. oryzae* (VAS22)

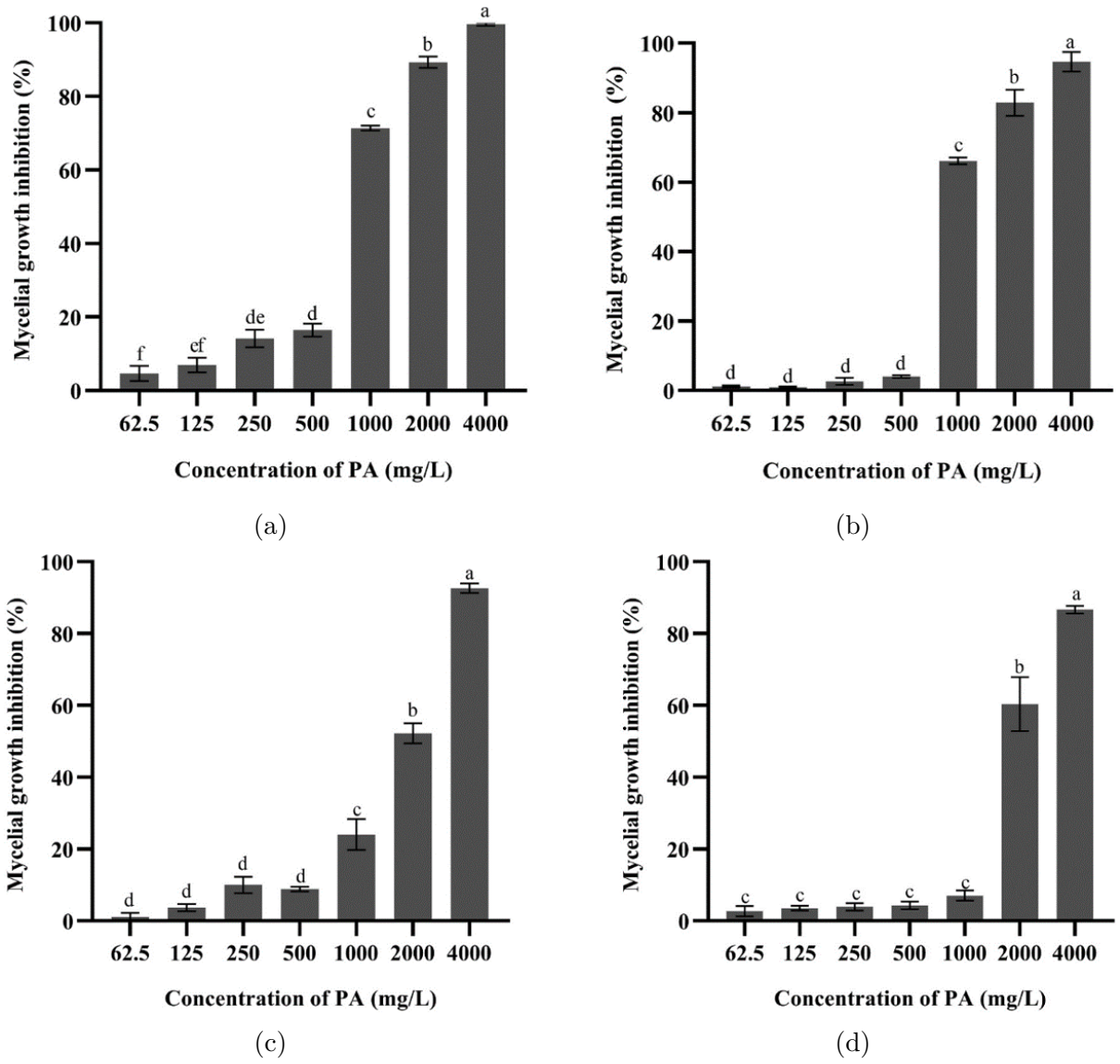

Figure 1.45: Mycelial growth inhibition (LIP23): (a) *F. oxysporum*; (b) *V. mali*; (c) *A. alternata*; (d) *B. cinerea*

Liang et al. (LIA24) reported that small concentrations of phytic acid (0.25% in weight) was enough to inhibit fungal growth of common wood-decaying fungi in three (*Trametes versicolor*, *Irpex lacteus* and *Gloeophyllum trabeum*) out of the four fungi tested. The forth fungi (*Rhodonia placenta*) had its growth significantly reduced with 4% of phytic acid, but its growth was not inhibited. Figure 1.46 presents the fungi growth of the four fungi tested, when incubated in a culture medium containing different concentrations of phytic acid. The pictures were taken after 14 days of incubation.

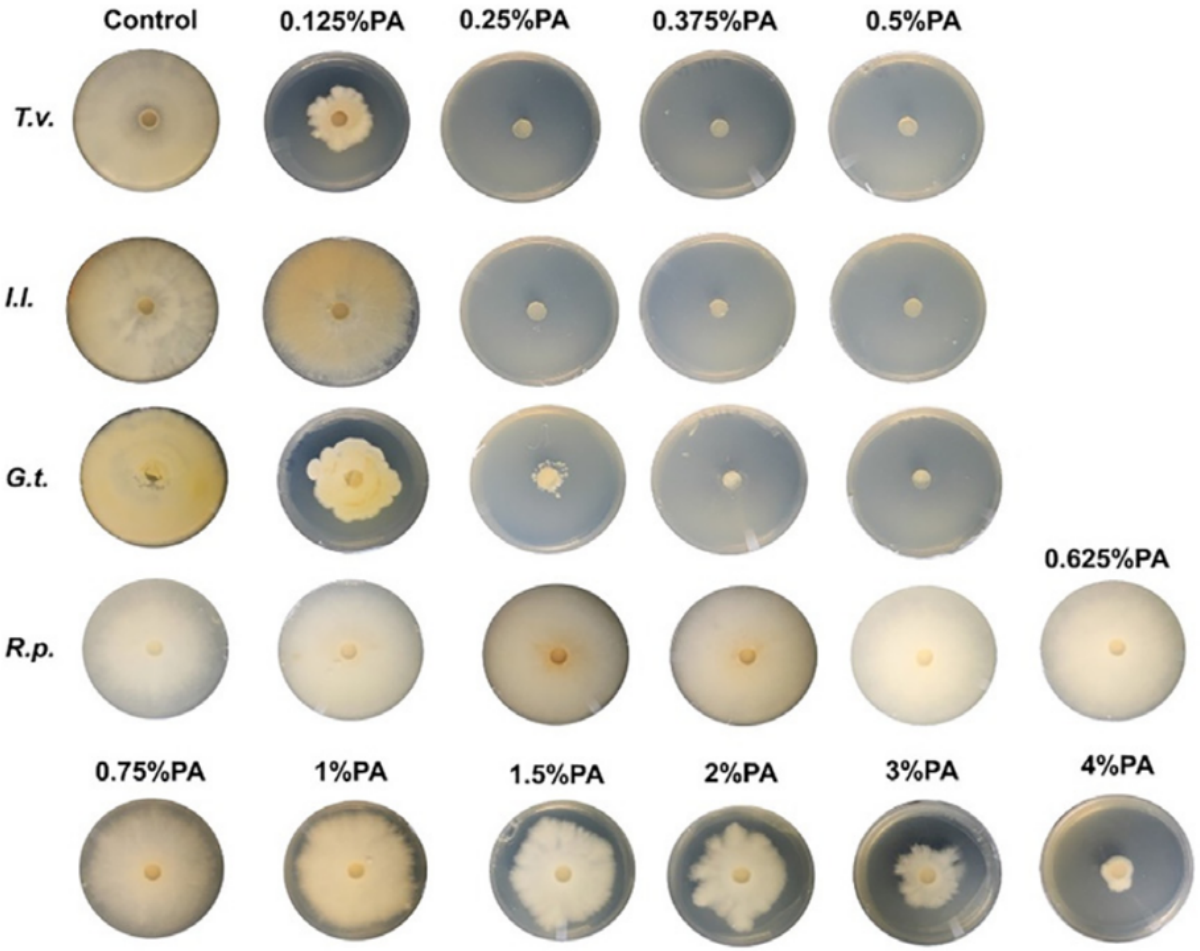

Figure 1.46: Wood-decaying fungi growth in culture medium amended with phytic acid in concentrations from 0.125% to 4% after 14 days (LIA24)
T.v. - *Trametes versicolor*; I.l. - *Irpex lacteus*; G.t. - *Gloeophyllum trabeum*; R.p. - *Rhodonia placenta*; PA - Phytic acid

1.10 Literature review conclusions

This Section is a summary of the main conclusions and the key points to be explored based on the observations made from the literature review. Then, the objectives of the thesis are restated and analyzed as a function of the conclusion obtained from the literature review.

1.10.1 Coupling fireproof treatment with acoustics and thermal performances of hemp wools

From the literature review, it was observed that the vegetal wools are an excellent material for acoustic correction and thermal insulation. This is linked to several factors including

the highly porous structure and its bio-based nature. Moreover, their hygroscopic behavior helps to regulate relative humidity in an inside environment. Adding these properties with the advantage of being composed of about 90% wt. renewable bio-based origin material, with low embodied carbon and energy, the vegetal wools consolidate themselves as a strong alternative to traditional materials for building insulation.

However, the material faces a limitation in its application due to its flammable nature. With a chemical constitution composed mainly of cellulose, hemicellulose and lignin, the vegetal wools are very reactive to fire, and require the application of fireproof treatments to reduce their flammability. For bio-based materials, the approach of the application of phosphorus- and nitrogen-based flame retardants is well established, due to synergetic effect between both components to promote char formation. Moreover, there are bio-based options for these type of flame retardants, which fits the nature of the vegetal wools.

Among the possible options, phytic acid is a promising phosphorus flame retardant, due to its bio-based origin and high percentage of phosphorus content (approximately 28% by weight). For nitrogen, urea seems to be a good fit due to its availability and price. Moreover, urea can contribute to swelling the fiber and facilitating the penetration of phosphorus and protecting the fiber against the acidity of phytic acid.

Between radiation and chemical grafting application methods, the latter was considered more adapted for the vegetal wools application, as it does not require specific equipments and facilitates easier upscaling. Then, two methods of chemical grafting were identified: by immersion and pulverization. The approach of immersion of vegetal wools in a solution containing flame retardants has been widely studied and can be considered an effective method. The pulverization method has been explored in a few studies, and although it appears to be a simple and effective approach, it requires further investigation, particularly regarding its homogeneity, efficiency, and scalability, key factors for a fireproof treatment at an industrial scale.

Independently of the application method, the most important parameter that directly influences the fire reaction parameters of the material is the phosphorus content after grafting. An amount of 0.5% to 1.0% has been shown to significantly reduce the flammability of bio-based materials, and even promoting a self-extinguishment behavior.

The treatment may lead to modifications not only in the chemical structure of lignocellulosic fibers but also in their microstructure, therefore affecting the functional performances of the vegetal wools. However, this possible impact has not been widely studied, and the link between the effects of the flame retardants in the micro-scale with the macro-scale acoustic and thermal performances has not been understood. As a multifunctional material, the relationship and integration between all properties are very valuable, and, for the case of vegetal wools, it needs more attention.

Therefore, it is important to characterize and evaluate treated and untreated hemp wools, with the goal of understanding the modification that it may cause on the material and how it could affect the functionality of the material. Experimental testing and modeling methods are fundamental tools to support the analysis.

Finally, the durability of fireproof treated vegetal wools is also questioned, particularly with regard to the biological aspects. Since phosphorus and nitrogen compounds are usually considered to be nutriments for the synthesis of nucleic acids, proteins and enzymes, and the chemical composition of lignocellulosic fibers are known to be a substrate for the development of many fungi species, the fireproof treatment of these fibers with phytic acid and urea could create favorable conditions for fungi proliferation. However, recent studies have shown that phytic acid can inhibit the fungal growth of certain species, which requires more investigation, especially in vegetal wools, but indicates a possible dual effect of phytic acid as a flame retardant and antifungal agent.

1.10.2 Objectives of the thesis

Based on the objectives outlined in the introduction of this thesis and the literature review presented in this Chapter, some questions have been answered, while others remain unanswered.

The flame retardants to be used for the fireproof treatment of fibers were defined. Phytic acid and urea are solid choices for the treatment of bio-based materials, because of their synergistic effect and their ability to promote char formation.

Two potential application methods were identified: through immersion and pulverization. The immersion method is commonly found in the literature and its efficacy is confirmed. However, it was observed that the studies usually treated small quantities of fibers, which makes it uncertain for large-scale application. The pulverization method, on the other hand, was not used in many studies, and their homogeneity, efficacy and scalability are questionable. Therefore, in order to select the ideal application method for the fireproof treatment of vegetal wools, they need to be investigated.

Then, independently of the method chosen, many parameters of the fireproof treatment will remain undefined. Therefore, the next objective consists of optimizing the treatment, while considering the production methods of vegetal wools and their fire reaction performances.

This thesis also aims to characterize the acoustic and thermal performances of hemp fiber and hemp wools, both before and after the application of the flame-retardant treatment. In addition, the microstructure of the materials will be investigated to identify potential modifications induced by the fireproof treatments, and their effects on the materials' functional properties.

In addition, the aim is to develop a durable material that is not susceptible to the development of fungi. Phytic acid and urea provide nutriments for fungi development, but fungi growth inhibition effect associated with phytic acid have been observed. This will be assessed for the characterization of the biological durability of the material after being treated.

Finally, the primary objective of this thesis is to validate the chosen methodology at an industrial scale, through the fabrication of fireproof treated hemp wools, using an optimized treatment method and assessing its effects on the material's acoustic and thermal performances.

Chapter 2

Materials and methods

For the development of fireproof treated hemp wools and to achieve the objectives of this thesis, the study is structured across three scales. The first scale focuses on the raw materials, specifically hemp fibers, which constitute the main component of the hemp wools, representing 90% of their weight. This part is presented in Chapter 3. The next scale involves the hemp wool prototypes. At this level, the hemp wools were manually prepared, and all analyses performed on them are presented in Chapter 4. Finally, at the industrial scale, hemp wool panels were produced using an industrial process, as presented in Chapter 5. The thesis organization is illustrated in Figure 2.1.

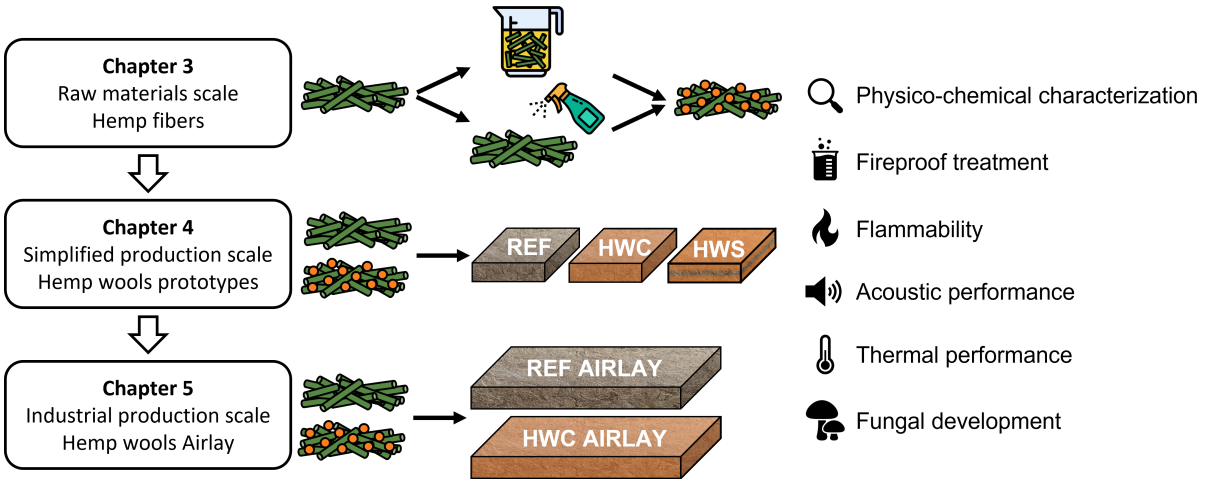

Figure 2.1: Scheme of thesis organization

In this Chapter, a description of the constituents of the vegetal wools, including the hemp fibers, thermoplastic fibers and flame retardants used for the fireproof treatment are presented in Section 2.1. The methods used for the analysis of the morphology and the physico-chemical characterization of the hemp fibers and wools are presented in Section 2.2. Then, the tests used for the characterization of the flammability, acoustic and thermal performances are presented in Sections 2.3, 2.4 and 2.5, respectively. Finally, the methods used for the evaluation of the sensitivity of hemp fibers and wools to the fungal development are presented in Section 2.6.

2.1 Formulation of vegetal wools

2.1.1 Hemp fibers

The hemp fibers used in this study were obtained from the company Agrochanvre, located in France. The fibers underwent the process of retting (Section 1.2) and cleaned, reducing the amount of unwanted hemp shives, that affect the quality of the hemp fibers as a raw material. The fibers presented a brownish coloration, as shown in Figure 2.2a.

The hemp fibers used for the hemp wools production came from another bale, but they were also provided by Agrochanvre, France. The fibers were retted and cleaned, presenting a good quality and a small quantity of hemp shives (Figure 2.2b). All the fibers used came from one single bale.

2.1.2 Thermoplastic fibers

The thermoplastic fibers consisted of a bi-component fiber (Trevira 256, Germany) that is commonly used for the fabrication of hemp wools (Figure 2.2c). They have a diameter of about 18 µm of diameter and are composed of poly(ether-sulfone) (PES) at their core, and copolyethylene (coPE) at the sheath. The melting point of the sheath is 127°C and the core is 256°C. During the process of manufacturing the hemp wools, the fibers are heated at temperatures above the melting point of the sheath material, which melts it and binds it with the hemp fibers, after cooling down. Therefore, thermoplastic fibers act as a binder in hemp wools, consisting of 10% of the hemp wools weight.



(a) (b) (c)

Figure 2.2: Constituents of the hemp wools: (a) Loose hemp fibers; (a) Hemp fibers used for hemp wools production; (b) Thermoplastic fibers

2.1.3 Flame retardants: phytic acid and urea

The flame retardants used in the fireproof treatment of the hemp fibers and wools consisted of using phytic acid (CAS: 83-86-3) in solution 50 wt.%, and urea (CAS: 57-13-6, purity $> 99.5\%$), shown in Figure 2.3.

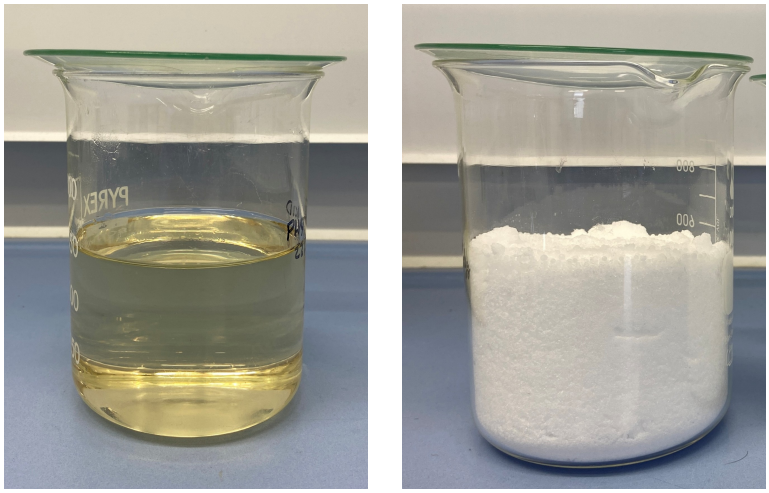

(a) (b)

Figure 2.3: Flame retardants used for fireproof treatment: (a) Phytic acid; (b) Urea.

2.2 Morphology and physico-chemical characterizations

In this Section, the tests involving the morphology and physico-chemical characterization of hemp fibers, thermoplastic fibers and hemp wools are presented. These tests were performed at the laboratory MAST/CPDM, from Université Gustave Eiffel, except for the airflow resistivity test that was performed at Cerema.

2.2.1 Homogeneity test

The immersion method ensures that all fibers come into contact with the solution, making it a homogeneous application method. However, such homogeneity cannot be guaranteed with the pulverization method. To assess this, a homogeneity test was conducted by spraying a colorant over the fibers. The amount of colorant used correspond to the mass ratio of 1, as it would be if the fibers were being treated with a flame retardant solution. The hemp fibers were spread on a surface, with half of the colorant applied to one side and the other half on the opposite side.

2.2.2 Weight and solid skeleton density variation

The weight evolution due to the grafting of the phosphorus and nitrogen molecules on the fibers, was measured before and after the application of the fireproof treatment, using a Mettler Toledo scale. The fibers were dried in oven at 60°C until constant mass before and after treatment, and their weight was measured. The results were expressed as percentages of the initial mass.

Subsequently, the fiber's solid skeleton density was measured, using the helium gas pycnometry method. The measurements were performed with a Micrometrics Accupyc II gas pycnometer (Figure 2.4). The method consists of adding a certain mass of fiber inside a recipient with a previously known volume. A second recipient is used as a reference, and both are filled with an inert gas (helium or nitrogen). By comparing the volume with and without the fibers inside the recipient, the equipment can provide the density of the fibers. For this test, a recipient with a volume of 100 cm^3 was used, and 17±1 g of fibers.

For hemp wool samples, the weight variation was assessed by measuring the weight of the cylindrical samples with 100 mm of diameter and 100 mm of height, and comparing it

with the reference. The weight variation is reported as the modification in the apparent density of these samples, given by Equation 2.1.

$$\rho_{ap} = \frac{m}{V_{ap}} \tag{2.1}$$

where ρ_{ap} is the apparent density; m is the measured mass; V_{ap} is the apparent volume, determined from measurements obtained with a caliper.

The solid skeleton density of the hemp wools samples followed the same protocol, but two different atmospheres were tested: under nitrogen and helium.

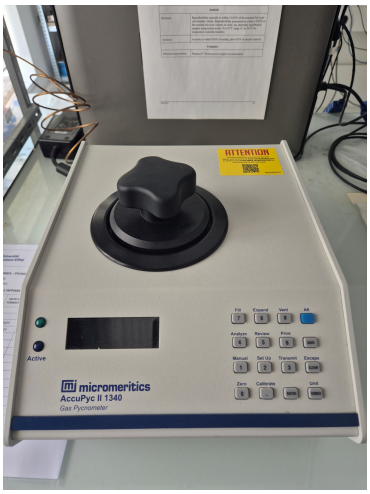

Figure 2.4: Gas pycnometer equipment

2.2.3 Fiber morphology observation

Hemp fiber morphology observations were made with a digital microscopy, model Keyence VHX-X1 (Figure 2.5). It allowed the observation of the overall physical aspect of the fibers before and after the treatment, such as their coloration and the surface's aspect and also, to search for particles of flame retardants that could remain on the fiber's surface after the treatment.



(a) (b)

Figure 2.5: Digital microscope

2.2.4 Fiber diameter

For the determination of the fiber's diameter before and after being fireproof treated, five fiber bundles for each treatment condition, with 5 cm of length each, were placed in a transparent plastic. The fibers were straightly placed but without being tensioned, as seen in Figure 2.6. Pictures were taken every 0.5 cm of each fiber, starting from the position 0.5 cm and ending in the position 4.5 cm. The pictures were taken with a digital microscope described in Section 2.2.3. The exact same fibers were fireproof treated, using the same methods and conditions as the hemp fibers used for the other tests. The measurement of fiber diameter was made before and after treatment, in the same position, and the relative variation was reported.

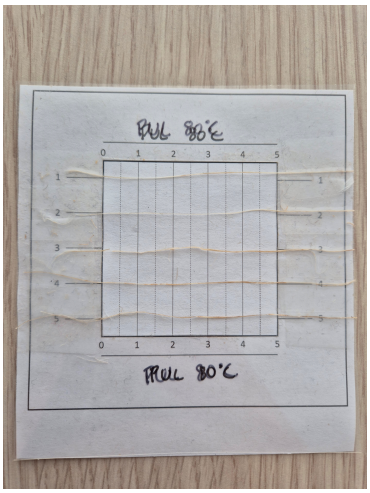

Figure 2.6: Setup for fiber diameter measurement

2.2.5 Airflow resistivity

Airflow resistivity (σ) (Section 1.4.2) is a parameter that measures a sample's resistance to airflow passage through it, following the standard ISO 9053-1:2018 (AFN18). The airflow resistance meter Mecanum SIGMA SIG2014 (Figure 2.7) was used. The equipment applies increments of airflow velocity and measures the pressure difference on both sides of the sample. Using Equation 2.2, it calculates the airflow resistivity.

For the hemp fiber analysis, the samples have 100 mm height and 100 mm diameter, with apparent densities varying between 30, 60 and 90 kg.m^{-3}, and stayed in the same room as the equipment for at least 72h before the test, to stabilize the temperature and water content of the hemp fiber samples. The room conditions were at 23.5±0.5°C and 40±5% of relative humidity. To hold the samples in place for the test, and avoid them falling, a metallic mesh was used in the bottom of the samples.

The hemp wool samples used for this test were assessed for apparent density before testing by weighting and measuring their dimensions with a caliper. The samples consisted of cylinders with 100 mm diameter and 40 mm height. They were placed in the measurement room for at least 72h before the test, with a temperature of 24.2 ± 0.3°C and a relative humidity of 36 ± 2%. A total of 4 measurements were made, one for each sample prepared and all hemp wool treatment conditions were evaluated.

For both hemp fibers and wools, 4 measurements were made for each treatment condition, and all conditions were assessed. The airflow resistivity is then calculated as shown in Equation 2.2.

$$\sigma = \frac{\Delta P A}{Q L} = \frac{\Delta P}{v L} \tag{2.2}$$

where ΔP is the pressure differential across the test sample; A is the surface area; Q is the measured volumetric flow rate; L is the sample's thickness; v is the airflow speed.



Figure 2.7: Air resistivity-meter equipment

2.2.6 Tortuosity

The tortuosity of the hemp wool samples was measured using an ultrasonic method for porous materials saturated by air, with the equipment Mecanum ultrasonic tortuosity-meter (Figure 2.8). The measurements were performed with the device in transmission configuration, in which the equipment measures the acoustic propagation time of laser-generated acoustic pulses. The first measurement is performed without the material, and the second with it. Due to the presence of the material, the acoustic pulse is retarded and its amplitude is reduced. Based on that, the phase velocity can be measured and used to calculate the tortuosity (ALL94; MOU01).



Figure 2.8: Ultrasonic tortuosity-meter equipment

2.2.7 Quantification of phosphorus content

The amount of phosphorus grafted onto the fibers, is one of the most important parameters influencing their fire performance. It was quantified using inductively coupled plasma atomic emission spectrometer (ICP-AES). The model used consists of the ULTIMA 2000

from Jobin Yvon Horiba Company (Figure 2.9a). The ICP-AES is a method that can be used to measure certain elements that are extracted from the fibers, and in the case of this study, the phosphorus element was analyzed.

As described by Hou et al. (HOU16), this technique is based on adding the sample to the instrument, where it is converted into an aerosol directed into the central channel of the plasma. The aerosol is quickly vaporized, as the ICP's core sustains a temperature of about 10000 K. Subsequently, the atoms are energized by radio frequency discharges, promoting the ions to excited states, which is followed by relaxation to the ground state, emitting a photon. Each photon has a characteristic energy, and the wavelength of them can be used to identify the elements from which they were originated.

In this thesis, the method was performed by attacking 0.30 g of fibers with 15 ml of nitric acid (CAS: 7697-37-2) and 15 ml of distilled water. The acid mineralized the fibers and extracted the phosphorus molecules that were grafted. The fibers and the solution were heated to 100°C and mixed under magnetic stirring for 4 hours (2.9b). After that, the mineralization was completed and the solution was filtered and diluted to 1.0 L (Figure 2.9c). Then, the diluted solution passed through the equipment, where a small quantity of the sample got in contact with the plasma, created from argon gas, exciting the atoms and emitting radiation energy when returning to their ground state.

The energy emitted from the samples was compared with reference samples, used for the calibration of the equipment, containing 1 ppm and 2 ppm of phosphorus molecules. With these samples, the equipment can estimate the concentration of phosphorus molecules present in the solution analyzed. At least 3 samples were collected from each hemp fiber specimen.

In the case of hemp wools, samples from the core and surface of the hemp wool panel have been taken for each treatment condition. By doing so, it was possible to compare the amount of phosphorus grafted in the different parts of the panel, and evaluate the homogeneity of the test.



(a) (b) (c)

Figure 2.9: ICP-AES procedure: (a) ICP-AES equipment; (b) Acid attack under magnetic stirring; (c) Filtration.

2.2.8 Chemical characterization of hemp fibers

Fourier transform infrared spectroscopy (FTIR) of the hemp fiber samples was used to identify the modification of the chemical structure of the hemp fibers before and after the fireproof treatment. The analyzes were performed using a Thermo Scientific Nicolet iS20 (Figure 2.10), with the Attenuated Total Reflection (ATR) sampling technique.

Before analysis, the samples were dried in oven at 60°C for 72h. A small sample of hemp fibers was manually compacted to reduce the empty spaces between fibers, and positioned in the equipment for analysis. Before each analysis, background spectra were obtained and subtracted from the fibers' spectra. A total of 32 scans were made for each sample in the range between 625 and 4000 cm^{-1}, with a spectral resolution of 0.25 cm^{-1}.



Figure 2.10: Fourier transform infrared spectroscopy equipment

2.2.9 Mass loss through thermogravimetric analysis

The thermal properties of the fibers were assessed by thermogravimetric analysis (TGA) (Figure 2.11). The TGA allows quick evaluation of the thermal behavior of the fibers, by thermally degrading them in a controlled environment. Through this test, the effects of the flame retardant can be observed, such as the earlier thermal degradation and the increase in the amount of residue, as explained in Section 1.6.2. In this research a model TA Instruments SDT650 was used. An amount of 15±3 g of fibers was used for each test, which started at 30°C up to 800°C, with a heating rate of 10°C.min^{-1}. The test was performed in an inert environment, with nitrogen gas, as well as in air, an oxidative environment. At least 3 measurements were made for each specimen condition.



Figure 2.11: Thermogravimetric analysis equipment

2.3 Flammability characterization

As presented in Section 1.6.3, the Euroclass classification takes into consideration multiple aspects of the fire reaction behavior of a material, such as its flammability, flame-spread, smoke production, the presence of flaming droplets and the acidity of released gas. However, the majority of the tests used to characterize all these properties are expensive and only available at a few specialized facilities.

Therefore, the tests used in this thesis allow the assessment of these fire reaction properties, but on a material scale, providing information about the general behavior of the flammability of hemp fibers and hemp wools. The tests used were the single-flame source test, Mass Loss Cone calorimeter (MLC) and smoke density test, performed at the Materia Nova laboratory.

2.3.1 Ignitability of hemp fibers and hemp wools

The single-flame source was used to assess the ignitability of the hemp fibers, following the standard EN ISO 11925–2:2020 (ISO20). A sample holder (Figure 2.12b) was used to contain the hemp fibers and create a sample with dimensions of 250 mm in height, 90 mm width and 30 mm thickness. This sample is placed inside a chamber (Figure 2.12a) and is mounted vertically. A flame with 2 cm of height and 45° inclination, gets in contact 2 cm above the base of the sample (Figure 2.12c). The flame was kept for 15s and the sample was observed for 60s after the beginning of the test. The flame burns the sample vertically and the height of the burned area is measured. In addition, it is observed whether the material continues to burn even after the flame is removed. At least 3 measurements were made for each specimen condition. For hemp wools, only those manufactured using the airlay method were tested and each condition was tested 12 times.

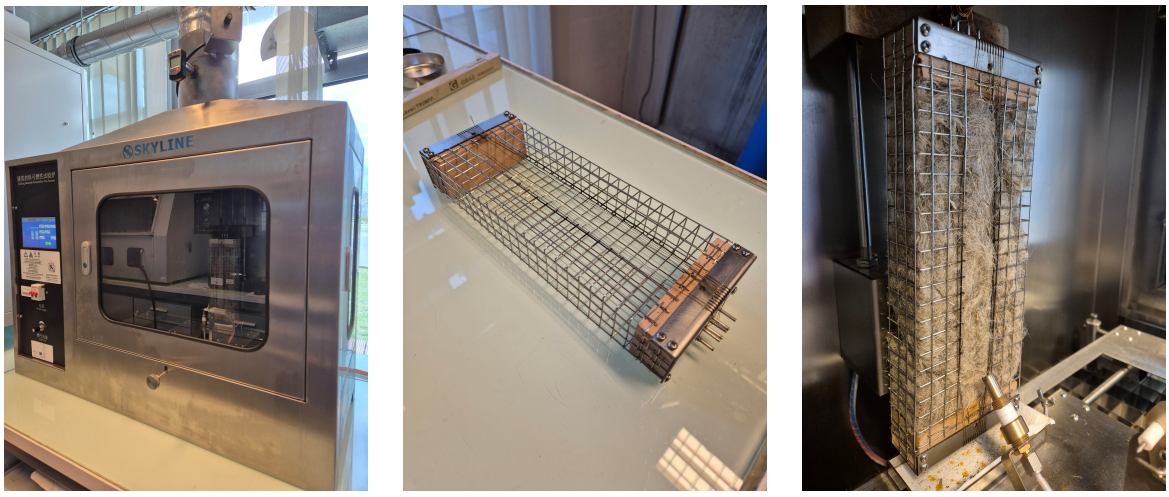

(a) (b) (c)

Figure 2.12: Single flame source test: (a) Chamber; (b) Sample holder; (c) Sample and flame position.

2.3.2 Fire reaction characterization

The Mass Loss Cone calorimeter test (Figure 2.13b) is one of the most effective tests to study the fire behavior of natural fibers on a material scale. The tests were performed with a cone calorimeter from FTT, Ltd., East Grinstead, West Sussex UK, equipped with a thermopile and chimney for heat release assessment, according to the ISO 17554:2014

- Reaction to fire tests standard (ISO14). The peak of heat release rate (pHRR), the total heat release (THR), the time to ignition and mass loss were determined during the test. The principle of the test is based on the measurement of an electrical signal by thermopiles, previously calibrated with different methane combustion flow rates.

Hemp fibers samples (Figure 2.13a), with the dimensions of 100x100x40 mm^3, and density of 60±2 $kg.m^{-3}$, were heated with a heat flux of 35 $kW.m^{-2}$. The combustion gases produced are captured by an exhaust duct system, filtered and released. At least 3 measurements were performed for each specimen. In the case of hemp wools, all samples were tested, including HWC, HWS, airlay and references. A total of 7 measurements were made for each condition. Figure 2.13c shows an ongoing test.



(a) (b) (c)

Figure 2.13: Cone calorimeter test: (a) Hemp fiber sample; (b) Cone calorimeter equipment; (c) Ongoing test.

For the verification of the calibration and correct functioning of the equipment, before each testing series, a reference sample made of polypropylene (PP) is tested. This sample has 3 mm of thickness and is produced by adding the polypropylene pellets in a 100x100x3 mm^3 mold (Figure 2.14a), and compressing it under heat. A temperature of 190°C and a pressure that starts at 20 bars and goes up to 150 bars are used. A Figure of the sample is presented in (Figure 2.14b). The PP sample is tested and it needs to have a time to ignition close to 60s and a peak heat release rate of 1000 ± 100 $kW.m^{-2}$. If it meets these criteria, the tests on the equipment can proceed.

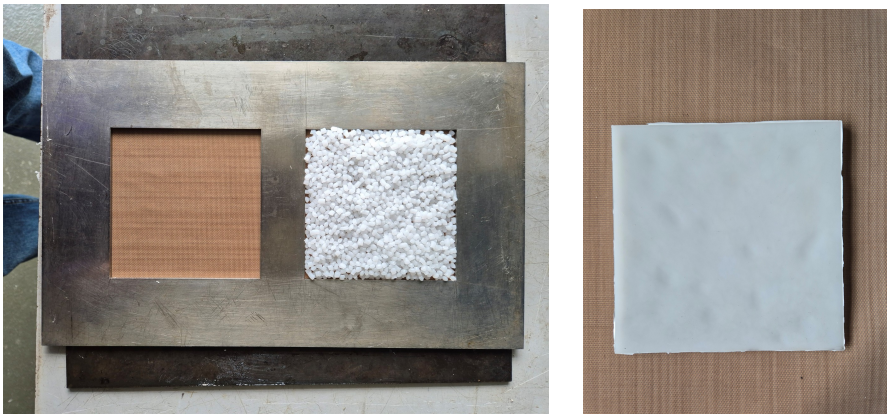

(a) (b)

Figure 2.14: Polypropylene sample preparation: (a) 100x100x3 mm^3 mold; (b) PP sample.

2.3.3 Smoke density

The smoke density test, also known as the Exit Sign Smoke Test, is standardized by ASTM D2843:2022 (AST22). In this test, there is a source of light on one side of a chamber, and a light receptor on the opposite side (Figures 2.15a and 2.15b). The receptor measures the opacity caused by the smoke of the sample that is burned inside the chamber, being an indicative parameter of the visibility of an environment in the event of a fire. The receptor is calibrated with lenses of 25%, 50%, 75% and 100% opacity before the test (Figures 2.15d and 2.15e). Moreover, the chamber contains an Exit sign in the back of the chamber, which can also serve as a visual reference for the opacity during the test. A sample of 4 g of hemp fiber was placed inside a chamber (Figure 2.15c), and it is continuously burned during the 4 minutes of test. During this time, smoke is released and the opacity is measured. The test ends after 4 minutes, and the ventilation system is activated.

For the hemp wools test, the mass of the samples was reduced to 2 g, as it was verified that this amount of material was enough to produce comparable results between the samples. Only the hemp wools fabricated by airlay had their smoke density production assessed.

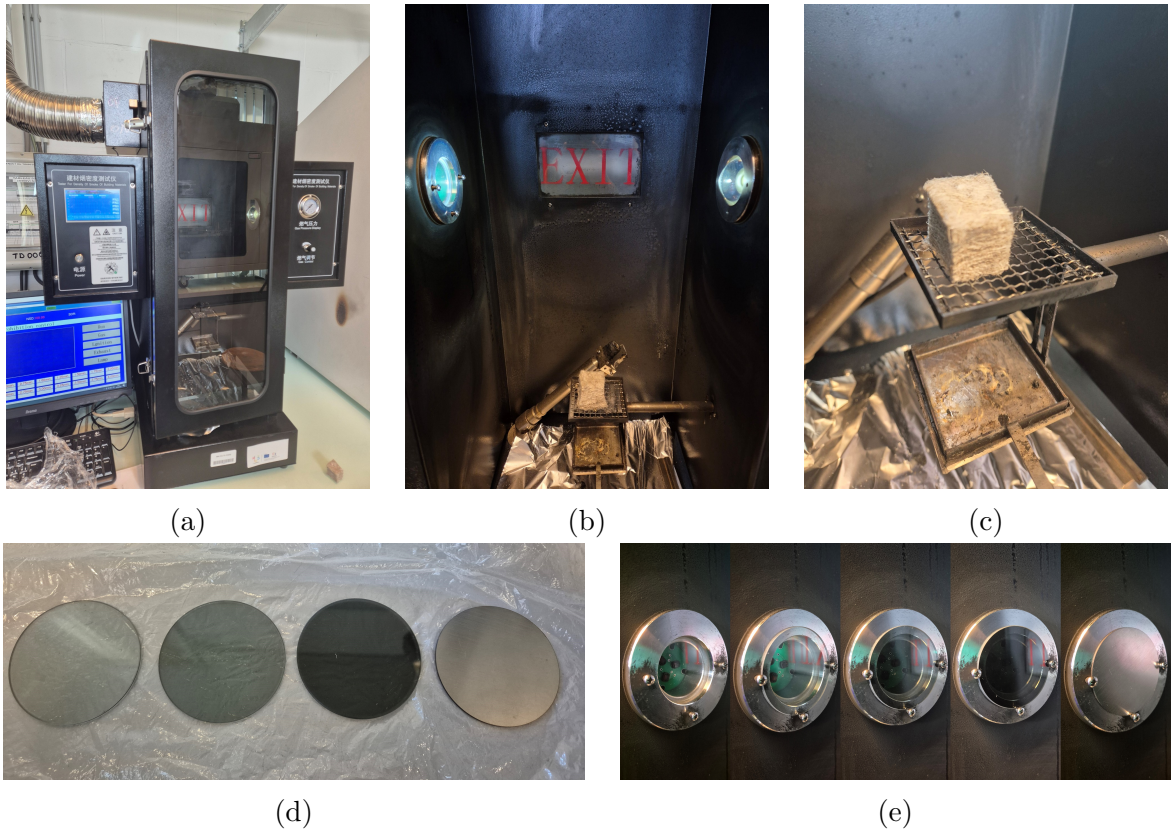

(a) (b) (c)

(d) (e)

Figure 2.15: Smoke density test: (a) Equipment; (b) Inside view; (c) Sample placement; (d) Calibration lenses with 25%, 50%, 75% and 100% of opacity; (e) Calibration lenses placed in front of the light sensor

2.4 Acoustic characterization

As seen in the literature review, the vegetal wools excel in absorbing sound, being an excellent material for acoustic correction (Section 1.4). However, with the application of a fireproof treatment and the possible associated modifications on the microstructure of

the fibers, the characterization of the hemp fibers and wools before and after treatment becomes fundamental for the understanding of the impacts of the treatment. The acoustic characterization of the hemp fibers and wools was performed at the facilities of Cerema.

The impedance tube, also known as the Kundt tube, is an equipment used to measure the acoustic properties of materials, including the sound absorption coefficient (α) (Section 1.4) and other intrinsic parameters, following the standard ISO 10534-2:2023 (AFN23).

It consists of a metallic tube with a sound source in one extremity and a rigid termination on the other end, which is considered to have an infinite impedance. A model Akustik Forschung – AcoustiTube AFD 1200 (Figure 2.16a), was used in this research. The tube's diameter was 100 mm and the frequency domain of measurements was in the range between 143 and 1993 Hz. The acoustic properties of the hemp fibers were measured using a wave at normal incidence and a three microphones configuration, which was initially developed by Iwase *et al.* (IWA98) and adapted by Salissou *et al.* (SAL10), by creating a cavity and placing the third microphone outside the impedance tube. This configuration allows the determination of intrinsic parameters of the material such as the dynamic density (ρ) and the dynamic bulk modulus (K), from the calculation of the characteristic impedance (Z_c) and wave number (k), as presented in Section 1.4.

In the case of hemp fiber testing, the samples have 100 mm of height and 100 mm of diameter (Figure 2.16b and 2.16c), with apparent densities of 30, 60 or 90 kg.m^{-3}. Before the test, the samples were placed in the room where the test was performed, in order to stabilize the water content and the temperature. The room conditions were at a temperature of 23.5±0.5°C and 40±5% of relative humidity. For each condition, 4 measurements were made, from both sides of the 2 samples prepared.

The difference between the hemp fibers and the hemp wools test lies in the sample's characteristics. In the case of the hemp wools, samples had 100 mm of diameter and about 40 mm of height, which were measured before each test. The apparent density of each sample was also measured, by weighting and measuring the dimensions with a caliper. Before each test, the samples were also placed in the same room as the measurements for at least 72h prior to being tested. The room conditions were of 24.2 ± 0.3°C and 36 ± 2%. The impedance tube test was made with all hemp wool samples. A total of eight measurements were made for each treatment condition, from both sides of the 4 prepared samples.



(a) (b) (c)

Figure 2.16: Impedance tube test: (a) Equipment; (b) Hemp fiber sample; (c) Sample inside the sample holder.

2.5 Thermal characterization

The thermal performance of the hemp wools are one of their main functional properties as an insulation material (Section 1.5). To assess the influence of the fireproof treatment on hemp fibers and wools, two tests were performed. The hot disc test presented in Section 2.5.1 was performed at Cerema, and the guarded hot plate presented in Section 2.5.2 was performed at Cetelor.

2.5.1 Thermal conductivity, diffusivity, and specific heat capacity on a transient state heat flux

Thermal conductivity, diffusivity, and specific heat capacity were measured by the Hot disc test, based on the standard ISO 22007-2:2015 (ISO22). This method is based on the transient plane source (TPS) and is used to measure the thermal conductivity of specimens with 0.01 to 500 $W.m^{-1}.K^{-1}$, being, therefore, adequate for natural fibers and vegetal wools. The equipment used is the model Hot Disk TPS 3500 (Figure 2.17a).

The equipment consists of a heating element probe made of a nickel spiral that is placed between two sheets of insulator of negligible specific heat. An electric current of constant power flows through the probe for a predefined period of time and heats it. The increase in temperature is measured over the time by the probe, which acts simultaneously as a sensor and a source of heat (Figure 2.17b). After that, it calculates the thermal conductivity, diffusivity and specific heat capacity of the material.

In this study, the hot disc sensor was placed between two specimens of hemp fibers (Figure 2.17c) with dimensions of 100 mm diameter and 50 mm height. During the test, the samples are placed inside a black metallic cover (Figure 2.17d), to reduce potential convective effects with the outside environment. The specimens have been tested for apparent densities of 30, 45, 60 and 90 $kg.m^{-3}$. Before each test, the fibers stayed at least 72h at the same conditions (temperature of 20.5°C ± 0.5°C and relative humidity of 43% ± 3%) of the laboratory, where the test was performed. At least 3 measurements were made for each specimen condition.

In the case of hemp wool analysis, the samples stayed in the same room where the test took place for at least 72h before the test, at temperatures of 23.8°C ± 0.1°C and relative humidity 31% ± 1%. For each measurement, the sensor was placed between two samples. Each treatment condition had 4 samples, therefore, samples 1 and 2 made one measurement, and samples 3 and 4 made a second measurement. Each pair of samples was measured five times. Each time, the position of one of the sides was inverted, to avoid any patterns in the result. The apparent density considered from each measurement, is the average from both samples that were tested. The results are expressed by the average of the 5 measurements of each pair (due to differences in the apparent density), and by the average of the 10 measurements from each condition.



(a) (b) (c)



(d)

Figure 2.17: Hot disc test: (a) Equipment; (b) Sensor over a hemp fiber sample; (c) Samples place on top of each other, with the sensor in between; (d) Black metallic cover.

2.5.2 Thermal conductivity on a steady-state heat flux

The guarded hot plate test is another test for the assessment of thermal conductivity of panels. This test is standardized by ISO 8302:1991 (ISO91). This test is based on the steady-state heat flux, where the sample is placed between a hot plate and a cold plate. The temperatures of the hot and cold plates from the equipment were set to 20°C and 0°C, respectively. The heat flows in one direction through the material and is measured by the electrical power supplied to maintain a steady-state.

In this study, this test was performed on samples of hemp wool panels with dimensions of initially 30x30x4 cm^3. Before testing, the panels were dried in oven at 60°C. To ensure that all the surface of the panels touched the plates, the height of 35 mm was used. Only one measurement for each condition was performed due to time limitation required to perform the test.

2.6 Sensibility to fungal development tests

As presented in Section 1.9, the biological durability of bio-based materials is often questioned, as their cellulose, hemicellulose, and lignin components are susceptible to fungal attack and subsequent growth. This concern increases with the application of a phosphorus-



Figure 2.18: Hemp wool samples inside the climate chamber

and nitrogen-based flame retardant, since both elements can be synthesized by the fungi to produce nucleic acids, proteins and enzymes. The tests performed in this thesis aim to identify the fungi that are naturally present in hemp fibers and verify their development under favorable conditions of temperature and humidity and in the condition of contamination. The tests presented in this Section were performed at the MAST/CPDM laboratory.

2.6.1 Fungal growth

At a first moment (T0) the fungi naturally present in every hemp fibers and hemp wools samples were identified. The treated hemp wool samples were divided into core and surfaces, to assess the homogeneity of the fungi development along the thickness of the panels prototypes.

After that, some samples were selected for incubation for the analysis of fungi growth in favorable environmental conditions. The samples selected were HF REF, HW REF, HWC 5%, HWC 10%, HWS 5% and HWS 10%, and were considered to be sufficient to assess the influence of the flame retardants on the fungi development. These samples were placed in individual boxes inside a climate chamber (Figure 2.18) at 30°C and 80% of relative humidity, for the duration of three months (T3) and six months (T6). The fungal growth was assessed by visual inspection of each sample and by the fungal extraction procedure described in the following Section.

2.6.2 Fungal extraction

The fungal extraction test was performed before (T0) and after incubation (T3 and T6). It was used to assess the presence of fungi colonies with potential to grow in the hemp fiber and hemp wool samples. This procedure was coupled with digital microscope imaging (see Section 2.2.3) to observe the fungi morphology and identify the species.

Before the test, a culture medium was prepared using 27 g of dehydrated potato dextrose mixture, 15 g of agar and 1 liter of distilled water. The culture medium was sterilized for 15 minutes at 121°C and 1 atm in an autoclave. Once cooled, the medium was poured into sterile Petri dishes with diameter of 90 mm for solidification.

To extract the molds from hemp fiber and hemp wool, a Stomacher® 400 Circulator

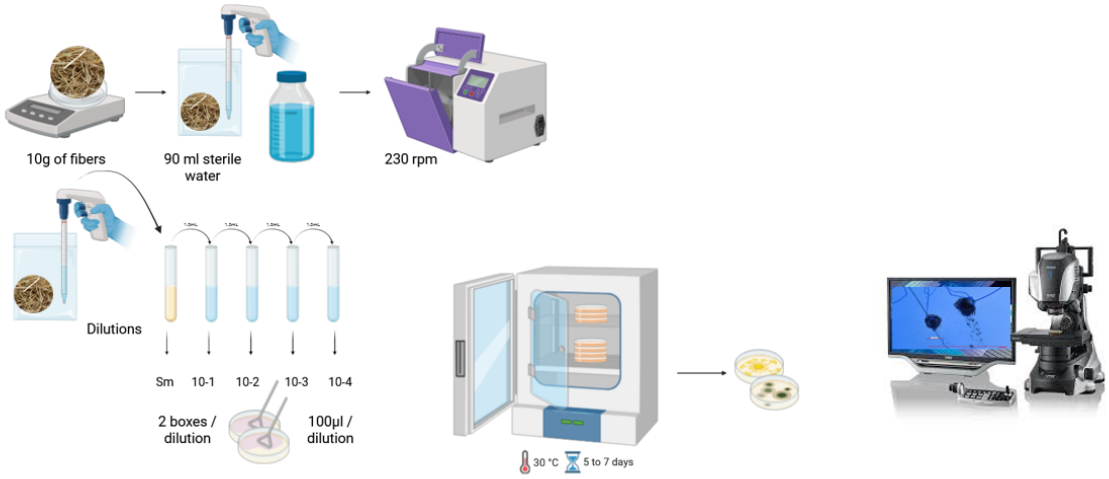

Figure 2.19: Schematic representation of the fungal extraction procedure

(Seward) was used. This method has previously been used by Delannoy et al. (DEL18). The equipment applies fast agitation, and is equipped with paddles that apply pressure in the pouches, forcing the extraction. The test protocol consisted of placing 10 g of hemp fiber or hemp wool in a sterile stomacher bag with 90 ml sterile water. The samples were agitated on stomacher equipment at 230 rpm for two minutes. After that, the liquid was collected and used to inoculate the Petri dishes filled with culture medium, which were incubated 30°C for 5 to 7 days.

After incubation, the molds were identified by macro- and microscopic observation. For microscopic observations, a scotch tape was used to remove the mold, and a drop of lactophenol blue was added for better microscopic visualization. The microscope used was the Keyence digital microscope presented in Section 2.2.3. A schematic representation of the fungal extraction test is illustrated in Figure 2.19.

2.6.3 Fungal impregnation

To evaluate fungal development in the case of an external contamination, hemp wool samples were impregnated with two species of fungi. This is an extreme approach that is not representative of the usual conditions found in buildings, but useful to identify the role of the flame retardants on fungal growth.

Two different methods were used, a wet and a dry methods, based on a method presented by Deborde (DEB25). The wet method involved the pulverization of a solution contaminated with the fungi *Penicillium spp.* or *Stachybotrys chartarum*, on the surface of the hemp wool samples. These samples were placed inside a closed recipient with small holes in the bottom (Figure 2.20). Another recipient filled with 2 to 3 cm of water was placed below the recipient containing the impregnated samples, with the goal to create a saturated environment, favoring the development of fungus. The humidity inside the recipient is estimated to be around 90% to 95% and the incubation phase took place during 28 days, inside a climate chamber at 30°C and 80% of relative humidity.

The second method involved the pulverization of the fungal spores, therefore, it is a dry method. A solution contaminated with *Penicillium spp.* and another with *Stachybotrys chartarum* stayed inside a closed bottle for a few days. During this time, the air inside the bottle was filled with the spores of these fungi. Using an air pump, these spores were pulverized over the hemp wool samples. After that, the samples were placed inside the same type of recipient as described in the previous paragraph, with the second recipient placed below, filled with water, to saturate the air inside and promote fungi growth (Figure



Figure 2.20: Setup with two recipients for the impregnation test

2.20). These samples were also incubated inside the same climate chamber at 30°C and 80% of relative humidity for 28 days.

In both methods, a Petri dish filled with the culture medium was pulverized in the same condition as the hemp wool samples, in order to verify the existence of contamination. Each week a picture was taken through the cover of the recipients, without opening them. After 28 days, a picture was taken without the cover and the quantification of the colonies was performed.

Chapter 3

Raw materials scale: Hemp fibers

As introduced in the outline of this thesis, this Chapter presents the first step toward the development of flame-retardant hemp wools (see Figure 3.1). Its main objective is to identify a fireproof treatment that both preserves the intrinsic properties of the hemp fibers and is suitable for industrial-scale application. The chapter is structured into four parts, as illustrated in Figure 3.2.

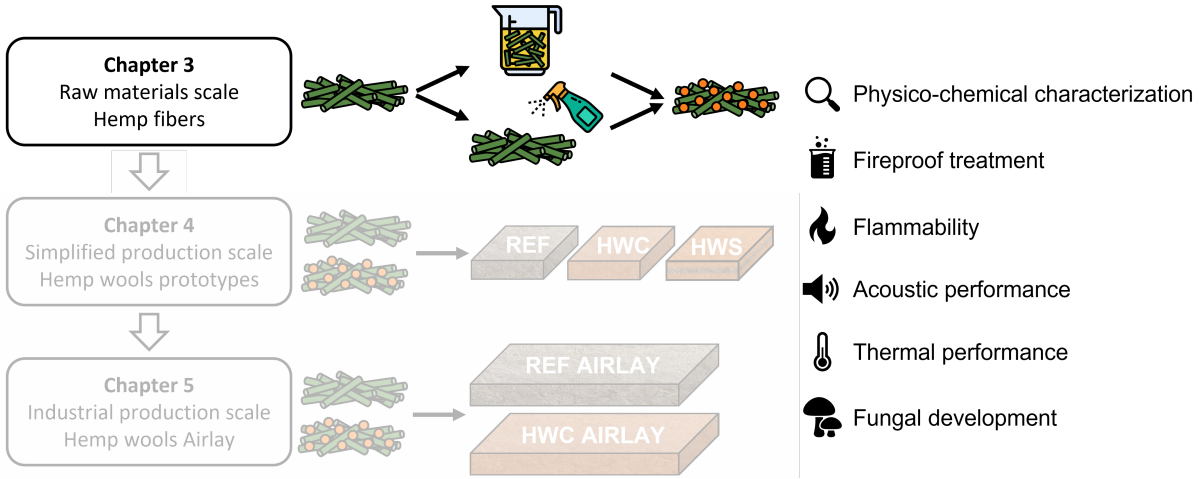

Figure 3.1: Scheme of thesis organization

In the literature review, it was observed that the fireproof treatment based on phytic acid and urea was an efficient method of reducing the flammability of bio-based materials. Taken into consideration the application of the vegetal wools as an insulation material for buildings, it is important that the treatment method be suitable for large scale production. Two application methods were identified: immersion and pulverization.

Therefore, these two methods need to be evaluated considering the treatment scalability as well as their effects on the bulk hemp fibers physico-chemical and flame-retardant properties. This evaluation is presented in the first Section 3.1 of this Chapter, which correspond to an article published in the Journal of Industrial Crops and Products, volume 228, in June 2025.

The literature review also highlighted that the acoustic properties of fibrous materials are strongly influenced by their microstructure and pore geometry. Therefore, the second part of this Chapter (Section 3.2) addresses the impact of phytic acid and urea treatment, applied through immersion and pulverization methods, on the acoustic performance of hemp fibers as well as the underlying mechanisms responsible for this impact. This work has been submitted to the Journal of Applied Acoustics.

The third part (Section 3.4) focus on the characterization of the thermal conductivity of hemp fibers, after the application of the fireproof treatment using the methods of

immersion and pulverization.

Finally, since the treatment consisted of phosphorus and nitrogen molecules, the durability of the material may be examined with respect to the potential development of molds. As highlighted in the literature review (Section 1.9.2), these molecules can be nutriments for fungi. Therefore, a study on the presence, identification and development of fungi was conducted in treated and untreated hemp fibers and is presented in Section 3.5.

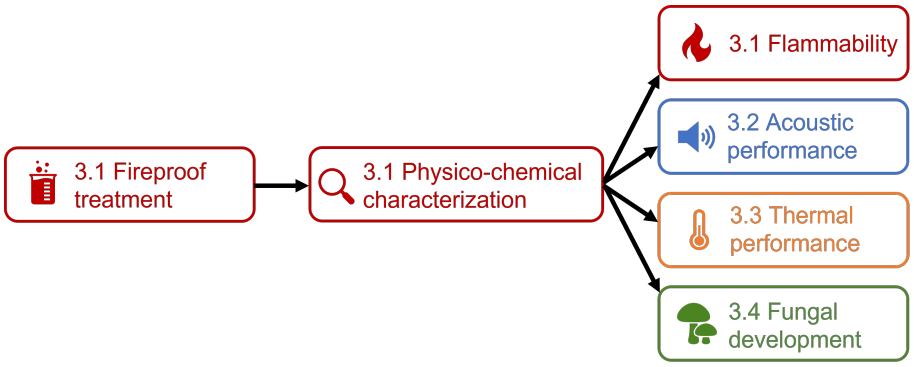

Figure 3.2: Parts of the Chapter 3

3.1 Article: Comparison of two flame-retardant treatment methods on bulk hemp fibers: towards a large-scale viability as a raw material for building insulation

Thomas Schatzmayr Welp Sá[1,2], Sandrine Marceau[1], Clément Piégay[2], Philippe Glé[2], Fouad Laoutid[3], César Segovia[4], Etienne Gourlay[5]

[1] CPDM, Université Gustave Eiffel - 14-20 Boulevard Newton, F-77454, Marne-la-Vallée, France
[2] Cerema, Université Gustave Eiffel, UMRAE - 11 Rue Jean Mentelin, F-67035, Strasbourg, France
[3] Laboratory of Polymeric and Composite Materials, Materia Nova Research Center - University of Mons (UMONS) - Av. Nicolas Copernic 3, 7000, Mons, Belgium
[4] CETELOR - Université de Lorraine, 27 Rue Philippe Seguin, 88051, Epinal, France
[5] Cerema, Equipe-recherche BPE - 11 Rue Jean Mentelin, F-67035, Strasbourg, France

Abstract

The high flammability of bio-based insulation materials derived from plant fibers is a major barrier to their widespread use, necessitating the development of effective flame-retardant treatments. This study aims to optimize the treatment of raw hemp fibers by comparing two environmentally-friendly application methods: immersion and spraying. The fibers are treated with a solution containing phytic acid and urea, as biobased sources of phosphorus and nitrogen. The efficiency of the treatments is assessed by characterizing the quantity of phosphorus grafted, the thermal degradation of the fibers by thermogravimetric analysis and their flammability using a mass loss calorimeter. Both application methods are effective, but the spraying method demonstrated superior performance, resulting in a higher level of phosphorus grafted to the fibers and a reduced heat release rate. Additionally, the formation of a protective char layer on the fiber surface helps to limit

flame propagation. Notably, this method requires ten times less treatment product than immersion, making it a highly scalable and efficient solution for the industrial production of flame-retardant insulating materials.

Keywords: *hemp fibers, bio-based material, flammability, fireproof treatment*

3.1.1 Introduction

The benefits of using bio-based materials in construction are numerous. They range from environmental aspects, linked to carbon capture and low-processing and low-energy intensive solutions (ARE21; GAL22; PIT21; ZIE20), to technical aspects, due to high-level performance in terms of acoustics (BER15; CHA16; PIE21) and hygrothermics (AMZ17; COL11; KOR16; MOU19). For building insulation, for example, lignocellulosic fibers provide multi-functional features that make them a strong alternative to conventional solutions.

However, the main drawback of natural lignocellulosic fibers is their high flammability (FRE14; KOZ20). During the thermal decomposition of bio-based materials, there is formation of levoglucosan, that decomposes into reactive species, which reacts with the oxidizing agent (usually the oxygen in the air) (HAJ20). Therefore, it fuels the combustion reaction maintaining and propagating the flame (see Figure 1). To overcome this problem, the use of flame-retardants (FRs) is needed. Different types of FRs are available and widely investigated for this purpose such as minerals, halogenated, phosphorus-based, nitrogen-based, silicon-based and nanometric compounds (COS17; MOR13; TAI22). Among these options, the phosphorus-based flame retardants seem to be one of the most promising, as they are considered to be non-toxic, unlike the halogenated ones, and can act by forming a carbonaceous layer (char) during thermal degradation and combustion of bio-based materials, reducing their flammability (COS17; HAJ20; KOZ20). This carbonaceous structure acts as a physical barrier, reducing the heat diffusion through the material, the oxygen penetration, the volatilization of combustible compounds and the flame spread (COS17; TAI22). This is illustrated in Figure 1. Furthermore, there are bio-based sources of phosphorus, such as phytic acid, which can be found in seeds and grains, which aligns with the purpose of working with bio-based materials (DAN13).

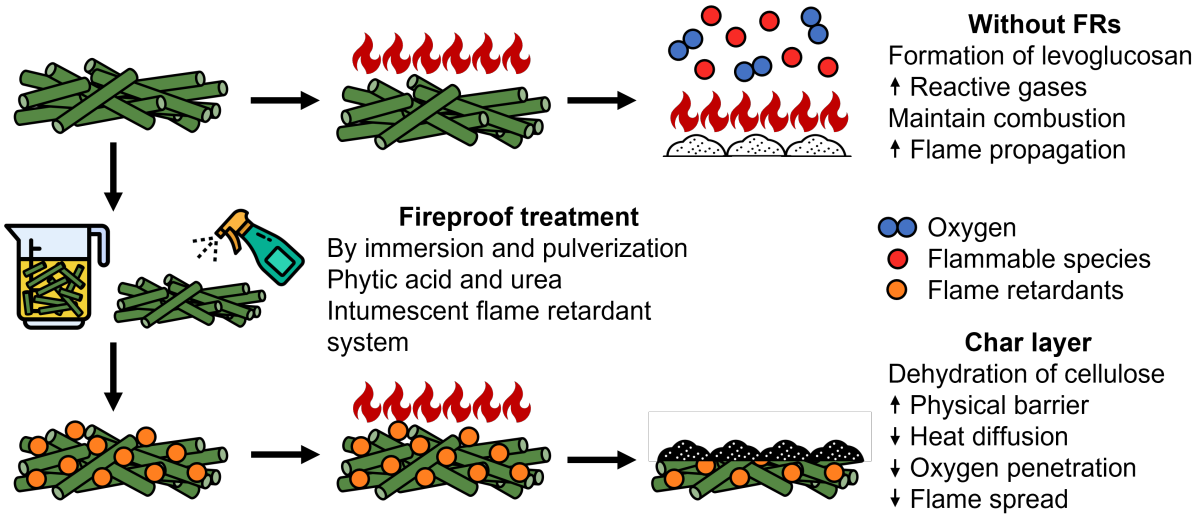

Figure 1: Scheme of the flame retardancy mechanism

The flame retardancy of phosphorus compounds can be improved by the combination with nitrogen-based products to form an intumescent flame retardant system (COS17; LAO09). Nitrogen flame retardants release gases when thermally degrading (COS17;

MOU20), which can lead to an expansion of the char layer, which will improve the protection of the lignocellulosic fibers against burning by reducing heat transfer between the heat source and the material's surface, and limiting the fuel transfer and the oxygen diffusion (LAO09). The synergism between phosphorus and nitrogen compounds have been previously explored and shown to be an interesting approach to reduce the flammability of bio-based materials (ANT22; MOU20; SYK21; TAI22; ZHA19).

Different techniques can be used for binding the phosphorus to natural fibers (HAJ18; KOZ20; TEI18). One of them consists in chemically grafting phosphorus through fiber immersion in a solution, followed by heating to activate covalent reaction and finishing by washing and drying steps (ANT22; DOR14; HAJ18; MOU20). Research has shown that reduced flammability of lignocellulosic fibers is directly associated with the phosphorus content achieved by the treatment (ANT22; HAJ18; MOU20; TAI22). Therefore, high phosphorus levels lead to improved char formation and lower flammability.

This immersion technique has proved effective in phosphorous grafting and flammability reduction (ANT22; DOR14; HAJ20; MOU20). However, given its multiple steps and demands for time, energy, and materials, it is important to assess its scalability for large-scale applications. The Table 1 presents the fireproof treatment details on natural fibers, by immersion, performed by studies found in the literature. Most of the studies treated low amount of fibers, and required some type of pre-treatment, increasing the number of steps, time and materials used. Furthermore, among the flame retardants used, only the phytic acid is considered to be a bio-based source of phosphorus, which corresponds well with the nature of vegetal fibers.

Table 1: Characteristics of the fireproof treatment by immersion

Type of fiber	Quantity treated	Phosphorus FR	Mass ratio FR/fiber (%)	Pre-treatment	Source
Flax	50 g	DAP[1], PA[2] and APP[3]	2.5-10	Removal of waxes and pectin with ethanol	(DOR14)
Flax	0.25 g	VPA[4]	400	-	(HAJ18)
Miscanthus and flax	0.25 g	C6, C8, C10 biphosphonic acids and VPA[4]	400-800	Removal of extractives with toluene/ethanol	(HAJ18)
Hemp	10 g	HEDP[5]	130	Steam explosion and bleaching	(MOU20)
Hemp	10 g	Phytic acid	3-7	Steam explosion and bleaching	(ANT22)

[1] Dihydrogen ammonium phosphate
[2] Phosphoric acid
[3] Ammonium polyphosphate
[4] Vinyl phosphonic acid
[5] 1-Hydroxyethylidene-1,1-diphosphonic acid

An alternative method, less frequently discussed in the literature (DEB23), involves applying flame-retardants via pulverization. This technique appears to require fewer resources and less time, but its efficiency and practical feasibility needs further investigation due to limited application reports.

The studies carried out to date have demonstrated the efficiency of the treatments used, but only on a few grams of fibers. There is a need to develop treatments that can be applied on an industrial scale to hemp fiber insulation materials, and to evaluate the impact of this treatment on their hygrothermal and acoustic performance. This is the

final objective of this research. Therefore, the first stage of this work is to compare two flame-retardant treatment techniques for fireproofing: one considered as the traditional method by immersion, and an alternative by pulverization. The objective is to optimize the treatment process for bulk hemp (Cannabis sativa) fibers, without any binder, with a focus on scalability for large-scale applications.

3.1.2 Materials and methods

3.1.2.1 Materials description

Bulk hemp fibers that were used for the evaluation of the two fireproof treatment methods have been obtained from AgroChanvre (France). These fibers have been previously retted and a portion of them can be seen in Figure 1a. The untreated hemp fibers used as reference are named as REF. For the treatment, a phytic acid (CAS: 83-86-3) in solution with a concentration of 50% in mass, and urea (CAS: 57-13-6, purity $>$ 99.5%) were used. Nitric acid (CAS: 7697-37-2) 65%, was also used for to perform the spectroscopy (ICP-AES) analysis.

3.1.2.2 Treatment

Before the treatment, the solution used was prepared by manually mixing 10 wt.% of phytic acid and 30 wt.% of urea, for 5 minutes, with distilled water. Two methods of application have been tested: by immersion and pulverization on 300 g of fibers. In the end of the treatment and before doing the following tests, the fibers had their water content and temperature stabilized at room temperature of 21$\pm$2°C and relative humidity of 35$\pm$5%.

The immersion method is based on previous works (ANT22; DOR14; HAJ20; MOU20), but has been adapted, for potential industrial-scale applications, by reducing the number of steps and simplifying the whole procedure. In this method, the fibers were fully immersed in the solution (see Figure 2a), at a solution-to-fiber mass ratio of 10 for 1 hour at room temperature. This method ensured a homogeneous application of the flame retardants in all fibers. Following immersion, the fibers were oven-dried at either 80°C or 120°C for 2 hours. They were then washed and dried in an oven at 60°C. Fibers treated by this immersion method are labeled IMM 80°C or IMM 120°C.

The pulverization method consisted on applying the solution with a spray, shown in 2c. This approach required significantly less solution than the immersion method, needing only enough to evenly coat the fibers. A solution-to-fiber mass ratio of 1 was determined to be sufficient for effective treatment without soaking. The fibers were spread out on a surface (Figure 2b) with half of the solution sprayed on one side. They were then flipped and the remaining solution was sprayed on the other side. After the application, the fibers were heated in an oven at either 80°C or 120°C for 2 hours, followed by drying at room temperature. Fibers treated by the pulverization method are labeled PUL 80°C or PUL 120°C.

3.1.2.3 Homogeneity test of the pulverization method

The homogeneity of the pulverization method was evaluated by the application of a blue-colored solution over the hemp fibers, simulating the same procedure as the application of the flame retardants. The fiber to solution mass ratio was of 1. 10 g of fibers were spread in a surface, and half of the solution was applied in one side of the fibers, and half of the solution on the other side. The homogeneity of the treatment was evaluated by a visual inspection.

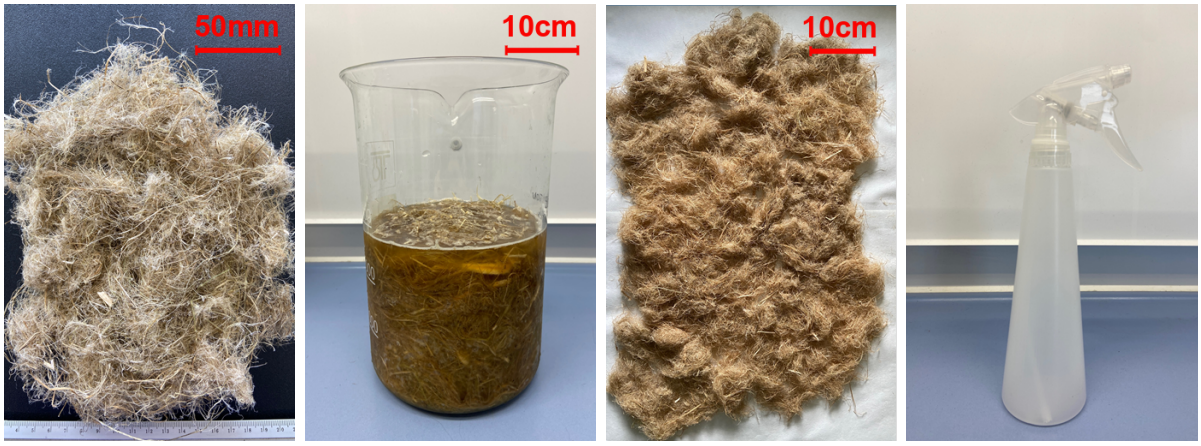

(a) (b) (c) (d)

Figure 2: Materials and treatment methods (a) Bulk hemp fibers; (b) Immersion method; (c) Pulverization method; (d) Spray used for pulverizing the solution

3.1.2.4 Weight, real density and fiber diameter assessment

To determine weight gain or loss after the treatment, the fibers were oven-dried and weighted before and after the treatment. A Mettler Toledo scale with a precision of 0.01 g was used to weight the material. The procedure consisted of drying the fibers at 60°C until constant mass, which was obtained until their mass variation from 3 measurements, obtained from 3 consecutive days, were lower than 0.5%. The same procedure was repeated after the treatment, and the results are reported as a percentage of the initial mass. The true density of the hemp fibers was determined using a Micrometrics Accupyc II helium gas pycnometer, with fibers pre-dried under the same conditions as described above.

Additionally, the diameter of five fiber bundles from each treatment condition was measured every centimeter along its length, both before and after the treatment. Measurements were taken on fiber bundles rather than individual fibers. To do so, fiber segments of approximately 5 cm in length were positioned straight, without tension, and images were captured every 0.5 cm using an optical microscope and a ruler, to identify the position. The evaluations of the fiber diameter were made using ImageJ software.

3.1.2.5 Fourier transform infrared spectroscopy (FTIR)

The Fourier-transform infrared spectroscopy spectra of all samples were obtained by a Thermo Scientific Nicolet iS20, using an Attenuated Total Reflection (ATR) sampling technique. Before analysis, the hemp fibers were dried in an oven for 3 days at 60°C. A small sample of hemp fibers was manually compacted to reduce the empty spaces between fibers, and positioned in the equipment for analysis. Before each analysis, the background spectra were obtained and subtracted from the fibers' spectra. A total of 32 scans were made for each sample in the range between 625 and 4000 cm^{-1}, with a spectral resolution of 0.25 cm^{-1}. The spectra are presented only up to 2000 cm^{-1}, in order to focus the analysis on the wavenumber range of interest.

3.1.2.6 Phosphorus content

The phosphorus content of treated fibers was determined using inductively coupled plasma atomic emission spectroscopy (ICP-AES) model ULTIMA 2000 from Jobin Yvon Horiba Company. Prior to ICP-AES analysis, 0.3 g of hemp fibers were digested using a nitric acid/distilled water (50/50) solution for 4 hours at 100°C, under magnetic stirring. The

remaining solution was filtered, and the phosphorus concentration was determined using calibration curves obtained from ICP-AES analysis of standard solutions at different concentrations. The test was repeated 10 times.

3.1.2.7 Thermal degradation

The thermal degradation of the treated and untreated fibers was assessed by thermogravimetric analysis (TGA) from TA Instruments model SDT650. Samples of 15±3 mg were heated from 30°C to 800°C, at 10°C.min^{-1}, under air. Three samples were tested for each condition, to ensure repeatability.

3.1.2.8 Fire reaction

Three different tests were used to characterize the fiber's reaction to fire. In all of them the samples weighted 24 g, which indicates an apparent density of 60 kg.m^{-3}. The single flame-source test was used to assess the ignitability of the hemp fibers, following the standard EN ISO 11925-2 (ISO20). The sample was burned for 15 seconds and is observed during 60 seconds after the test begins. The height of the burned area was measured and three samples were tested for each condition.

The mass loss calorimeter test ISO 5660-1 (ISO15) was used to quantify the flammability of the hemp fibers. The samples used had dimensions of 100x100x40 mm^3, and they were exposed to a heat flux of 35 kW.m^{-2}. This test provides numerous comparable parameters regarding the flammability of a materials: time to ignition (TTI), heat release rate (HRR), peak HRR (pHRR), total heat release (THR) and mass loss rate were measured. This test was repeated four times for each condition.

A smoke density apparatus was also used to assess the effects of the treatment on smoke opacity, following the ASTM D2843 (AST22). Samples of 4 g of hemp fiber were burned during 4 minutes and the opacity of the air in the chamber was measured. The results are reported as a curve of the absorptivity versus time. This test was repeated 2 times.

3.1.3 Results and discussion

3.1.3.1 Homogeneity test

Images of the hemp fibers before and after the homogeneity test are shown in Figure 3. Figure 3a shows the raw hemp fibers spread in a surface before the application of the colorant. Then, Figure 3b shows the aspect of the fibers after full application of the colored solution on both sides. Even though the small amount of solution used (fiber to solution mass ratio of 1), it can be seen that an evenly spread of the colored solution is achieved.

3.1.3.2 Physical properties

The results for the mass and diameter variations after flame retardant treatments are reported in Table 2. All treated samples showed an increase in mass after the treatment. The weight increase of the immersed fibers was 3.2% for IMM 80°C and 5.1% for IMM 120°C. In contrast, the pulverized samples exhibited a much higher weight increase, with gains of 14.3% for PUL 80°C and 12.8% for PUL 120°C. These differences are due to the different finishing methods applied during treatment. In fact, since immersed fibers are washed, non-grafted phosphorylated molecules are removed and only covalently bonded molecules remain. On the contrary, pulverized fibers are not washed, and thus the weight

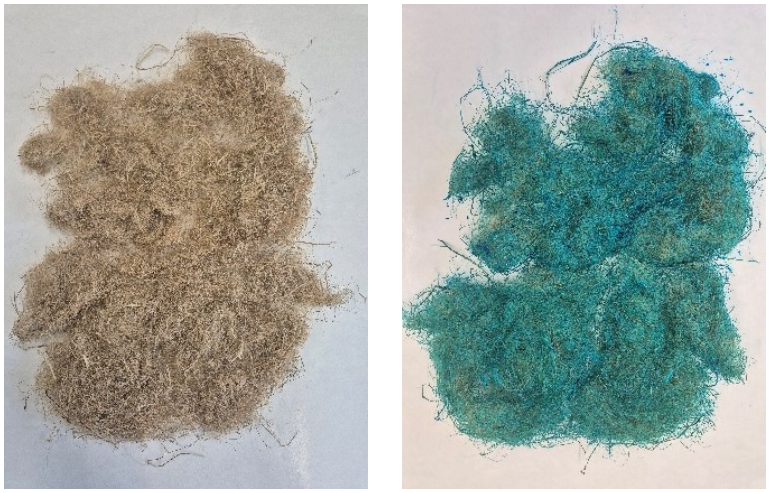

(a) (b)

Figure 3: Homogeneity test (a) Bulk hemp fibers before spraying; (b) Fibers after full application of the colorant

increase is higher and correspond to the initial reagents amount used, grafted and non-grafted.

Another reason behind the difference in mass increase observed between the immersed and pulverized fibers, was identified by measuring the mass change on a sample (REF W 80°C) that underwent the same treatment steps as the immersed fibers, but without the use of the flame retardants. In other words, the fibers from this sample were immersed in water for 1 hour, then were heated at 80°C and were finally washed and dried. This sample allowed the assessment of the effects of water immersion, heating and rinsing alone. A 5% mass decrease was observed, attributed to the partial removal of waxes, pectin, and ashes. Therefore, the actual weight increase due to phosphorus grafting in the IMM 80°C and IMM 120°C samples is higher than the measured values.

Even with the weight increase from the treated hemp fibers, the real density of them barely changed, and no significant differences were found. All fibers presented a density near 1.50 g.cm^{-3}, which are in accordance with the literature (PER15). In theory, considering that the fibers are shaped as a perfect cylinder, with a height h, a diameter d, a mass m and a density ρ, the fiber's density can be expressed as the Equation 1.

$$d = 2 \cdot \sqrt{\frac{m}{\pi \cdot h \cdot \rho}} \tag{1}$$

As the treated hemp fiber mass increased and their real density remained the same or slightly decrease, a diameter increase is expected. By considering the mass and the density variations of the treated samples, and that the fiber's height is big enough so it does not change when the fibers are treated, the Equation 1 gives the expected percentage increment of the diameter from the treated samples, when compared to the reference fibers. The samples IMM 80°C, IMM 120°C, PUL 80°C and PUL 120°C presented an expected diameter increase of 1.5%, 3.3%, 7.2 % and 6.7%, respectively.

In order to verify this phenomenon, images of the same hemp fibers were made before and after the treatment. Figure 4 illustrates two examples of diameter measurement, with images taken before (4a and 4c), and after (4b and 4d) treatment. In both cases, the marks on the fibers show that they did not twist or shift during treatment, allowing precise location of the measured positions. That was, however, not always the case. Frequently, the fibers shifted, twisted, or separated from their bundles after being treated, making the comparison between them difficult. Two examples are shown in Figure 5, where Figure

5a and Figure 5c show two images made before treatment, and Figure 5b and Figure 5d show two images made after treatment. In both cases, it is possible to see that the fibers rotated their position when compared to their initial position (indicated by the arrows), which caused a large difference in their diameter when observed from the microscope. Like those cases, measurements were excluded if the fiber's position was unclear before and after treatment, or if fiber bundles had attached or detached in certain areas. Additionally, fibers that were visibly twisted were also excluded, as they are not perfectly round and this affected measurement accuracy. For each condition, 45 measurements were taken, with about half discarded for these reasons.

Morphological analysis of the fiber bundles evidences that the treated samples generally showed a diameter increase of 6% and 8%, in respect to their initial size, except for sample IMM 80°C, which showed no change. These results are shown in Table 2, alongside their standard error. However, significant variation between measurements led to a high standard deviation, limiting the relevance of comparisons among treated samples despite careful measurement protocols. Despite this, the overall trend of diameter increase suggests an effect of the treatment on fiber morphology.

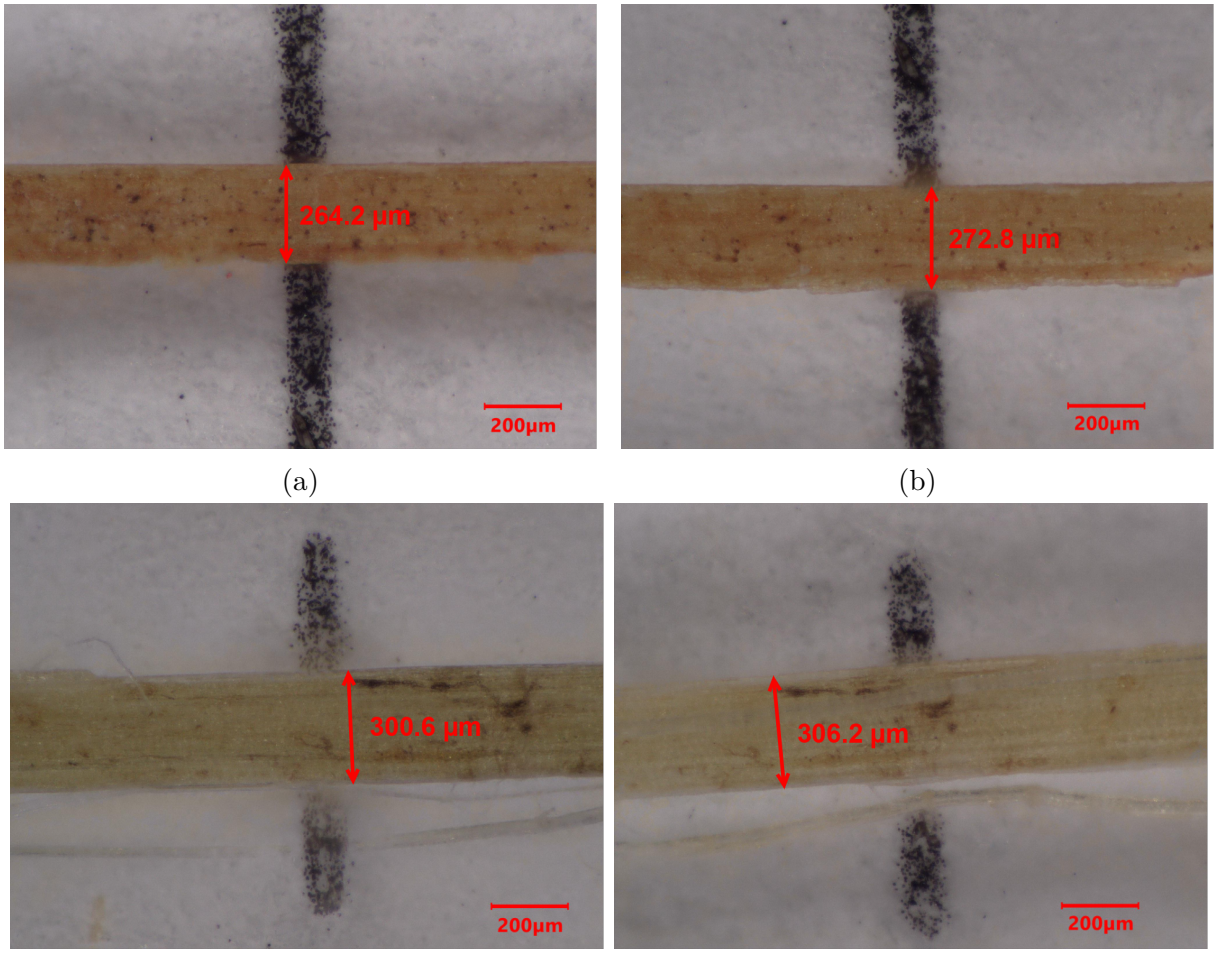

Figure 4: Example of measurement of fiber diameter. (a) and (c) Before the treatment; (b) and (d) After the treatment

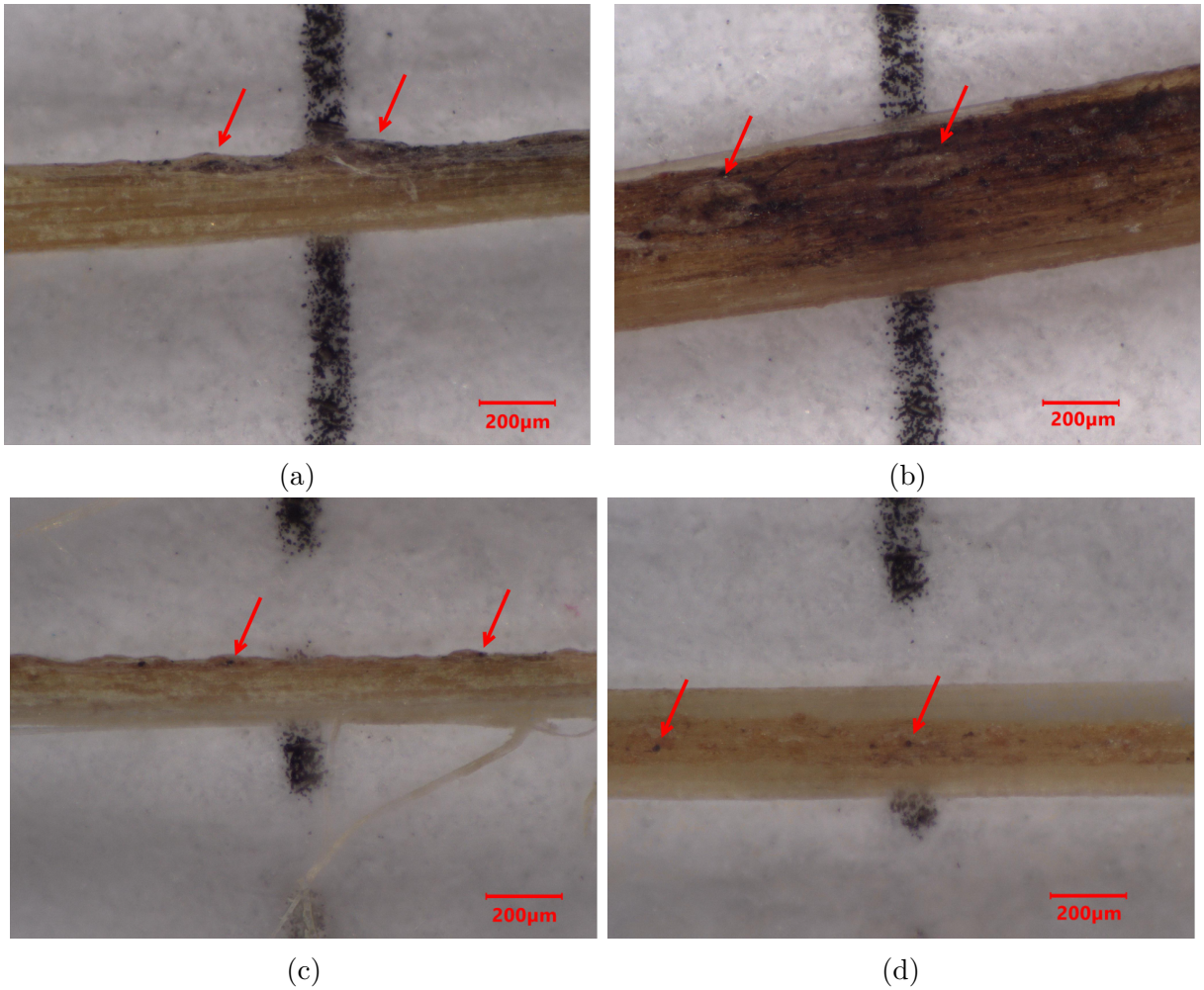

(a) (b)

(c) (d)

Figure 5: Example of a discarded measurement of fiber diameter. (a) and (c) Before the treatment; (b) and (d) After the treatment

Table 2: Mass and fiber diameter change

Sample	Mass variation (%)	Diameter variation (%)	Real density ($g.cm^{-3}$)
REF	-	-	1.503±0.004
REF W 80°C	-5.0±0.7	-1±5	-
IMM 80°C	3.0±0.8	0±5	1.504±0.002
IMM 120°C	5.1±1.7	6±6	1.479±0.003
PUL 80°C	14.3±4.6	8±4	1.496±0.003
PUL 120°C	12.8±2.4	6±3	1.489±0.002

3.1.3.3 Fourier transform infrared spectroscopy analysis

The FTIR-ATR spectra from all hemp fiber samples are presented in Figure 6. The treated samples were compared to the reference to identify the changes in the spectra after the treatment. The peaks linked to the bonds between plant fibers and phytic acid are indicated with a dashed line in the Figure. At 790 cm^{-1}, a bond between phosphorus, oxygen and carbon was identified (TAI22). The peaks at 1240 cm^{-1} and 1450 cm^{-1}, correspond to the P=O bonds absorption (LIS15; MAR15; TAI22). The presence of these peaks confirms the formation of covalent bonds between the phosphorus molecules from the phytic acid and the cellulose and hemicellulose from the hemp fibers. The peak 1630 cm^{-1} originates from the N-H bonds, which comes from the use of urea as a flame

retardant (MAR15).

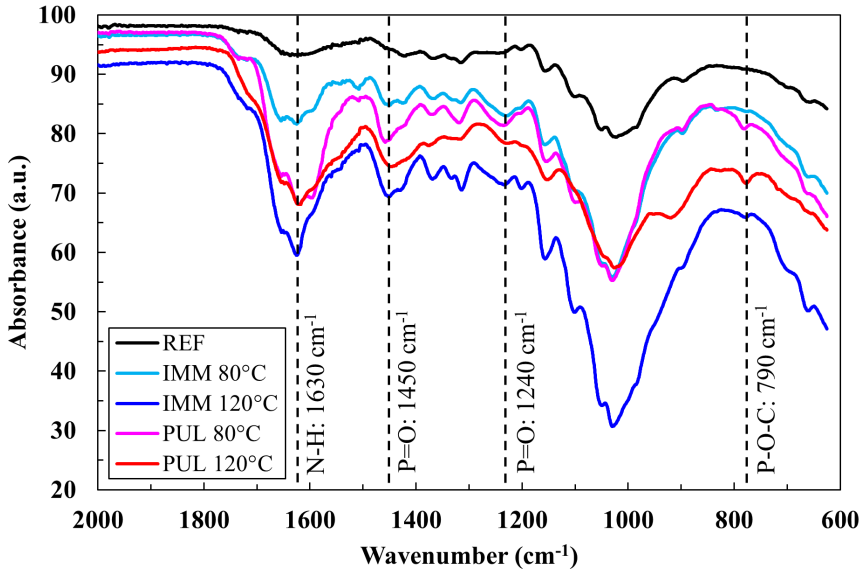

Figure 6: FTIR spectra of treated and untreated hemp fibers

3.1.3.4 Phosphorus content

A significant decrease in the hemp fibers flammability is expected with the grafting of phosphorus, as presented by Antoun et al. (ANT22). Therefore, the fiber's phosphorus content was measured and the results are reported on Table 3. The fibers treated by immersion, at 80°C and 120°C, presented a phosphorus content of 0.61% and 0.66%, respectively. A paired t-student test showed that both phosphorus contents are statistically similar between themselves. The fibers treated by pulverization achieved a higher phosphorus concentration, reaching 1.85% and 1.56%, for the fibers treated at 80°C and 120°C, respectively. The higher phosphorus content presented by the pulverization method, in comparison with the immersion method, was explained by the absence of washing at the end of the treatment.

3.1.3.5 Thermal degradation

The thermal degradation curves of the hemp fibers and their derivatives are presented on Figures 7 and 8, revealing two main stages of mass loss. For the reference fibers, degradation starts at 230°C, corresponding to the breakdown of the hemicellulose fraction, due to its low crystallinity and reduced thermal stability (DOR14; YAN07). This is followed by the cellulose degradation, which continues up to 380°C. Then, a second mass loss takes place between 380°C and 500°C, corresponding to a further degradation of products formed in the initial stage, known as humins (BAU21). The lignin does not have an evident peak as it degrades gradually in multiple stages between 150°C and 700°C (COS17; ZHA14).

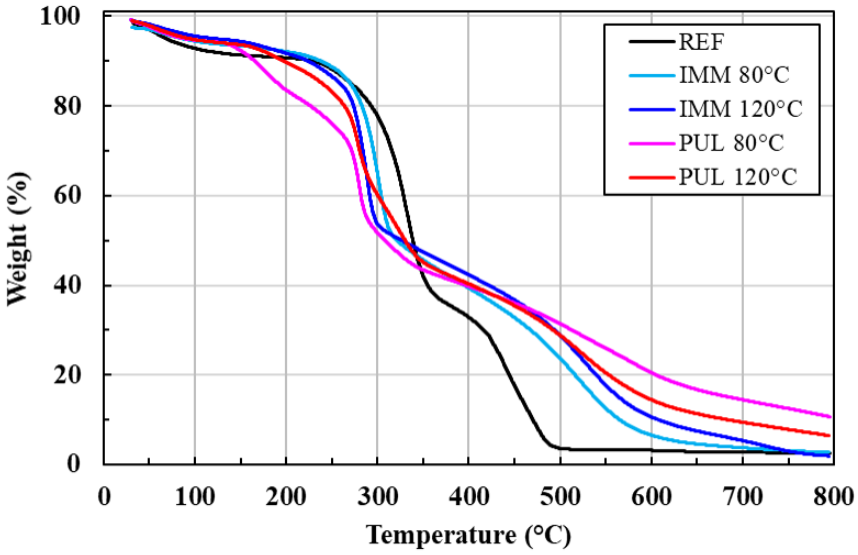

Figure 7: TGA curves from treated and untreated hemp fibers

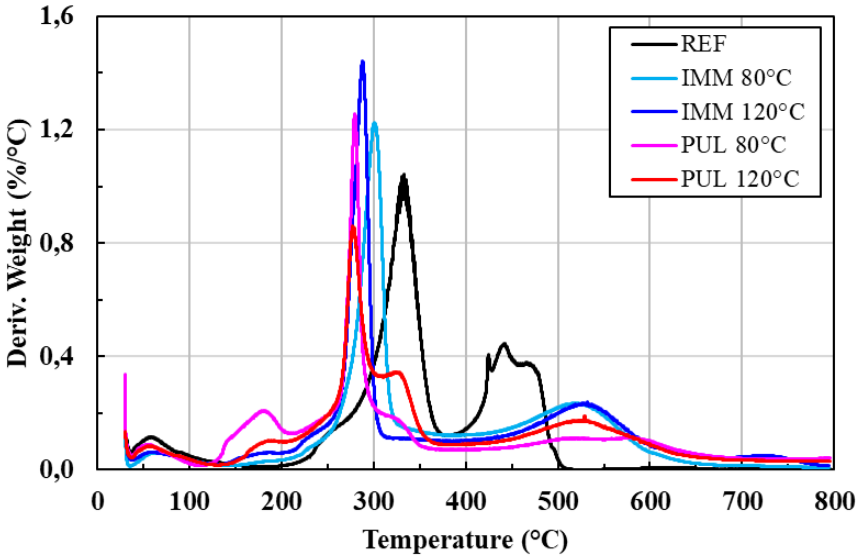

Figure 8: DTG curves from treated and untreated hemp fibers

In the case of treated fibers, premature thermal degradation is observed. In fact, the peak of the first degradation step occurs at 333°C for untreated fibers and between 277 and 304°C for modified fibers. This shift is related to changes in the degradation pathways of cellulose and hemicellulose due to dehydration catalyzed by the phosphorus flame retardant (HAJ20). The accelerated dehydration of cellulose promotes char formation, which protects the inner parts of the fibers and increases the residue formed during thermal degradation (HAJ20; MOU20; TAI22). This is confirmed by TGA analysis that highlight that the amount of the residue formed at 500°C is higher for treated fibers (between 23% and 31%) compared to only about 4.2% for the untreated fibers. At 750°C, the immersed fibers show no significant increase in residue compared to the reference sample, whereas pulverized fibers maintain high residue levels, 10.0% and 8.7%, for the fibers treated 80°C and 120°C respectively. These results are summarized in the Table 3 along with phosphorus content measured by ICP-AES.

Table 3: Peak DTG, residues at 500°C and 750°C and phosphorus content

Sample	Peak DTG (°C)	Residue 500°C (%)	Residue 750°C (%)	P content (%)
REF	333±1	4.2±0.6	2.4±1.0	0.08±0.01
IMM 80°C	304±2	23.5±0.2	2.1±0.8	0.61±0.16
IMM 120°C	294±5	26.4±2.1	2.2±0.3	0.66±0.24
PUL 80°C	277±4	30.4±0.8	10.0±0.6	1.85±0.40
PUL 120°C	277±1	29.5±3.7	8.7±2.8	1.56±0.26

The TGA results also demonstrated a good correlation with the phosphorus content of the fibers. It is evident that higher phosphorus content corresponds to a greater amount of residue remaining during thermal degradation, particularly at temperatures above 500°C. This indicates that the quality of the char formed is enhanced, providing better protection for the fibers and increasing the mass retained during the test.

3.1.3.6 Fire reaction

The mass loss cone calorimeter test provided several valuable parameters for characterizing the fire behavior of the treated hemp fibers. The evolution of the heat release rate (HRR) as a function of temperature for the reference and treated fibers is shown in Figure 9, with a summary of all test results on Table 4.

First of all, the reference fibers presented a quick ignition, with a TTI of about 3.5 seconds. The samples IMM 80°C and IMM 120°C, delayed the ignition to 5.3s and 6.0s, respectively, and the samples PUL 80°C and PUL 120°C, delayed it even more, having a TTI at about 11.0s and 9.5s, respectively, as shown in Figure 4. This indicates the tendency to increase the fibers resistance to ignition after the treatment.

Significant improvements were also observed in the pHRR, and THR. The average of the pHRR from the reference fibers was of 109 $kW.m^{-2}$. The samples IMM 80°C, IMM 120°C, PUL 80°C and PUL 120°C had an average of 92 $kW.m^{-2}$, 70 $kW.m^{-2}$, 49 $kW.m^{-2}$ and 57 $kW.m^{-2}$, respectively, representing a reduction of 16%, 36%, 55% and 48%. The THR, measured from the beginning of the test, until the flame extinction, showed a substantial decrease for the treated fibers, reaching nearly 90% for the pulverized fibers. The overall reduction in fiber's flammability aligns with their phosphorus content, shown in Table 3. All treated samples exhibited a significant enhancement of fire-retardant behavior, particularly the pulverized fibers, which contain a higher phosphorus level. These results are in accordance with the residue increase observed in the TGA.

Table 4: Cone calorimeter results

Sample	TTI (s)	pHRR ($kW.m^{-2}$)	THR ($MJ.m^{-2}$)
REF	3.5±1.9	109±7	13.2±0.6
IMM 80°C	5.3±4.2	92±15	7.5±0.9
IMM 120°C	6.0±4.0	70±6	2.9±0.3
PUL 80°C	11.0±1.2	49±9	1.5±0.6
PUL 120°C	9.5±3.0	57±13	1.8±0.4

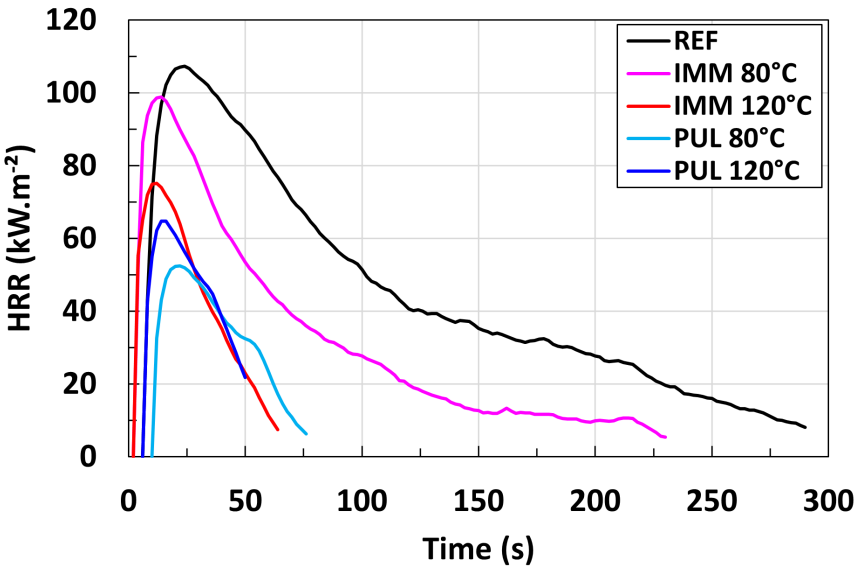

Figure 9: HRR curves of treated and untreated hemp fibers as a function of time

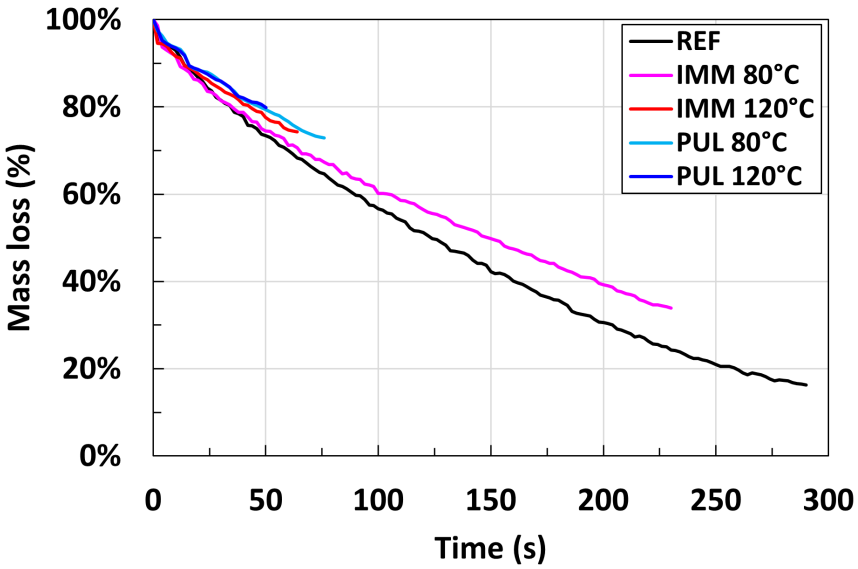

Figure 10: Mass loss during the cone calorimeter test

The mass loss curves over the duration of the test are shown in Figure 10. During the tests, flames extinguished much faster for most treated fibers. The reference fibers burned intensively, with an average burning duration of about 4.5 minutes, leaving an average final mass of 17% of the initial mass. The IMM 80°C sample showed a slight enhancement, with an average burning time of just under 4 minutes and a final mass was of 34%. Significant improvement was observed for the other treated fibers. The IMM 120°C sample had an average burning duration of 1 minute and 9 seconds, preserving 70% of the initial mass. Both pulverized samples burned for only 50 seconds, preserving 77% of their initial mass.

Figure 11 illustrates the appearance of the fibers after testing. A char layer is observed on all treated samples, evidencing the effect of the phosphorus-based treatment. This char helped the treated samples retain their shape, allowing them to be removed from the mold intact. In contrary, the reference sample was highly deteriorated, fragile and unable to maintain its form. The reduction of burning time and the increase of the remaining

masses is linked to the formation of these char layer barrier on top of the fibers, creating a protection to the unexposed fibers.

Notably, samples IMM 120°C, PUL 80°C and PUL 120°C retained, at some extent, their fiber morphology of the fibers, which can be correlated to their improved performance. In contrast, portions of the IMM 80°C sample developed a smooth surface, losing the original fiber structure.



REF IMM 80°C IMM 120°C PUL 80°C PUL 120°C

Figure 11: Hemp fibers aspect after the cone calorimeter test.

3.1.3.7 Ignitability and smoke production

The ignitability of the fibers was assessed using the single flame source test. The results are presented in the Figure 12. All the fibers presented a burned area below 15 cm, which meets the requirements for the European classification (Euroclass) classes E and F. The immersed fibers, despite not showing a statistically significant reduction in the burned area height when compared to the reference fibers, they cease burning as soon as the flame was removed. For the pulverized fibers, a statistically significant reduction in burned area was observed, and they also stopped burning immediately after the flame was removed.

The smoke density test provides additional insight into the reaction to fire analysis of both treated and untreated hemp fibers, by examining smoke production during combustion. Results are expressed as the light absorption percentage, or absorptivity, as a function of time, as seen in Figure 13. Higher absorptivity indicates less light passing through the smoke to reach the detector. Initially, smoke density rises quickly to a peak before starting to decrease, which happens due to chamber's bottom opening, that allow airflow and smoke exit. At a certain point, the rate of smoke production falls below the rate at which smoke exits, causing the curves to decline.

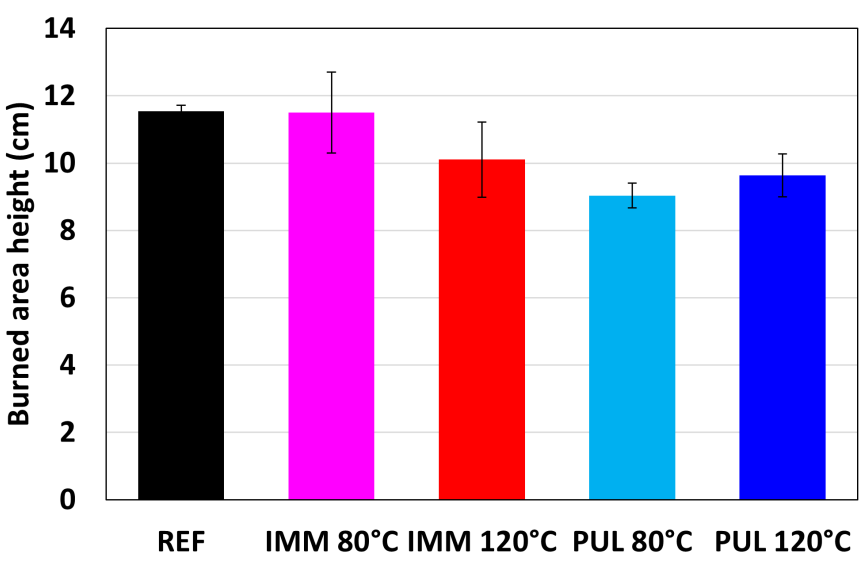

Figure 12: Burned area height from the single flame source test

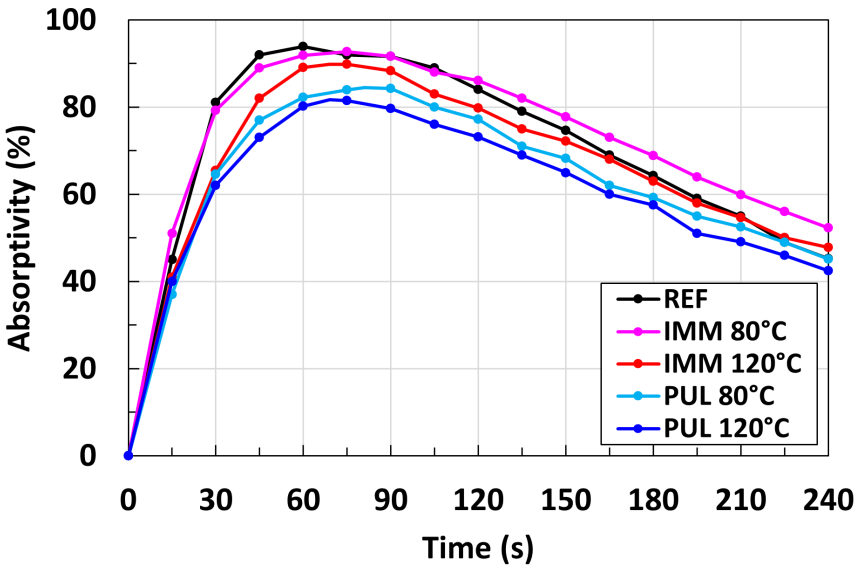

Figure 13: Absorptivity as a function of the test duration

The IMM 80°C fibers showed no improvements regarding the smoke production with a smoke production rate similar to that of the reference fibers. Both achieved comparable maximum absorptivity, 93.9% for reference fibers and 92.8% for IMM 80°C fibers. In contrast, the IMM 120°C, PUL 80°C and PUL 120°C samples presented a reduced smoke production rate and lower maximum absorptivity values, reaching peaks of 89.8%, 84.5% and 81.7%, respectively.

3.1.3.8 Comparison between immersion and pulverization treatments

Based on the results presented, both treatment methods effectively reduce the flammability of the hemp fibers, although key differences exist. Notably, the pulverization method resulted in higher phosphorus content in the fibers due to the absence of a final washing step, leading to reduced flammability and smoke production, which makes this method advantageous in flame- retardant performance.

From a technical and industrial scaling perspective, each treatment method has positive and negative aspects. The pulverization method uses a FR/Fiber mass ratio of 1, instead of 10 for the immersed fibers, requires fewer washing and drying steps, and yields fibers that remain loose, making it a less resource-, time-, and energy-intensive approach.

Conversely, it was noted that the fireproof treatment imparts a viscous texture to the fibers when handled, a sensation not experienced with the immersed fibers. This characteristic is attributed to the absence of a washing step in the pulverization treatment, which leaves non-grafted flame-retardant on the fiber surface. Therefore, this method may not be suitable for applications involving frequent user contact, such as textiles. In such cases, the immersion method is preferable, as it effectively removes any residual substances from the fiber surface.

Additionally, some side effects of the treatment on the fibers were noted, including an increase in weight and a tendency for the fiber diameter to increase as well. However, the real density of the fibers remained unchanged. These changes at the fiber level could also influence the acoustic and thermal performance of the fibers in applications such as building insulation.

3.1.4 Conclusion

Hemp fibers stacks were treated with a bio-based flame-retardant system, combining phytic acid and urea, using two application methods: immersion and pulverization. As opposed to the techniques previously seen in the literature (Table 1), the methods presented in this study aim to be adapted to an industrial production level, treating a large quantity of fibers while being efficient in the amount of flame retardant used and the number of steps required for the whole treatment. The results showed that the thermal and flame-retardant properties of the fibers were affected by both the treatment method and drying temperature.

For the immersion method, although both fiber samples had similar phosphorus content, the fibers treated at 120°C exhibited greater residue at 500°C during TGA, lower pHRR and THR during mass loss calorimeter test, and a lower smoke production, in respect to untreated fibers and those treated by immersion at 80°C.

With the pulverization method, flammability results were similar across both temperatures, despite a higher phosphorus content in fibers treated at 80°C. Therefore, treating fibers at lower temperatures is preferable, as it reduces energy use, costs, and avoid potential fiber degradation.

The compounds used for the flame-retardant treatment of hemp fibers and the pulverization application method can be used to treat fibers on a large scale and manufacture insulating materials based on plant fibers. This work has demonstrated the effectiveness of this treatment in raw fibers. One of the prospects of this work is to manufacture insulating panels using industrial processes to validate these results on a material scale.

In addition, as the treatment of the fibers can have an impact on their diameter, the characterization of their hygrothermal and acoustic performance will also be carried out in order to study their influence on the functional properties of the fibers.

3.2 Article: Impact of a phosphorus-based fireproof treatment on the acoustic performances of bulk hemp fibers

Thomas Schatzmayr Welp Sá[1,2], Sandrine Marceau[1], Clément Piégay[2], Philippe Glé[2], Fouad Laoutid[3], César Segovia[4], Etienne Gourlay[5]

[1] CPDM, Université Gustave Eiffel - 14-20 Boulevard Newton, F-77454, Marne-la-Vallée, France
[2] Cerema, Université Gustave Eiffel, UMRAE - 11 Rue Jean Mentelin, F-67035, Strasbourg, France
[3] Laboratory of Polymeric and Composite Materials, Materia Nova Research Center - University of Mons (UMONS) - Av. Nicolas Copernic 3, 7000, Mons, Belgium
[4] CETELOR - Université de Lorraine, 27 Rue Philippe Seguin, 88051, Epinal, France
[5] Cerema, Equipe-recherche BPE - 11 Rue Jean Mentelin, F-67035, Strasbourg, France

Abstract

Bio-based materials are a relevant alternative to traditional building materials particularly due to their carbon sequestration and storage properties. However, their high flammability limits their use and the application of a fireproof treatment is needed. Since fireproof treatments may alter the fibers and the acoustic properties depend on the material's microstructure, it is essential to evaluate the impact of such treatments. The goal of this paper is to evaluate the performance of hemp fibers, before and after fireproof treatment. Also, it aims to understand the impact that it can have on their microstructure using acoustic parameters. The sound absorption of four treated formulations and one untreated reference configuration was evaluated with an impedance tube using a three microphones characterization method. This method allows the indirectly determination of the characteristic parameters of the pore network within the samples using equivalent fluid modeling. In addition, the use of homogenization models such as Tarnow's enables the estimation of the effective radius of the fibers in the samples. Thus, an increase in the fiber radius was observed after fireproof treatment, providing a possible explanation for the experimentally observed decrease in airflow resistivity and viscous dissipative effects, as well as the reduction in acoustic absorption in the treated hemp fiber stacks.

Keywords: *hemp fibers, bio-based material, acoustic, sound absorption, fireproof treatment*

3.2.1 Introduction

To face the challenge of reducing carbon emissions, the building industry is adapting and transitioning to more sustainable practices. The growing interest in the use of bio-based materials arises from the need to create less impactful alternatives to substitute traditional materials (GAL22). Moreover, bio-based products have a higher percentage of renewable embodied energy as well as carbon sequestration and storage properties when compared to inorganic mineral, organic fossil fuel, and innovative engineered processes (GRA21). This leads to a material with low, or even negative, global warming potential values (GRA21; ZIE20). In this context, vegetal fibers have been used as raw material to manufacture insulation products due to their lightness and excellent acoustic (BER15; GUM22; PIE18) and thermal performances (EL-16; PIE20; VOL15).

However, their application in the building sector is restricted due to their high flammability (AMZ17; KOZ20). Therefore, the application of a flame retardant is necessary.

Among the many solutions for flame retardant treatment of fibers, only a few are compatible with the bio-based nature of vegetal fibers (SAC25). Two different fireproof treatment methods, based on phosphorus and nitrogen flame retardants, have been proposed to reduce the flammability of hemp fibers, expand the material's application possibilities and ensure its fire safety in bio-based applications (KOZ20; SAC25).

A promising approach for bio-based materials is the use of phosphorus-based flame retardants, which act by forming a char layer that blocks external heat, oxygen penetration and flame spread (SAC25; TAI22). The phosphorus molecules are grafted in the cellulose through different techniques, such as radiation (HAJ19; SON15; TAI22), chemical grafting by immersion (ANT22; HAJ18; SAC25) or pulverization (LEE23; SAC25). Regardless of the technique employed, due to the chemical modification of natural fibers, an impact on their microstructure is expected (LAZ13). Authors have reported fiber swelling caused by the treatment and the use of urea (ANT24; ISO13), a source of nitrogen that has a synergetic flame retardant effect with phosphorus-based flame retardants (ANT24; LAO09; TAI22).

In order to optimize the effectiveness of bio-based acoustic insulators and guarantee fire safety during their use, it is important to first understand the impact of phosphorus-based fireproof treatments on the acoustic performance of bulk hemp fiber stacks. The results obtained can then be used in the case of panels manufactured by the industrial thermo-bonding process.

Understanding the inner structure of fiber stacks and the impact of flame retardants on this structure is essential for studying the acoustic performance of fibrous materials. Indeed, morphological parameters such as the fiber size distribution, as well as parameters such as porosity or airflow resistivity related to their arrangement, influence the viscous and thermal dissipation of sound waves within the pore network (ARE10; LUU17; PIE21; TAS08).

In the scientific literature, few studies have investigated the link between the flammability or flame retardancy of natural fibers and their acoustic performance. These studies address the flammability and acoustic performance of natural fibers or composites, either without the application of fireproof treatments (FAT11) or by using various types of flame retardants (LYU20). However, these studies do not analyze the potential influence of flame-retardant treatments on the acoustic performance of the material. Sun et al. (SUN24) demonstrated a clear impact of their fireproof treatment on the sound absorption capacity of a bamboo, cellulose and glass fibers composite, but the origin of this impact was not assessed.

Considering the importance of the pore network and morphological characteristics of fibers in the acoustic properties of fibrous media, it is relevant to quantify and evaluate the potential impact of fireproof treatments on them. To do so, a first step involves conducting material-scale characterizations on both treated and untreated fiber stacks to quantify their respective acoustic properties. Subsequently, it will be necessary to evaluate the effects of the treatment at the pore network scale by analyzing key parameters obtained through acoustic characterization methods. In fact, parameters of the pore network such as porosity, airflow resistivity, tortuosity, viscous and thermal characteristic lengths and static thermal permeability contribute to viscous and thermal acoustic dissipation phenomena (JAO20). Finally, on the fiber scale, it will be important to assess the impact of fireproof treatment on the density and morphology of the fibers.

The determination of the acoustic parameters of the pore network makes it possible to use and validate the semi-phenomenological JCAL modeling method for treated and untreated fiber stacks by comparing it with the experimental measurements (CHA91; JOH87; LAF97). In addition, to account for the dimensions of natural fibers and assess the effects of fireproof treatments, it seems appropriate to use micro-macro homogenization

modeling approaches. The Tarnow model (TAR96) uses a micro-macro approach by providing an analytical relationship between airflow resistivity and an equivalent fiber radius. This model was validated by Piégay (PIE18) for hemp and flax wools, considering a perpendicular airflow and random fiber distribution.

In this paper, the first Section describes the materials used for the preparation of the samples and for the treatment of them, as well as the methods for their physico-chemical and acoustic characterization. Then, in Section 4.1.4, the characterization results are presented as well as the material's sound absorption performance. A compression model is used to compare samples with equivalent initial mass. Moreover, the characteristic parameters of the pore network are evaluated and the sound absorption of hemp fibers is modeled using the JCAL model. In the end of this Section, an estimation of the fiber radius is performed using the Tarnow model. Finally, Section 4.1.5 concludes the article by presenting the main findings and future perspectives.

3.2.2 Materials and methods

3.2.2.1 Materials description

The hemp fibers used in this work come from the agricultural exploitation AgroChanvre (France). They were previously retted (LEC21; THY06). Bulk hemp fibers referenced in this paper as HF REF have not been treated with flame retardants. They can be seen in Figure 1a. For fibers that have been treated, their references are detailed in Section 4.1.2.2.

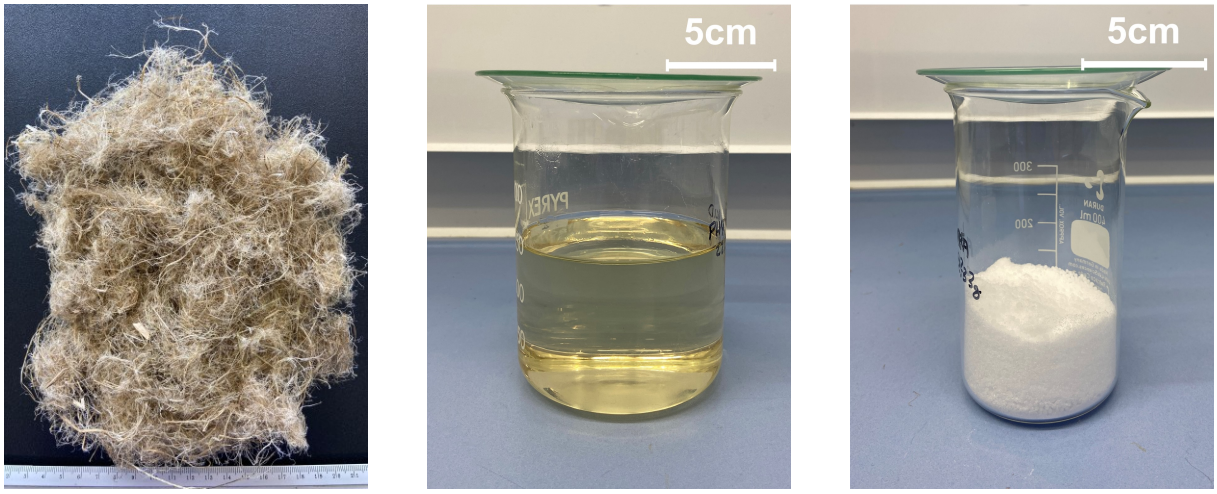

(a) (b) (c)

Figure 1: Materials used for treatment (a) Bulk hemp fibers; (b) Phytic acid; (c) Urea

3.2.2.2 Fireproof treatment of hemp fibers

For the fireproof treatment of the hemp fibers, phytic acid (CAS: 83-86-3) in solution 50 wt.% (Figure 1b), and urea (CAS: 57-13-6, purity > 99.5%) (Figure 1c), were used. Nitric acid (CAS: 7697-37-2) 65% of concentration was also used to perform the spectroscopy (ICP-AES) analysis.

The fireproof treatment of hemp fibers consists of applying a solution of 10 wt.% of phytic acid and 30 wt.% of urea, with two different methods: by immersion (Figure 2a) and pulverization (Figure 2b) as detailed in a previous work (SAC25). After application of the solution, in both methods, the fibers are heated in an oven to activate the covalent reaction between the phosphorus molecules and the cellulose and hemicellulose (grafting)

(HAJ20; TAI22). Two different temperatures were used during the treatment, 80°C and 120°C, for two hours. After heating, the immersed fibers were washed with distilled water to remove the ungrafted particles that remained over the fibers and then dried in an oven at 60°C for 72h. The pulverized fibers did not require a washing step and were therefore directly dried in an oven. Table 1 presents the samples and their nomenclature.

Table 1: Fireproof treatment method and samples nomenclature

Sample	Method	Temperature
HF REF	-	-
HF IMM 80°C	Immersion	80°C
HF IMM 120°C	Immersion	120°C
HF PUL 80°C	Pulverization	80°C
HF PUL 120°C	Pulverization	120°C

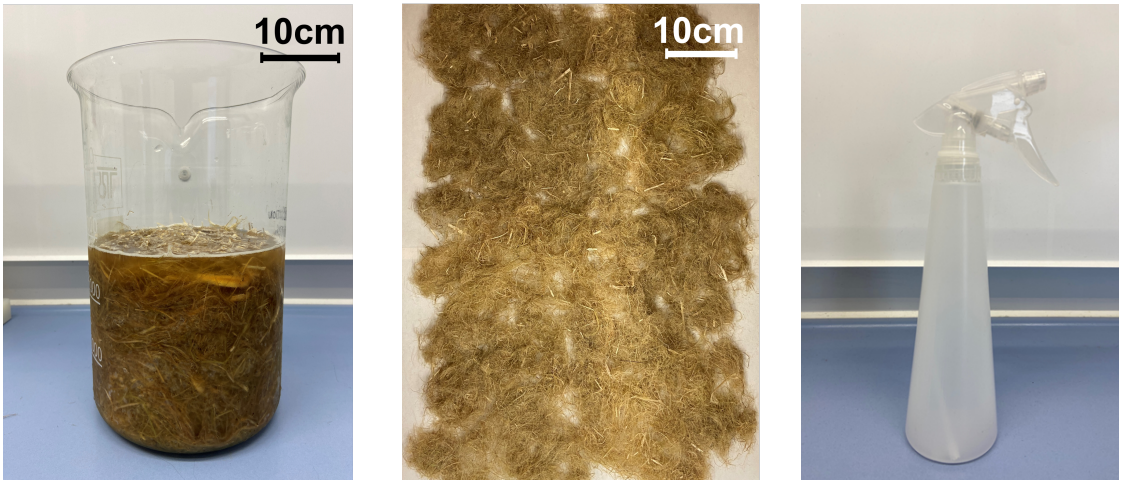

(a) (b) (c)

Figure 2: Materials and treatment methods (a) Immersion method; (b) Pulverization method; (c) Pulverizer

3.2.2.3 Chemical characterization

The phosphorus content on treated hemp fibers was determined using inductively coupled plasma atomic emission spectroscopy (ICP-AES) model ULTIMA 2000 from Jobin Yvon Horiba Company. The method used was adapted from previous works (HAM97; TAI22). Prior to ICP-AES analysis, 0.30 g of hemp fibers were digested using a nitric acid/distilled water (50%/50%) solution for four hours at 100°C, under magnetic stirring. The remaining solution was filtered, and the phosphorus concentration was determined using calibration curves obtained from ICP-AES analysis of standard solutions at different concentrations. The test was repeated 10 times.

3.2.2.4 Acoustic properties

An impedance tube, model AcoustiTube AFD 1200, with normal wave incidence and a three microphones configuration was used (see Figure 3a) to characterize the sound absorption coefficient (α) of hemp fibers, according to the standard ISO 10534-2:2023 (AFN23). The tube's diameter was 100 mm and the frequency domain of measurements was in the range between 150 and 2000 Hz. The three microphones configuration was

initially developed by Iwase *et al.* (IWA98) and adapted by Salissou *et al.* (SAL10), by placing the third microphone outside the impedance tube. This configuration allows the determination of intrinsic parameters of the material such as the dynamic density (ρ) and the dynamic bulk modulus (K), from the calculation of the characteristic impedance (Z_c) and wave number (k).

Prior to the test, the hemp fibers were kept in the measurement room for three days, to stabilize their temperature and humidity. The room conditions were 23.5±0.5°C and 40±5% of relative humidity. All samples had 100 mm of height and diameter (Figures 3b and 3c), and three densities were tested: 30, 60 and 90 kg.m^{-3}, in order to obtain an overview of their acoustic performance within the apparent density range of typical insulation materials. For each condition, four measurements were made, from both sides of the two samples prepared.



(a) (b) (c)

Figure 3: (a) Impedance tube; (b) Cylindrical stack of hemp fiber; (c) Hemp fibers inside the sample holder for impedance tube measurements

3.2.2.5 Fiber density and sample porosity

To determine the impact of the treatment on the mass of the fibers, they were oven-dried and weighed before and after the treatment. A Mettler Toledo scale with a precision of 0.01 g was used to weigh the material. The procedure consisted of drying the fibers at 60°C until constant mass, which was obtained until their mass variation from three measurements, obtained from three consecutive days, were lower than 0.5%. The same procedure was repeated after treatment and the results are reported as a percentage of the initial mass. For this analysis, an additional sample of reference fibers that were only washed and dried at 80°C was added (REF W 80°C). This sample was used to specifically identify the effects of the flame retardants that were used for treatment and to distinguish them from the effect of washing in the immersion case.

The skeleton density (ρ_s) of the hemp fibers was determined using a Micrometrics Accupyc II helium gas pycnometer, with fibers pre-dried under the same conditions as described above. With this result, the porosity (ϕ) of each sample was calculated using Equation 1. The apparent density of the hemp fiber stacks is represented by the variable ρ_{ap}.

$$\phi = 1 - \frac{\rho_{ap}}{\rho_s} \tag{1}$$

3.2.2.6 Indirect characterization of acoustic parameters

In order to assess the impact of the fireproofing treatment on the pore network of the stack of fibers, it seems appropriate to determine the five other characteristic parameters in addition to porosity, related to the effects of visco-thermal dissipation within them.

From the works of Panneton and Olny (OLN08; PAN06) an estimation of the airflow resistivity (σ), tortuosity (α_∞), viscous characteristic length (Λ), thermal characteristic length (Λ') and static thermal permeability (Θ_0), can be obtained, based on the experimental values of porosity (ϕ) and two intrinsic parameters: dynamic density (ρ) and dynamic bulk modulus (K). These parameters are obtained experimentally by Kundt tube characterization (JAO20). The equations used for the estimation of the acoustic parameters are stated in Equation 2 to 6 (JAO20).

$$\sigma = \lim_{\omega \to 0} -\omega Im(\rho) \tag{2}$$

$$\alpha_\infty = \frac{\phi}{\rho_0}\left(Re(\rho) - \sqrt{Im(\rho)^2 - \frac{\sigma^2}{\omega^2}}\right) \tag{3}$$

$$\Lambda = \frac{\alpha_\infty}{\phi}\sqrt{\frac{2\eta\rho_0}{\omega Im(\rho)}\left[\frac{\alpha_\infty \rho}{\phi} - Re(\rho)\right]} \tag{4}$$

$$\Lambda' = 2\sqrt{\frac{\kappa}{C_p\rho_0\omega}\left[-Im\left[\left(\frac{\gamma P_0 - \phi K}{\gamma P_0 - \gamma\phi K}\right)^2\right]\right]^{-1}} \tag{5}$$

$$\Theta_0 = \frac{\phi\kappa}{C_p\rho_0\omega}\Bigg/\sqrt{-Re\left[\left(\frac{\gamma P_0 - \phi K}{\gamma P_0 - \gamma\phi K}\right)^2\right]} \tag{6}$$

where ω the angular frequency, P_0 the air pressure at equilibrium, ρ_0 the static air density, η is the dynamic viscosity of air, κ the thermal conductivity of air, C_p the heat capacity of air at constant pressure, γ the air heat capacity ratio.

3.2.2.7 Sound absorption modeling approach

The Johnson-Champoux-Allard-Lafarge (JCAL) model (CHA91; JOH87; LAF97), which considers a non-uniform pore section geometry, was used to gather information about the visco-inertial and thermal dissipative effects of the hemp fiber samples and their pore geometry. The dynamic density (ρ) and the dynamic bulk modulus (K) are calculated by Equations 7 and 8. These parameters are then used to calculate the characteristic impedance of the material (Z_c) and the wave number (k), which are used to calculate the sound absorption coefficient.

$$\rho = \frac{\rho_0\alpha_\infty}{\phi}\left[1 - j\frac{\sigma\phi}{\rho_0\alpha_\infty\omega}\sqrt{1 + j\frac{4\eta\alpha_\infty^2\rho_0\omega}{\Lambda^2\sigma^2\phi^2}}\right] \tag{7}$$

$$K = \frac{\gamma P_0}{\phi}\left[\gamma - (\gamma - 1)\left(1 - j\frac{\phi\kappa}{\Theta_0 C_p\rho_0\omega}\sqrt{1 + j\frac{4\Theta_0^2 C_p\rho_0\omega}{\kappa\phi^2\Lambda'^2}}\right)^{-1}\right]^{-1} \tag{8}$$

The simulations carried out using the six input parameters were compared with the experimental results obtained with the impedance tube, to validate the relevance of the JCAL model for fireproof treated and untreated vegetal fiber stacks. This model has already been used in the literature for modeling the sound absorption properties of fibrous

materials, such as hemp fibers (GLE19), typha fibers (KHO25), textile waste (RUB23), vegetal wool (GLE13; PIE19).

3.2.2.8 Compression model

Sound absorption is a parameter that is sensitive to variations in the material's apparent density and mass. Therefore, the Castagnède (CAS00) compression model can be used to predict the sound absorption of compressed or expanded samples in one dimension, by determining suitable values for the parameters characteristic of the JCAL approach. In this study, since experimental testing was conducted on samples with the same final apparent density and the mass of the treated samples varied with the treatment, the compression model was used to simulate the sound absorption performance of samples with equivalent initial quantities of fiber. In doing so, the effects of the treatment could be directly observed and analyzed.

The model consists of the determination of five parameters of the JCAL model, presented in Section 4.1.3, while considering a compression factor (n). The thermal permeability does not account for this factor but is instead estimated by an approximation (LEI18). The compression factor, n is defined as the ratio between the thickness of the material before (h_i) and after (h_n) being compressed (Equation 9). The new acoustic parameters can be calculated as shown in Equations 10 to 15. The variable R_f, is the fiber radius estimated by the Tarnow model, which will be presented in Section 3.2.2.9.

$$n = \frac{h_i}{h_n} \tag{9}$$

$$\phi_n = 1 - n(1 - \phi) \tag{10}$$

$$\sigma_n = n\sigma \tag{11}$$

$$\alpha_{\infty n} = 1 - n(1 - \alpha_\infty) \tag{12}$$

$$\Lambda_n = \frac{\Lambda}{\sqrt{n}} + \frac{R_f}{2}\left(\frac{1}{\sqrt{n}} - 1\right) \tag{13}$$

$$\Lambda'_n = \frac{\Lambda'}{\sqrt{n}} + \frac{R_f}{2}\left(\frac{1}{\sqrt{n}} - 1\right) \tag{14}$$

$$k'_0 = \frac{\phi\Lambda'^2}{8} \tag{15}$$

3.2.2.9 Micro-macro modeling approach

To evaluate whether the treatment has an effect on the fiber radius, it is possible to use a micro-macro homogenization approach such as Tarnow modeling, which provides analytical relationships between resistivity and microstructural parameters of the fiber stack (TAR96). This model is based on the hypothesis of cylinders (fibers) with the same radius placed in a regular or random configuration, with an airflow parallel or perpendicular to the fibers. A relationship is stipulated between airflow resistivity and the radius of the fibers (R_f), the material's porosity and the dynamic viscosity of the air (η). The condition of fibers randomly distributed with an airflow perpendicular to them, as described by Equation 7, was selected based on observations from Glé (GLE13).

The Tarnow model has been validated by Piégay *et al.* (PIE18), in the case of vegetal wools. Therefore, the Tarnow model can be used to assess the modification on an effective radius of the fibers after treatment, and to explain their effects on the macro-scale acoustic performance.

$$R_f = \sqrt{\frac{4\eta(1-\phi)}{\sigma[0.64ln(\frac{1}{1-\phi}) - 0.737 + (1-\phi)]}} \tag{16}$$

3.2.3 Results and discussion

3.2.3.1 Weight and density

The effect of the treatment on the fibers' mass is reported in Table 2. Fibers treated with flame retardants showed an increase in mass. The increase was smaller for the samples treated by immersion, with a mass variation of 3.0% for the sample IMM 80°C and 5.1% for the IMM 120°C. A more significant mass increase was observed in the pulverized fibers with values of 14.3% and 12.8% for the samples PUL 80°C and PUL 120°C, respectively. The difference in mass variation between the treatment methods can be explained by the lack of a washing step at the end of the pulverization treatment method. Sample REF W 80°C was the only one to exhibit a reduction in mass after treatment, with a mass variation of -5.0%. This indicates that the mass increase on the flame retardant treated samples comes from the products that are bounded with the fibers during the treatment.

The skeleton density of the fibers is reported in Table 2. A small decrease of 0.01 g.cm^{-3} and 0.02 g.cm^{-3} in the density is observed in the samples PUL 120°C and IMM 120°C, compared to the reference fibers, respectively. Samples IMM 80°C and the PUL 80°C did not show any significant change, presenting values around 1.50 g.cm^{-3}. These results indicate that the treatment did not significantly impact the density of the hemp fibers, therefore no influence from the density on the acoustic properties is expected.

Table 2: Physico-chemical characterization results

Sample	Fiber density (%)	Mass variation (%)	Phosphorus content (%)
REF	1.503±0.004	-	0.08±0.01
REF W 80°C	-	-5.0±0.7	-
IMM 80°C	1.504±0.002	3.0±0.8	0.61±0.16
IMM 120°C	1.479±0.002	5.1±1.7	0.66±0.24
PUL 80°C	1.496±0.002	14.3±4.6	1.85±0.40
PUL 120°C	1.489±0.002	12.8±2.4	1.56±0.26

3.2.3.2 Phosphorus content

The phosphorus content of the hemp fibers is reported in Table 2. Reference fibers only present 0.08% of phosphorus in their composition. The fibers treated by immersion, at 80°C and 120°C, presented a phosphorus content of 0.61% and 0.66%, respectively, which are statistically similar between themselves. Pulverized fibers achieved a higher phosphorus concentration, reaching 1.85% and 1.56%, for fibers treated at 80°C and 120°C, respectively. Since pulverized fibers are not washed at the end of the treatment procedure, a higher amount of flame retardants remain in the fibers. For the immersed fibers, only the molecules bounded with the fibers remained.

3.2.3.3 Acoustic properties

The sound absorption curves of the reference hemp fibers as a function of frequency, for the densities of 30, 60 and 90 kg.m^{-3}, are shown in Figure 4, represented by black straight lines. These curves correspond to the averages of four measurements and the gray area highlights the maximum and minimum values observed during the measurements. This gray area indicates a low dispersion between average, maximum and minimum values for all samples. The effects of the apparent density of the fiber stacks are demonstrated, showing an increase in absorption across the entire frequency range, and a shift of the first peak of absorption to lower frequencies.

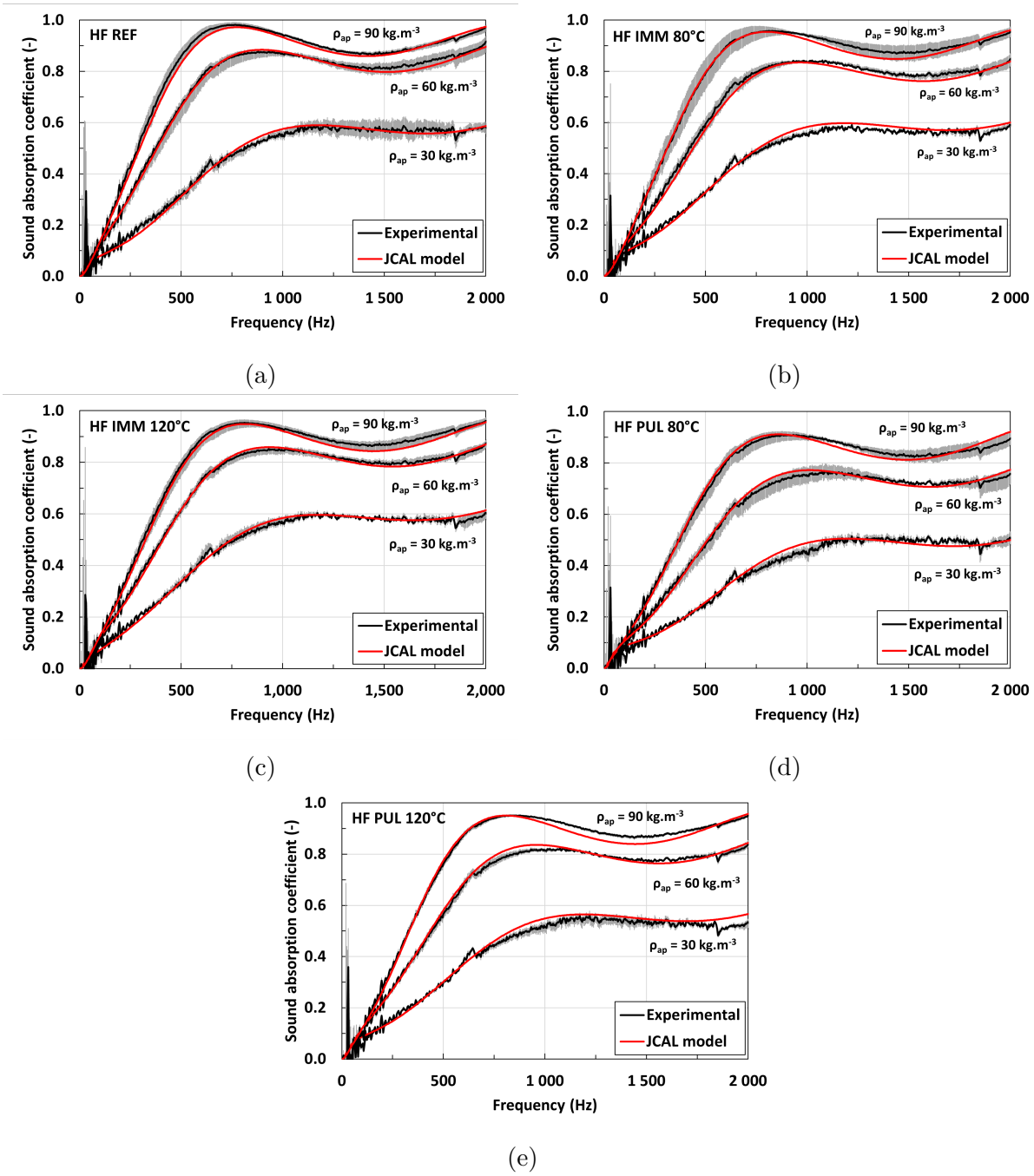

Figure 4: Sound absorption coefficient - Comparison between experimental and JCAL-modeled curves : (a) HF REF; (b) IMM 80°C; (c) IMM 120°C; (d) PUL 80°C; (e) PUL 120°C

The JCAL model was used to validate the results obtained by comparing simulations with experimental curves. The acoustic parameters were calculated using Equations 2 to 6 and with them the dynamic density (ρ) and the bulk modulus (K) were calculated (Equations 7 to 8). The JCAL model curves are also represented in Figure 4 by straight red lines.

The results show a good correlation between the average experimental and modeled curves. The relative error is presented in Table 3. Overall, the JCAL model curves accurately represent the experimental results, presenting relative errors below 4% and remaining close to the average values or within the range defined by the minimum and maximum measurements.

Table 3: Relative error between experimental and JCAL modeled curves from 200 to 2000 Hz

Sample	Apparent density ($kg.m^{-3}$)	Relative error (%)
REF	30	3.1
	60	1.4
	90	1.6
IMM 80°C	30	3.3
	30	2.4
	30	1.4
IMM 120°C	30	2.2
	60	1.3
	90	1.9
PUL 80°C	30	3.7
	60	2.1
	90	1.8
PUL 120°C	30	4.0
	60	1.7
	90	1.8

However, to correctly evaluate the effects of the fireproof treatment on the sound absorption of hemp fibers, the same initial amount of fibers must be considered in the fiber stacks. As shown previously in Table 2, the mass of the samples increases with the treatment, especially for the pulverization treatment. For this reason, the Castagnède compression model is used to determine the coefficients of the JCAL method corresponding to the same initial quantity of fibers.

3.2.3.4 Evaluation of characteristic pore network parameters

Therefore, the approach employed was to use a compression model to create sound absorption curves of equivalent mass. The characteristic parameters of the porous structure of materials were adjusted using the compression factor and Equations 10 to 15. The adjusted parameters are shown in Figure 5.

These parameters can not only be used to model the sound absorption through the JCAL model, but it also provides information about the material's pore network. Therefore, it can be evaluated to understand the influence of the treatment on the sound absorption of the treated hemp fiber stacks.

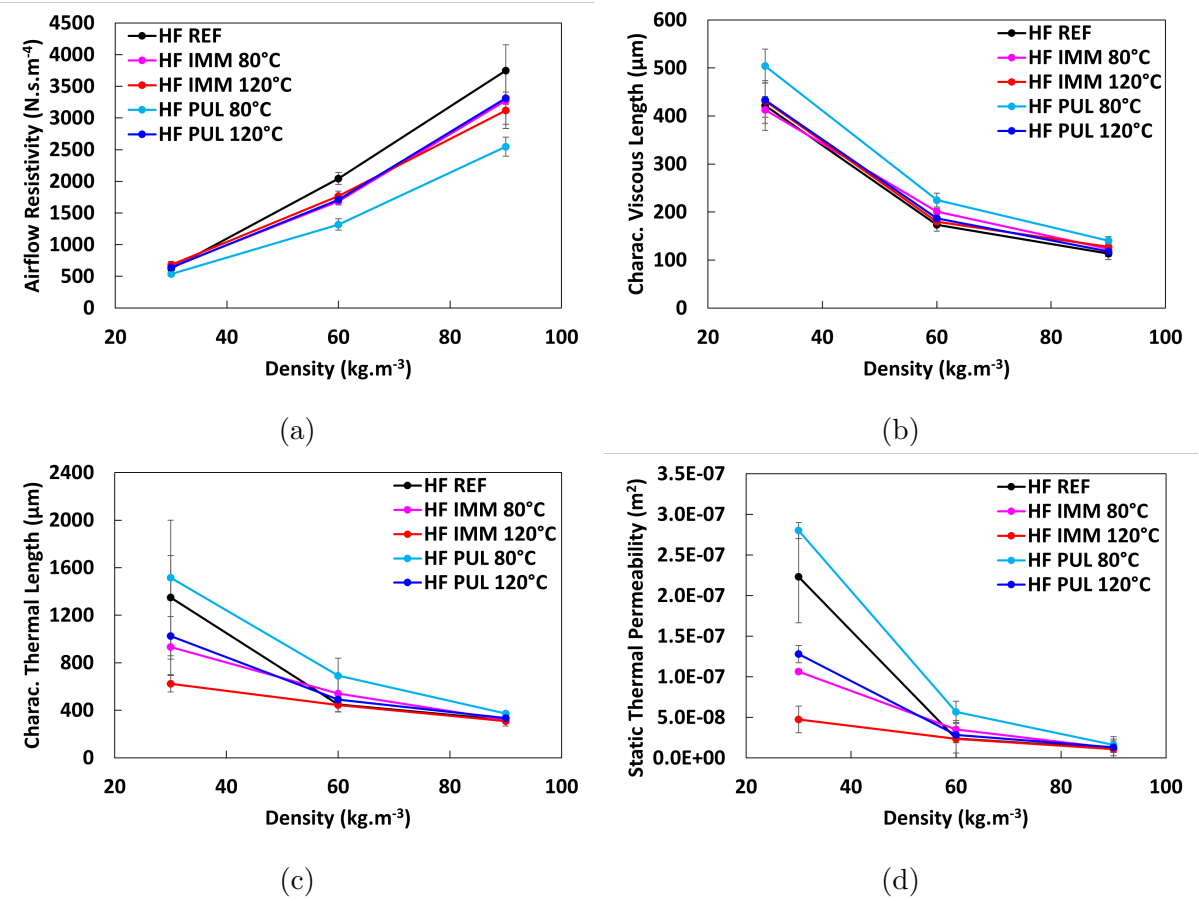

Figure 5: Characteristic parameters of the porous structure of hemp fiber samples with equivalent mass: (a) Airflow resistivity; (b) Characteristic viscous length; (c) Characteristic thermal length; (d) Thermal permeability

As demonstrated in Section 4.1.4.1, the fibers solid skeleton density values did not change significantly with treatment. Thus, based on Equation 1, it can be stated that the porosity of the stacks does not change substantially after treatment and is primarily dependent on the apparent density of the samples. For samples at 30, 60 and 90 kg.m^{-3}, the corresponding porosities were 0.98, 0.96, and 0.94, respectively.

The tortuosity is not represented graphically because its values ranged between 1.00 and 1.02 for all samples, indicating that hemp fibers do not effectively impact the path of sound waves passing through the sample. This result is in agreement with Piégay (PIE19).

The results of airflow resistivity, presented in Figure 5a, show that at 30 kg.m^{-3}, the airflow resistivity values provided by the samples are very low, ranging from 534 to 681 N.s.m^4. At 60 kg.m^{-3}, the differences between fireproof treated and untreated samples are highlighted by the decrease in airflow resistivity. Samples REF, IMM 80°C, IMM 120°C, PUL 80°C, and PUL 120°C presented airflow resistivity values of 2045, 1685, 1764, 1317 and 1710 N.s.m^4, respectively. This indicates an impact of the treatment on this parameter. At 90 kg.m^{-3}, the same behavior is observed. The airflow resistivity of the reference sample reached the highest value among all samples at 3746 kg.m^{-3}, while samples IMM 80°C, IMM 120°C, and PUL 120°C presented similar values around 3100 and 3300 kg.m^{-3}. Sample PUL 80°C presented the lowest resistivity with a value of 2547 N.s.m^4.

Regarding the characteristic viscous and thermal lengths (Figures 5b and 5c), only sample PUL 80°C exhibited a significant change compared to the reference fibers. Both values increased, indicating larger pore sizes and lower viscous and thermal losses that

lead to lower sound absorption at low and high frequencies, respectively. This result can be explained by the fact that the treated stacks are reconstituted with the same apparent density as untreated ones, despite being composed of hemp fibers with grafted phosphorus. A more open pore structure also facilitates the airflow permeability, therefore, it complies with the airflow resistivity results. Finally, the results of static thermal permeability (Figure 5d) were obtained by an estimation, and the original values presented a high standard deviation, making the comparison between samples inconclusive.

3.2.3.5 Acoustic performance comparison

With the new characteristic parameters of the pore network, the dynamic density and bulk modulus were calculated, and the sound absorption of samples with equivalent mass was modeled. These curves, for initial densities (ρ_{ap0}) of 30, 60 and 90 kg.m^{-3}, are shown in Figure 6.

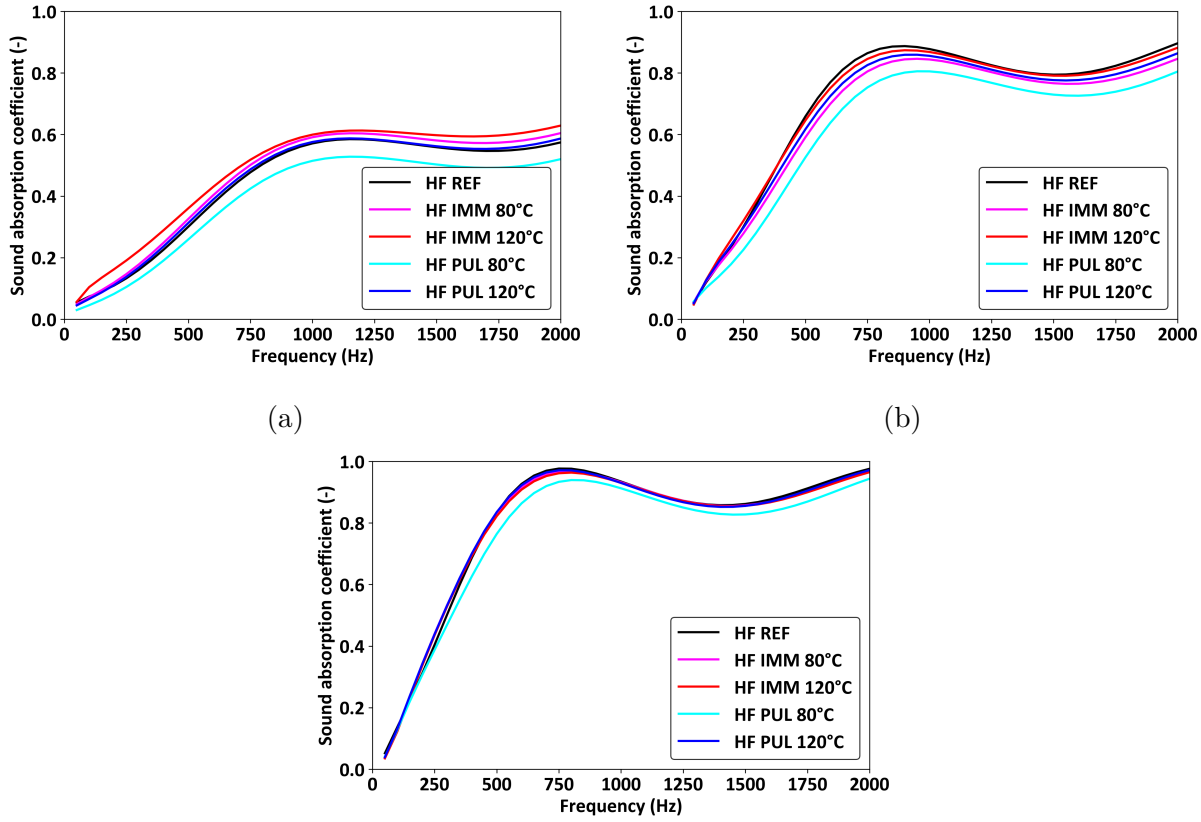

Figure 6: Sound absorption coefficient comparison between hemp fibers stacks of equal mass with different treatment methods: (a) $\rho_{ap0} = 30$ kg.m^{-3}; (b) $\rho_{ap0} = 60$ kg.m^{-3}; (c) $\rho_{ap0} = 90$ kg.m^{-3}

To assess the impact of the treatment on sound absorption performance, a relative difference between each type of treatment and the reference is determined for each density value. This relative difference corresponds to the average value between the reference and treated samples, in the range of frequency between 200 and 2000 Hz, shown in Table 4.

At 30 kg.m^{-3}, the treated samples presented higher sound absorption than the reference, up to 8.3% higher on average, for the sample IMM 120°C. The exception was the sample PUL 80°C that presented a 9.3% lower sound absorption than the reference fibers on average. At 60 kg.m^{-3}, all samples presented lower sound absorption than the reference but with very similar values, except sample PUL 80°C, that presented a reduction

of 7.7%. At 90 kg.m^{-3}, the treated samples curves converge to the reference curve, with differences lower than 2.3%. Overall, the sample with the largest performance reduction in all densities was the PUL 80°C, which is the one that has the highest phosphorus content, as shown in Table 2.

Table 4: Relative differences between the reference and treated samples from 200 to 2000 Hz

Sample	Apparent density (kg.m^{-3})	Relative difference (%)
REF x IMM 80°C	30	4.3
	60	-3.6
	90	0.0
REF x IMM 120°C	30	8.3
	60	-0.5
	90	-0.2
REF x PUL 80°C	30	-9.3
	60	-7.7
	90	-2.3
REF x PUL 120°C	30	1.4
	60	-2.1
	90	0.0

As previously mentioned, the pulverized samples are not washed at the end of the treatment, allowing the phytic acid and urea particles to remain on the fiber surface. Therefore, it is hypothesized that this residue affects the fiber microstructure and reduces their ability to absorb sound waves. This impact will be further explored in the following Section.

3.2.3.6 Estimation of the effective radius of fibers

With the information gathered about the hemp fiber stacks, it is possible to estimate an effective fiber radius from Tarnow's modeling in the configuration shown in Section 3.2.2.9. The relationship for determining this value is given by Equation 7. Using the porosity values presented in Section 4.1.4.4 and the airflow resistivity values from the JCAL model, the estimation of the effective radius of the fibers is calculated and reported in Figure 7.

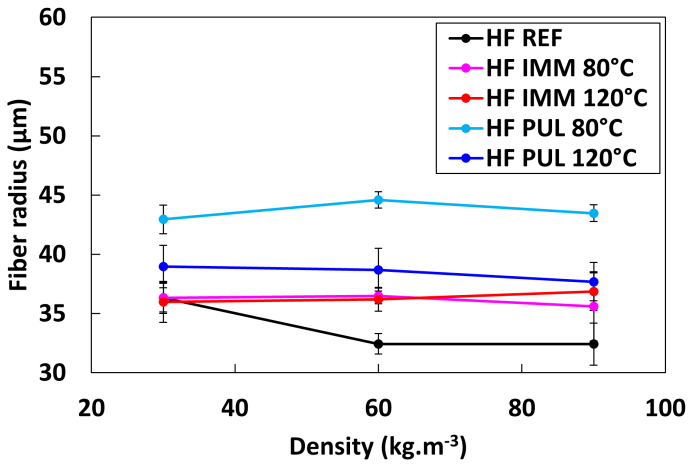

Figure 7: Hemp fiber radius estimation by the Tarnow model

The estimated fiber radius values vary slightly with density due to changes in airflow resistivity. For the sake of comparison, the values commented are from the density of 60 kg.m^{-3}. The effective radius estimated for the reference fibers was of 32.4 µm. This value is higher than what is usually reported in the literature for elementary hemp fibers (around 20 µm) (PIE19; SAU18), but the fibers in this study have not been "opened" or processed in any way to separate them from their bundles. Therefore, they can remain agglomerated, which increases the expected fiber radius. These results are, then, relevant.

Samples IMM 80°C, IMM 120°C and PUL 120°C showed a small increase in their radius of 10%, estimating a radius of about 35 µm to 36 µm. The PUL 80°C sample showed a greater increase in the fiber radius (25%), reaching 40.5 µm.

Through these results, it can be observed that the fireproof treatment applied on the hemp fibers leads to a moderate impact on the microstructure and pore geometry, due to an increase in fiber radius. This increase appears to be related to the use of the flame retardant. There are several possible explanations, but these will require further investigation to be verified. A first explanation could be that the treatment coats the fibers, adding a slight thickness to the surface. The consistency of the treatment could also lead to the creation of fiber agglomerates that stick together. Finally, it is also possible that the nature of the treatment could cause a swelling of the fibers. In all cases, the increase in the radius of the fibers leads to a reduction of the fiber stacks airflow resistivity and thus a slight reduction of the acoustic dissipation of waves by viscous effects at low frequencies. Furthermore, the reduction in viscous dissipation tends to shift the first peak of absorption to higher frequencies. However, this loss of sound absorption is very limited and the fireproof treated stacks of hemp fibers remain excellent sound absorbers, making these fibers good candidate as raw material for sound absorption panels.

3.2.4 Conclusion

In the present study, the acoustic properties of fireproof treated hemp fibers were evaluated. Through the acoustic properties, it was possible to describe the pore geometry and to estimate the effective radius of the fibers in the treated and untreated cases.

The treatment involved either immersing hemp fibers in a solution of phytic acid and urea or spraying this solution onto the fibers. Both methods enable the grafting of phosphorus onto the fibers and incorporate urea as a nitrogen source to achieve a synergistic effect for improved flame retardancy. Besides, both approaches resulted in a limited reduction in the sound absorption performance of hemp fibers.

Through the analysis of the acoustical parameters, obtained through direct measurements and indirect characterization based on impedance tube characterization, it was revealed that the treatment affected mainly the airflow resistivity, with a reduction of the viscous dissipation effects.

Moreover, through a micro-macro approach using the Tarnow model, the effective radius of hemp fibers was estimated, and an increase was observed. This increase was observed in all treated samples but was higher in a pulverized sample, which presented a higher amount of phosphorus grafted. The microstructure of the fiber stacks has a direct relationship with the acoustic performance of the material, and the increase in the effective fiber radius seems to be the reason behind the decrease in sound absorption. Further investigations are required to understand the reasons for the increase in effective fiber diameter after treatment. This could be done using SEM-type imaging techniques to experimentally assess fiber diameter and compare their morphology before and after treatment.

Despite this limited impact on the sound absorption of hemp fibers, the fireproof treatment used in this research expands considerably the field of potential applications of

hemp fibers and their manufactured products as bio-based insulators. Furthermore, they remain excellent sound absorbers, even after the fireproof treatment.

3.4 Thermal properties of fireproof treated hemp fibers

In the previous Sections of this Chapter, the impact of the fireproof treatment on the microstructure, physico-chemical properties and acoustic behavior of treated hemp fibers was evaluated. Another key functional aspect of these fibers is their thermal properties, which was assessed with the hot disc equipment, as specified in Section 2.5.1 and are presented in this Section.

The room conditions of temperature and humidity during measurements varied slightly the days that they were done. They are reported in the Table 3.5. As observed, the temperature remained stable during the days of measurement, between 19°C and 20°C. In contrary, the humidity varied considerably, between 40% and 52%, since the laboratory room where the equipment was placed was not regulated for relative humidity. As hygroscopic materials, with an increase in humidity, the hemp fibers can retain a higher humidity and increase the thermal conductivity measured. Therefore, the values obtained should be evaluated carefully, as the room conditions varied significantly between days of measurement.

Table 3.5: Temperature and humidity during measurements

Measurement	Temperature (°C)	Humidity (%)
D30	19.5 ± 0.4	40 ± 2.6
D45	20.0 ± 0.3	52 ± 0.7
D60	19.3 ± 0.2	45 ± 2.4
D90	19.8 ± 0.3	49 ± 0.3

3.4.1 Apparent density

The hemp fiber samples prepared target an apparent density of 30, 45, 60 and 90 kg.m^{-3}. Since the samples did not hold in position effectively, due to the lack of any sort of binder, the dimensions of them were measured and the effective apparent density was obtained. The effective apparent density was effectively 37.5, 46.5, 63.0, and 94.5 kg.m^{-3}, respectively. These changes happened especially due to a reduction in height, and a small increase in the radius of the samples.

3.4.2 Thermal conductivity, diffusivity and specific heat

The thermal conductivity, diffusivity and specific heat results are presented in Figure 3.8. Between 30 and 60 kg.m^{-3}, the thermal conductivity is constant at around 0.067 W.m^{-1}.K^{-1}. For a density of 90 kg.m^{-3}, it increases to around 0.078 W.m^{-1}.K^{-1}. The effect of fiber density is therefore clearly visible, whereas the variations between the different treatments are not significant. Any effect that the treatment might have on the thermal conductivity is overshadowed by the influence of the apparent density.

However, as mentioned in the beginning of this section, the humidity of the room did not stay constant during measurements and it could have impacted the measurements, specially for the measurement at 30 kg.m^{-3}. As the relative humidity was lower, these values are expected to be lower as well, due to a lower water content presented at the fibers. Since the values obtained were similar to the ones at 45 and 60 kg.m^{-3}, it means

the apparent density of 30 kg.m^{-3} might be too low and the effects of radiation start to be more significant.

In Figure 3.8b, the evolution of thermal diffusivity as a function of fiber's apparent density is presented. It can be noted that the diffusivity decreases as fiber apparent density increases, converging to about 0.6 mm^2.s^{-1}, which are in the same order of magnitude as wood fibers (0.37 mm^2.s^{-1}) and wood wools (0.76 mm^2.s^{-1}) presented by Palumbo et al. (PAL18). The lower value for the wood fibers can be explained by their higher apparent density of 230 kg.m^{-3}, whereas the wood wools had a density of 55 kg.m^{-3}, closer to the fibers presented in this study. Similarly to the thermal conductivity results, no significant differences are observed for fibers that have been treated.

The specific heat values of the treated samples were slightly higher for the samples at lower apparent density, but above 60 kg.m^{-3}, all samples presented the same specific heat at about 1.5 kJ.kg^{-1}.K^{-1}. The values are similar to those reported by Schiavoni et al. (SCH16) for hemp insulation materials, ranging from 1.6 to 1.7 kJ.kg^{-1}.K^{-1}.

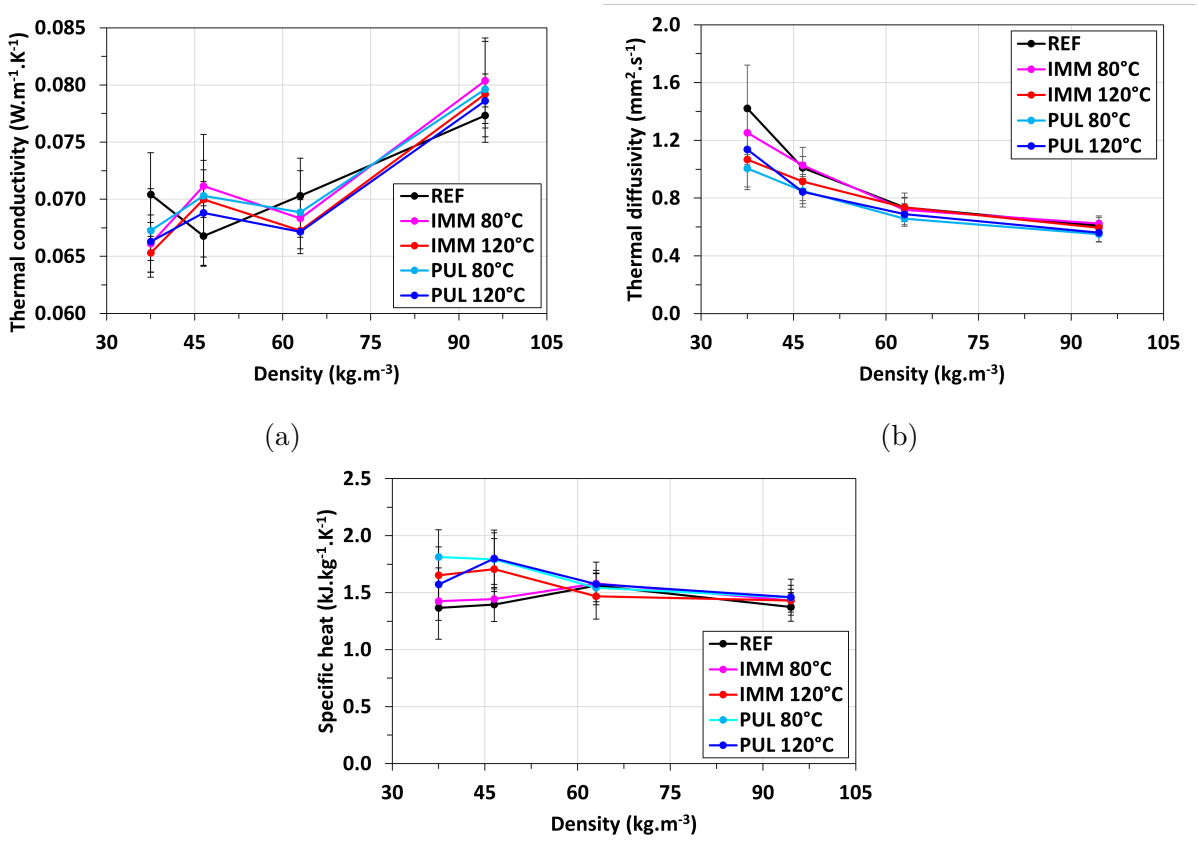

Figure 3.8: Thermal conductivity, diffusivity and specific heat results of treated and untreated hemp fibers

3.5 Fungal development on hemp fibers

In addition to the characterization of the impact of different fireproof treatment methods on the performance of hemp fibers, their susceptibility to fungal growth was also evaluated to ensure the durability of the treated fibers over time. To do so, the presence and identification of the fungi present in the fibers before (T0) and after 3 (T3) and 6 months (T6) of incubation in favorable growth conditions (30°C and 80% RH), was performed. The incubation test and the identification procedure are detailed in Sections 2.6.1 and 2.6.2.

The presence of fungi was evaluated in all hemp fiber samples (HF REF, HF IMM 80°C, HF IMM 120°C, HF PUL 80°C and HF PUL 120°C), before incubation. At T0, it was detected the presence of one colone of *Penicillium spp.* in two samples: HF REF and HF PUL 120°C. This species of mold is naturally present in the environment, and it is likely the origin of the fungi. It has a white colony with a green-colored center, with a powdery aspect (Figure 3.9). The immersed samples and sample HF PUL 80°C did not present any mold. Therefore, no particular influence of the presence of phosphorus and nitrogen molecules, originated from the flame retardants, is observed. Furthermore, the heating step also did not influence the presence of mold, since the pulverized samples heated at 80°C did not have mold, and the samples heated at 120°C did.

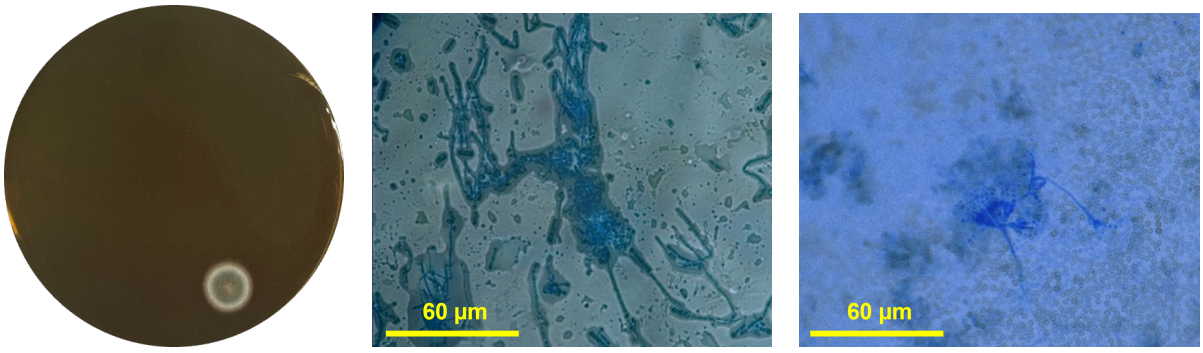

(a) (b) (c)

Figure 3.9: Identification of *Penicillium spp*: (a) At the Petri dish; (b) and (c) Digital microscope images

Then, sample HF REF was selected for incubation to assess the development of *Penicillium spp.* in natural untreated hemp fibers if it was exposed to favorable conditions for the its growth. The incubation lasted up to 6 months in a climate chamber at 30°C and 80% relative humidity, and the presence of fungi was verified and identified after 3 months (T3) and 6 months of incubation (T6).

At T3, the presence of the mold *Chrysonilia sitophila* was observed in the reference sample. This mold presents white colonies with a filamentous aspect that quickly become orange and have a fast growth (Figure 3.10). It is found in cereals, bread, silos and hot and humid environments. This specie was probably present in the hemp fibers but in a dormant state, and could only proliferate when favorable environment conditions were obtained.

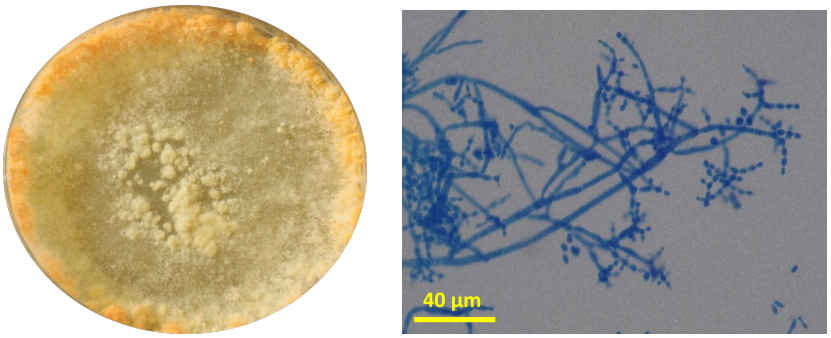

(a) (b)

Figure 3.10: Identification of *Chrysonilia sitophila*: (a) At the Petri dish; (b) Digital microscope image

Finally at T6, after six months of incubation, no mold was found in the reference fibers. The absence of the *Chrysonilia sitophila* indicates that the colonies nourished

themselves from all substrate needed for their development and died when there were no more nutrients left.

In conclusion, although mold was detected on two fiber types at T0 and on the reference fibers at T3, the absence of visible contamination indicates that, even under favorable temperature and humidity conditions, the fungi did not proliferate on the fibers.

3.6 Conclusion

The objective of this Chapter was to evaluate the influence of a fireproof treatment on hemp fibers by testing different methods of treatment application and conditions. The effectiveness of the treatment method was assessed as well as its influence on the properties of the fibers: their microstructure and their acoustic and thermal performances.

Confirming the observations from the literature review, the fireproof treatment based on phytic acid and urea is a solid choice as it was effective in reducing the flammability of the hemp fibers. This was observed in both treatment methods (immersion and pulverization) proving that the pulverization method can be an option to the well-established immersion method. A difference was observed on the influence of the grafting temperature, where it was expected that higher temperatures would lead to higher phosphorus grafted, but this was valid only for the immersion method. Further investigation of the optimal duration and temperatures of the heating step is needed, when considering the pulverization method.

The pulverization method was able to graft a higher phosphorus content onto the hemp fibers. This was associated with major difference on the flame retardants application methods. The immersion method requires a washing step at the end of the treatment, to remove the ungrafted molecules. As a dry method, or at least a method without the full immersion of the fibers in liquid solution, the pulverization method does not require this step, and the grafted and ungrafted phosphorus molecules remain present on the fibers. This resulted in a lower flammability of the pulverized hemp fiber samples.

Another important difference between the treatment methods is the amount of flame retardants used for each treatment. The immersion method required 10 times more solution prepared than the weight of the fibers to fully submerge them. In contrast, the pulverization method was performed with a solution to fiber mass ratio of 1, which is therefore 10 times less solution than the immersion method.

Taking into account that the pulverization method requires fewer steps and less material, along with the observations described above, it was considered as the most efficient treatment for hemp wool panels. Therefore, this method will be applied for the treatment of hemp wools in the following Chapters.

In terms of acoustic performance, a slight impact of the treatment was observed on the sound absorption of the treated samples at 60 $kg.m^{-3}$. This impact was more important on the samples with higher amount of phosphorus. At the other densities, no significant differences were observed, except for sample PUL 80°C. By investigating the characteristic parameters of the pore geometry, it was observed a reduction in the airflow resistivity. For characteristic viscous and thermal lengths, only sample PUL 80°C presented a significant change compared to the reference. Its values increased, demonstrating a tendency to increase their pore size.

Using a micro-macro approach with the Tarnow's model, the fiber radius was estimated. All treated samples showed an increase in their estimated radius, but a more important increase was observed in the pulverized samples that had a higher phosphorus content. Therefore, an impact of the treatment is observed on the hemp fibers, that can lead to a small reduction on their sound absorption performance. However, the treated

hemp fiber remains as excellent absorbers and can still be used as raw material for fireproof treated insulation.

Concerning thermal performances, no direct impact related to the use of flame retardants was observed. The influence of humidity and especially the apparent density are more relevant to impact the values of thermal conductivity, diffusivity and specific heat. Since the treatment leads to changes in apparent density, it can affect the thermal properties indirectly.

Fungal development analysis has shown that molds present in the air can be naturally found in hemp fibers. A specie commonly found in plants, seeds, and grains was also identified under favorable conditions of temperature and humidity, indicating that it is possible to have dormant molds in hemp fibers, which are waiting for optimal conditions to grow and proliferate. Only single colonies were identified before and after incubation, and no visual proliferation of the mold was observed, demonstrating that even under favorable conditions, the fungi analyzed did not proliferate.

This Chapter provided relevant information on the fireproof treatment and the effects linked to its application on functional properties and on the biological durability of hemp fibers. This was performed with the main raw material of the hemp wools. It is then relevant to advance to the scale of hemp wools and understand the manufacturing process and optimize the treatment for this material.

Chapter 4

Simplified production scale: Hemp wool prototypes

Chapter 3 showed that the flame retardant treatment selected from the literature review reduced the flammability of hemp fibers. When comparing the immersion and pulverization treatment methods, the latter proved to be the most efficient and effective, due to higher phosphorus content present in treated fibers, less steps required during treatment, and less flame retardants used.

Since the characterizations were performed on raw hemp fibers, it is necessary to validate the results obtained on insulating wool, taking into account the addition of synthetic fibers and the manufacturing process of hemp wools. In Chapter 4, small-scale hemp wool prototypes are manufactured and fireproof treated, with the goal to optimize the fireproof treatment at the scale of hemp wools and to define the treatment used in the next steps of this research (Figure 4.1).

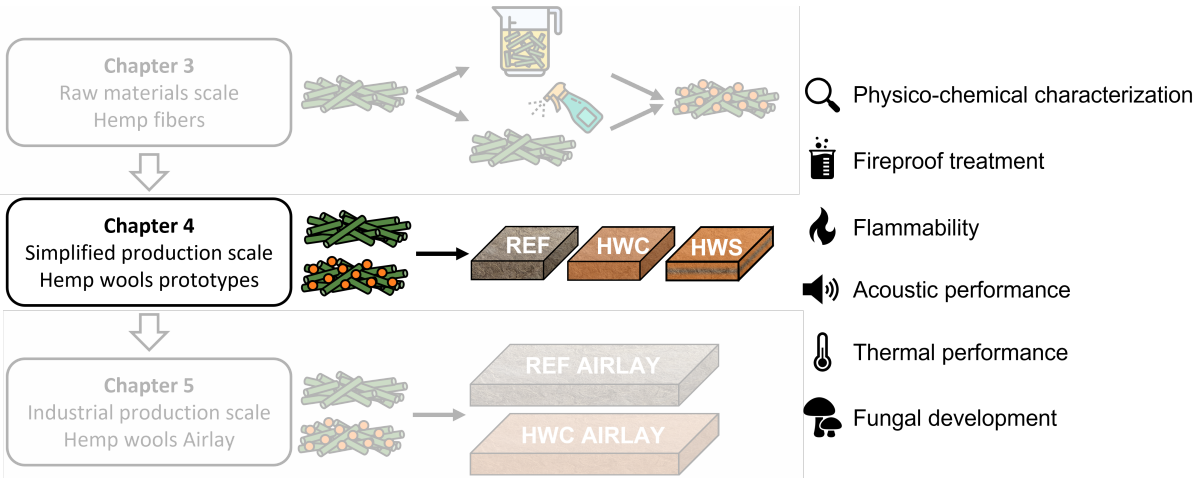

Figure 4.1: Scheme of thesis organization

This Chapter is composed of 6 parts divided into 4 Sections, as illustrated in Figure 4.2. It starts with Section 4.1, an article that will be submitted to Applied Acoustics, presenting the hemp wool prototype manufacturing and treatment process, their physico-chemical characterization, the evaluation of the impacts of the fireproof treatment on the sound absorption of hemp wools, and the analysis of the resulting effects on the characteristic parameters of the pore geometry. The treatment consisted of applying different concentrations of flame retardants at two distinct stages during the manufacturing of the hemp wools, either before or after forming the panels. Then, through a sensitivity analysis, it was identified which parameters change the most the sound absorption coefficient after treatment.

Subsequently, in Section 4.2 the thermal properties were evaluated, considering the different treatments tested, in order to assess the influence of the flame-retardants concentration and application procedure.

Then, in Section 4.3 four different concentrations of flame retardants applied before or after the production of hemp wool were evaluated in this Chapter, with the aim of optimizing the treatment and defining the optimal treatment method for industrial scale production (Chapter 5). Therefore, in this Section, a comparison between the fire reaction of the different hemp wool prototypes is presented.

Finally, mold identification and development are also assessed for hemp wools, and their results are presented in Section 4.4.

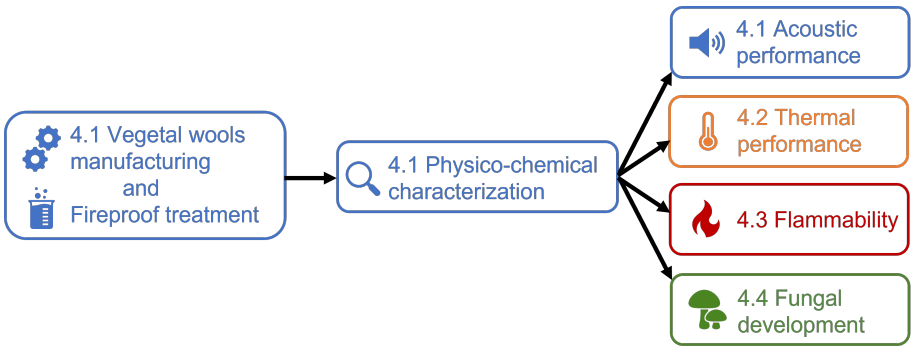

Figure 4.2: Parts of the Chapter 4

4.1 Article: Investigation on the sound absorption performance of fireproof treated hemp wools

Thomas Schatzmayr Welp Sá[1,2], Sandrine Marceau[1], Clément Piégay[2], Philippe Glé[2], Fouad Laoutid[3], César Segovia[4], Etienne Gourlay[5]

[1] CPDM, Université Gustave Eiffel - 14-20 Boulevard Newton, F-77454, Marne-la-Vallée, France
[2] Cerema, Université Gustave Eiffel, UMRAE - 11 Rue Jean Mentelin, F-67035, Strasbourg, France
[3] Laboratory of Polymeric and Composite Materials, Materia Nova Research Center - University of Mons (UMONS) - Av. Nicolas Copernic 3, 7000, Mons, Belgium
[4] CETELOR - Université de Lorraine, 27 Rue Philippe Seguin, 88051, Epinal, France
[5] Cerema, Equipe-recherche BPE - 11 Rue Jean Mentelin, F-67035, Strasbourg, France

Abstract

Hemp wool panels, typically composed of hemp and thermoplastic fibers, represent a sustainable alternative to conventional insulation, offering strong sound absorption capabilities. However, their high flammability restricts their use in buildings. Phosphorus- and nitrogen-based flame retardants have emerged as promising solutions, but their impact on the microstructure of vegetal wools—and consequently on their acoustic performance—remains poorly understood. Since fiber size, morphology, and organization strongly govern sound absorption, different treatment processes may lead to distinct outcomes. In this study, hemp wool panels were fireproofed using two production methods, and their acoustic performance was assessed in relation to pore geometry parameters. Results show a slight reduction in sound absorption in the treated samples, particularly for those with higher phosphorus content. Significant modifications in porosity, airflow

resistivity, and thermal characteristic lengths were observed. Despite the small loss in performance, the fireproof treated hemp wools remained as excellent absorbers, fitting its use as an alternative sustainable insulator.
Keywords: *hemp wool, bio-based material, acoustic, fireproof treatment*

4.1.1 Introduction

Hemp wools are panels designed for building insulation, coupling sustainability and excellent functional performance. Their application is becoming increasingly relevant in the context of sustainable construction, as they represent an alternative to traditional insulation materials derived from mineral and petroleum sources. In addition to being renewable and recyclable, hemp fibers contribute to carbon sequestration during growth and provide both thermal and acoustic comfort, making hemp wool an attractive solution for reducing the environmental footprint of buildings (ARE21; HAB21).

The main component of the hemp wools, composing about 90% of its weight, is the hemp fibers. After being harvested, these fibers are submitted to the retting process, which allows micro-organisms and bacteria to consume the binding substances present in the hemp fiber, such as pectin, facilitating defibrillation operations (ABO10; MAR14). Then, decortication, scutching and hackling processes are employed to improve fiber quality, by removing unwanted non-fibrous materials such as hemp shives, and separating fiber agglomerates as far as possible (FRE12; THY06).

For the fabrication of insulation panels, the vegetal wools can be produced using an airlay technique associated with a thermo-bonding process. In this method, the vegetal fibers are mixed with a small amount of thermoplastic fibers (generally around 10% of the material's weight), which acts as a binder in this system (ROY11). The mixed fibers passes through an air stream to evenly distribute the fiber web, forming a light panel (AYA23; HYS16). Then, the fibers are heated and compressed to reduce the panel thickness and consolidate the panel. At this moment, the thermoplastic fibers partially melt and are subsequently cooled down, forming bonds with the hemp fibers (ROY11). The temperature applied depends on the melting point of the polymer used, but it is usually around 115°C to 215°C (JOM13; ROY11; TOM10).

Regardless of the production method, hemp wools, as a bio-based material, have a weakness, which is their high flammability (AMZ17; KOZ20). It limits their application and reliability as an alternative material for building insulation. A solution to this problem is the use of flame-retardants. Phosphorus-based flame-retardants have shown an interesting improvement on bio-based materials flammability, while preserving their intrinsic nature by using bio-based phosphorous-based additives, such as phytic acid (ANT22; HAJ18; MOU20; SAC25; TAI22). They act by accelerating the kinetics of thermal degradation and favoring the formation of a char layer during combustion. This char layer reduces flame spread, oxygen diffusion and heat shield (LAO09; TAI22). Moreover, the phosphorus-based flame-retardants can be used in association with nitrogen-based counterparts to enhance char yield and thermal stability, thereby further reducing the flammability (COS17; KOZ20; TAI22). The aim of the treatment is to graft phosphorus molecules onto the fibers and reduce their fire reaction (SAC25).

Based on a previous study on flame-retarded hemp fibers with a combination of phytic acid and urea (SAC25), two application methods of treatment are possible, by immersion of the fibers in solution or by pulverization of the solution over the fibers. Given the production processes of the hemp wools and the time and energy required in each of these methods, the pulverization method was selected. Furthermore, two possibilities of application were identified: pulverization of all fibers, before the production of panels, targeting the grafting of phosphorus molecules in the whole panel; or the production of

the panels followed by the pulverization of their surfaces only.

Despite the benefits of flame-retardant treatment on the flammability of hemp wools, concerns arise about the acoustic performance. In fact, the acoustic performance of fibrous materials is strongly related to their microstructure and pore geometry, and changes in the morphology or chemical structure of the fibers could lead to modification of the acoustic performance of the materials (ARE10; LUU17; LUU17; PIE18; PIE21).

However, the impact of fireproof treatments on the acoustic performance of materials is not widely explored. Few studies analyzed the sound absorption of treated bio-based materials, such as low-density fiberboards (LEE23), recycled technical textiles (DAN21), and bamboo pulp foam (YUE24). In some cases, the application of flame retardants let to an overall improvement in the sound absorption, while in others, it resulted in a reduction. However, no clear explanation of how the flame-retardant treatments impacted the acoustic performance has been established. There is a lack of investigation on the effects of the applied treatments on the microstructure and pore network of the materials, that could be useful to understand the real impact of the fireproof treatment on the acoustic performance of vegetal wools.

In this context, characteristic parameters of the pore geometry can be a useful tool for evaluating the viscous and thermal dissipation effects before and after fireproof treatment, and correlate them with the pore network structure. From previous studies (AYA23; CHA16; JAO20; KHO25), the Johnson-Champoux-Allard-Lafarge (CHA91; JOH87; LAF97) (JCAL) modeling method has been shown to provide a pertinent simulation of the sound absorption of fibrous materials based on these parameters. This method is based on the equivalent fluid theory and assumes the solid skeleton as a rigid body or motionless. It uses parameters related to the material's pore geometry to describe the viscous and thermal effects that occur in the pores.

Another approach is through homogenization methods, such as the models from Tarnow (TAR96) and Umnova (UMN09). These models are based on a self-consistent homogenization approach but in which the energy consistency condition is replaced by a zero vorticity condition at the unit cell boundary. They provide analytical relationships between parameters of the fiber morphology (effective radius and porosity) and characteristic parameters of the pore network, used in the JCAL model. Therefore, this approach allows for the use of macro-scale properties to understand the microscopic geometry of the hemp wools.

In this study, hemp wool prototypes will be developed and treated using phosphorus- and nitrogen-based flame retardants, with the aim of evaluating the effects of the treatment on the material's sound absorption. The investigation of the characteristic parameters of the pore network aligned with homogenization models based on micro-macro approaches, allowed the identification of the treatment impact on the organization and morphology of the fibers.

4.1.2 Materials and methods

4.1.2.1 Materials description

Bulk hemp fibers, from AgroChanvre (France), were used for the production of hemp wools. These fibers were previously retted (LEC21; THY06) and cleaned, presenting a small number of shives. All hemp fibers used in this study were taken from one single bale. A bi-component fiber TREVIRA 256 (Germany), made of poly(ether-sulfone) (PES) on the core, and copolyethylene (coPE) on the sheath, with about 18 µm of diameter, was used as the binder of the hemp wools. The melting point of the sheath is 127°C and the core is 256°C (data provided from manufacturers). For the fireproof treatment, phytic acid (CAS: 83-86-3) in solution 50 wt.%, and urea (CAS: 57-13-6, purity > 99.5%) were

used. Nitric acid at 65% concentration (CAS: 7697-37-2) was also used for spectroscopy (ICP-AES) analysis.

4.1.2.2 Hemp wool prototype production

In this section, the steps taken during the manufacturing of hemp wools will be described and detailed. The whole process was divided into five major steps (Figure 1): fibers opening; fibers mixing; treatment application and panel preparation; panels heating; and samples preparation.

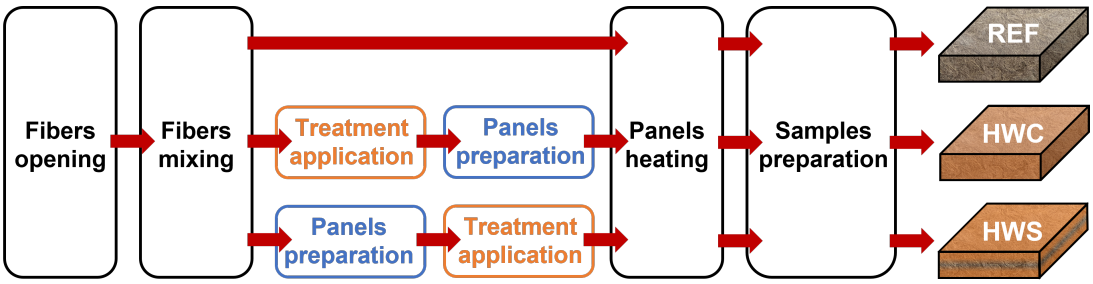

Figure 1: Schematic representation of the hemp wool panels production

Fibers opening: The first step consists of "opening" the fibers, which means separating the elementary fibers from their bundle. Bulk hemp fibers are mainly composed of technical fibers, i.e., fiber bundles of elementary fibers, and usually, these technical fibers are strongly intertwined with each other. Therefore, to ensure a good mixing between hemp and thermoplastic fibers, they need to undergo a preceding step, that untangles them and separates the elementary hemp fibers from their bundles.

An amount of 4.5 kilograms of hemp fibers were processed using a fiber-opening machine Laroche 500 equipped with two metallic cylinders. The first has pointed spikes at a density of 2 spikes per cm^2, and the second is equipped with lining teeth, at a density of 10 per cm^2. Together, both modules served to open and separate the entangled fibers. This process also helped clean the fibers by removing unwanted hemp shives. After passing through the equipment, the fiber lengths were reduced to approximately 5 to 15 cm. The same procedure was performed with 0.5 kg of bi-component fibers, which helped to untangled them. This process is shown in Figure 2.



(a) (b)

Figure 2: Fiber opening process: (a) Hemp fiber; (b) Thermoplastic fiber

Fibers mixing: The process of mixing the fibers started with spreading the hemp fibers over a large surface and the bi-component fibers were evenly distributed on top of them, as homogeneously as possible. The bi-component fibers accounts for 10% of the hemp wool's mass. This step helps prevent the formation of zones with high or low concentration of thermoplastic fibers. Then, these fibers passed twice in the opening machine to mix, in order to achieve the desired homogeneity. The whole fiber mixing process is illustrated in Figure 3. After mixing the fibers, they were weighted and separated in plastic bags containing the same amount of fibers each, for the target goal of 60 kg.m^3 for each panel.



(a) (b) (c)

Figure 3: Fiber mixing process: (a) Fibers spread in a large surface; (b) Mixing process (c) Mixed fibers aspect

Fireproof treatment of hemp wools and panel preparation: The fireproof treatment solution was prepared by mixing the phytic acid, urea and distilled water, under magnetic stirring at 300 rpm for 10 minutes. The solution to fiber mass ratio used was of 1, which allowed for proper dispersion of the solution without saturating the fibers. Four different solution concentrations were tested: 1%, 3%, 5% and 10% of phytic acid and 3%, 9%, 15% and 30% of urea, respectively.

Two possible methods of solution application were identified. The first method consisted of spreading the fibers in a recipient and pulverizing the solution over them. The fibers were continuously mixed and pulverized until the whole solution was applied. The fibers were then placed manually in molds with dimensions of 30x30x5 cm^3, making the panels. The samples treated by this method are labeled as HWC (hemp wool core).

In the second method, the procedure is done in the opposite order. Firstly, the panels are prepared in the molds with the untreated mixed fibers and then pulverized at their surfaces on both sides with the flame retardant solution, with half of the solution sprayed on one side of the panel and half on the other. This method is referenced as HWS (hemp wool surface). Table 1 summarizes the samples and the concentration of phytic acid and urea.

Panels heating and samples preparation: Then, the hemp wools in the molds passed through an oven with two main purposes. Firstly, it melts the copolyethylene, which is found in the outer layer of the bi-component fiber, and after cooling, it bonds with the hemp fibers, acting as a binder in the hemp wool (ROY11). Secondly, heat is necessary for the grafting of phosphorus molecules with the hemp fibers (HAJ20; MOU20; SAC25).

Table 1: Fireproof treatment concentration and samples nomenclature

Sample	Phytic acid (%)	Urea (%)	Treatment
HW REF	-	-	-
HWC 1%	1%	3%	Core
HWC 3%	3%	9%	Core
HWC 5%	5%	15%	Core
HWC 10%	10%	30%	Core
HWS 1%	1%	3%	Surface
HWS 3%	3%	9%	Surface
HWS 5%	5%	15%	Surface
HWS 10%	10%	30%	Surface

A conveyor belt passes through the oven at a speed of 0.5 m.min^{-1}. The oven, model Santex Santatherm Thermobonding Oven, consists of two chambers that form an airflow of hot air. For the manufacturing of the hemp wool panels, the temperature of both chambers were set to 140°C. After passing through the oven, the material is cooled down with fresh air at room temperature, for the solidification of the bi-component fibers. The whole procedure takes about 15 minutes.

The panels passed through the oven three times. The first time was executed with the panels still inside the mold, for the consolidation of them. The second time was done for better consolidation of the panel and a longer exposure to heat, improving the grafting of the phosphorus. The third time was carried out without the mold, to reduce the thickness of the panels from 50 mm to 40 mm. The heating process is presented in Figure 4.



(a) (b) (c)

Figure 4: Fiber heating process: (a) Mixed fibers placed in 30x30x5 cm^3 molds; (b) Heating process: (c) Hemp wools panels prototypes

After that, cylindrical samples were cut from the panels with 100 mm of diameter, using a band saw, for the acoustic characterization of the hemp wools. A total of 4 samples were cut for each formulation, as shown in Figure 5.

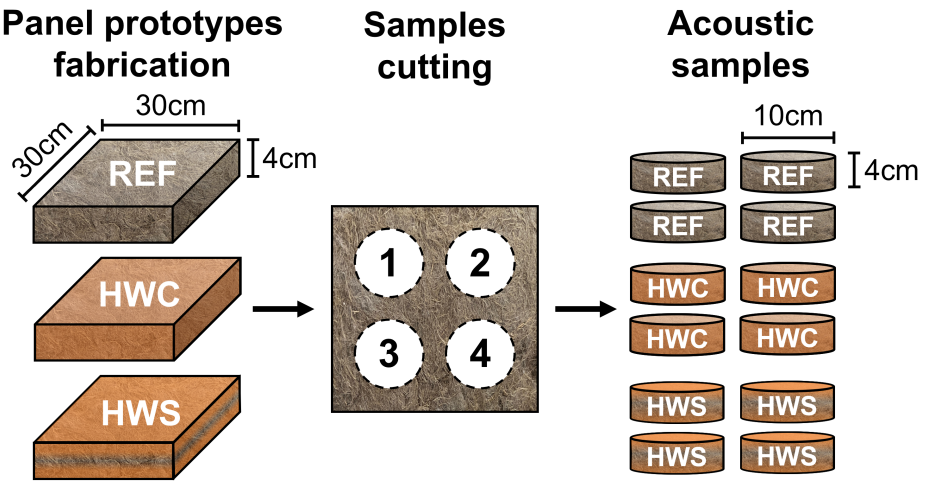

Figure 5: Schematic representation of the acoustic samples preparation. Orange zones represents the area treated with flame-retardants.

4.1.2.3 Chemical characterization

The phosphorus content of the hemp wools was measured with the inductively coupled plasma atomic emission spectroscopy (ICP-AES) technique, with an equipment model ULTIMA 2000 from Jobin Yvon Horiba Company. A sample of 0.3 g of hemp wool was digested using a nitric acid/distilled water (50/50) solution for 4 hours at 100°C, under magnetic stirring. The remaining solution was filtered, and diluted in a 1 l volumetric flask. The phosphorus concentration was determined using calibration curves obtained from ICP-AES analysis of standard solutions at different concentrations. The test was repeated 4 times for each sample. The phosphorus content was assessed at the surface and in the center of each sample, to verify the homogeneity of both treatment application methods, i.e. surface or core.

4.1.2.4 Airflow resistivity

The airflow resistivity (σ) was measured directly using a Mecanum SIGMA SIG2014 airflow resistance-meter, following the procedure of the standard ISO 9053-1:2018 (AFN18). For this test, the same cylindrical samples from the impedance tube test were used. A total of 4 samples per condition were tested. Prior to testing, the samples' water content and temperature were stabilized for 72h in the same room where the measurements were conducted, with room conditions of 23.5 ± 0.5°C and 40 ± 5% relative humidity.

4.1.2.5 Density and porosity

The density of the solid phase of the hemp wools was determined using a Micrometrics Accupyc II gas pycnometer. The test was performed in two conditions: helium gas and nitrogen gas. Both gases are inert, but have different size of molecules, which can demonstrate the presence of very small pores that the helium molecules can penetrate, and the nitrogen gas cannot. In both conditions, the fibers were pre-dried at 60°C for 72h. The open porosity of each sample was calculated using the apparent density (ρ_{ap}) of the sample and the material's skeleton density (ρ), through Equation 1.

$$\phi = 1 - \frac{\rho_{ap}}{\rho} \tag{1}$$

4.1.2.6 Impedance tube

The sound absorption performance of the hemp wool samples was measured with an impedance tube, model AcoustiTube AFD 1200, with a three microphones configuration (IWA98; SAL10), and following the standard ISO 10534-2:2023 (AFN23). The tube's section had 100 mm and the frequency domain of measurements was in the range between 143 and 1993 Hz.

The samples were cut in a cylindrical shape with 100 mm diameter with a band saw. Their height was 40 mm, as specified during the production description of the panels in Section 4.1.2.2. The panels produced had a target density of 60 kg.m^{-3} using the same amount of fibers for each formulation. However, with the addition of the flame retardants, some variations in the panels' apparent density were observed. For each condition, 4 samples were prepared and each was tested on both sides, totaling 8 measurements for each condition. To stabilize the water content and the temperature of the hemp wool samples, they stayed in the measurement room for 72h before the test, with room conditions of 23.5 ± 0.5°C and 40 ± 5% relative humidity.

4.1.2.7 Tortuosity

The hemp wool's tortuosity was measured using an ultrasonic method for porous materials saturated by air, with the equipment Mecanum ultrasonic tortuosity-meter. The measurements were performed with the device in transmission configuration, in which the equipment measures the acoustic propagation time of laser-generated acoustic pulses, with and without a material (ALL94; MOU01).

4.1.2.8 Indirect characterization of the pore network parameters

Some characteristic parameters of the pore network were indirectly obtained based on studies by Panneton and Olny (OLN08; PAN06). These parameters allow for the characterization of the pore network of the hemp wool samples and the evaluation of the impact of the fireproof treatment on them. Equations 2 to 4 were used to determine the viscous characteristic length (Λ), thermal characteristic length (Λ') and static thermal permeability (Θ_0), respectively (JAO20). The dynamic density (ρ) and dynamic bulk modulus (K) were obtained experimentally using the impedance tube with the 3 microphones method described in Section 4.1.2.6.

$$\Lambda = \frac{\alpha_\infty}{\phi}\sqrt{\frac{2\eta\rho_0}{\omega Im(\rho)}\left[\frac{\alpha_\infty\rho}{\phi} - Re(\rho)\right]} \tag{2}$$

$$\Lambda' = 2\sqrt{\frac{\kappa}{C_p\rho_0\omega}\left[-Im\left[\left(\frac{\gamma P_0 - \phi K}{\gamma P_0 - \gamma\phi K}\right)^2\right]\right]^{-1}} \tag{3}$$

$$\Theta_0 = \frac{\phi\kappa}{C_p\rho_0\omega}\Big/\sqrt{-Re\left[\left(\frac{\gamma P_0 - \phi K}{\gamma P_0 - \gamma\phi K}\right)^2\right]} \tag{4}$$

4.1.3 Modeling

4.1.3.1 JCAL model

The sound absorption performance of the hemp wool samples was simulated using the Johnson-Champoux-Allard-Lafarge (JCAL) model (CHA91; JOH87; LAF97). This approach considers the movement of the fluid phase (air) through a pore network based on a

non-uniform geometry. Under the assumption of a rigid skeleton (PIE18), only the visco-inertial and thermal dissipative effects are taken into account. In this case, the sound absorption coefficient can be determined with two intrinsic parameters: dynamic density (ρ) and dynamic bulk modulus (K). The JCAL method establishes analytical relationships between the intrinsic parameters of the material and the characteristic parameters of the pore networks, shown in Section 4.1.2.8 and the porosity shown in Section 4.1.2.5. These relationships are represented as Equations 5 and 6.

$$\rho = \frac{\rho_0 \alpha_\infty}{\phi}\left[1 - j\frac{\sigma\phi}{\rho_0\alpha_\infty\omega}\sqrt{1 + j\frac{4\eta\alpha_\infty^2\rho_0\omega}{\Lambda^2\sigma^2\phi^2}}\right] \tag{5}$$

$$K = \frac{\gamma P_0}{\phi}\left[\gamma - (\gamma-1)\left(1 - j\frac{\phi\kappa}{\Theta_0 C_p\rho_0\omega}\sqrt{1 + j\frac{4\Theta_0^2 C_p\rho_0\omega}{\kappa\phi^2\Lambda'^2}}\right)^{-1}\right]^{-1} \tag{6}$$

4.1.3.2 Tarnow model

The estimation of the fiber radius can be done by using a micro-macro approach, where through macro-scale parameters can be used to estimate micro-scale characteristics of the material. The Tarnow model provides analytical relationships between resistivity and microstructural parameters of the fiber stack (TAR96), under the hypothesis of cylinders (fibers) with the same radius placed in a regular or random configuration, with an airflow parallel or perpendicular to the fibers. Therefore, a relationship between airflow resistivity and fiber radius (R_f) is stipulated, along with the material's porosity and the dynamic viscosity of the air (η), as shown in Equation 7.

Four different scenarios are possible through the combination of fiber organization and airflow: regular or random fiber distribution, airflow parallel to fibers or perpendicular. Based on a study from Glé (GLE13), the condition of random fiber distribution with perpendicular airflow is the most adequate for hemp wools. The Tarnow model has been validated by Piégay *et al.* (PIE18), in the case of vegetal wools.

$$R_f = \sqrt{\frac{4\eta(1-\phi)}{\sigma[0.64ln(\frac{1}{1-\phi}) - 0.737 + (1-\phi)]}} \tag{7}$$

4.1.3.3 Umnova model

Another approach for the estimation of the fiber radius is the Umnova model (UMN09). This model is based on the homogenization theory, which assumes the existence of a representative volume of the material and a separation between micro and macro scales. It also considers the slip effects that occurs in the pore surfaces when the characteristic pore size becomes comparable to a saturating gas molecular mean free path (l_{mean}). This parameter depends on the fluid viscosity, density and temperature. For air at normal conditions it is about 60 nm. Since the pore size in hemp wools are significantly higher than 60 nm, the air is in the continuum regime, and the slip effects can be neglected.

In this case, assuming an airflow perpendicular to the fibers, the Umnova model provides a relationship between the fiber radius, airflow resistivity and air viscosity, given by Equation 8.

$$R_f = \sqrt{\frac{16\eta(1-\phi)}{\sigma(-2ln(1-\phi) - 2\phi - \phi^2)}} \tag{8}$$

4.1.4 Results and discussion

4.1.4.1 Density and porosity

The pycnometer results performed under nitrogen and helium atmospheres are presented in Table 2. The density of the sample did not vary significantly with the treatment for both types of gas. Under nitrogen, the range of values is between 1.43 and 1.45 kg.m^{-3} and from 1.44 to 1.46 kg.m^{-3} under helium. The values are slightly lower when measuring density in nitrogen because the molecules are larger than Helium. As a result, nitrogen fills less space in the pycnometer capsule and measures a higher volume occupied by the fibers, leading to a slightly lower density. However, the difference between the results are lower than 1%, indicating that both methods are valid for the determination of the solid skeleton density of the fibers.

Table 2: Real and apparent density of hemp wools

Sample	Density - N_2 kg.m^{-3}	Density - He kg.m^{-3}	Apparent density kg.m^{-3}	Porosity - He (-)
HW REF	1.445 ± 0.003	1.460 ± 0.003	60.9 ± 3.7	0.958 ± 0.002
HWC 1%	1.447 ± 0.001	1.460 ± 0.004	66.0 ± 1.3	0.955 ± 0.001
HWC 3%	1.450 ± 0.003	1.459 ± 0.002	70.4 ± 2.1	0.952 ± 0.001
HWC 5%	1.448 ± 0.002	1.454 ± 0.003	75.0 ± 10.7	0.948 ± 0.006
HWC 10%	1.454 ± 0.003	1.457 ± 0.002	86.3 ± 8.6	0.941 ± 0.005
HWS 1%	1.443 ± 0.001	1.449 ± 0.003	56.1 ± 3.3	0.961 ± 0.002
HWS 3%	1.435 ± 0.002	1.447 ± 0.006	57.3 ± 7.5	0.960 ± 0.005
HWS 5%	1.438 ± 0.002	1.446 ± 0.003	60.7 ± 4.5	0.958 ± 0.003
HWS 10%	1.442 ± 0.001	1.453 ± 0.003	64.2 ± 4.7	0.956 ± 0.003

Table 2 also presents the apparent density of each formulation. They are obtained from measurements of size and weight from all four samples made from each treatment condition.

It can be noted that the apparent density of HWC samples increases linearly with the amount of flame-retardants applied, increasing from 60.9 kg.m^{-3} for the HW REF to 86.3 kg.m^{-3} for HWC 10%. A statistical analysis one-way Anova and Tukey HSD tests, showed significant difference between samples (p-value = 0.0006), which was found to occur between the reference and samples HWC 5% and HWC 10%. Statistically, there is no difference between the reference and samples HWC 1% and HWC 3%. HWS samples also presented increasing apparent density, between themselves, but at a lower rate, as only their surfaces were treated. From statistical one-way Anova tests, no significant differences were observed between HWS and reference samples (p-value = 0.207).

As a result of the solid skeleton density and apparent density of each sample, their open porosity was calculated using Equation 1. The solid skeleton density values used in the calculation were the ones obtained through the helium pycnometry, and the values are reported in Table 2. The reference sample presented a porosity of 0.958. HWC samples presented a reduction in their porosity with values between 0.955 (HWC 1%) and 0.941 (HWC 10%). Compared to the reference, all samples are significantly different, except HWC 1%, as shown by an one-way Anova analysis (p-value = 0.000). HWS samples presented porosity values around 0.956 and 0.961, and did not show any significant difference compared to the reference, as confirmed by an one-way Anova and Tukey HSD tests (p-value = 0.014, but the differences occur between samples HWS 10% and HWS 1% and HWS 3%).

Knowing that the fiber's real density barely change with the treatment, and the fact

that each panel was made with the same amount of fibers and had the same volume of 30x30x4 cm^3, the new volume occupied by the fibers can be estimated using Equation 9.

$$V_f = \frac{\rho_{ap} V_p}{\rho_f} \tag{9}$$

where ρ_{ap} is the apparent density, ρ_f is the real density of the fibers, V_f is the volume occupied by the fibers and V_p is the volume of the panel.

By comparing each sample with their respective reference, a relative change of volume is obtained, and presented in Table 3. Samples HWC demonstrate a clear increase in their volume with the increase in the flame-retardants used, reaching 41.6% increase for sample HWC 10%. It is worth noting that all fibers in these samples were treated prior to the panel production process.

In contrast, for samples HWS, no clear behavior of the volume change is observed, since a volume reduction is observed in samples HWS 1% and HWS 3%, and an increase in sample HWS 10%. Because the HWS samples were only treated at their surface and after their production, they are considered less homogeneous, and are not suitable for evaluating the impact of the treatment on the volume occupied by the fibers.

Table 3: Volume occupied and fiber radius change with treatment

Sample	% Volume difference
HW REF	-
HWC 1%	7.8%
HWC 3%	15.5%
HWC 5%	22.8%
HWC 10%	41.6%
HWS 1%	-7.7%
HWS 3%	-5.5%
HWS 5%	0.4%
HWS 10%	5.6%

4.1.4.2 Phosphorus content

The phosphorus content presented at the core and surface of the hemp wools is shown in Figure 6. HWC samples presented a similar phosphorus content at both their core and surface, indicating that this treatment method leads to homogeneous grafting of phosphorus molecules throughout the entire sample. The phosphorus content plays a key role in reducing the flammability of hemp wools, with its content increasing proportionally to the amount of phytic acid applied.

HWS samples were treated only at their surfaces. The results show that the phosphorus content was zero at the core of the prototypes (square orange marks), whereas the surface presented increasing values of phosphorus content, similar to the ones observed in the HWC samples. These results show that with the treatment applied to the panels after manufacture, only the surfaces of the panels are treated, and that the core has a phosphorus content of zero, similar to the reference sample.

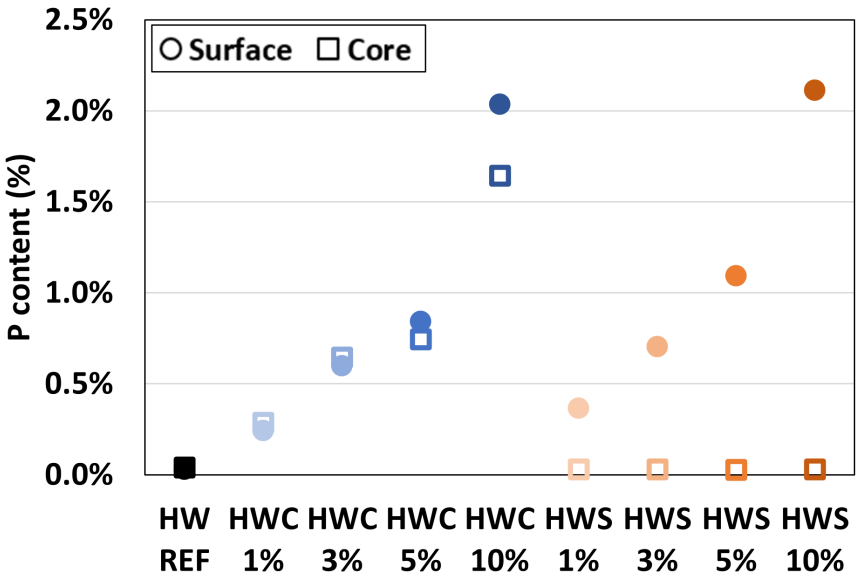

Figure 6: Phosphorus content of hemp wools

4.1.4.3 Sound absorption coefficient

The sound absorption of the hemp wools has been obtained with the impedance tube test. The average curve from 8 measurements are shown in Figure 7 for samples HWC and HWS. These samples were manufactured with the same procedure and used the same amount of fibers for each panel. Therefore, samples cut from panels (Figure 5) are expected to have, on average, the same amount of fibers, even though their masses and apparent densities are different after treatment. In other words, the curves presented in Figure 7 do not have the same apparent density, but rather the same amount of fibers.

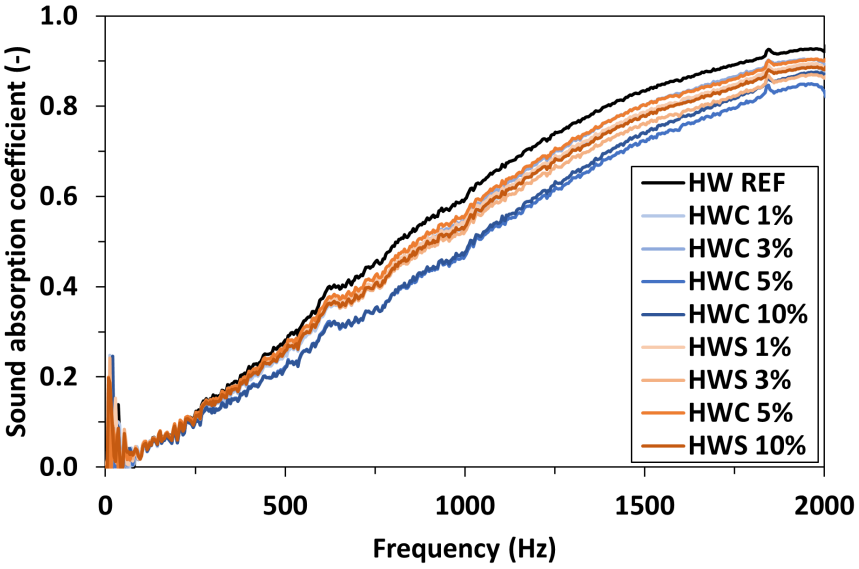

Figure 7: Sound absorption comparison between HWC and HWS with equivalent amount of fibers

To quantify the change in sound absorption in the treated samples, the relative difference between them and the reference was determined. This was done for each data point in the range of frequencies between 200 and 2000 Hz, and the average relative difference was obtained.

Samples HWC presented a reduction in their average sound absorption that was, at some extent, proportional to the flame-retardants concentration applied. Indeed, samples HWC 5% and HWC 10% have shown the largest reduction in their ability to absorb the sound waves energy, despite their higher density presented in Table 2. These samples presented a sound absorption performance 16.5% and 15.4% lower than the reference, as shown in Table 4, respectively. These samples have a higher amount of phosphorus grafted, as shown in Section 4.1.4.2, indicating an impact of the treatment on the fibers and, consequently, a reduction in acoustic performance. This impact will be explored further in Section 4.1.4.4.

Samples HWS had a smaller reduction in performance, varying between 4.5% to 9.0% (Table 4), with no significant differences between themselves, indicating a smaller influence of the flame-retardant concentration. The HWS sound absorption curves are placed between HWC 5% and HWC 10% and the reference sample. Since only the surfaces of these samples are treated, and their core is equivalent to the reference sample, this result is logical.

Table 4: Relative difference on the sound absorption between the reference and treated samples from 200 to 2000 Hz

Sample	Relative difference (%)
REF x HWC 1%	8.1%
REF x HWC 3%	6.1%
REF x HWC 5%	16.5%
REF x HWC 10%	15.4%
REF x HWS 1%	6.3%
REF x HWS 3%	9.0%
REF x HWS 5%	4.5%
REF x HWS 10%	7.7%

4.1.4.4 Characteristic parameters of the pore geometry

The characteristic parameters of the pore geometry are linked to the pore network and the elements characteristic of fiber's morphology, which were assessed through direct or indirect methods. Figure 8 presents the porosity values calculated from the apparent and real densities of each formulation, on the primary y-axis. These results have been presented and discussed in Section 4.1.4.1. It should be noted that all hemp wools are highly porous, with porosity values between 94% and 96%.

The tortuosity values of hemp wool are also shown in Figure 8, in the secondary y-axis. The values ranged between 1.12 and 1.24, and are slightly higher than the tortuosity values, between 1.01 and 1.08, obtained by Piégay (PIE19) for untreated hemp wools. However, they remain low, indicating that the fibers do not significantly interfere with the path traveled by the sound waves through the material.

The air resistivity values are presented in Figure 9. From measurements, the reference hemp wools have shown an airflow resistivity of 6000 N.s.m^{-4}, while HWC samples presented values below 5000 N.s.m^{-4}, and HWS samples with values between them. This indicates a tendency of the fireproof treatment to increase the permeability to airflow passage through the samples. However, using one-way ANOVA and Tukey HSD tests it was observed that all samples are considered statistically similar to each other.

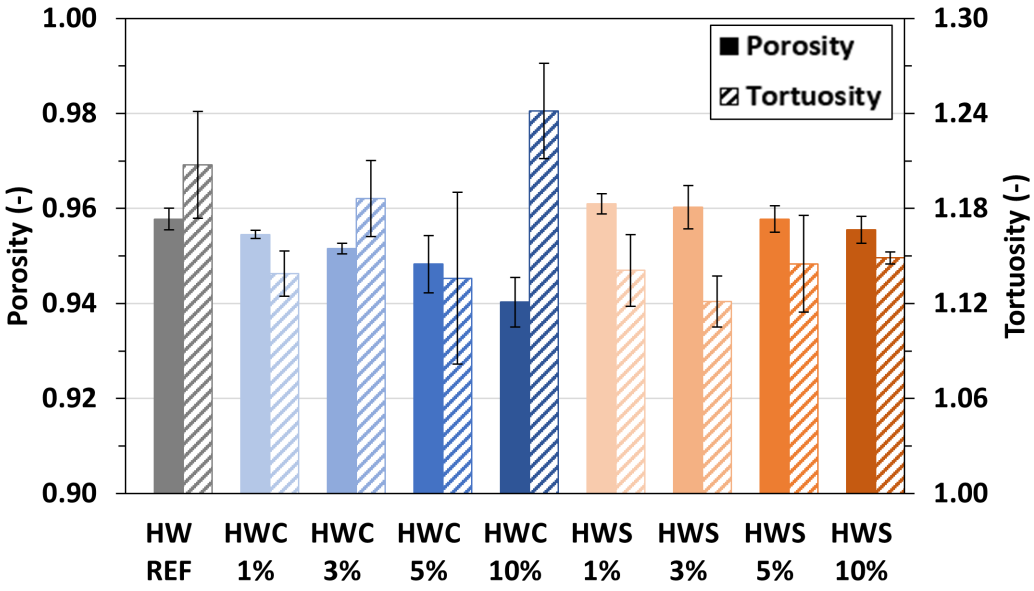

Figure 8: Porosity and tortuosity of hemp wools

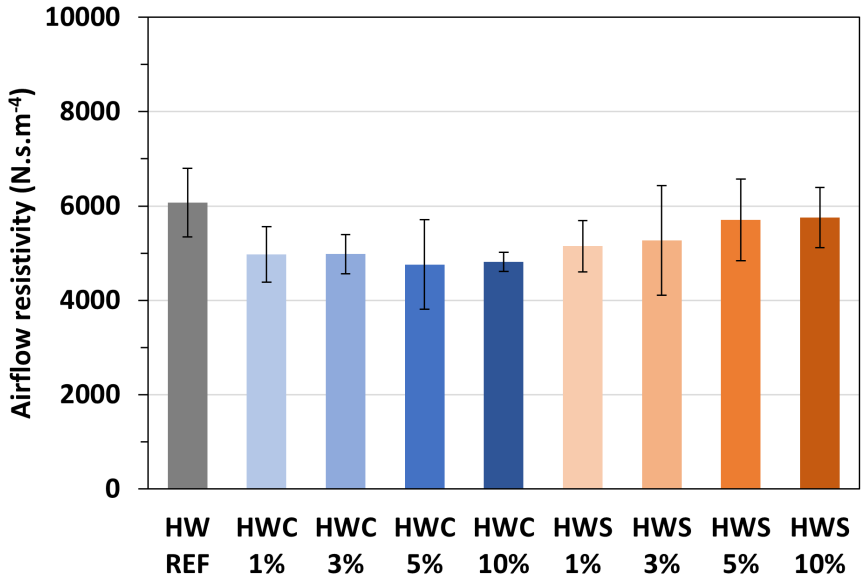

Figure 9: Airflow resistivity of hemp wools

The characteristic viscous and thermal lengths and static thermal permeability results are presented in Figure 10, with the first two parameters associated to the primary y-axis and the latter to the secondary one. For both characteristic viscous and thermal lengths values presented a small tendency to increase in the treated samples. However, statistical analysis has shown that there is no significant difference between the characteristic viscous length results.

For the characteristic thermal length, only the reference statistically differed to some treated samples (HWC 5%, HWC 10%, HWS 1% and HWS 3%). Moreover, the characteristic thermal length values are approximately twice of their respective characteristic viscous length, which was also observed in previous studies (PIE19). A higher characteristic viscous and thermal lengths indicate larger pores and connection between pores, which lead to lower dissipation of the viscous and thermal effects. Moreover, a higher pore size also facilitates the air permeability, which explains the reduction in airflow resistivity. These results are consistent with the reduction in sound absorption observed

in Figure 7. The thermal permeability values presented, in some cases, high dispersion, which makes it difficult to draw conclusions. Overall, no significant changes are observed between samples.

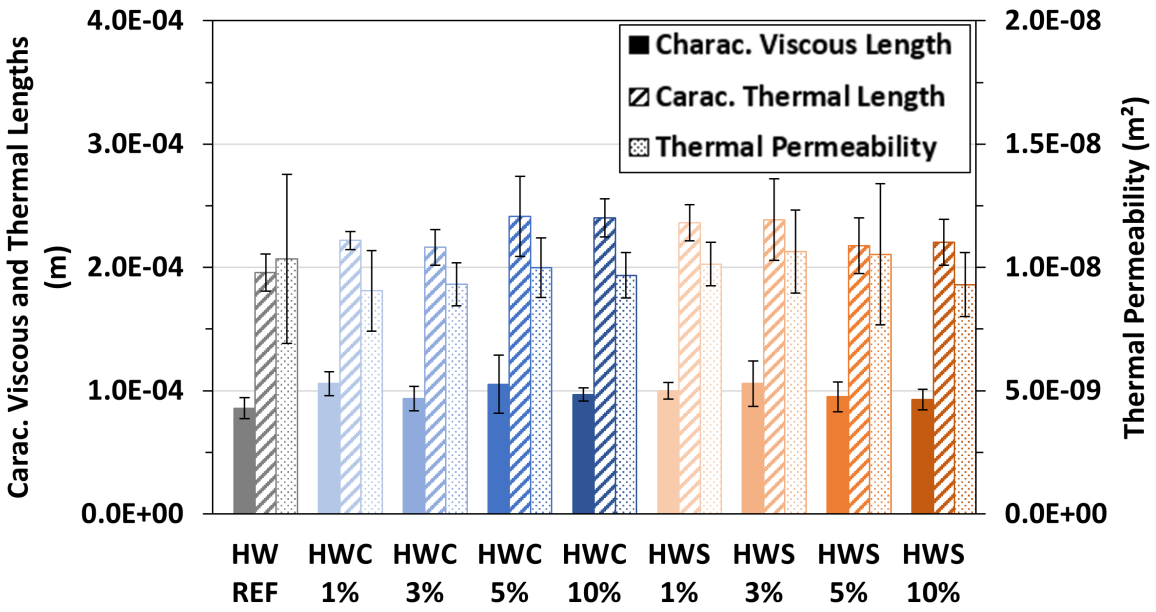

Figure 10: Characteristic viscous and thermal lengths (primary y-axis) and thermal permeability (secondary y-axis)

Based on these results, it can be seen that the application of the fireproof treatment leads to some changes in the characteristic parameters of the pore geometry of the hemp wools. To complete this analysis, it is relevant to evaluate the effects of the treatment on the fibers themselves taking advantage of models with a micro-macro approach.

4.1.4.5 Estimation of the fiber radius

The estimation of the fiber radius in the hemp wools was performed using the Tarnow and Umnova models, as specified in Sections 4.1.3.2 and 4.1.3.3. The results are presented in Figure 11.

The values obtained from the Umnova model are about 23% to 25% higher than the values from the Tarnow model, which indicates a difference of about 5 µm. In both models, the HWS samples presented values similar to the reference fibers, indicating that, even with their surfaces treated, it did not significantly affect the other parameters used for the estimation of the fiber radius, such as airflow resistivity and porosity (as seen in Section 4.1.4.4).

However, as a result of the changes in porosity and airflow resistivity, the HWC samples presented an increase in their estimated fiber radius, which clarifies the reasoning for the reduction in airflow resistivity observed in Section 4.1.4.4. Since these hemp wool samples have all fibers treated, and have a homogeneous distribution of phosphorus molecules throughout their thickness (Section 4.1.4.2), the impact of the treatment is also more significant. Using the Tarnow values, this increase in the estimated fiber radius is about 17%, 23%, 32% and 45% for the samples HWC 1%, HWC 3%, HWC 5% and HWC 10%, respectively.

Therefore, the application of the flame retardants in all fibers can lead to an impact in the microstructure of the hemp wools, whereas the application of the treatment only at the surface, does not lead to significant changes in the properties of the material.

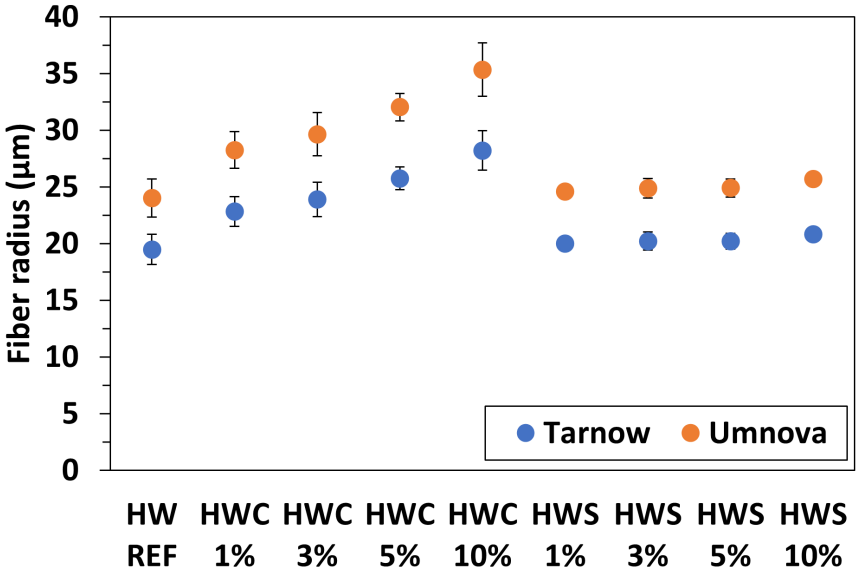

Figure 11: Estimation of fiber radius in hemp wools using Tarnow (TAR96) and Umnova models (UMN09)

4.1.5 Conclusion

In the present study, hemp wool prototypes were developed and fireproof treated with phytic acid and urea, using two different methods: by treating all fibers before the production of the panels (HWC samples), or by treating the surface of the panels, after their production (HWS samples). These samples were characterized in terms of their physico-chemical properties and acoustic performance.

The physico-chemical characterization consisted of the assessment of the real density, apparent density, and phosphorus content of the samples. The real density results showed variations lower than 0.02 kg.m^{-3}, between treated and untreated samples. The apparent density, on the contrary, has shown a significant linear increase for samples HWC as the amount of flame-retardants applied increased. For the HWS samples, their values also increase linearly, but without significant differences from the HW REF apparent density. On the chemical side, the phosphorus content of the HWC samples was homogeneous on the core and at the surface of the samples. The HWS samples presented significant amount of phosphorus at their surfaces, and no phosphorus at their core.

The sound absorption of the fireproof treated hemp wools was slightly reduced with the treatment. This was more significant on samples HWC 5% and HWC 10%, as the amount of flame-retardants applied was higher. Samples HWS, presented a sound absorption curve between the reference and the HWC curves, as their core remained untreated. The analysis of the characteristic pore geometry demonstrated a significant impact of the treatment on the porosity, airflow resistivity and thermal characteristic length.

This work can be completed by an image analysis of the morphology of the fibers, and the assessment of the fiber radius, which could provide more information about the origin of the flame-retardants impact on the hemp wool. Furthermore, a sensitivity analysis could be carried out to determine which parameter is being most impacted, and influencing acoustic absorption the most after the treatment application.

Despite this reduction, all hemp wool samples remained as excellent absorbers, showing that the fireproof treatment based on phytic acid and urea does not hinder the development of treated hemp wools. In contrary, it enables new applications in a safe manner and establishes vegetal wools as an alternative to traditional acoustic insulation materials.

4.2 Thermal properties of fireproof treated hemp wool prototypes

The thermal properties were evaluated using the hot disc test and the guarded hot plate, as specified in Sections 2.5.1 and 2.5.2. During the measurements made with the hot disc, the room conditions presented an average temperature of 23.7 ± 0.3 and average relative humidity of 31% ± 2%. With the low variation in the room conditions, it is ensured that no external variable impacted the results.

4.2.1 Thermal conductivity

To perform an analysis in the hot disc test, two samples were prepared for each formulation, as presented in Section 2.5.1. As shown previously in Section 4.1.4.1, the apparent densities of the hemp wool prototypes change with the treatment condition. Therefore, the results presented in this Chapter will be as a function of the apparent density of the samples.

The values obtained for the thermal conductivity using the hot disc test are presented in Figure 4.12. The thermal conductivity results can be divided into two main groups of values. The first one is a group of results for densities between 50 and 70 kg.m^{-3}. In this group are found the references, all HWS samples and a few HWC samples (those with lower density, independently of the treatment concentration). In this group, no difference is observed between samples, and they all present a thermal conductivity that range between 0.52 and 0.64 W.m^{-1}.K^{-1}. At this range of densities, Piégay (PIE19) obtained values of thermal conductivity of hemp wools between 0.55 and 0.64 W.m^{-1}.K^{-1}

Above 70 kg.m^{-3}, another behavior is noted. As the density increases, the thermal conductivity also tends to increase. Piégay (PIE19) observed the same behavior for densities above 60 kg.m^{-3}. Below that, the author states that the effects of the radiation becomes more significant affecting the measured effective thermal conductivity. The same effects occurs in this thesis, given the shape of the curve, especially the results below 60 kg.m^{-3}. Measurements at lower densities are necessary to observe the effects of radiation in more clearly.

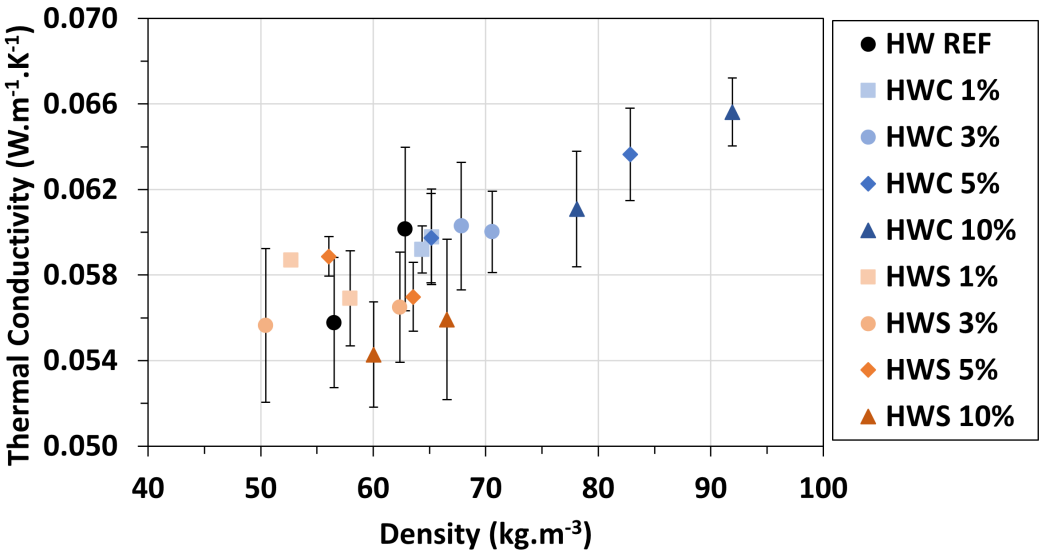

Figure 4.12: Thermal conductivity results using the hot disc test

No significant impact directly linked to the concentration of flame retardants or the

application method is observed. Similar to the results obtained for hemp fibers (Section 3.4.2), the influence of the changes in apparent density is more influential on the effective thermal conductivity than other parameters directly associated with the treatment.

The thermal conductivity of the hemp wool prototypes was also measured using the standardized method guarded hot plate, frequently used in the industry to provide reference values of thermal conductivity and R. Differently from the hot disc test, which is base on a transient regime, the guarded plate test perform measurements in a stationary regime. Another difference is that the before testing in the guarded hot plate, the samples were dried in oven, whereas for the hot disc test they were simply stabilized with the room's relative humidity. As seen in Section 1.5.2 in the literature review, due to the hygroscopic behavior of the lignocellulosic fibers, their water content plays an important role in their effective thermal conductivity.

This test was performed before the cut of samples for other tests, so whole panels of 30x30x4 cm^3 were used. The possibility of using bigger samples is one of the advantages of this test. To ensure that the whole panel touched the plates, a small compression was applied to the panels, resulting in a thickness of 35 mm.

The thermal conductivity results are reported in Table 4.5. The test was done only once for each treatment condition, therefore, no measurement of error is given. The thermal conductivity values ranged between 0.036 and 0.039 $W.m^{-1}.K^{-1}$, and no differences were observed between samples, indicating that the fireproof treatment applied does not significantly impact the thermal conductivity of the hemp wools. In comparison with the hot disc test, the values obtained are significantly lower, due to the difference methodology and different water content of the fibers (by being dried before testing in the guarded hot plate test).

For a slightly lower apparent density (between 40 and 60 $kg.m^{-3}$) Deborde (DEB25) obtained thermal conductivity values of hemp fiber panels around 0.037 and 0.042 $W.m^{-1}.K^{-1}$, using a testing method based on stationary regime. Using a guarded hot plate, Korjenic et al. (KOR16) reported a thermal conductivity of hemp insulation products between 0.039 and 0.050 $W.m^{-1}.K^{-1}$. Therefore, the results obtained in this study are consistent.

For comparison with commercial products, the hemp wools are usually reported with a thermal conductivity of 0.038-0.041 $W.m^{-1}.K^{-1}$ (LEK15). For comparison, the results reported in this thesis are of the same order of magnitude as the values found in the industry for mineral wools.

Table 4.5: Thermal conductivity from guarded hot plate test

Sample	Thermal Conductivity ($W.m^{-1}.K^{-1}$)
HW REF	0.036
HWC 1%	0.038
HWC 3%	0.038
HWC 5%	0.039
HWC 10%	0.039
HWS 1%	0.037
HWS 3%	0.036
HWS 5%	0.037
HWS 10%	0.036

4.2.2 Thermal diffusivity and specific heat

The thermal diffusivity and specific heat were also measured during the hot disc test. The thermal diffusivity varied slightly between samples, but no particular tendency was noted. The values ranged from 0.4 to 0.9 $mm^2.s^{-1}$, with the average around 0.6 $mm^2.s^{-1}$. This is the same result from the hemp fibers presented in Section 3.4.2. For comparison, Palumbo et al. (PAL18) obtained the thermal diffusivity of wood fibers and wood wools with values of 0.37 and 0.76 $mm^2.s^{-1}$, respectively. The equipment used for measurement was and electronic thermal properties analyzer, which relies on the transient state regime.

For the specific heat, all treated samples presented values around 1.3-1.5 $kJ.kg^{-1}.K^{-1}$, except sample HWS 10% that presented values above 2.0 $kJ.kg^{-1}.K^{-1}$. The reference samples presented a specific heat of 1.7-1.8 $kJ.kg^{-1}.K^{-1}$, similar to Schiavoni et al. (SCH16) and above the majority of the treated samples. This indicates a small influence of the treatment that was not observed on the hemp fibers.

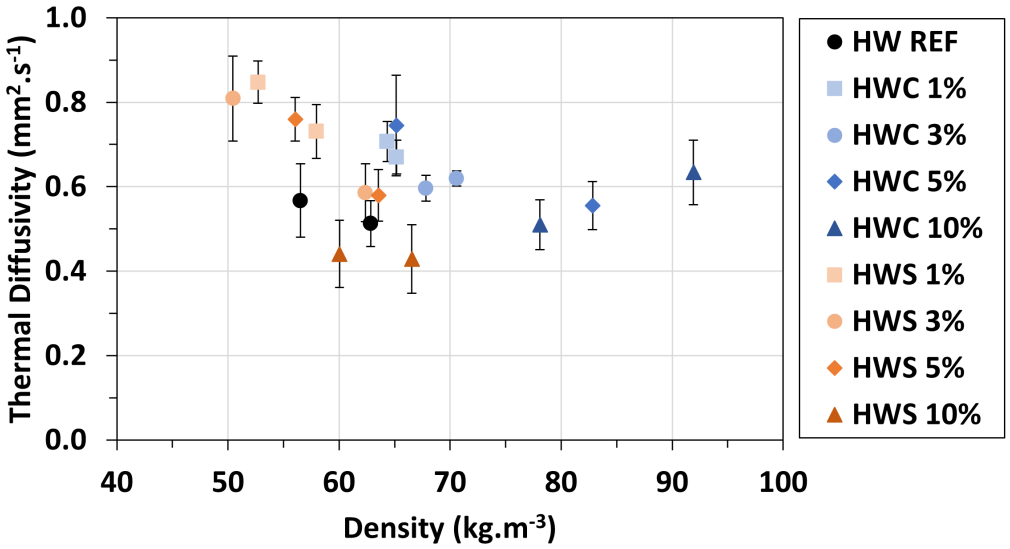

(a)

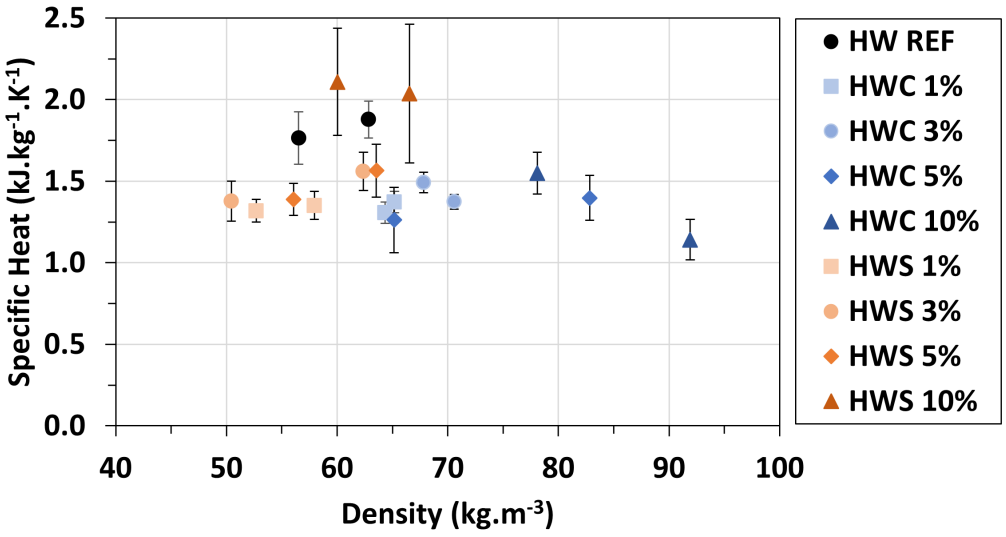

(b)

Figure 4.13: Thermal properties of hemp wool prototypes: (a) Thermal diffusivity; (b) Specific heat

4.3 Fireproof treatment and flame retardancy of hemp wool prototypes

4.3.1 Fire reaction assessment

In addition to the results just presented on the acoustic behavior of prototypes treated with the two types of flame retardant treatments, the mass loss cone calorimeter test was used to assess their fire reaction, as specified in Section 2.3.2. The aspect of the samples before and after the test is presented in Figure 4.14.

Sample HW REF underwent complete combustion and the fibers became white and extremely fragile. Since they were not treated, the lignocellulosic fibers depolymerized into levoglucosan which decomposes in low molecular weight species with very high flammability (HAJ20). The volatiles formed react with oxygen, and maintain the combustion and flame propagation processes.

All treated samples presented char formation, which is the black layer covering the fibers. The phytic acid release acidic molecules that catalyses the dehydration reaction of the cellulose and the hemicellulose, promoting the formation of char (HAJ20). For sample HWC 1%, it can be observed that some zones remained white, indicating that there was not enough flame retardants applied. The same occurred in sample HWC 3%, but at a lower intensity. Sample HWC 5% presented a dense char formation, without any white zones, which indicates that this amount of flame retardants was able to cover and effectively change the degradation pathway of all fibers to form char. Finally, sample HWC 10% formed a very dense char layer at the top of the sample, which prevented heat from penetrating into the deeper layers of the sample. Consequently, the sample is fully preserved, maintaining its natural color.

The HWS samples presented char formed on the top of their samples, but their core were white after the test, since they were not treated. The char layer was very thin and not homogeneous in the sample HWS 1% and HWS 3%. The sample HWS 5% presented a denser char, however, it was noted that it was not enough to block the external heat, and the interior still underwent combustion. An even denser char was formed in the sample HWS 10%, and a smaller white zone was observed in these samples. Moreover, due to the dimensions of the samples, and the characteristics of the test, the heat could penetrate the samples from the sides, which were not treated, nor protected during the test. Therefore, even with a thick and dense char layer formed on the top, the core was vulnerable from the heat in all four sides of the sample. A test with samples with larger dimensions might provide slightly different results.

For each treatment condition, four measurements were made. A good reproducibility was observed in all samples, with the exception of sample HWC 10%, which will be discussed further in this Section. For the HW REF sample, one measurement was discarded due to incorrect setup of the equipment. The other three samples were tested and their curves are presented in Figure 4.15, to illustrate the reproducibility of the test.

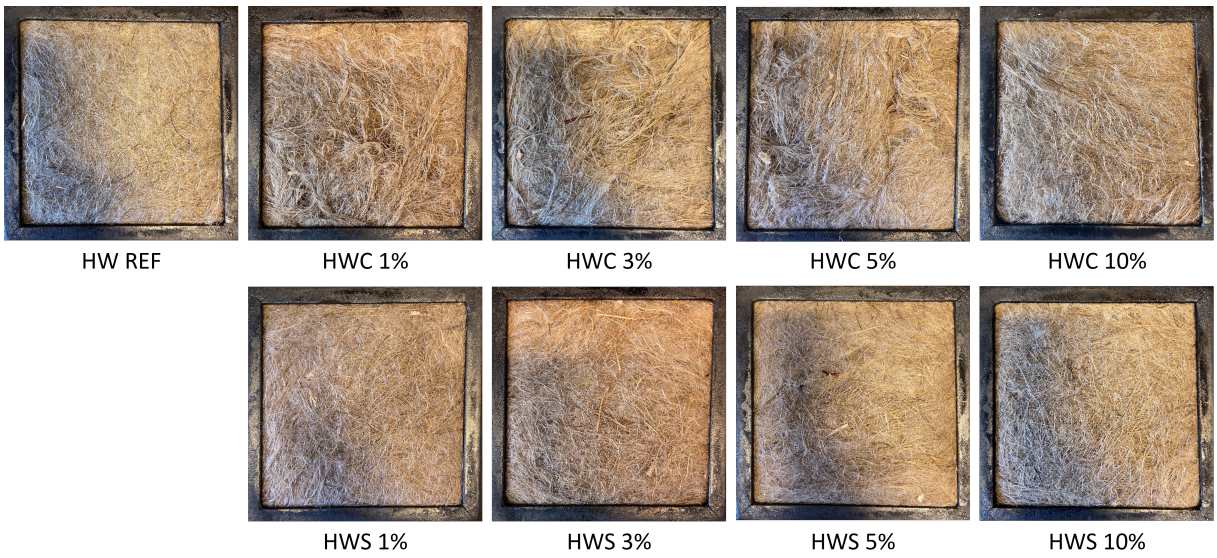

(a)

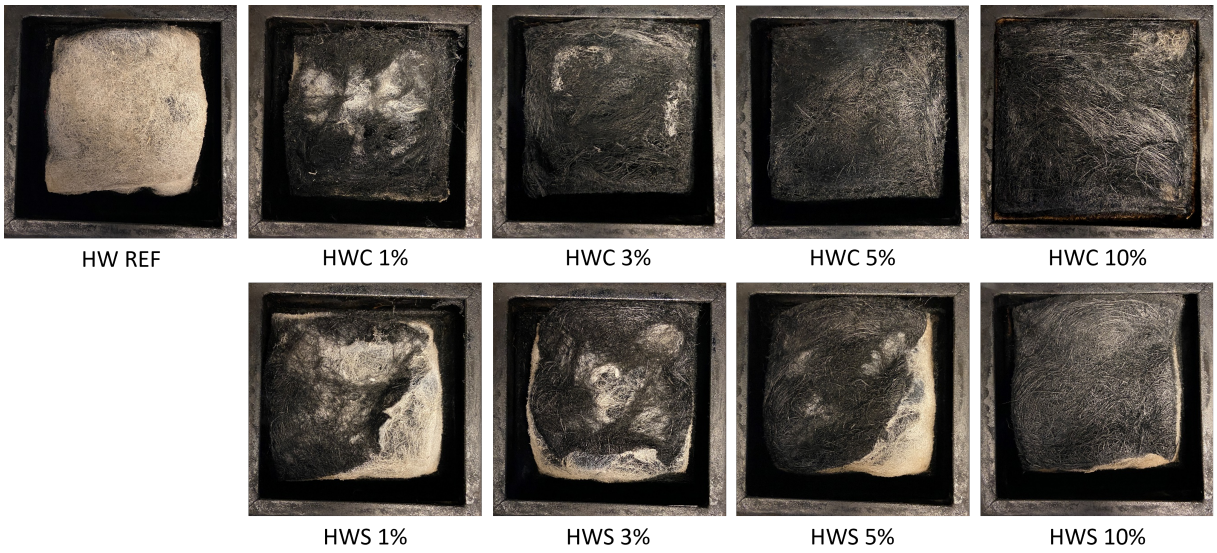

(b)

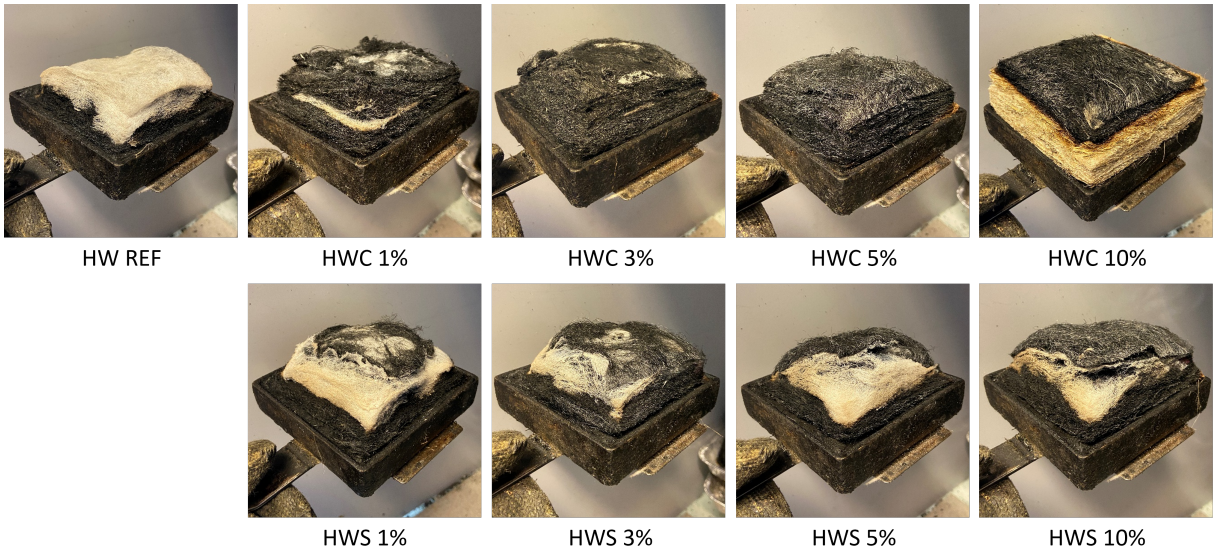

(c)

Figure 4.14: Hemp wools samples aspects for mass loss cone calorimeter test: (a) Before testing; (b) and (c) After testing

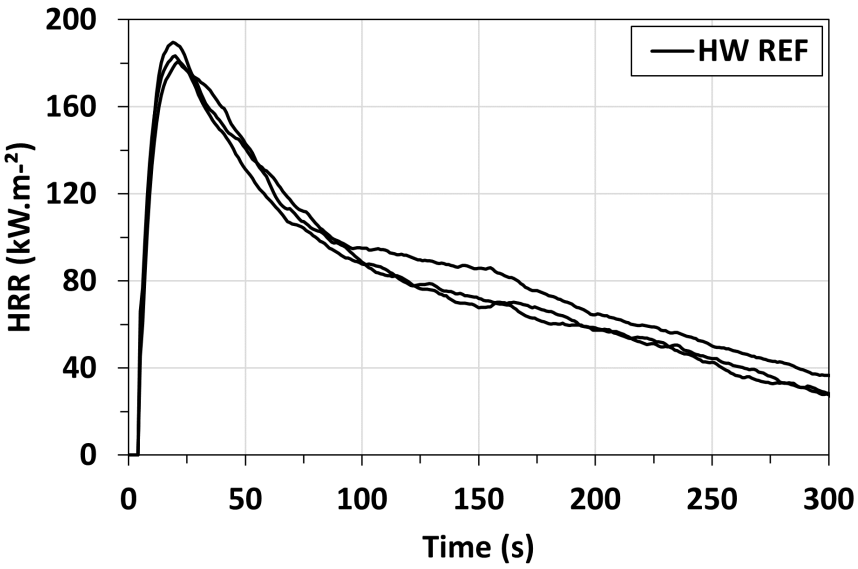

Figure 4.15: Heat release rate curves from mass loss cone calorimeter tests of HW REF samples

The curve of heat release rate over time that better represents the average behavior of all four measurements, for each treatment condition, is presented in Figure 4.16. Then, the results of peak heat release rate (pHRR) and total heat released (THR) are presented in Figure 4.17.

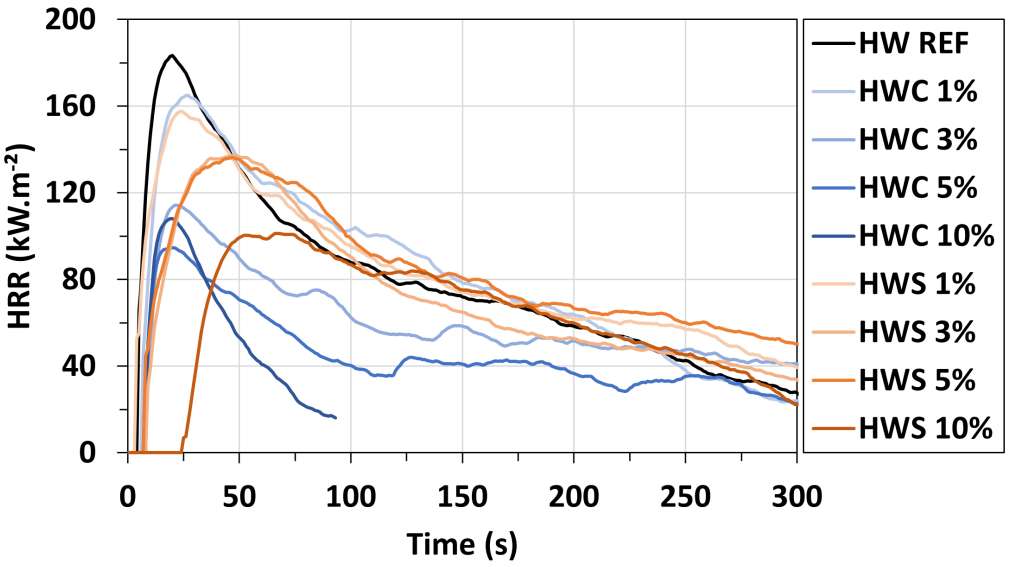

Figure 4.16: Heat release rate curves from cone calorimeter tests of fireproof treated hemp wool prototypes

From the curves, it can be observed that the reference sample (in black) presents a sudden increase in HRR, reaching a very high peak in a short time. The HRR decreases, but remains high throughout the whole test. It is also noted that the samples with 1% phytic acid and 3% urea slightly reduced the pHRR value. This represented an average reduction of 9% for the HWC 1% sample and 18% for the HWS 1% sample. However, their THR remained unchanged when compared to the reference (Figure 4.17b).

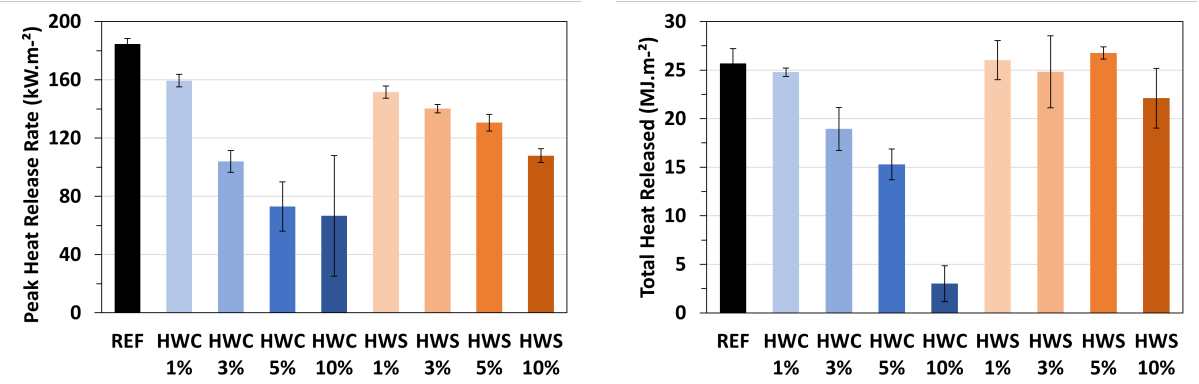

(a) (b)

Figure 4.17: Cone calorimeter results: (a) Peak heat release rate; (b) Total heat released

HWC samples (in tones of blue) present a significant reduction of pHRR, and a much lower HRR during the test. Samples HWC 3%, HWC 5% and HWC 10% presented an average reduction of 37%, 53% and 64% in the pHRR, respectively, and a reduction of 27%, 40% and 88% in the THR. As presented in the literature review, the phosphorus content is the main component responsible for the reduction in the fire reaction (see Section 1.6). Here, this is also observed as pHRR and THR decreased with the increase in phosphorus content (Figure 4.17).

A particular result worth detailing is the HWC 10%. Among the four measurements, one had to be discarded and another one did not ignite. In fact, the char layer was formed over the sample and even after more than 2 minutes of exposure to the heat and the sparks, it did not ignite. This samples was not considered for the average values of pHRR and THR. The other two samples had a very different behaviors and are shown in Figure 4.18. One sample ignited rapidly after 8s and presented a high pHRR, with the flame extinguishing at 93s. The other sample took 37s to ignite and presented a low pHRR and THR, with flame extinguishing at 99s. Therefore, the average values observed should be considered with caution.

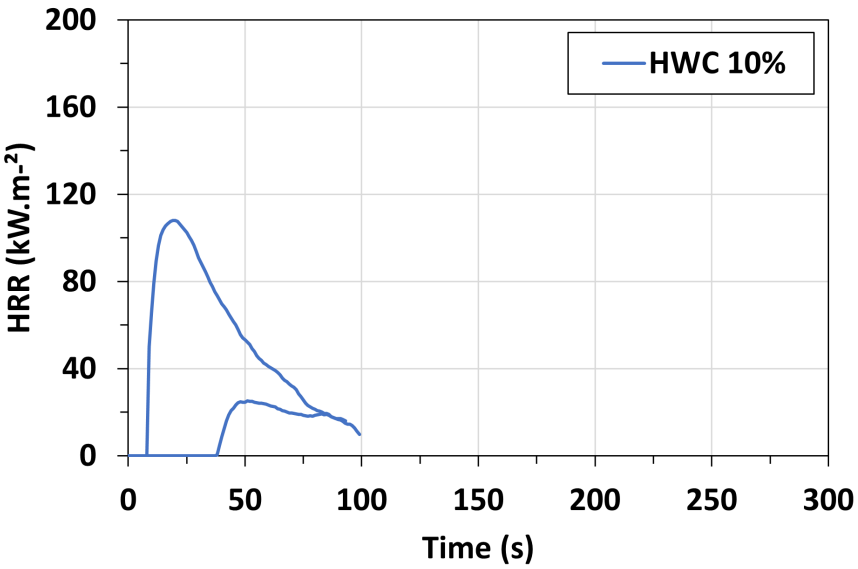

Figure 4.18: Heat release rate curves from cone calorimeter tests of HWC 10% samples

Despite these results with the sample HWC 10%, it was noted that this sample was the only one to have fast flame extinguishment (or even no ignition). Samples HWC 3%

and HWC 5% significantly reduced both pHRR and THR, but a small flame was still observed for a long duration, over 5 minutes.

The HWS samples also reduced the pHRR but in a lower magnitude than the HWC samples. The average reduction was of 24%, 29% and 42% for samples HWS 3%, HWS 5% and HWS 10%, respectively, when compared to the reference. Moreover, it was observed that these samples delayed their peaks, due to the high concentration of phosphorus on their surface.

However, after the peak, the HRR remained high, similar to the reference sample, which happened due to the untreated core of the samples that burned vividly. This led to insignificant changes in THR for samples HWS 3% and HWS 5%, and a reduction of 14% for the sample HWS 10%. As mentioned before, it was noticed that the heat could enter through the sides of the samples, so even with a dense char layer, the core still burned. For comparison, HWS 10% presented a fire reaction behavior equivalent to HWC 3%, with much higher amount of flame retardants applied.

4.3.2 Relationship with phosphorus content

As presented in the literature review in Section 1.6.5, through Figures 1.35a and 1.35b, the phosphorus grafted content has a strong relationship with the parameters of pHRR and THR of lignocellulosic fibers. This was also observed in the hemp fibers presented in this study, in Section 3.1 (SAC25).

From the results obtained with the mass loss cone calorimeter test for the hemp wool prototypes, these relationships are presented in Figure 4.19. For the HWC samples a linear correlation a R^2 of 0.72 is obtained, but a better correlation is obtained when an exponential correlation is made with R^2 of 0.84. The exponential correlation was also used by Antoun et al. (ANT22). The HWS sample presented a good correlation between pHRR and the average phosphorus content with a R^2 of 0.88. The linear correlation fits well because it is limited to phosphorus content of 1%.

The correlation between THR and phosphorus content presented an excellent linear correlation for the HWC samples, but not a good one for the HWS samples. This occurred due to the homogeneity of the treatment. Since all the fibers are treated in the HWC samples, their fire behavior is homogeneous and a good correlation is found between THR and phosphorus content. In contrary, the HWS samples are only treated in the surface, and their surface have high phosphorus content that contributes to the formation of char and the reduction in flammability. Thus, the average phosphorus content, in this case, is not an interesting method to analyze the phosphorus content of the material, since its distribution is hot homogeneous. This heterogeneity led to an imprecise correlation of THR and phosphorus content.

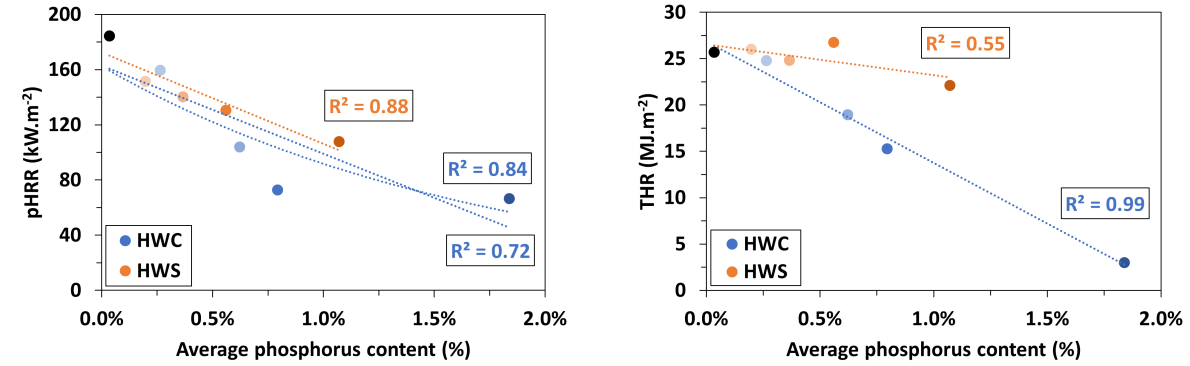

(a) (b)

Figure 4.19: Correlation between fire reaction parameters and average phosphorus content from hemp wool prototypes: (a) pHRR; (b) THR

Instead of relying on the phosphorus content to correlate the fire reaction performance, the amount of phytic acid applied can be used. The advantage of this is that the amount of phytic acid applied is an input parameter to the treatment. These correlations are shown Figure 4.20. The graphics show the same tendencies, with very similar R^2 from Figure 4.19.

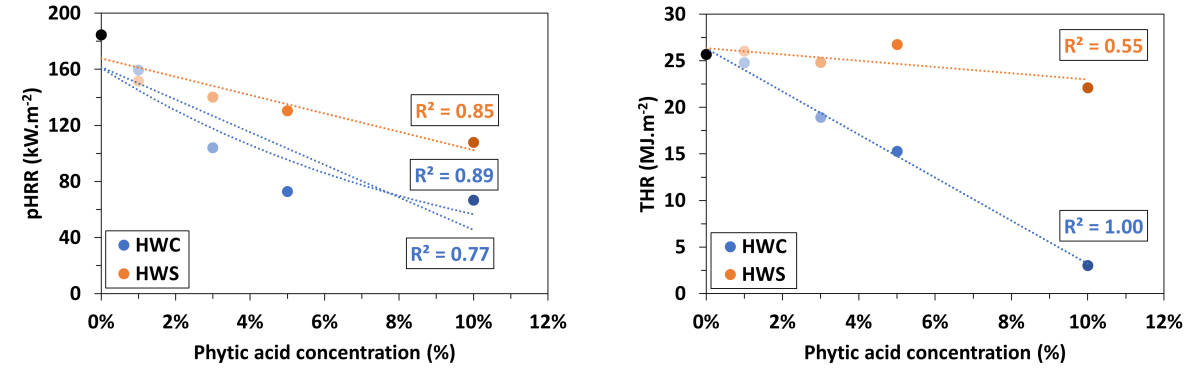

(a) (b)

Figure 4.20: Correlation between fire reaction parameters and phytic acid applied: (a) pHRR; (b) THR

Once again, a strong linear relationship between THR and phytic acid was observed for the HWC samples. Using the correlation equations from THR x phosphorus content (Equation 4.10) and THR x phytic acid concentration (Equation 4.11), a relationship between the phytic acid concentration and the phosphorus grafted can be stipulated (Equation 4.12).

$$THR = -1309.10P + 26.85 \tag{4.10}$$

$$THR = -231.21PA + 26.33 \tag{4.11}$$

$$P = 0.1766PA + 0.0004 \tag{4.12}$$

Where THR is the total heat released in MJ.m^{-2}, P is the percentage of phosphorus content and PA is the phytic acid concentration applied in the treatment.

With the correlation between the phosphorus content and the phytic acid it is possible to obtain the main chemical parameter associated with the treatment without performing any test, and predict a fire reaction behavior only knowing the amount of flame retardant used.

Knowing the relationship between phosphorus content and the phytic acid concentration used in the treatment, it is possible to calculate the treatment efficiency in grafting the phosphorus molecules in the hemp wools. This efficiency varies slightly with the amount of of phytic acid considered, so the range used in this thesis will be considered (between 1% and 10%). Since the molar mass of phytic acid is 660.03 g.mol^{-1} and it has 6 molecules of phosphorus (6 x 30.974 g.mol^{-1}), the mass fraction of phosphorus in phytic acid is 28.16%. The treatment's efficiency is then calculated by the ratio of the amount of phosphorus grafted (P), divided by the maximum amount of phosphorus grafted (28.16% of the amount of phytic acid applied (PA)), as shown in Equation 4.13.

$$Eff = \frac{P}{0.2816PA} \tag{4.13}$$

The values obtained were 94%, 74%, 56% and 65% for the treatment performed at HWC 1%, HWC 3%, HWC 5% and HWC 10%, respectively. Considering the handmade treatment process and the possibility of automating this process with a spray system linked to the manufacture of the panels, this value could be improved.

Figure 4.21 presents the mass loss curves obtained with the cone calorimeter test. It can be seen that the reference sample is the one with the faster mass loss, reducing its mass to about 50% in two minutes and to less than 20% after five minutes. Samples with 1% of phytic acid also presented similar behavior, indicating that the amount of flame retardants was not enough to preserve the sample's mass.

HWC 3% and 5% presented a significant improvement, taking 3 minutes to achieve the same 50% of mass and retaining more than 30% of their masses after 5 minutes. This is linked to the char formation that was able to protect the inner layers of the samples, preserving their masses. As mentioned previously, the sample HWC 10% was the only one that presented self-extinguishment behavior, and since the test stopped at flame-out, the curve only goes to 100s. Even so, it is possible to see a significant reduction of degradation kinetics.

The HWS samples presented a mass loss kinetics between the reference and the HWC samples. Because their cores were not treated, thermal degradation occurred, causing significant mass loss. The increase in the remaining mass, when compared to the reference, is linked to the formation of char in the upper layer of the sample.

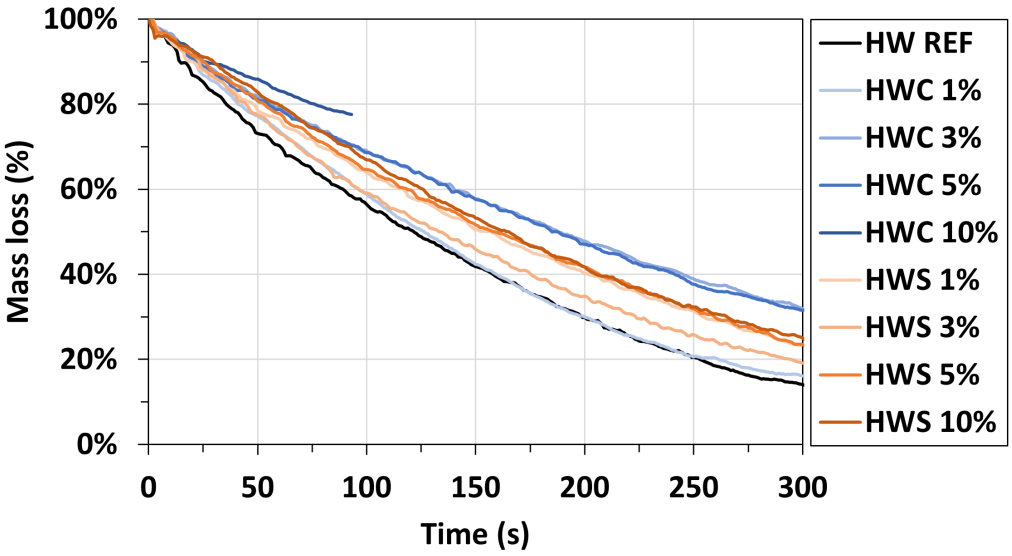

Figure 4.21: Mass loss curves during cone calorimeter tests

4.3.3 Flame-retardant hemp wool prototypes

In conclusion, based on these results, one treatment condition was selected to be used for the production of fireproof treated hemp wools at an industrial scale. Between HWC and HWS samples, it was decided that the HWC ones were preferable, due to the homogeneity of the treatment and the assurance that all fibers would be treated. This played an important role in the final aspect of the samples and in the total heat released after the cone calorimeter test.

The flame retardants concentration selected was 5% phytic acid and 15% urea. The HWC 5% sample showed a dense char formation, preservation of its form, and significant reduction in pHRR and THR parameters. Lower amount of flame retardants presented zones that were fully combusted, indicating a lack of flame retardants for a homogeneous treatment. In contrary, the sample HWC 10% presented very interesting results, even showing no ignition in one sample, however, it uses double of the amount of flame retardants than HWC 5% sample. Considering the nature of the material, and the motivation of producing material with low energy and carbon footprint, it was decided that the optimal sample for the treatment at industrial scale, that will be presented in Chapter 5, was the HWC 5%.

4.4 Fungal development on fireproof treated hemp wools

Susceptibility to fungal growth in hemp wool prototypes was evaluated by fungal incubation and identification (Sections 2.6.1 and 2.6.2, respectively) and impregnation (Section 2.6.3) tests. The incubation test was used to identify the fungi that are naturally present in the hemp wool samples and to assess their development during 6 months of incubation under favorable conditions of temperature and relative humidity. This approach considers a natural development of fungi that are already found in hemp wools.

The impregnation test considered a more aggressive approach, in which hemp wool samples were pulverized with mold colonies via wet and dry methods. This approach allowed analysis of whether the phosphorus- and nitrogen-based flame retardants would promote the development of fungi in the case of contamination.

4.4.1 Development of fungi in hemp wool prototypes in favorable conditions

Samples HW REF, HWC 5%, HWC 10%, HWS 5% and HWS 10% were incubated in a climate chamber at 30°C and 80% of relative humidity for 6 months. Hemp wool samples were divided into core and surface, due to different chemical compositions relative to the fireproof treatment, as observed in Section 4.1.4.2. The presence of fungi and their identification were obtained before incubation (T0), after 3 months (T3) and after 6 months (T6). The results are presented in Table 4.6 and are discussed in the following.

Table 4.6: Presence of fungi before and after incubation

Sample	Fungi presence		
	T0	T3	T6
HW REF	-	*Chrysonilia sitophila*	*Fusariumm spp.* *Trichoderma harzianum*
HWC 5%	-	*Chrysonilia sitophila*	-
HWC 10%	-	*Chrysonilia sitophila*	-
HWS 5%	*Aspergillus niger*	*Chrysonilia sitophila*	-
HWS 10%	*Aspergillus niger*	*Chrysonilia sitophila*	-

Before incubation, no presence of mold was detected in samples HW REF, HWC 5% and HWC 10%. In samples HWS 5% and HWS 10%, the mold *Aspergillus niger* was observed, both at their surface and core. This specie presents the formation of white colonies with black spots, with a filamentous aspect (Figure 4.22). They are typically found in indoor environments therefore, it is not surprising to find them in hemp wools. This contamination is likely to come from the air rather than from the retting process.

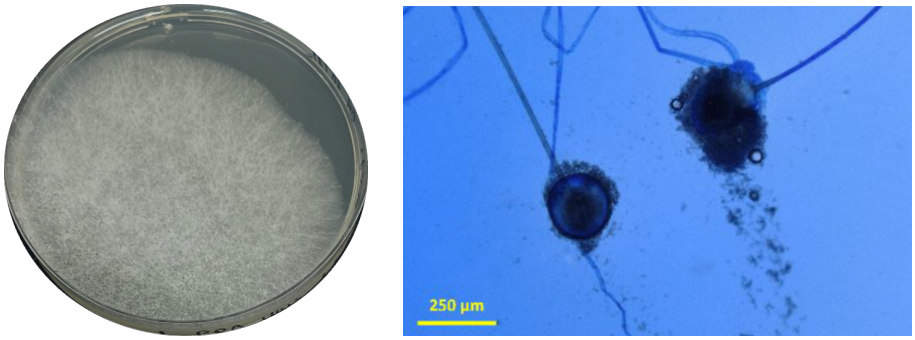

(a) (b)

Figure 4.22: Identification of *Aspergillus niger*: (a) At the Petri dish; (b) Digital microscope image

After 3 months of incubation, the presence of *Chrysonilia sitophila* was identified in all samples. This mold was also present in the hemp fibers shown in Section 3.5. It was hypothesized that cross contamination between samples could have occurred, since this type of result is not expected. At 6 months of incubation, this specie was no longer found, as observed in the hemp fibers, reinforcing that it was a punctual contamination that occurred at 3 months of incubation. However, the hypothesis that all samples naturally contained this mold species in a dormant state, developing once optimal growth conditions were met, is not discarded.

At 6 months, two other fungal species were detected and identified in the HW REF sample, *Fusarium spp.* and *Trichoderma harzianum*. The former forms orange-colored

colonies with cotton-like aspect (Figure 4.23), and the latter forms white-colored colonies with a filamentous aspect (Figure 4.24). These species are commonly found in plants and soils. Therefore, it is likely that they were already present in the fibers before incubation and were able to proliferate once they found optimum conditions for their growth. No other fungi species were detected in the HWS and HWC samples.

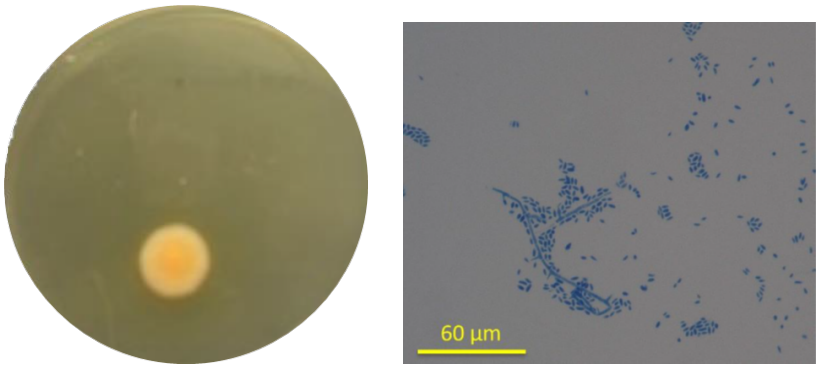

(a) (b)

Figure 4.23: Identification of *Fusarium spp.*: (a) At the Petri dish; (b) Digital microscope image

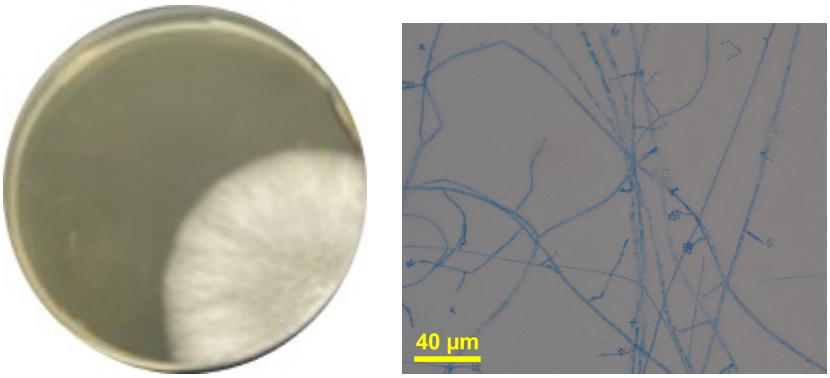

(a) (b)

Figure 4.24: Identification of *Trichoderma harzianum*: (a) At the Petri dish; (b) Digital microscope image

This fungal identification and analysis showed that some fungi present in the air can contaminate the hemp wool, such as *Aspergillus niger* found before incubation in samples HWS 5% and HWS 10%, and the *Penicillium spp.* found in the hemp fibers (Section 3.5). Moreover, some fungi can be present in hemp fibers, but remain dormant until favorable growth conditions are found, which is the case of *Chrysonilia sitophila* after three months of incubation and *Fusariumm spp.* and *Trichoderma harzianum* after 6 months. In all cases where a mold was identified, only single colonies were found, indicating their presence, but without strong proliferation.

In summary, no particular negative influence of the fireproof treatment on the development of fungi was observed, despite their phosphorus and nitrogen-based composition. The HWC samples, which have all fibers treated, and present a homogeneous distribution of the phosphorus and nitrogen molecules, did not present any fungi at any incubation time. HWS samples presented the same fungi at their surface and at their core, even though only the surface of these samples have been treated.

As observed in the literature review (Section 1.9.2), phytic acid can inhibit fungi growth of certain species of fungi (LIP23; LIA24). In fact, it is possible to observe that

the samples with a homogeneous treatment of all fibers (HWC samples) did not present any mold colony, neither before nor after 6 months of incubation. This may possibly indicate the action of phytic acid in inhibiting the development of molds in hemp wools.

In conclusion, no direct relationship was observed between the concentration of fire-proof treatment nor the phosphorus content, and the development of fungi in this test. However, it can be stated that the treatment was not detrimental but rather beneficial to the susceptibility of hemp wools to fungal development, inhibiting their growth.

4.4.2 Development of fungi in contaminated hemp wool prototypes

The fungi development of hemp wools were also assessed in the scenario of contaminated fibers with incubation under favorable conditions (Section 2.6.3). This is an extreme approach that is not representative of the usual conditions found in buildings. Two methods were tested, a wet method with the pulverization of a contaminated solution with *Penicillium spp.* and another with *Stachybotrys chartarum*. These molds were selected because they were found at T0 before incubation in some hemp wool samples and in the reference hemp fiber sample. The second method is a dry method, where the spores of *Penicillium spp.* were pulverized over the samples.

Before testing in hemp wool samples, the wet and dry methods efficacy was evaluated using Petri dishes filled with a culture medium, as specified in Section 2.6.3. The evaluation consisted of verifying the development of fungi colonies after 7 days of incubation at 30°C and 80% of relative humidity. The aspects of the Petri dishes after incubation are presented in Figure 4.25.

The Petri dishes pulverized with a solution containing *Penicillium spp.* and another with *Stachybotrys chartarum* presented a very strong development of the fungi, covering the whole surface and consuming the majority of the culture medium. The Petri dish used for the control of the dry method, was pulverized with the spores of *Penicillium spp.* and three small colonies were formed. These observations indicate that the wet method was able to apply a higher number of fungi colonies and represent a method with stronger contamination.

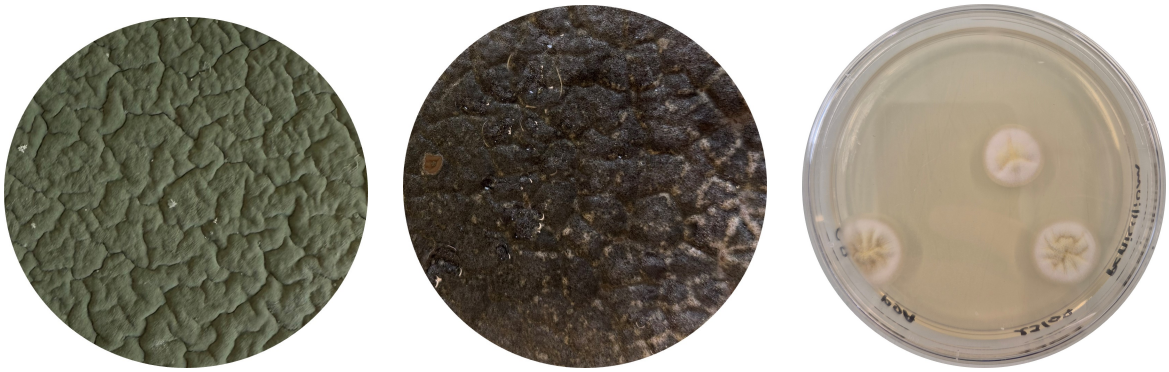

(a) (b) (c)

Figure 4.25: Verification of fungi impregnation methods: (a) Wet method - *Penicillium spp.*; (b) Wet method - *Stachybotrys chartarum*; (c) Dry method - *Penicillium spp.*

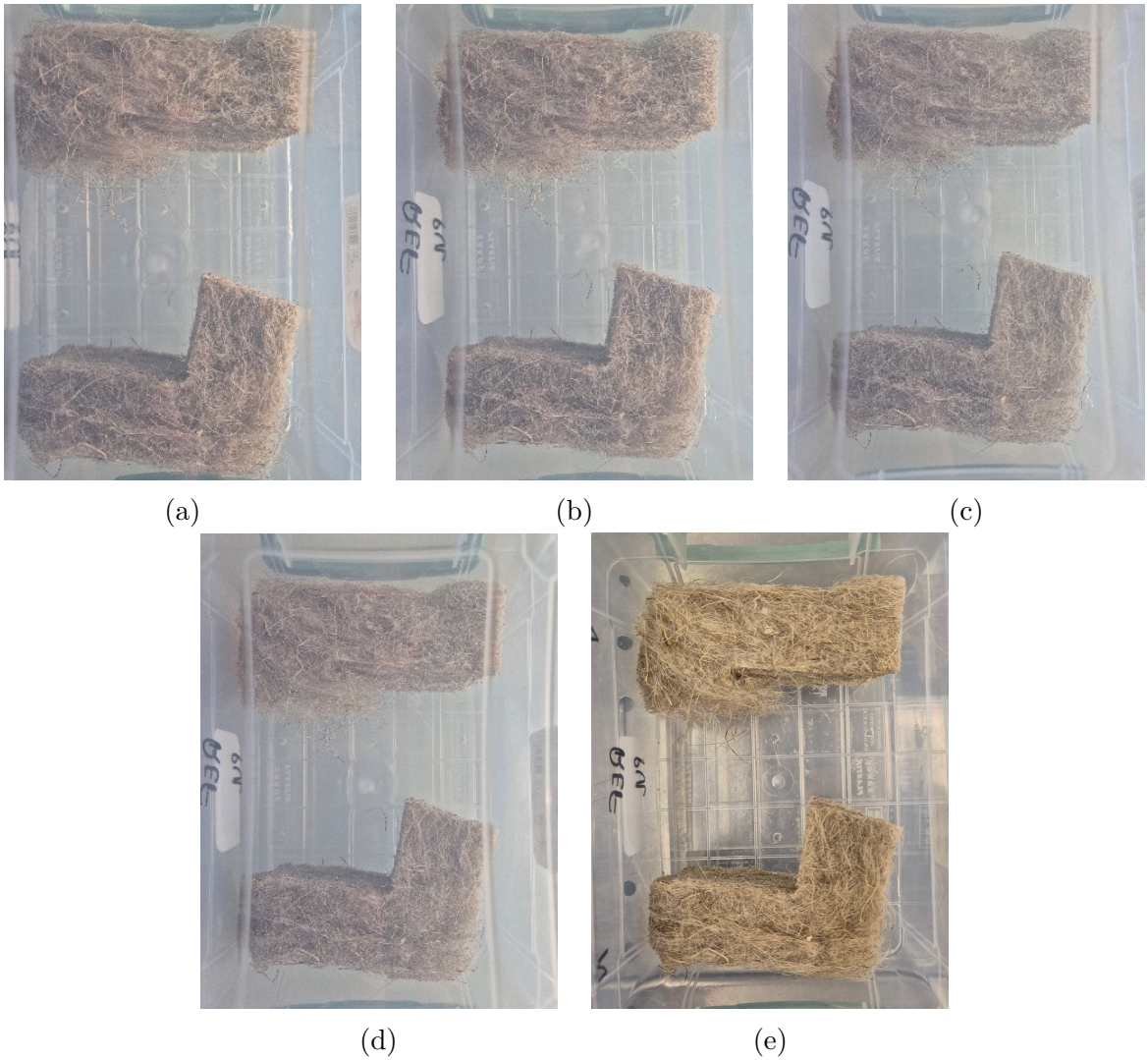

Figure 4.26: Monitoring of HW REF sample during incubation after impregnation: (a) Before incubation; (b) 7 days of incubation; (c) 14 days; (d) 21 days; (e) 28 days (without the cover)

Figure 4.26 shows the aspect of the samples before incubation and after 7, 14, 21 and 28 days of the HW REF sample. Visually, no fungi development was observed, even after 28 days of incubation, independently of the impregnation method. The same pictures were taken for all other samples, and no visible fungi growth was observed.

The identification of the fungi colonies after 28 days detected the presence of *Penicillium spp.* in the reference hemp wool samples when impregnated with the wet and dry methods. The aspect of the Petri dishes with the mold is shown in Figure 4.27. The presence of *Stachybotrys chartarum* was not observed.

The treated samples HWC 5% and HWC 10% did not present any fungi, in both methods, despite being directly contaminated with a high concentration of fungi colonies. These results indicate that in the reference wools, the fungi found conditions to sustain their life, without proliferation, while in the treated wools the conditions did not allow the permanence of the fungi. Therefore, the treatment acts as a fungicide, despite being composed of phosphorus and nitrogen. The inhibition of fungi growth caused by the presence of phytic acid was observed in previous studies (LIP23; LIA24), which can explain the absence of fungi in the treated samples.

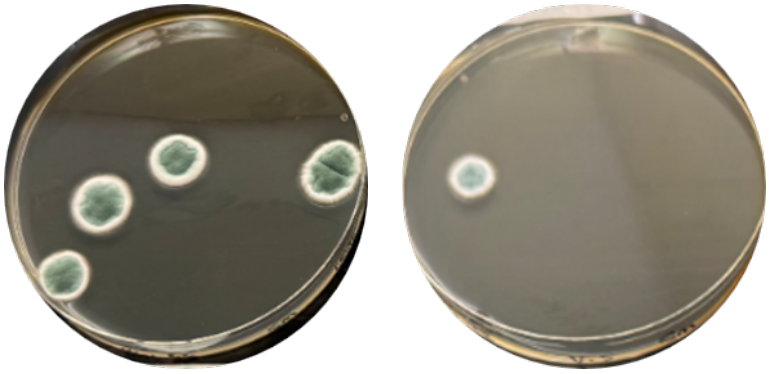

(a) (b)

Figure 4.27: Presence of *Penicillium spp.* from the HW REF sample: (a) Wet method; (b) Dry method

4.5 Conclusion

After defining pulverization as the ideal method for the application of the flame retardant solution in Chapter 3, during the manufacturing of hemp wool prototypes two other possibilities were identified. The first possible method consisted of treating all hemp and thermoplastic fibers before the production of hemp wool panels (HWC), and the second method by treating the surface of the hemp wool panels after production (HWS).

These two methods were tested and evaluated in terms of physico-chemical characterization, reaction to fire behavior, acoustic and thermal performances and sensibility to fungal development of the hemp wool prototype. The optimization of the fireproof treatment also included the evaluation of the concentration of phytic acid and urea, in the concentrations of 1%, 3%, 5% and 10% in mass for phytic acid and 3%, 9%, 15%, 30% for urea.

The chemical modification of the hemp wool prototypes was assessed through measurements of phosphorus content in their core and surfaces. HWC and HWS samples presented increasing values of phosphorus with increase in flame retardant concentration, but the in the HWC samples this concentration was homogeneous throughout the material, whereas in the HWS samples they are only on the surface.

The chemical modification of the fibers led to an apparent density increase in the HWC samples, but no significant difference was observed in the HWS samples. It also influenced the flammability of the hemp wools. The mechanisms of flame retardancy were evidenced, as a char layer was formed over the fibers, reducing heat penetration, flame spread and oxygen diffusion.

However, the fire reaction behavior was not the same in all samples. The samples treated with 1% and 3% of phytic acid presented fully combusted zones after the MLC test, indicating that the amount of flame retardants applied was not enough to produce a homogeneous char layer. In samples treated with higher phytic acid concentration (5% and 10%), the presence of a denser char formation was observed. In the HWS samples, since the phosphorus was only grafted at the surface, the core remained vulnerable to the heat and underwent full combustion, even with high quantities of flame retardants. The size of the samples might have played a role in this result, as the heat could easily reach the lower layers of the samples through the sides.

A strong correlation between the total heat released and the phosphorus content was observed for the samples HWC, linked to a homogeneous treatment. Another strong correlation between the total heat released and the amount of phytic acid used for treatment was also observed. This allowed the development of a relationship between the amount

of phosphorus and the amount of phytic acid applied. With that, a treatment efficiency was found to be between 64% to 77%.

On the acoustic side, the treatment led to a reduction of the sound absorption coefficient of the hemp wool prototypes. This reduction was more significant in HWC samples, especially those with higher amount of phosphorus grafted (HWC 5% and HWC 10%), reaching a maximum relative reduction of 16.5%. HWS samples presented intermediate values of sound absorption between the reference and HWC samples, where the relative reduction of sound absorption was between 4.5% and 9.0%. Through the analysis of the characteristic parameters of the pore geometry, the parameters that significantly changed after the fireproof treatment were the porosity and the characteristic thermal length.

Regarding the thermal parameters, the treatment does not affect the thermal conductivity directly, but rather indirectly through the increase in apparent density of the HWC samples. The specimens that presented any significant increase belonged to the HWC 5% and HWC 10% formulations, which contains the highest amount of phosphorus grafted. Therefore, the treatment may impact indirectly the thermal conductivity of the hemp wool prototypes.

The biological durability tests detected the presence of a fungus that are commonly found in indoor environments before incubation. After six months of incubation in favorable environmental conditions for the fungi development, two species of molds that are usually found in plants and soils were observed in the reference hemp wool. No fungi colonies were found in the treated samples.

The impregnation of *Penicillium spp.* led to the formation of some colonies in the HW REF sample, that were not visible to the naked eye. No colonies were formed after incubation in the treated samples, indicating a beneficial effect of the flame retardants on the prevention of fungal growth, in particular the phytic acid. However, this needs further study considering other bio-based materials and a larger variety of fungi species.

In this Chapter, new findings related to the impact of the fireproof treatment on the functional performances, fire reaction and biological durability of hemp wools were presented. The treatment was optimized to the condition of HWC 5%, which is the pulverization of the fibers with the treatment solution containing 5% phytic acid and 15% urea, before the panels production. This condition combines significant reduction on the flammability of hemp wools, and moderate quantities of flame retardants.

This treatment method will be used in the following Chapter for the production of fireproof treated hemp wool panels in an industrial-scale. This will allow the verification of the treatment procedure considering the particularities of a large-scale production, and the characterization of their fire reaction, acoustic and thermal performances and the biological durability.

Chapter 5

Industrial production scale: Hemp wool airlay panels

In the previous Chapters, the fireproof treatment have been defined, tested and optimized in bulk hemp fibers and hemp wool prototypes. The pulverization of a flame retardant solution containing 5% phytic acid and 15% urea in mass, in all fibers, before the panels formation, was considered as the optimal treatment method, when considering the time and energy required, the amount of materials and the flammability of the treated hemp wools.

The treatment definition is a major step for the development of flame retardant hemp wool panels. However, the production method that are usually employed in the industry for the fabrication of hemp wool panels differs considerably from the method used for the prototypes fabrication. Different production methods can lead to different characteristics, performances or problems.

Therefore, to fulfill the main goal of this thesis, the properties and performances of a fireproof treated hemp wool panel, produced through a method used in the industry, will be assessed (Figure 5.1). This Chapter aims to demonstrate the viability of the treatment and production methods developed throughout this thesis, considering a large-scale production of flame retardant hemp wool panels.

Through the study of the physico-chemical properties, fire reaction, acoustic and thermal performances and sensibility to fungal development of treated and untreated hemp wool panels, it will be possible to characterize the material and provide reference values to be comparable with insulation products commercialized in the market.

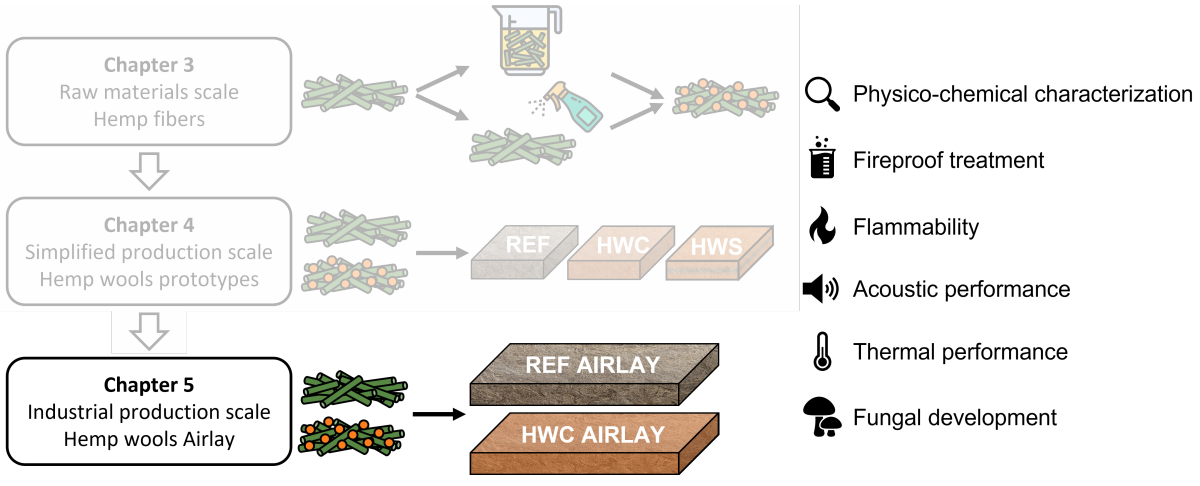

Figure 5.1: Scheme of thesis organization

This Chapter is divided into six parts, as demonstrated in Figure 5.2. The first

part consists of the description of the production method using an airlay procedure with a thermal-bonding method to consolidate hemp wool panels (Section 5.1). Then, the physico-chemical characterization of the airlay hemp wools are presented in Section 5.2. Finally, from Section 5.3 to 5.6, the fire reaction, acoustic performance, thermal properties and fungal development are presented, respectively.

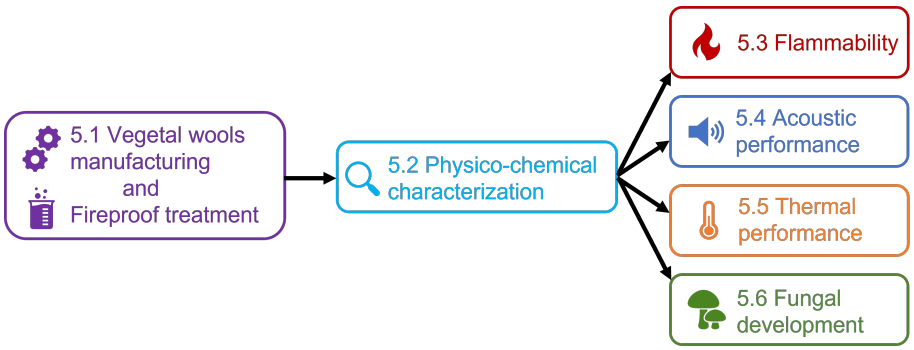

Figure 5.2: Parts of the Chapter 5

5.1 Hemp wools manufacturing by airlay

The production of hemp wool panels by the airlay method can be divided into five steps, illustrated in Figure 5.3 (AYA23). The first step included the use of the fiber opening machine to untangle and open the fibers and mix hemp and thermoplastic fibers, similar to the procedure described in Section 4.1.2.2. For each panel produced, 13.5 kg of hemp fibers and 1.5 kg of thermoplastic fibers are required, and two panels were produced, one reference and one treated panels. A total of 27 kg of hemp fibers and 3 kg of thermoplastic fibers were used.

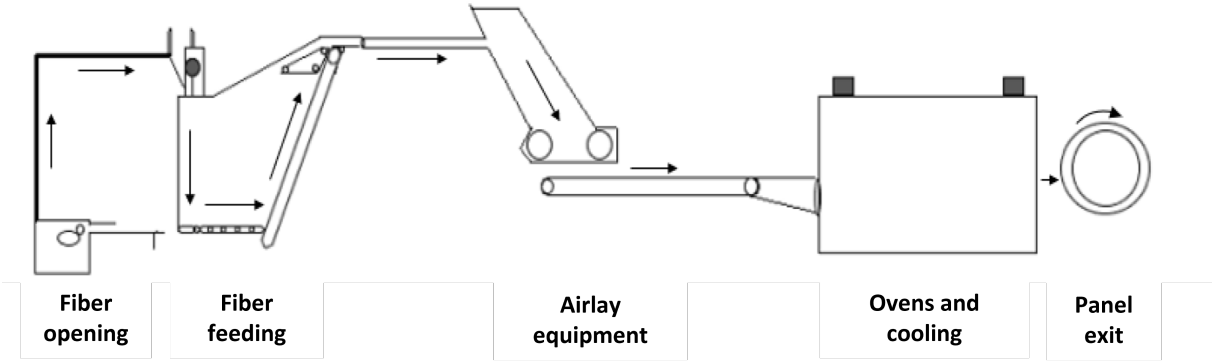

Figure 5.3: Schematic representation of the airlay production (AYA23)

5.1.1 Fireproof treatment

Before being sent to the next step, the fibers were fireproof treated. The fireproof treatment consisted of a solution of phytic acid, urea and distilled water, prepared with the same conditions as described in Section 4.1.2.2. For the hemp wools produced with the airlay method, only one condition of treatment was evaluated, due to the amount of materials used to produce each panel. Based on the results of Chapter 4, the condition chosen was with 5% phytic acid and 15% urea. The materials used and the solution prepared are presented in Figures 5.4a to 5.4d.

The application method adopted was through the pulverization of the solution in all fibers, before panel production. It is, therefore, similar to the condition HWC 5%,

developed in Chapter 4 for hemp wool prototypes. Each kilogram of fibers was spread inside a carton box (Figure 5.4f), and sprayed with a spray bottle (Figure 5.4e) filled with the treatment solution. During this procedure, the fibers were mixed and turned multiple times, in order to pulverize all the fibers as homogeneously as possible.

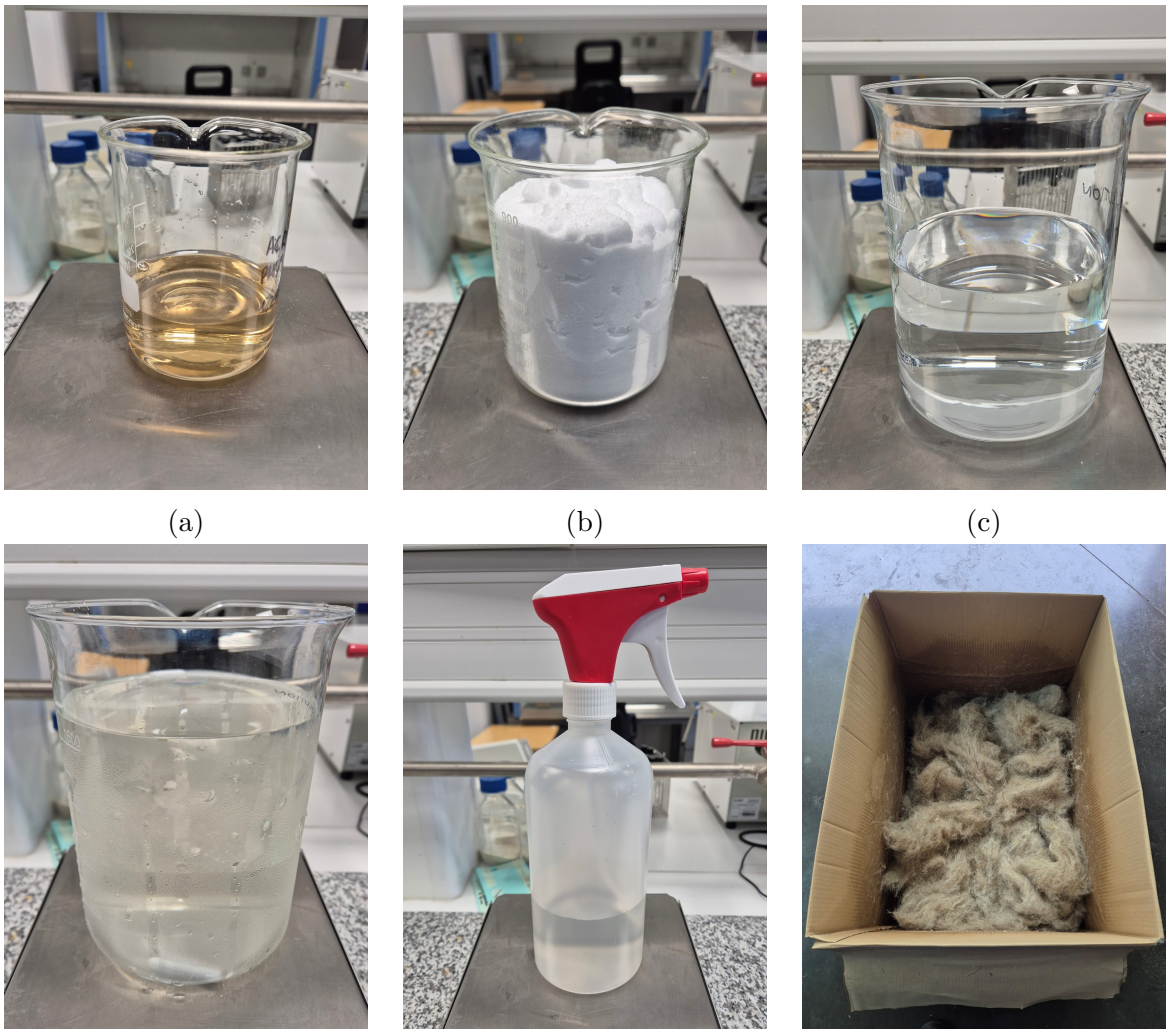

(a) (b) (c)

(d) (e) (f)

Figure 5.4: Fireproof treatment of hemp wools: (a) Phytic acid; (b) Urea; (c) Distilled water; (d) Solution; (e) Spray used for application; (f) Pulverization of hemp wools

After the application of the fireproof treatment, the fibers were oven-dried at 80°C for 1 hour. This duration was enough to significantly reduce the water content of the fibers, and allowed for the continuation of the hemp wool fabrication.

5.1.2 Airlay production

To begin the production of hemp wools, the dried fibers were sent to a feeder (Figure 5.5a), which can help regulate the flow of fibers to the airlay equipment. The airlay equipment is fed with fibers in a chimney. Depending of the feed speed, therefore the quantity of fibers, the apparent density of the panels can be regulated. After that, the fibers are dispersed in an air stream through perforated rotating cylinders to form a web on a conveyor. The speed of the discharge rollers controls the thickness of the panels.

Panels with two densities were produced for each treatment condition: one with a higher density, target for 60 $kg.m^{-3}$ similarly to the prototype panels produced in Chapter 4, and a second with lower density. This was done by controlling the speed of the rollers

that charge and discharge the airlay equipment. Therefore, the apparent density is not a parameter that can be directly controlled, but rather indirectly through the adjustments of conveyor belts speeds and cylinders rotations.

When exiting the airlay equipment, the panel with the highest density had approximately 150 mm of thickness (Figure 5.5b), and the panel with the lowest density had approximately 100 mm (Figure 5.5c). As seen in these Figures, the first couple of meters of the panel that exit the airlay machine, do not have a homogeneous distribution of the fibers, because the equipment is not charged with fibers in the beginning of the process. However, after the first couple of meters, the thickness of the panels is homogeneous, as seen in Figure 5.5d. Figures 5.5e and 5.5f present the thickness and fiber distribution of the panels with higher density and lower density, respectively.

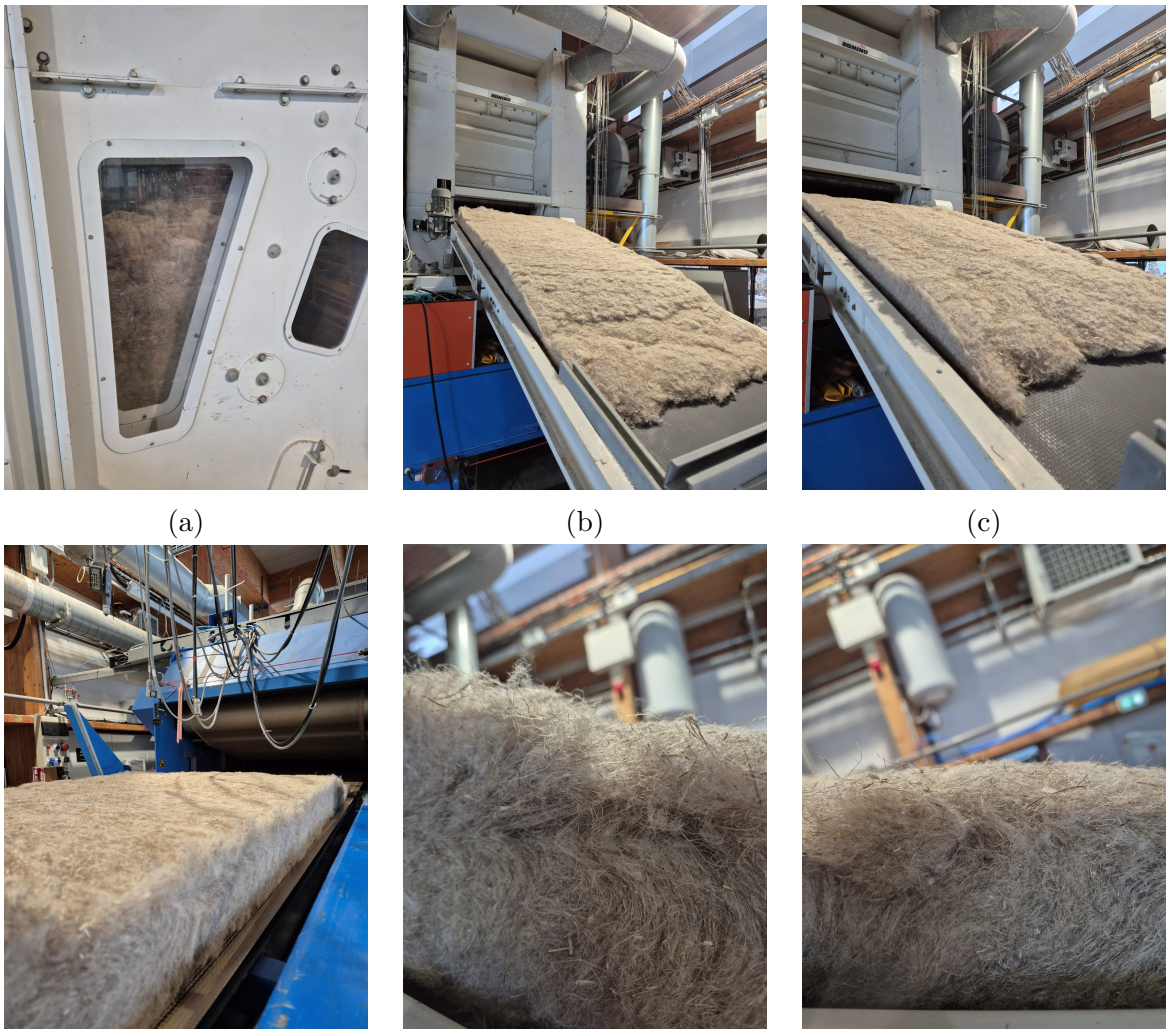

(a) (b) (c)

(d) (e) (f)

Figure 5.5: Airlay production process: (a) Feeder of mixed hemp and thermoplastic fibers; (b) Airlay panel with higher density; (c) Airlay panel with lower density; (d) Homogeneous thickness of panels after the couple of meters; (e) Distribution of fiber from the airlay panel with higher density; (f) Distribution of fiber from the airlay panel with lower density

Given the two treatment conditions (reference and treated in the HWC 5% condition) and two densities (referenced as lower and higher), four samples of hemp wool panels produced by the airlay method were prepared: HW REF AL- for the reference sample with lower density; HW REF AL+ for the reference with higher density; HWC 5% AL- for the treated sample at lower density; and HWC 5% AL + for the treated sample with higher density.

5.1.3 Panels heating

After exiting the airlay equipment, the panels passed through the oven in a conveyor belt at a speed of 0.5 m.min^{-1}, as described in Section 4.1.2.2, for the thermo-bonding process (Section 1.3). The oven temperature was set to 140°C, for melting the copolyethylene present in the sheath of the thermoplastic fibers. After being subsequently cooled down with fresh air, the polymer solidified and formed bonds with the hemp fibers, consolidating the panels. Moreover, heat is also an important step to graft the phosphorus molecules from phytic acid with the hemp fibers, as mentioned in Section 1.6. This process took about 15 minutes, and the panels passed twice in the oven. This is one less passage than the amount used in prototype manufacturing. However, in order to optimize the process at the industrial production level, considering the time and energy consumption, the number of passages in airlay production was reduced to two.

During each passage of the fibers through the oven, the hemp wools thickness was reduced. The oven consists of two chambers, and is equipped with rollers with controlled height, that are used adjust the panel's thickness. In the first passage, the first roller was set to reduce the thickness of the panels with higher apparent density from 150 mm to 100 mm. The second roller reduced the thickness from 100 mm to 50 mm. The panel with lower density had its thickness reduced from 100 mm to 80 mm and 80 mm to 50 mm, in the first and second rollers, respectively. The second passage in the oven reduced the thickness of all panels to 40 mm. The aspect of the panels after they pass in the oven is presented in Figures 5.6a and 5.6b.



(a) (b)

Figure 5.6: Hemp wools produced by airlay method: (a) Reference panel (HW REF AL); (b) Treated panel (HWC 5% AL)

Compared to prototype fabrication, one less passage through the oven was applied. It was considered that two passages was enough for the proper consolidation of the panels, at the desired thickness. However, this means that the pulverized fibers were exposed to heat for a shorter duration, which may impact the phosphorus grafting reaction with the hemp fibers.

The last step consisted of cutting the samples for fire reaction tests and acoustic and thermal measurements, as mentioned in Section 4.1.2.2. The fire reaction samples consisted of square-shaped samples with dimensions of 100x100x40 mm^3. The acoustic samples consisted of cylinders with 100 mm diameter and 40 mm height.

5.2 Physico-chemical properties of airlay hemp wool panels

Before having their performances assessed, these samples were characterized in terms of physical properties, including solid skeleton density, apparent density and porosity, and chemical properties, through the assessment of the phosphorus content grafted during treatment. These characterizations were compared to the results obtained for the prototype samples HW REF and HWC 5%, presented in Chapter 4. These samples were prepared with the same treatment conditions as the airlay samples, and differ mainly in how they were manufactured.

5.2.1 Solid skeleton density, apparent density and porosity

The solid skeleton density of the reference and treated airlay hemp wools was assessed through gas pycnometry, under helium and nitrogen atmospheres, as specified in Section 2.2.2. The results are reported in Table 5.1.

The HW REF AL and HWS 5% AL sample presented solid skeleton density of 1.448 g.cm^{-3} and 1.463 g.cm^{-3}, respectively, when assessed under helium gas, and 1.435 g.cm^{-3} and 1.455 g.cm^{-3}, when under nitrogen. The lower values obtained in the measurements performed with nitrogen are due to the bigger molecule size, that cannot fill the smaller pores that the helium molecule can. However, similarly to the results from the hemp wool prototypes (Section 4.1.4.1), the difference between nitrogen and helium measurements was lower than 1%, indicating that both methods are valid. Noticeably, the treatment can lead to a slightly increase of the solid skeleton density, around 0.02 g.cm^{-3}.

Comparing to the prototype samples HW REF and HWC 5% produced in the Chapter 4, the airlay reference sample presented a solid skeleton density slightly lower, and the treated HWC 5% AL sample presented values that are slightly higher. Both variations are in the order of 0.01 g.cm^{-3}

The samples prepared for the acoustic characterization were used to assess the apparent density of the hemp wools, using the methodology described in Section 2.2.2. These samples had 100 mm diameter and 40 mm thickness, and were individually measured and weighted. Their values, and their respective porosity, calculated with Equation **??** using the solid skeleton density obtained with the measurements done under helium gas, are presented in Table 5.1.

Table 5.1: Apparent density of airlay hemp wool samples

Sample	Solid skeleton density - He (g.cm^{-3})	Solid skeleton density - N_2 (g.cm^{-3})	Apparent density (kg.m^{-3})	Porosity (Helium) (%)
HW REF AL-	1.448 ± 0.003	1.435 ± 0.002	51.6 ± 3.7	96.4
HW REF AL+			66.1 ± 4.4	95.4
HWC 5% AL-	1.463 ± 0.003	1.455 ± 0.002	62.0 ± 3.7	95.8
HWC 5% AL+			79.6 ± 4.2	94.6

It can be seen that the goal of producing two densities of hemp wool panels was successfully achieved. The reference samples presented an apparent density of 51.6 kg.m^{-3} at the low density condition and 66.1 kg.m^{-3} at high density condition, indicating a difference of about 15 kg.m^{-3}. The low and high density conditions for the treated samples were 62.0 and 79.6 kg.m^{-3}, respectively. As the parameters set in the airlay equipment were the same for the production of the samples at equivalent densities, these differences

between the reference and the treated conditions come from the treatment itself, similar to the results obtained in Chapters 3 and 4.

In the prototype samples the difference between the apparent density of the HWC 5% and HW REF samples was 14 kg.m^{-3} (Table 2). The same order of magnitude of the variation is observed in the airlay samples. For the lower density samples the difference was 10 kg.m^{-3}, and for the higher density, 14 kg.m^{-3}. Therefore, in characterization results of the airlay samples densities are consistent compared to the prototypes.

All samples presented a very high porosity, at about 94-96%. A small reduction in porosity is observed with the treatment, which is due to the changes in apparent density, since the solid skeleton densities hardly changed.

5.2.2 Phosphorus content

As presented in the previous Chapters, the chemical characterization provide valuable information about the hemp wools flammability, due to the relationship between phosphorus content and fire reaction parameters, such as pHRR and THR.

The samples for ICP-AES were extracted from the core of the hemp wool panels, and their result for phosphorus content is presented in Figure 5.7. For comparison purposes, the ICP results of the prototype samples HW REF and HWC 5% were also added.

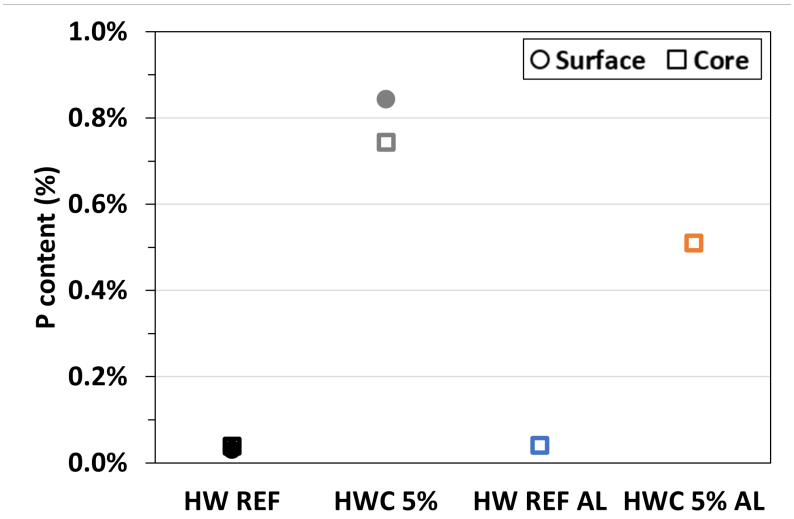

Figure 5.7: Phosphorus content of airlay hemp wools

It can be observed that the reference airlay sample (HW REF AL) presented almost no phosphorus content (0.04%), similar to HW REF and the reference fibers presented in Chapter 3. The treated airlay sample (HWC 5% AL) showed a phosphorus content of 0.51 ± 0.08%. This value is lower than the 0.79% ± 0.29% observed in its prototype counterpart (HWC 5%).

This reduction could be associated with two reasons. The first one is the reduction of the heating step duration. During the production of the prototypes, each panel passed three times through the oven, totaling about 18 minutes inside the heating chamber, whereas in the airlay method, each panel passed twice through the oven, which is an equivalent of 12 minutes of heat. The heating step is an important part of the treatment, as it promotes grafting of the phosphorus molecules into the cellulose and hemicellulose.

Another possible reason behind the reduced phosphorus content, is the fact that the airlay method has more steps with contact between the fibers and equipments. After being pulverized with the flame retardant solution, the fibers come in contact with the fiber-opening machine, the feeder, the airlay equipment, and multiple conveyor belts.

It was hypothesized that the contact between the fibers and these equipments might generate friction and remove the flame retardant particles. In contrast, the formation of the prototype panels after the fibers were treated was manually executed, which means there is considerably less contact between the fibers and other surfaces. Moreover, because the heating time was reduced, less phosphorus molecules were grafted and more molecules were vulnerable to being removed by friction.

During the analysis of the phosphorus content of the hemp wool prototypes, a correlation between the phosphorus content and the phytic acid used was determined (Equation 4.12). The ICP result of airlay hemp wools does not fit this equation, indicating that the production method interferes in the treatment and the chemical characteristics of the treated fibers. Recalculating the treatment efficiency using Equation 4.13, the airlay method reaches an efficiency of 36%.

In contrast to the results obtained for the characterization of the densities and porosity, the airlay production method influenced the chemical constitution of the fibers after treatment, by presenting lower values of phosphorus grafted. In the sequence, the flammability of these hemp wools will be assessed to verify their flame retardancy behavior.

5.3 Fire reaction of fireproof treated hemp wool airlay panels

The characterization of the fire reaction and smoke production of the airlay hemp wools consisted of the single-flame source, the cone calorimeter and the smoke density test, as described in Sections 2.3.1, 2.3.2 and 2.3.3, respectively.

5.3.1 Single-flame source test

The single-flame source test was performed with the reference and treated airlay samples. The results are shown in Figure 5.8. Both samples presented burned heights below 15 cm, after 60s of ignition, indicating that they have limited flame spread. This is one of the key requirements in the Euroclass for a classification between B and E. The burned height of the reference sample was on average 11.2 cm whereas HWC 5% AL presented a burned height of 7.2 cm, indicating a reduction of the flame-spread property after the fireproof treatment.

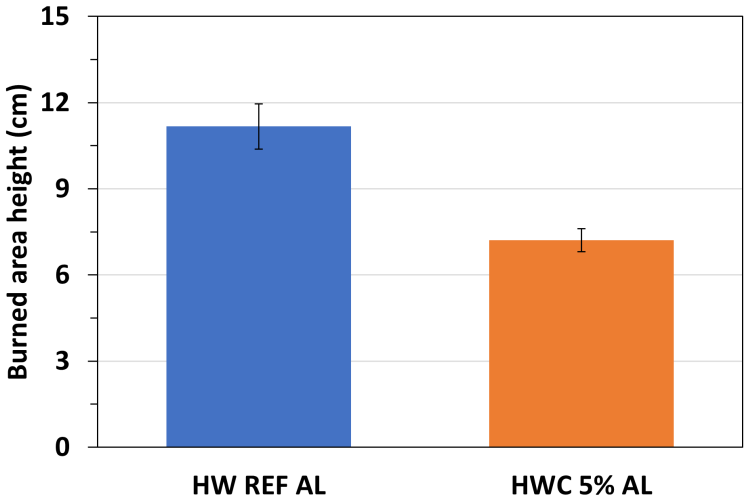

Figure 5.8: Burned height from airlay hemp wools

During this test, the time for the flame to extinguish was observed and measured, and a significant difference was observed between the treated and untreated hemp wools. The HW REF AL samples presented a time to extinguish, after the flame was removed, of 82 ± 27 seconds, while the HWC 5% AL flame extinguished immediately after removing the flame source.

5.3.2 Mass loss cone calorimeter

The mass loss cone calorimeter test was performed on 8 samples for each condition of treatment and apparent density. The aspects of the samples before and after the test are presented in Figure 5.9. It can be seen that the untreated sample presented the same coloration and form as the untreated prototype sample presented in Figure 4.14 in Section 4.3. This sample underwent complete combustion, presenting a white coloration and a very fragile structure (Figure 5.9b).

In contrast, the treated sample formed a solid char layer that protected the lower layers of the samples (Figure 5.9d). In Figures 5.9e and 5.9f, it can be seen that the lowest part of the sample was preserved, retaining its natural color and form, due to the char layer formed on top of it. This was observed in most of the samples, others were fully covered by the char layer.

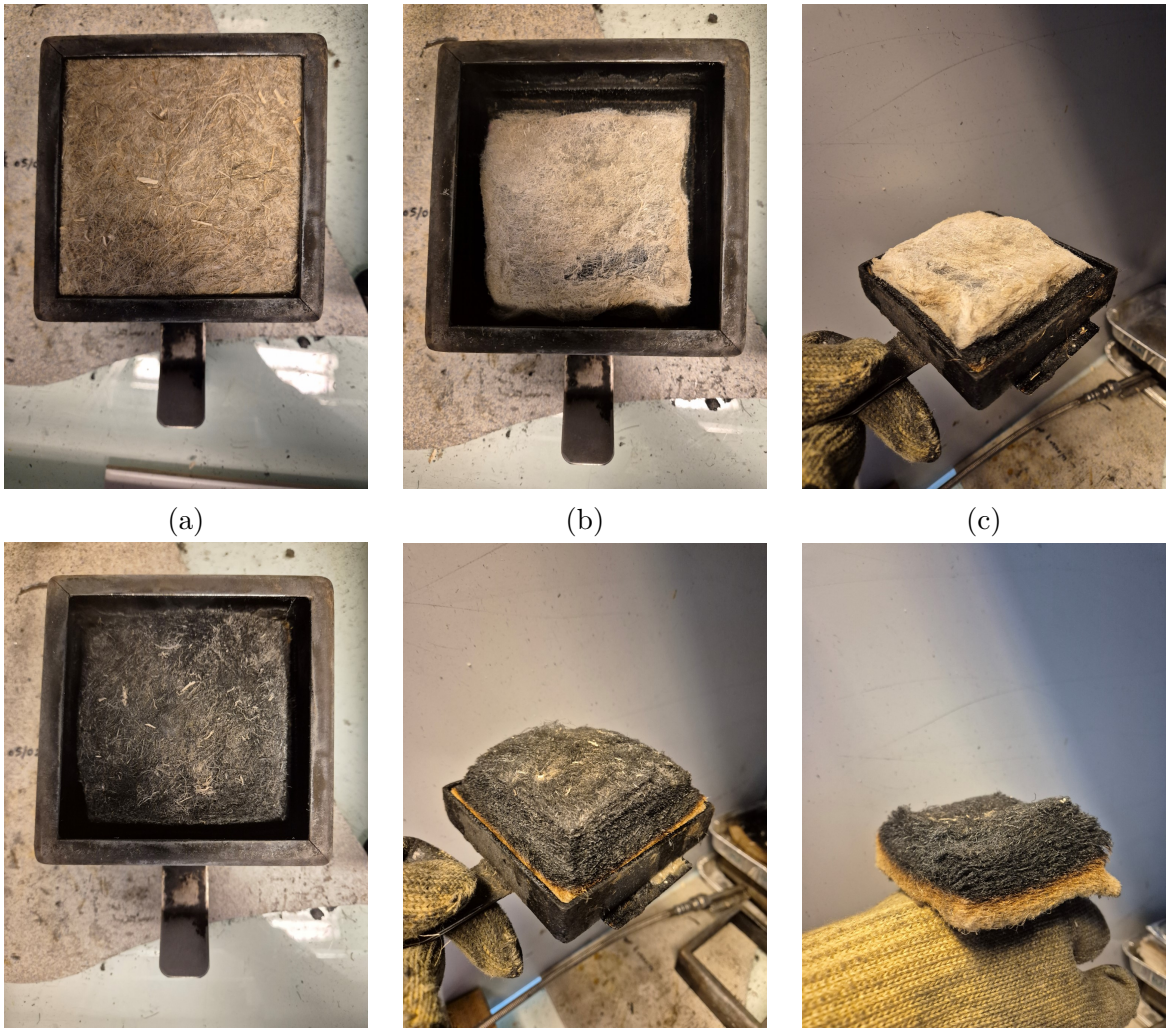

(a) (b) (c)

(d) (e) (f)

Figure 5.9: Visual aspect of cone calorimeter samples: (a) Before testing; (b) Top view of HW REF AL after; (c) Isometric view HW REF AL after; (d) Top view of HWC 5% AL after; (e) Isometric view HWC 5% AL after; (f) Side view HWC 5% AL after

For each condition of treatment and density, seven measurements were tested. Among those, one of each was discarded due to incorrect setup of the test, or results that deviated from the other six. The results of all samples for the HW REF AL+ and HWC 5% AL+ are presented in Figure 5.10.

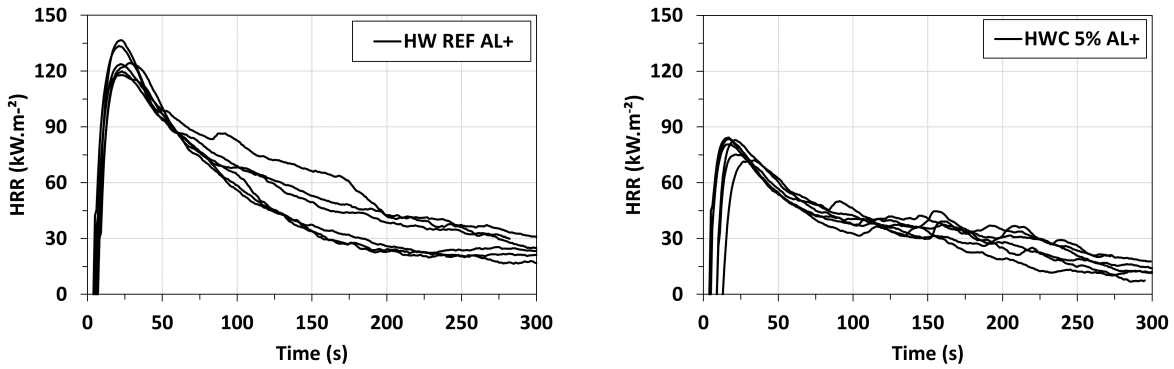

(a) (b)

Figure 5.10: Heat release rate curves from mass loss cone calorimeter tests: (a) Samples HW REF AL+; (b) Samples HWC 5% AL+

A good reproducibility can be observed between samples. Therefore, for the comparison between treated and untreated samples, as well as different densities, the HRR curve that better represents the average behavior of each sample was selected. The heat release rate curves over time are presented in Figure 5.11.

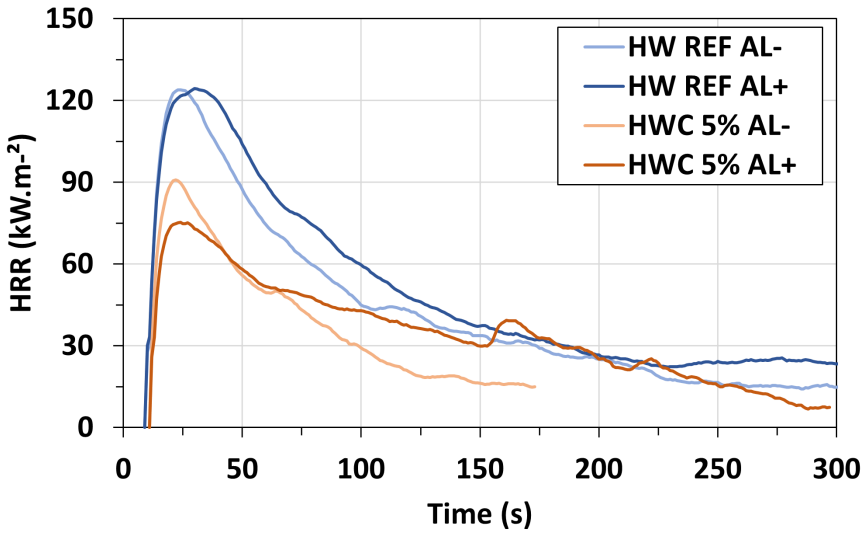

Figure 5.11: Heat release rate over time from airlay hemp wools

Noticeably, no significant differences are observed between densities. Samples HW REF AL- and HW REF AL+ presented the same format of curve, describing similar kinetics of degradation, and the same values of pHRR on average. For the treated sample, no significant change in the pHRR is observed either. These results are also reported in Figure 5.12a.

When comparing treated and untreated samples, HWC 5% AL- showed a reduction of 27% in pHRR compared to HW REF AL-, and sample HWC 5% AL+ a reduction of 37% compared to HW REF AL+.

However, when it comes to the total heat released, the samples with higher densities presented higher values than the samples with lower densities (Figure 5.12b). Because higher density samples have higher mass, they have more material to be combusted, which leads to higher THR. The fireproof treatment reduced THR values in 50% and 43%, for the treated samples at low and high densities, respectively.

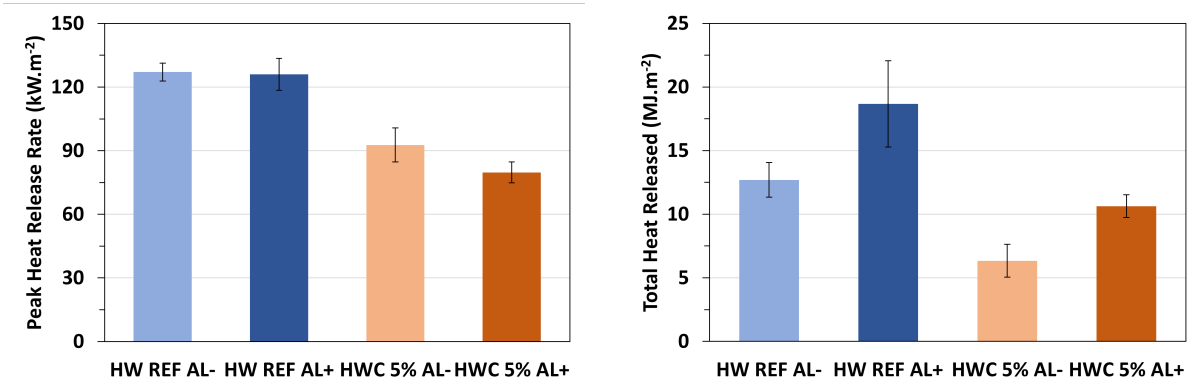

(a) (b)

Figure 5.12: Mass loss cone calorimeter results: (a) Peak heat release rate; (b) Total heat released

The mass loss curves over time during the MLC test are shown in Figure 5.13. Both untreated samples presented a fast kinetics of degradation, burning continuously for long durations and retaining low amount of weight at the end of the test. The flame was extinguished on average in less than 5 and 7 minutes for the HW REF AL- and HW REF AL + samples, respectively, and their remaining mass was 14% and 24%. The increase in density led to longer time until flame extinguishment, due to higher amount of fibers, but also a higher relative final mass. The same can be observed in the treated samples. Samples HWC 5% AL- and HWC 5% AL+ had their flames extinguished on average at about 3 and 5 minutes, respectively, and a final mass of 38% and 50%. The test duration and the residual mass after the cone calorimeter test are presented in Table 5.2

Table 5.2: Test duration and residual mass after MLC test for airlay hemp wool samples

Sample	Test duration (s)	Residual mass (%)
HW REF AL-	284 ± 28	14 ± 2
HW REF AL+	414 ± 75	24 ± 9
HWC 5% AL-	169 ± 33	38 ± 8
HWC 5% AL+	305 ± 28	50 ± 5

Two distinct kinetics of degradation were observed depending on the density analyzed. Both samples with lower density, treated and untreated presented similar rate of degradation. The main difference between them, is that the flame extinguished earlier, preserving a higher mass at the end of the test. On the other hand, higher density samples presented a distinguished behavior. The treated samples presented a slower rate of thermal degradation, and a significantly higher residual mass, while the untreated sample degraded for longer and presented half of the mass remaining. The comparison of the rate of degradation between samples of different densities was avoided due to the residual mass parameter being presented as a relative value.

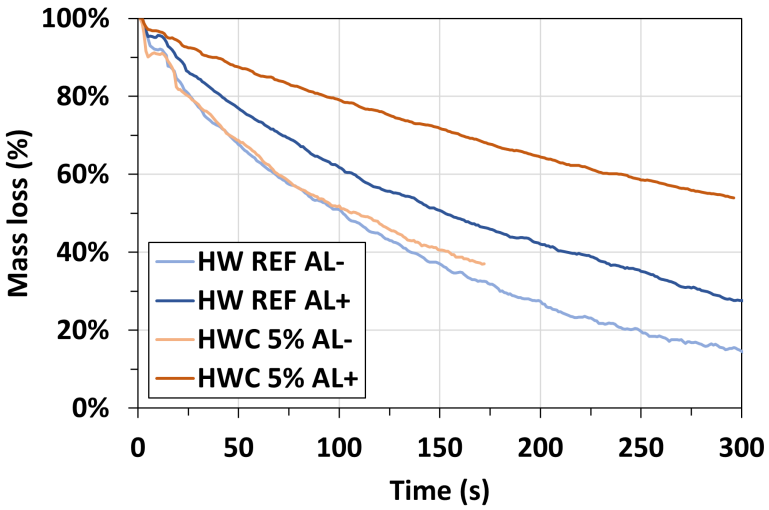

Figure 5.13: Mass loss over time during MLC tests from airlay hemp wools

5.3.3 Smoke density test

Samples weighting 2g were cut from hemp wool panels, and used for the assessment of smoke production, as described in Section 2.3.3. A total of 5 samples were tested for each treatment condition. In this test, no differentiation was made between lower and higher density samples, since their difference would be too subtle for a sample weighting 2g. All samples were cut from panels with lower densities.

The smoke density results are shown in Figure 5.14. For both samples, in the first 30 seconds of the test, almost no smoke is observed. During this time, the fibers are heating and the humidity is evaporating. After that, pyrolysis starts, breaking the cellulose, hemicellulose and lignin chains and releasing volatiles and gases that form the smoke. In the treated sample, this process is accelerated, because of the catalytic effect of the phosphorus molecules on the thermal degradation of cellulose and hemicellulose. Therefore, a clear peak of absorptivity was detected by the equipment, resulted from the high production rate of smoke. This peak was on average 31.8% of absorptivity at 75s after the beginning of the test. After this peak, the smoke density inside the chamber decreases quickly. For the reference sample, a wider peak was formed between 90s and 105s, but at a lower magnitude, with an average of 22.4%.

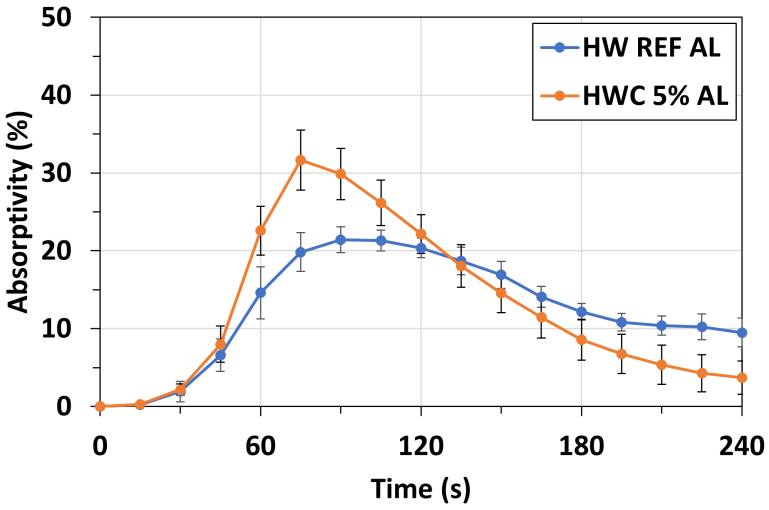

Figure 5.14: Absorptivity over time during smoke density test from airlay hemp wools

After two minutes of test, the absorptivity measured by the equipment was similar for the reference and treated sample, due to the char formation on the treated sample, and consequently the reduction on the combustion reaction rate, and due to maintenance of the high levels of smoke being produced by HW REF AL. Then, until the end of the test, the reference sample showed a slow reduction of the smoke density inside the chamber, but was kept at higher levels than the treated sample, which significantly reduced the smoke density.

The fire reaction characterization of the hemp wools allowed the assessment of multiple parameters including ignitability, heat release rate over time and smoke production, which provide an overview of the fire behavior of the fireproof treated hemp wools. Compared to the hemp wools produced in Chapter 4, the treated airlay wool presented a lower phosphorus content. However, a significant reduction in the flammability is observed in comparison to the HW REF AL sample, which proves the efficacy of the optimized treatment method applied.

5.4 Acoustic performance of fireproof treated hemp wool airlay panels

The fireproof treatment of the hemp wool airlay panels affects the physico-chemical properties of the material, as shown in Section 5.2. Thus, it is relevant to evaluate how these changes influence the acoustic performance of hemp wools, in particular their capacity to absorb sound waves.

5.4.1 Sound absorption coefficient

The acoustic performance of the hemp wool airlay panels was assessed by measuring the sound absorption coefficient through the impedance tube test, as described in Section 2.4. Each sample was tested on both sides, totaling eight measurements for each condition. The sound absorption curves for each sample and each treatment condition are presented in Figure 5.15.

Due to the variation in the sample's apparent density, some dispersion was observed. This dispersion is, however, logical to the variation in apparent density. For example, the two lowest sound absorption curves in the HW REF AL- condition (Figure 5.15a), presented an apparent density of 47.1 kg.m^{-3}. The two highest curves, an apparent density of 55.8 and 55.0 kg.m^{-3}. The same occurs for the HW REF AL+: the lowest curve had an apparent density of 59.6 kg.m^{-3}, whereas the two highest curves have an apparent density of 71.4 kg.m^{-3}. Since the results are consistent with the variation of the apparent density, the use of the average sound absorption curve and the average apparent density is relevant.

The average curves of sound absorption for each sample are presented in Figure 5.16. For reference, the sound absorption curves of the prototype reference (HW REF) and HWC 5% samples, both presented in Chapter 4, were also added.

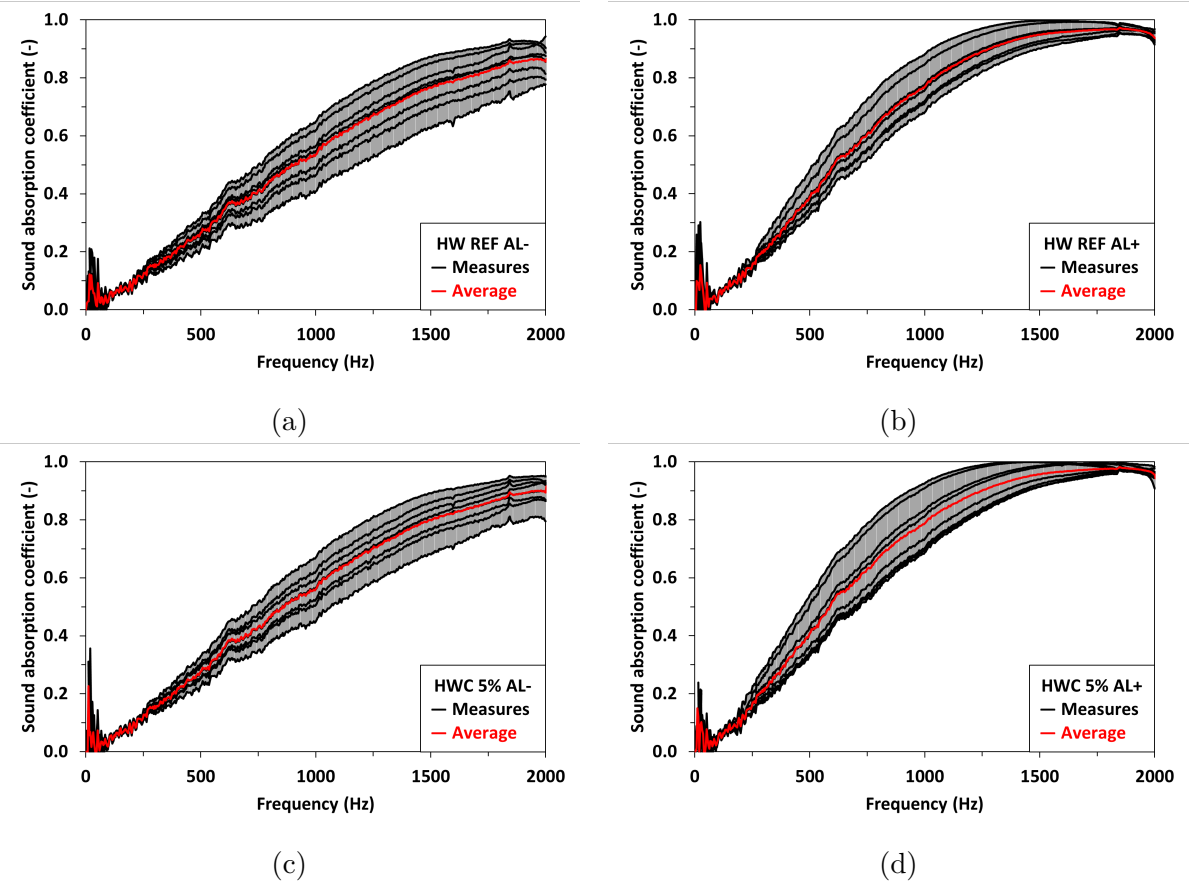

Figure 5.15: Sound absorption curves of each sample tested for each treatment condition and density evaluated: (a) HW REF AL-; (b) HW REF AL+; (c) HWC 5% AL-; (d) HWC 5% AL+

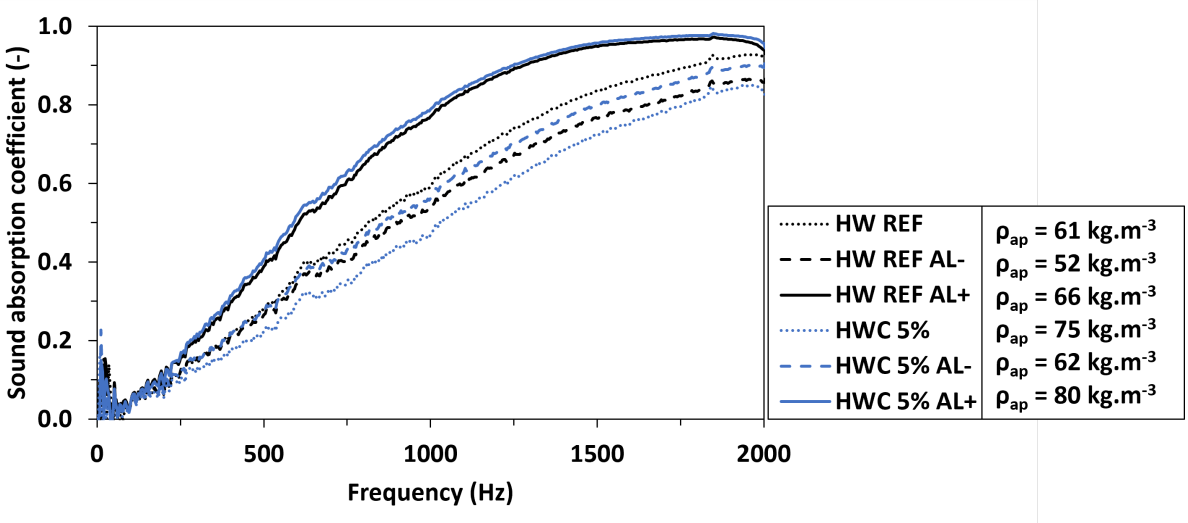

Figure 5.16: Sound absorption curves from airlay hemp wools

Through the analysis of the sound absorption curves of the reference samples, including those produced by airlay and the prototype, the effect of the apparent density is highlighted. Sample HW REF AL- has the lower apparent density at 52 kg.m^{-3}, and presented the lowest values of sound absorption in all range of frequency. It is then followed by the HW REF at an apparent density of 61 kg.m^{-3}, and finally the HW REF AL+ with an apparent density of 66 kg.m^{-3}. In the latter, the sound absorption was

significantly improved, increasing the absorption at lower frequencies, and forming a peak of absorption at about 1700 Hz.

Interestingly, for the treated samples, the expected relationship between acoustic absorption and apparent density was not followed. The prototype sample HWC 5%, with an apparent density of 75 kg.m^{-3}, presented the lowest sound absorption. However, the lowest density is found in the sample HWC 5% AL-, with 62 kg.m^{-3}. This difference is quite significant, but the sound absorption is slightly higher than the HWC 5%, throughout all range of frequency. Then, the sample HWC 5% AL+ showed a significant increase in absorption capacity, shifting the curve to lower frequencies and forming a peak of absorption, similarly to the HW REF AL+ sample.

The comparison between treated and untreated prototype samples presented in Section 4.1.4.3 of Chapter 4, showed lower performance of the treated samples, which can be seen here through samples HW REF and HWC 5%. However, this impact was not observed in the airlay samples. The samples that were produced under the same conditions of target apparent density led to similar acoustic absorption performance.

It is noted that the airlay method of production was beneficial for the acoustic performance of the hemp wools. This is even more pronounced in the treated samples, in which performance was comparable to that of the reference samples and significantly superior to the HWC 5% prototype, even with a lower density. This effect is likely linked to a better dispersion of the fibers, creating a well-distributed and random fiber net, which increases the viscous and thermal dissipation effects and better absorb sound waves (LUU17).

The changes in these effects can be confirmed through the analysis of the characteristic parameters of the pore geometry that describes the visco-inertial and thermal effects that occur in the pore structure of the hemp wools. The assessment of these parameters also allows for evaluation of the influence of the airlay production method, as a significant improvement was observed in treated hemp wools.

5.4.2 Characteristic parameters of the pore geometry

It has been shown that the airlay production method played a role in the acoustic performance of the hemp wools, in particular for the treated sample. To understand this influence, the analysis of the characteristic parameters of the pore geometry becomes pertinent, especially when compared with a similar material produced with another production method, such as the hemp wool prototypes from Chapter 4.

The six characteristic parameters of the pore geometry were obtained for the airlay hemp wools. The values of porosity were presented in Section 5.2.1, but are also shown in Figure 5.17. Since the solid skeleton density of all samples, are very similar to each other, the main difference in the values of porosity originates from the difference in apparent density of the samples. Therefore, the samples produced targeting higher densities are less porous than the lower density samples. Also, since the treated samples are also slightly more denser, their porosity is also smaller. However, all sample are very porous with porosity values above 94%.

The tortuosity results are also presented in Figure 5.17, in the second y-axis. The values range between 1.11 and 1.23, and a large standard deviation was obtained during measurements. Effectively, these tortuosity values can be considered to be low, which represented a material that does not have impose constraints in the sound wave pathway through the material. However, these values are slightly higher, when compared to the values obtained by Piégay (PIE19) and by Ayadi (AYA23) for hemp wools, which were found to be between 1.01 and 1.08.

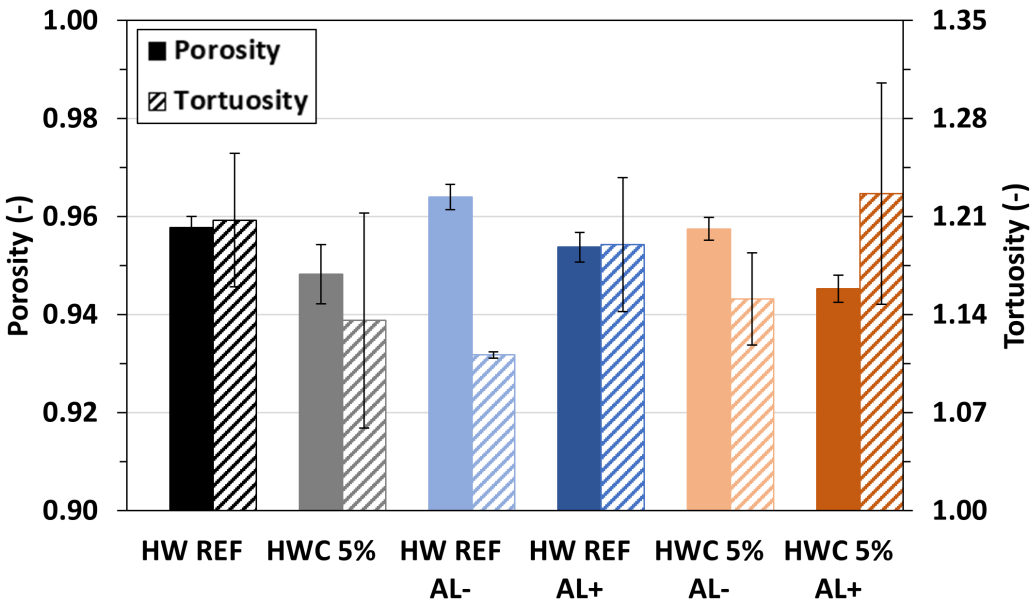

Figure 5.17: Porosity and tortuosity of airlay hemp wools

The values of airflow resistivity obtained directly with measurements using the resistivity-meter, are presented in Figure 5.18. By comparing the results of the samples that targeted lower density (HW REF AL- and HWC 5% AL-), the airflow resistivity increased from 5000 to 6000 N.s.m^{-4}, respectively. They are of the same order of magnitude as the hemp wool samples developed by Ayadi (AYA23), which had the same thickness, lower apparent density, and reported a airflow resistivity of 5000 N.s.m^{-4}. An increase is also observed in the samples with higher density, where HW REF AL+ showed an airflow resistivity of 7000 N.s.m^{-4} and HWC 5% AL+ a value of 9000 N.s.m^{-4}.

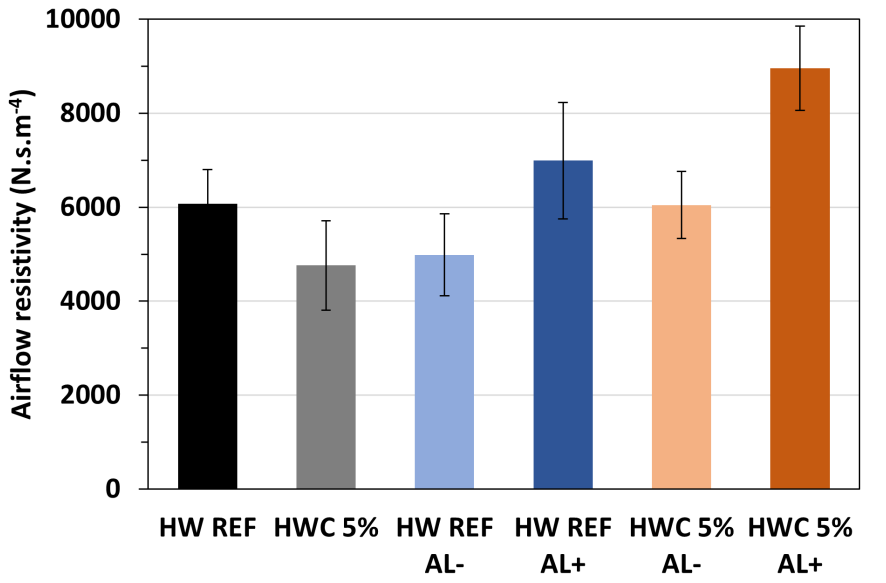

Figure 5.18: Airflow resistivity of airlay hemp wools

Therefore, the fireproof treatment on airlay samples led to an increase in airflow resistivity. This tendency is contrary to the one observed in the prototype samples, where the treatment reduced the airflow resistivity, possibly associated with an increase in fiber radius linked to the application of flame retardants.

The reason behind the different behavior obtained for the airflow resistivity on the treated prototypes and on the airlay samples, lies on the production method. During the production of the prototype samples, the fibers were placed in the molds manually, as homogeneously as possible, aiming for a random fiber distribution. However, the manual placement of the fibers may not well distribute the fibers and some level of compression was needed, which can induce a particular orientation of the fibers.

During airlay production, the panels are formed by stacks of fiber layers on top of each other, and before passing through the oven and having their thickness reduced, the fibers are oriented on the z-axis (Figure 5.19a). After being passed through the oven, moving on the conveyor belt in the x-axis direction, the fiber layer stacks can be observed in the samples (Figure 5.19b). In the XZ plane, the fibers are inclined, forming an angle that goes up to 45° with the x-axis, as observed in Figure 5.19c. This fiber orientation is formed due to the passage of the panel in the x-direction and the compression with the rollers inside the oven. The fibers that were oriented on the z-axis are laid down and form an angle with the horizontal. When observed in the plane YZ, the fibers presented a horizontal orientation in the y-axis, as seen in Figure 5.19d. The fiber orientation observed in the airlay hemp wools gives the material an anisotropic character.

In comparison, the hemp wool prototypes did not have the same method of preparation. The fibers were placed in the molds and compressed manually, which induces the orientation of the fibers to be horizontal on the XY-plane. Since fiber orientation influences the sound absorption performances of hemp wools (LEI18; LUU17), its difference between hemp wool prototypes and airlaid explains the difference observed in sound absorption and airflow resistivity. This is especially notable in the comparison between the HWC 5% and HWC 5% AL samples, where the airflow resistivity of the airlay samples is significantly higher.

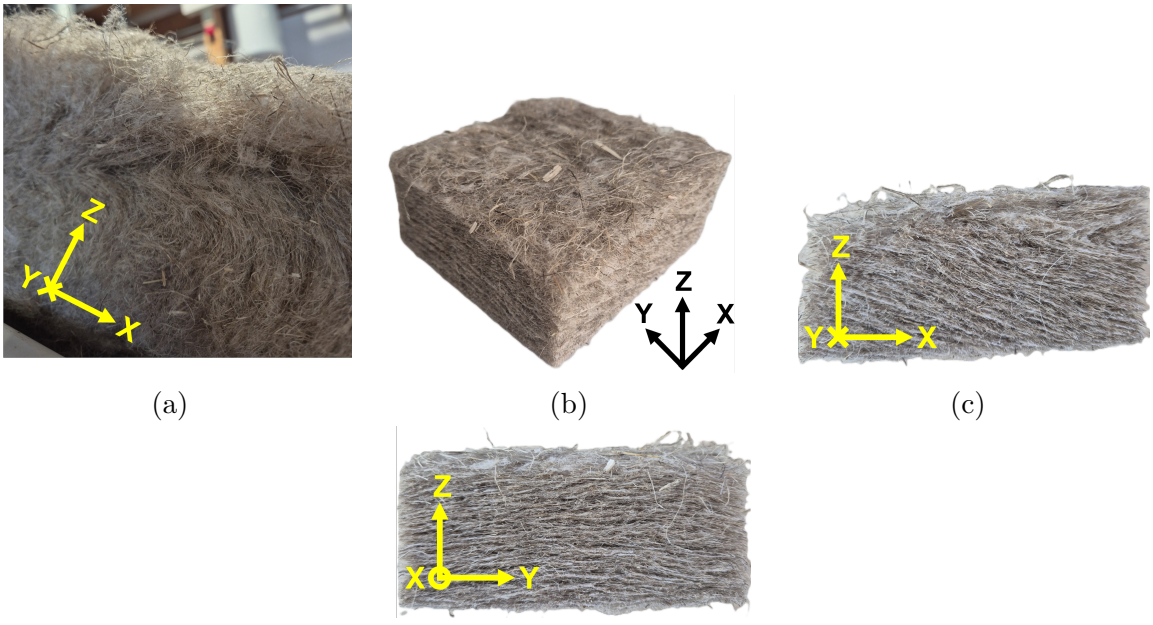

(a) (b) (c)

(d)

Figure 5.19: Airlay HW samples fiber distribution: (a) After airlay production, before passing in the oven; (b) Cut sample after production; (c) X, Y and Z coordinates in a sample as a reference

Another reason for the difference in airflow resistivity of the HWC 5% prototype sample and the HWC 5% AL sample is the dispersion of the fibers after being treated. Since the fibers get wet after being sprayed with flame retardants, the manual handling

of the fibers may have clumped some small fibers together, increasing the effective fiber radius and reducing the surface available for energy dissipation through viscous effects. The airlay method ensures a better dispersion of the fibers, avoiding fiber clumping.

In the reference samples, this difference between the prototype and airlay samples is not observed, which might be associated with the absence of the treatment application, therefore, during the preparation of the panel, the fibers were dry and remained separated from each other even after being manually handled. Therefore, the differences between the fiber distribution and orientation of the HW REF and HW REF AL samples are not as different as the treated samples.

The results for characteristic viscous and thermal lengths are presented in Figure 5.20. For the viscous length, samples HW REF AL-, HW REF AL+, HWC 5% AL- and HWC 5% AL+ presented values of 111 μm, 82 μm, 101 μm and 68 μm, respectively. Two tendencies can be observed: the first one is the reduction of the characteristic viscous length as the apparent density of the samples increase, which happens due to the increased amount of fibers occupying the same volume and consequently reducing the space between the pores. The second observation is associated with the use of flame retardants. In both densities, the characteristic viscous length values are reduced in the treated samples, which may be associated with the presence of flame retardant particles present over the fibers that slightly reduce the space between pores.

The same observations can be made for the characteristic thermal length. The values obtained were 276 μm, 186 μm, 230 μm and 146 μm, for the samples HW REF AL-, HW REF AL+, HWC 5% AL- and HWC 5% AL+, respectively. Therefore, the pore sizes are also reduced with the increase in density and due to the application of flame retardants. Noticeably, the values of the characteristic thermal length of the hemp wools are about two times the values obtained for the characteristic viscous length, which is coherent with the observations from Piégay (PIE19).

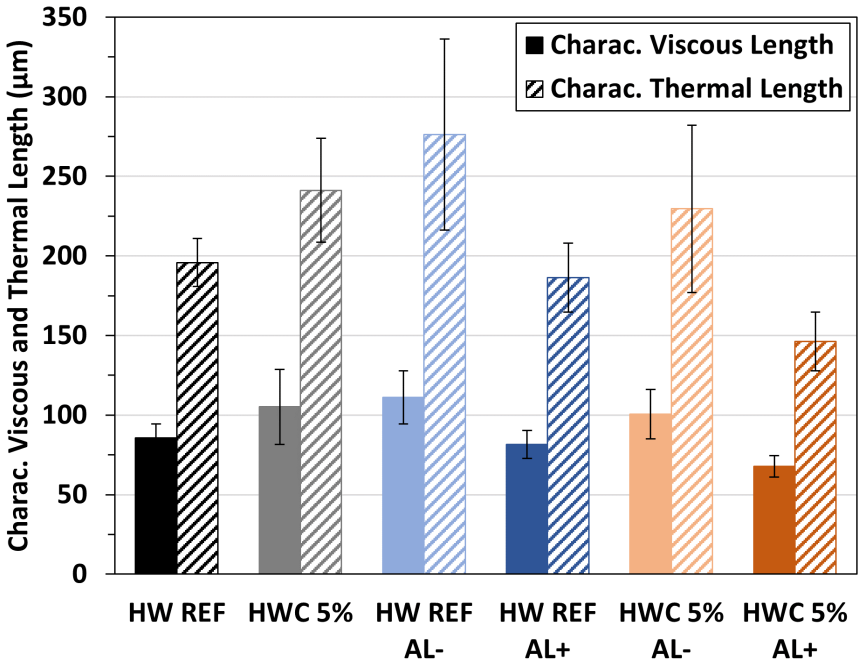

Figure 5.20: Characteristic viscous and thermal length results of HW REF and HWC 5% prototype and airlay samples

The thermal permeability values showed a very high dispersion, hindering the comparison between samples. Despite that, it was observed that changes in apparent density

did not impact this property significantly, and the use of flame retardants presented a tendency to reduce the thermal permeability of hemp wools.

In conclusion, the flame-retarded hemp wools, produced through airlay method, demonstrated an excellent performance to absorb sound. Their performance was significantly superior to its prototype counterpart, which was associated with characteristics of the airlay production method that allows the formation of a well-distributed random fiber web. Associated with that, and with fibers dispersion and orientation, an increase in airflow resistivity was observed in the treated samples produced with the airlay method, when compared with the prototype sample.

It is then clear that the apparent density, the fireproof treatment and the production method can influence the performance of the hemp wools as an acoustic insulator. Next, to cover their main functional properties, their thermal performance will be assessed.

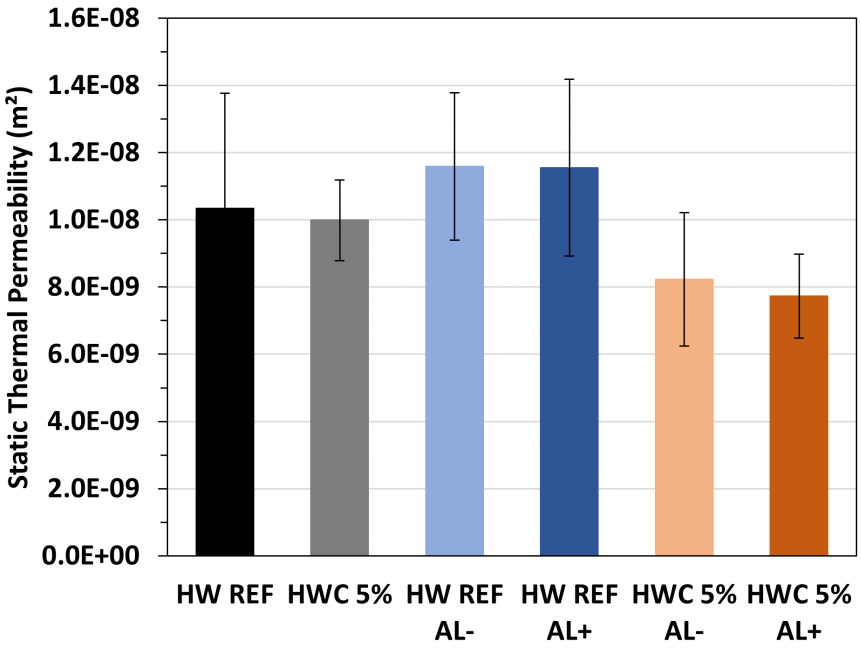

Figure 5.21: Thermal permeability results of HW REF and HWC 5% prototype and airlay samples

5.5 Thermal properties of fireproof treated hemp wool airlay panels

Similarly to the hemp wool prototypes, the thermal properties of the hemp wool airlay panels were assessed using the hot disc and the guarded hot plate test, as specified in Sections 2.5.1 and 2.5.2. The measurements were made with a room temperature of 23.7 ± 0.3 and an average relative humidity of 31% ± 2%.

5.5.1 Thermal conductivity of airlay hemp wools

The thermal conductivity samples were prepared as described in Section 2.5.1. Their thermal conductivity values of the airlay hemp wools, as a function of their apparent density, are presented in Figure 5.22. The results obtained for HW REF and HWC 5% prototype samples are presented alongside the airlay samples, for comparison.

The thermal conductivity of the HW REF AL samples presented a tendency to increase when the apparent density increased from 53 kg.m^{-3} up to 68.5 kg.m^{-3}, going from 0.057

to 0.062 $W.m^{-1}.K^{-1}$. No difference was observed between the HW REF AL samples with the two lowest apparent density. HWC 5% samples presented a linear increase in thermal conductivity values, starting at 0.056 $W.m^{-1}.K^{-1}$ for the sample with a density of 57.7 $kg.m^{-3}$, to 0.064 $W.m^{-1}.K^{-1}$ for the sample with a density of 81.4 $kg.m^{-3}$.

Both treated and untreated airlay samples presented similar thermal conductivities as their prototype counterparts. The conclusions obtained from this test are similar to those obtained in Section 4.2.1 for hemp wool prototypes: the apparent density governs the thermal conductivity results, and the airlay samples, produced with the same method but aiming for two different densities, confirmed it. At densities lower than 60 $kg.m^{-3}$, no difference was observed between samples, which could indicate the radiation effects becoming more relevant. Moreover, no significant difference associated directly with the application of the fireproof treatment is observed, despite the changes in chemical composition.

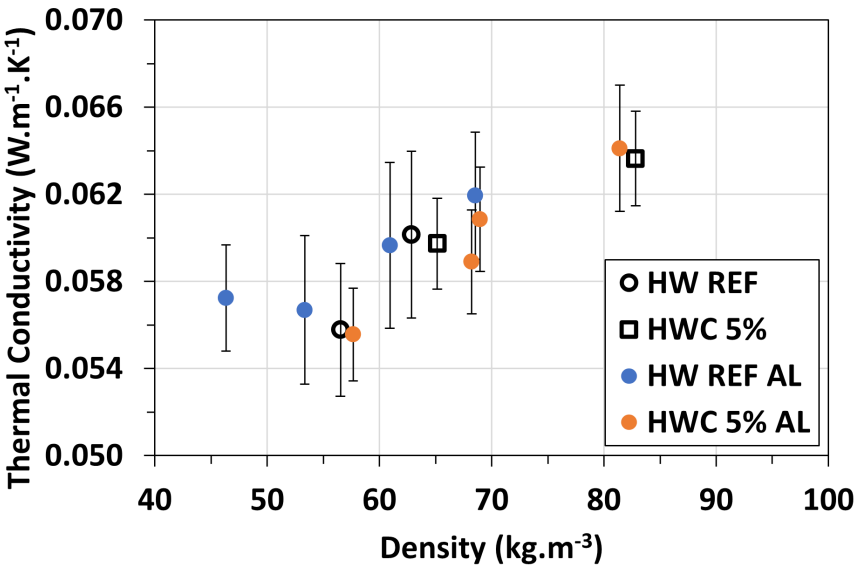

Figure 5.22: Thermal conductivity of airlay hemp wools

Thermal conductivity of airlay samples was also assessed by the guarded hot plate test, using panels with dimensions of 30x30x4 cm^3. Differently from the hot disc test, this method relies on the steady-state heat flux regime. Also, for this test, the samples had their water content reduced in an oven (Section 2.5.2). A small compression was applied on the panels, reducing the thickness to 35 mm, in order to ensure the contact of the whole panel with the equipment's plates. Due to time limitations, only one sample of each condition was tested.

Both HW REF AL samples, with lower and higher densities, presented thermal conductivity values of 0.039 $W.m^{-1}.K^{-1}$, slightly higher than the HW REF prototype sample, that had 0.036 $W.m^{-1}.K^{-1}$. The HWC 5% AL samples presented a thermal conductivity of 0.038 $W.m^{-1}.K^{-1}$, independently of the apparent density of the samples. In this test, the thermal conductivity of hemp wools did not change significantly with the flame retardant treatment, even after the increase in apparent density. Testing with more samples is required to draw conclusions.

5.5.2 Thermal diffusivity and specific heat

The thermal diffusivity results and specific heat of airlay hemp wools are presented in Figure 5.23. Regarding the thermal diffusivity results, the HW REF AL presented values ranging 0.53 and 0.70 $mm^2.s^{-1}$, and a slightly tendency to decrease as density increases.

The thermal diffusivity of the HWC 5% AL samples had almost the same range of values from their references, and no evident behavior is observed as density changes. The comparison with the hemp wool prototypes also did not provide any further information.

For the specific heat, the treatment appears to reduce this parameter, since the references presented values around 1.7-1.8 kJ.kg^{-1}.K^{-1} and the treated samples around 1.4-1.6 kJ.kg^{-1}.K^{-1}. The same range of values were observed in the prototypes, showed in Section 4.2.2. No specific influence of the apparent density is observed. Also, no difference is observed in the specific heat in the samples produced by the airlay method or the prototypes.

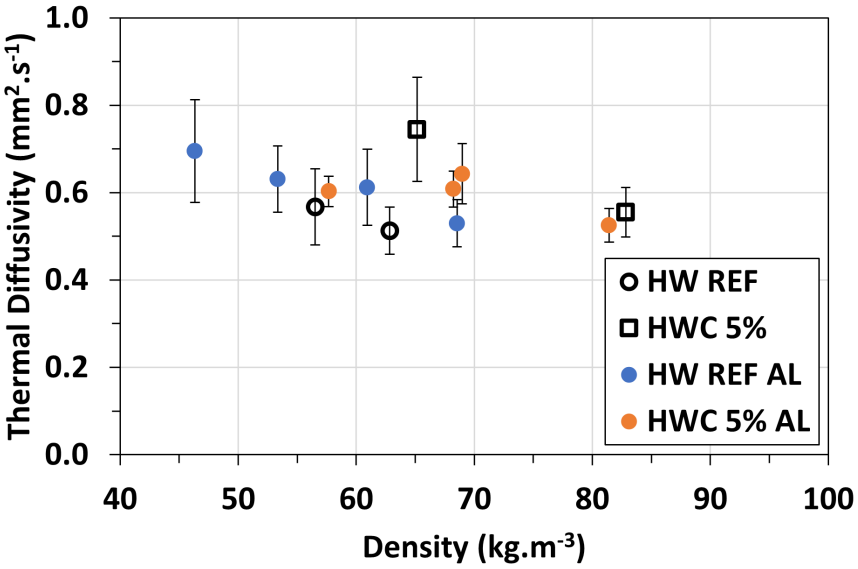

(a)

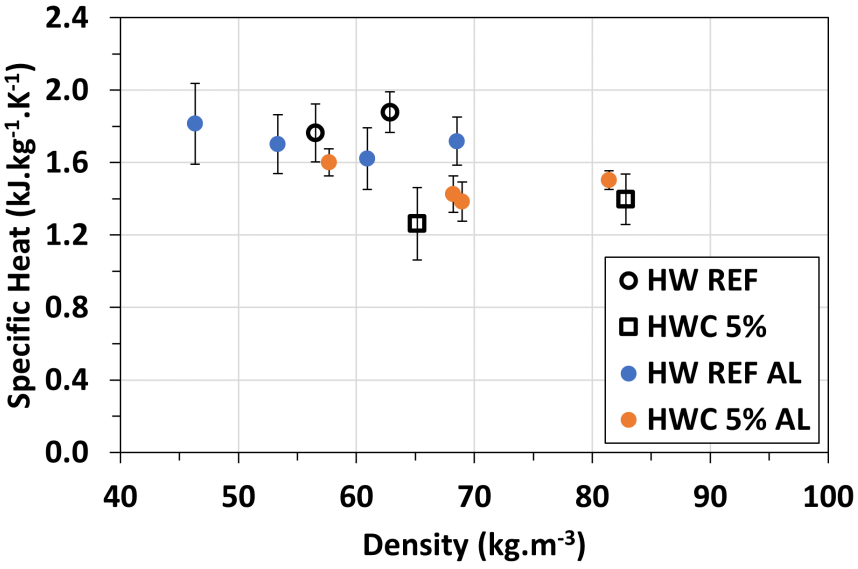

(b)

Figure 5.23: Thermal properties of airlay hemp wool panels: (a) Thermal diffusivity; (b) Specific heat

Overall, the same conclusions made for the hemp wool prototypes were observed for the airlay samples. The thermal conductivity has a direct relationship with the apparent density, when above 60 kg.m^{-3}. Below that, the effects of radiation becomes more significant and affects the effective thermal conductivity of the panels. The measurements

performed with a steady-state heat flux equipment, obtained similar values of thermal conductivity as other hemp wools and other insulation materials that are found in the market. No influence of the treatment nor apparent density was observed on the thermal diffusivity. In contrast, the specific heat of the hemp wools slightly decreases when they are treated.

5.6 Fungal development of fireproof treated hemp wool airlay panels

The functional performances of the airlay hemp wools have been assessed. Then, the last Section of this Chapter covers the sensibility of this material for the development of fungi. Given the results obtained for hemp fibers, presented in Chapter 3 and hemp wool prototypes presented in Chapter 4, it was observed that the treatment does not promote fungal growth, but may instead contribute to the fungi growth inhibition.

To support these results, the fungal growth in airlay hemp wools was assessed directly by exposing the material to a strong contamination condition, which is the impregnation test described in Section 2.6.3. This test evaluated fungal development under the condition of a contamination of mold and does not represent the normal conditions that hemp wools would be exposed to as building insulation. In the wet method, *Penicillium spp.* and *Stachybotrys chartarum* were used to impregnated the airlay samples and in the dry method, only *Penicillium spp.* was used.

As shown in Section 4.4.2, the wet and dry methods of fungi impregnation were verified in Petri dishes filled with a culture medium. It indicated that the wet method led to Petri dishes fully covered by the molds, indicating strong contamination. The dry method was also contaminated but with only a few colonies, representing a lighter attack.

The aspect of sample HW REF AL before and after 7, 14, 21 and 28 days of incubation is presented in Figure 5.24. Even after incubation, no fungal growth was visible. The same occurred in the HWC 5% AL samples.

Then, fungal identification (Section 2.6.2) was performed to verify and identify the presence of fungi after 28 days of incubation. In the reference airlay sample, colonies of *Penicillium spp.* were found when the impregnation was done with the wet method, but no colonies of *Stachybotrys chartarum* neither *Penicillium spp.* with the dry method were not found. For the treated airlay sample, the presence of a single colony of *Penicillium spp.* was observed on the wet method. The other conditions did not present colonies formed.

These results indicated that the fungi *Stachybotrys chartarum* did not find optimal conditions to survive, be it temperature, humidity or substrate, since no colonies were found in the hemp wool panels presented in this Section or in Section 4.4.

Moreover, *Penicillium spp.* was only found when the impregnation was done with the wet method and its presence was observed in the reference with a few colonies being identified and in the treated hemp wool sample with a single colony. In Section 4.4.2, the treated samples did not present any single colonies after incubation, which was linked to phytic acid inhibiting the growth of fungi, as seen in the literature review. In the airlay samples, one single colony was found, indicating that the treatment may help control the development of *Penicillium spp.*, yet this specie might still find conditions to survive.

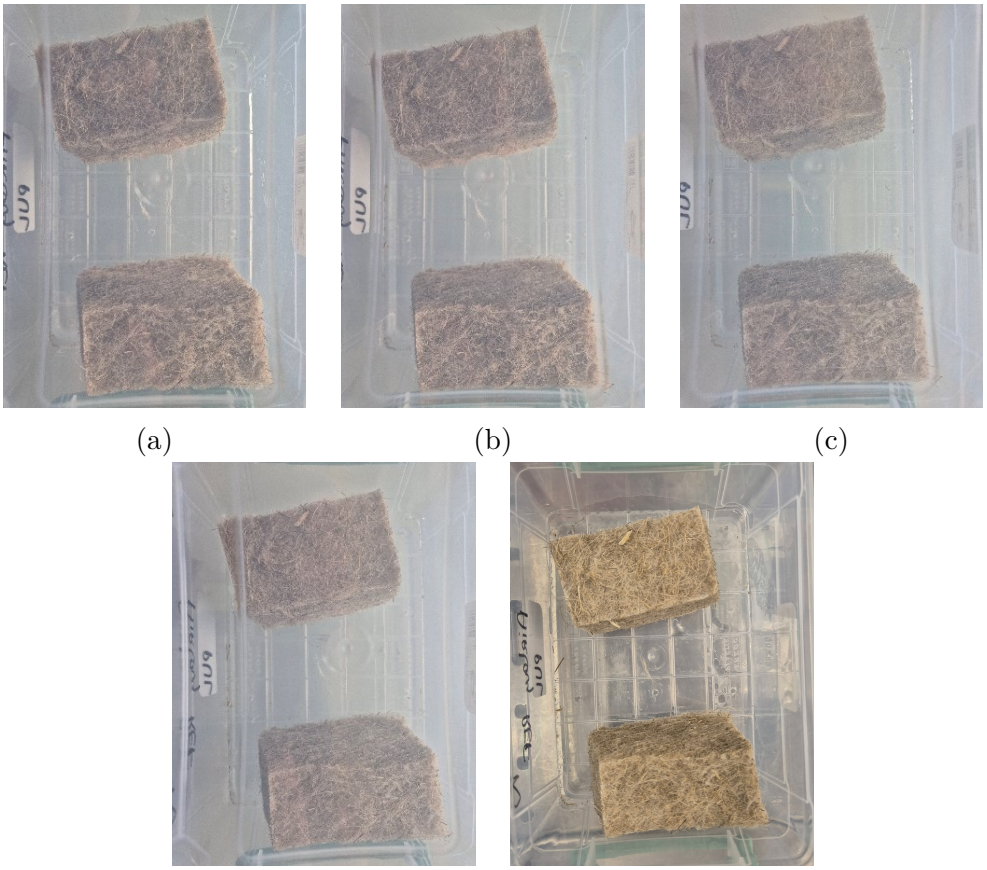

(a) (b) (c)

(d) (e)

Figure 5.24: Monitoring of HW REF AL sample during incubation after impregnation: (a) Before incubation; (b) 7 days of incubation; (c) 14 days; (d) 21 days; (e) 28 days (without the cover)

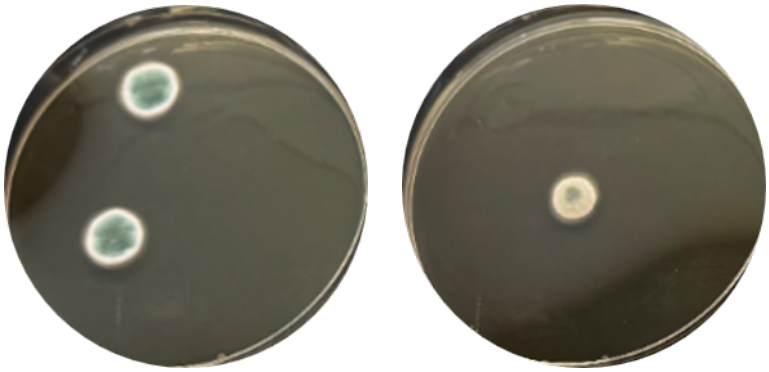

(a) (b)

Figure 5.25: Presence of *Penicillium spp.*: (a) HW REF AL sample with the wet method; (b) HWC 5% AL sample with the wet method

5.7 Conclusion

This Chapter covered the development, the treatment and the assessment of the fire reaction, acoustic and thermal performances and the sensibility to fungal development of hemp wools produced in an industrial-scale using an airlay method.

Based on the conclusions from Chapters 3 and 4, a fireproof treated hemp wool was produced using the thermo-bonding and airlay production processes, with the treatment

consisting of the pulverization of a solution of 5% phytic acid and 15% urea in all fibers, before panel production. For a fair comparison of its flammability, functional properties and biological durability, a reference panel was produced with the same production conditions, without the treatment.

For each condition, panels with two different apparent densities were produced. The treated samples presented higher apparent densities, similarly to the observations made for hemp fibers and hemp wool prototypes, which are associated with the changes in chemical composition of the fibers constituents.

The treated airlay sample has shown a phosphorus content of about 0.5%, lower than the amount of 0.8% from the same formulation in prototype, which can be explained by the different procedures applied during the panels production. For the prototypes, the fibers were distributed in the panels manually, whereas for the airlay method, the fibers have to pass through multiple machines. The friction between the equipments and the fibers could have removed some part of the phosphorus that was not grafted onto the cellulose and hemicellulose. Furthermore, the prototypes passed three times through the oven, and the airlay samples passed only twice, which reduced the grafting time for the formation of covalent bonds between the phosphorus and the hemp fibers.

Even with only 0.5% of phosphorus content, a significant improvement in the fire reaction of HWC 5% AL samples was observed. When compared to the reference, the cone calorimeter indicated a reduction of 27-37% in pHRR and 43-50% in THR, depending on the sample's density. It was also observed that denser samples had a slower kinetics of degradation and a longer burning duration. The higher density contributed to the formation of a denser char.

In the single-flame source test, the burned height and the time for the flame to extinguish were significantly reduced in the treated hemp wool sample. Regarding smoke production, the treated samples produced smoke at a higher rate in the first 75s of testing, when compared to reference samples. This behavior is associated with the early thermal degradation effect caused by the catalysis of the cellulose dehydration reaction. Then, the rate of smoke production quickly decreases, and after two minutes of testing the visibility becomes better than the reference sample, due to the char formed reducing the combustion reaction.

In terms of acoustic performance, it was observed that the samples produced in the same conditions (with the same target apparent density) led to similar sound absorption curves, regardless of whether the samples were treated or not. This indicates that the treatment did not cause any negative change in the sound absorption capacity of the hemp wools, in contrast to what was observed in the prototypes.

The evaluation of the characteristic parameters of the pore geometry allowed a deeper understanding of the influence of the treatment on the acoustic performance of the hemp wools. Significant changes were observed in the porosity, airflow resistivity and in the characteristic viscous and thermal lengths.

Due to the increase in apparent density, the porosity reduced slightly with the treatment application. However, all samples can still be considered highly porous (94% to 96%). The airflow resistivity of the treated airlay samples were higher than the reference, which was the opposite effect to that observed in the prototypes. Two reasons were attributed to this result. The first one is the fibers orientation. Since the airlay production forms panels through the stack of fiber layers homogeneously distributed on top of each other, an anisotropic material is created. The manual fabrication of the prototypes might have induced a particular orientation of the fibers, which can affect their airflow resistivity. Another reason is that the manual handling of the fibers during prototype production might have caused the clumping of some fibers. In the airlay production this is avoided, and a better dispersion of the fibers is promoted.

The thermal and viscous lengths presented a tendency to be reduced as the density increases, since higher amount of fibers occupying the same volume leads to the reduction of the space between and inside the pores. These properties also presented a slight tendency to reduce with the application of the treatment, which might be associated with the presence of flame retardant particles over the fibers.

Thermal conductivity results demonstrated a clear influence of the apparent density when above 60 $kg.m^{-3}$. Below that, the influence of the radiation effect becomes more significant, and affects the effective thermal conductivity of the hemp wools. No direct influence of the flame retardants was observed in the thermal conductivity, but rather an indirectly effect associated with the increase of apparent density when the hemp wools are treated. The guarded hot plate results, commonly used by the industry to characterize their isolation panels, presented similar values of thermal conductivity to the prototypes, and other hemp wools and insulation materials available in the market.

Finally, the sensibility to fungal development was assessed with the impregnation of *Penicillium spp.* (wet and dry methods) and *Stachybotrys chartarum* (wet method). Fungi colonies of *Penicillium spp.* were found in the reference and treated airlay samples impregnated with the wet method. In Chapter 4, no fungi colonies were observed in the treated samples, indicating that phytic acid could be inhibiting fungal growth, as observed by previous studies as well. In the airlay treated samples, one single colony was found, which reinforces the need of further testing to verify the antifungal effect of phytic acid. However, considering the results with the airlay samples and the prototype samples, even with a strong contamination of fungi and an incubation in optimal conditions of humidity and temperature, no fungi was visible in the hemp wool samples.

Conclusion and Perspectives

General conclusion

Vegetal wools are materials developed for building insulation, due to their multifunctional properties, such as acoustic absorption capacity, thermal insulation and a hygroscopic nature. Moreover, they are bio-based materials with low environmental impacts, since they are mainly composed of vegetal fibers, a renewable source with carbon sequestration and storage properties. Therefore, thanks to these multiple benefits, vegetal wools are more than an alternative to traditional building insulation materials originated from mineral and petroleum sources.

As a plant-derived bio-based material, vegetal wools face a major challenge: their inherent flammability, which limits their use in wall systems. This thesis proposes an innovative approach for developing bio-based insulating materials by designing flame-retardant hemp wool panels treated with a flame retardant that is itself bio-based, and applicable, as far as possible, to an industrial scale. The aim was to provide an environmentally compatible solution that enhances fire resistance while maintaining the bio-based nature of the material. Furthermore, the study evaluated the effects of the flame-retardant treatment on the acoustic and thermal performances, as well as on the susceptibility to fungal growth, in order to ensure the preservation of the material's multifunctional properties and biological durability. To achieve these objectives, the research was structured in three main stages dedicated to the development and assessment of the treated hemp wool panels.

The work began at the raw material scale, through the study of hemp fibers, the material that comprises about 90% of hemp wools' mass. The hemp is a plant with fast growth, widely available, that requires little water and is resistant to droughts and pests. In this step, the flame retardants were defined based on the literature review, composed of phytic acid, a bio-based source of phosphorus molecules, and urea, an accessible source of nitrogen. Together, these components have a synergetic effect and can form an intumescent flame retardant systems to reduce the flammability of the hemp fibers, while respecting the nature of the material. With the flame-retardants chosen, it was important to define how to apply them, considering a large-scale application as an insulation material. Two methods were identified and tested: by immersion and pulverization. The first one was the more frequently used in previous studies, but required more steps involving pre-treatments and drying, that the pulverization did not need. However, less information about the pulverization was available, and questions about the efficacy of the method and its homogeneity raised.

With fire reaction tests, both methods proved the efficacy of the flame-retardants chosen, by successfully grafting phosphorus molecules on hemp fibers and significantly reducing their flammability. On the acoustics side, a reduction in the sound absorption performance of hemp fiber stacks was observed. This result was associated with the modification of the fibers microstructure, such as their radius. No direct influence of the treatment was observed on the thermal properties, but rather indirectly through the

increase of the apparent density of the treated hemp fibers.

The definition of the application method came down to the procedure itself, where significant differences were observed between them. The pulverization method delivered a homogeneous treatment using a tenth of the amount of flame retardants needed in the immersion method, and avoiding the need of drying steps. Therefore, considering an industrial application, the pulverization method was selected.

After that, the treatment needed to be optimized for hemp wools. So, at this point, the study passed to the next scale, which consisted of hemp wool prototypes. These prototypes were produced with 90% of hemp fibers and 10% of thermoplastic fibers, with a simplified method of hemp wool production that consisted of opening and mixing the fibers, panels preparation by placing the fibers manually in molds, heating in oven at 140°C and sample cutting. This simplified method allowed the assessment of multiple fireproof treatment conditions, including variation of flame retardants concentration and two possible application methods: the treatment could be either done in all fibers, before the panels preparation (HWC samples), or after it, by only treating the surface of the panels (HWS samples).

The main difference between both methods was observed in their phosphorus content and how it was distributed in the material. In HWC samples, this phosphorus was homogeneously distributed, which led to higher average phosphorus content and a significant increase in apparent density. HWS samples, in contrast, presented phosphorus molecules grafted only at their surface, showing lower average phosphorus content than HWC samples and an apparent density similar to the reference hemp wools. This difference influenced the fire reaction of the hemp wools, where HWC samples presented a significantly lower flammability, than the reference and HWS samples.

Both methods reduced the sound absorption capacity of the hemp wool prototypes, and this reduction was more important on samples with higher phosphorus content. An investigation carried out on the characteristic parameters of the pore geometry of each sample identified a tendency to reduce the porosity and airflow resistivity of the treated samples. Through a homogenization model using a micro-macro approach, an increase in the estimated fiber radius of the HWC samples, which contain a higher phosphorus content, was observed.

Regarding thermal properties, a linear increase in thermal conductivity is observed with an increase in the apparent density of the samples, if it is above 70 $kg.m^{-3}$. Below that, the effects of radiation become more significant and affect the effective thermal conductivity of the hemp wools. Using a stationary regime testing method, the effective thermal conductivity of all hemp wool panels was similar to other hemp wools and insulation materials available on the market.

These results showed that different treatment methods led to different impacts on the physico-chemical and functional properties of the hemp wools. Taking into consideration the flammability aspects, and the quantity of materials used for treatment, the treatment condition of HWC 5% was considered the optimal method for producing flame retardant hemp wools.

To confirm the feasibility of this treatment method in industrial scale, it needed to be validated by producing and treating hemp wool panels using a production method that is used by vegetal wool manufactures. This was performed by fabricating hemp wool panels using the airlay method, and the treatment condition selected. Also, two distinct apparent densities were produced for each treatment condition.

The apparent density of the treated hemp wools increased with the treatment application as observed for the prototypes, and a lower phosphorus content was obtained. This was associated lower grafting time, due to reduced passages through the oven during

panels production, and friction between the fibers and the equipments.

Even with reduced phosphorous content grafted, a significant improvement in the fire reaction parameters of the hemp wool was observed, such as a reduction between 27-38% of pHRR and 43-50% of THR, when comparing treated and untreated hemp wools. The reduction of the burning time while submitted to an intense heat flux, and the reduction of the mass loss rate showed the importance of the char layer in extinguishing the fire and protecting the inner layers of the panels.

Some positive effects of the production by the airlay method were observed in the acoustic results. The sound absorption performance did not change in the treated sample, in contrast to the results observed in the prototypes, even with the reduction of the treated airlay hemp wools porosity. Associated with this, a tendency to increase airflow resistivity was observed, which is possibly related to an improved random fiber distribution and the anisotropic fiber orientation resulted from the airlay production.

In the thermal properties, no particular influence of the production method neither of the treatment was observed. The apparent density appears to be the main property that dictates the effective thermal conductivity results.

Moreover, as the treatment relied on phosphorus- and nitrogen-based compounds, particular attention was given to the potential impact on fungal susceptibility. The fungal species naturally present in hemp fibers and wools were identified, and their growth was examined both under favorable conditions and under conditions of intentional contamination. Interestingly, the results revealed that the treatment—particularly the use of phytic acid—appears to inhibit fungal growth. This finding highlights a potentially dual functionality of phytic acid, acting not only as a flame retardant but also as an antifungal agent, thereby reinforcing the innovative and multifunctional character of the proposed bio-based treatment.

To conclude, this thesis developed flame-retardant hemp wool panels through a treatment process optimized for large-scale implementation. This innovative approach expands the potential applications of hemp-based insulation materials and contributes to the sustainable advancement of building technologies by offering a viable, bio-based alternative to conventional insulation products.

Perspectives

Although this work provided significant results for the development of flame-retardant hemp wool panels and advanced scientific understanding of the relationships between fire-retardant treatment, physico-chemical properties, acoustic and thermal performance, and fungal susceptibility, new questions and challenges have emerged.

Fireproof treatment of lignocellulosic fibers

The treatment applied in this thesis was initially defined based on the literature on vegetal fibers. However, further optimization could be pursued, particularly by evaluating the potential benefits of incorporating urea. Phytic acid served as the primary flame retardant in this study, and considering the feasibility of industrial-scale production, the role of urea requires further investigation. Although some studies have addressed this topic, additional research exploring different proportions of flame retardants and variations in bio-based raw materials could significantly enhance current knowledge.

The method for applying the flame-retardant solution was developed throughout this thesis, from raw fibers to prototypes and airlay wools. Notably, a substantial difference in phosphorus content, and consequently in treatment efficiency, was observed between

prototypes and airlay samples, suggesting that the application process in airlay production has room for improvement.

In prototype samples treated only on the surface (HWS samples), it was observed that heat could penetrate the sides and ignite the interior. It would be valuable to assess whether this behavior persists in larger samples. Moreover, surface treatment may be sufficient for thinner samples, depending on the penetration depth of the treatment. Investigating these scenarios would provide a more comprehensive understanding of the treatment's potential, which was beyond the scope of this thesis.

It is also important to consider the phenomenon of smoldering fire when producing insulation panels for buildings. This phenomenon has not yet been extensively studied with bio-based materials, and could be investigated in untreated and treated vegetal wools.

Finally, the fire behavior results obtained in this study offered significant insights into the performance of treated and untreated hemp wools. However, the tests employed did not allow classification according to the Euroclass system. Conducting standardized Euroclass tests on hemp wool airlay panels would be an important step toward promoting their production and use as a sustainable alternative to conventional insulation materials.

Characteristics and performances of vegetal wools

It was demonstrated that the treatment formulation, application methods, and the production process of vegetal wools can significantly influence their physico-chemical properties and functional performances. Several key factors warrant further investigation to complement the findings of this thesis.

First, fiber orientation plays a crucial role in the functional performance of vegetal wools. Future work could include a comparative analysis of fiber distribution between prototypes and airlaid samples. In addition, imaging techniques could be employed to assess changes in fiber diameter following treatment and to validate the results predicted by homogenization models.

Given that the performance of vegetal wools depends on multiple interrelated factors, a multi-criteria optimization strategy could be implemented, linking their microstructure to macro-scale properties. For acoustic performance, a meta-material approach could be explored to further optimize the sound absorption capabilities of vegetal wools.

Phytic acid potential as flame-retardant and antifungal product

In this work, the assessment of fungal growth in hemp fibers and wools indicated that the treatment may inhibit fungal development. This effect has been reported in recent studies and is attributed to the use of phytic acid. Further investigation using other bio-based materials and different fungal species would help to better understand the potential of phytic acid as a dual-function agent, acting not only as a flame retardant but also as an antifungal substance.

Generalization to other vegetal fibers

Hemp fibers were selected for this study due to their favorable cultivation characteristics and wide availability in Europe. However, this approach could be extended to other types of biomass that may be more relevant to different countries and regions. Given the diversity of lignocellulosic fibers, vegetal wools with a range of properties could potentially be developed. In the existing literature, the variety of vegetal wools studied remains

limited, and research on flame-retardant treated vegetal wools is even scarcer, highlighting significant opportunities for innovation.

Building scale validation

The development of flame-retardant vegetal wool panels in this thesis spanned from raw material selection to panel production. The next stage in the life cycle of these panels is their application in buildings. Validating the results obtained in this thesis through building-scale testing and monitoring would enable the assessment of their real-world performance, confirming their effectiveness as sustainable and high-performance insulation materials.

Life cycle assessment of fireproof treated hemp wools

One of the main advantages of using vegetal wools lies in their environmental benefits, inherited from their bio-based nature, carbon sequestration and storage capabilities, and renewability. For flame-retardant hemp wools, it is essential that the applied fireproof treatment aligns with environmental sustainability principles, ensuring that the additives do not compromise the material's bio-based character or recyclability. Consequently, conducting a life cycle assessment of the fire-retardant treated hemp wools is crucial to quantify the environmental impact of the treatment and to identify key areas for improvement during both the treatment and panel production processes.

Bibliography

Abot, A. (2010, November). *Caractérisation des fibres longues de chanvre (Cannabis sativa) en vue de leurs utilisations dans des matériaux composites.*

AFNOR, A. F. d. N. (2018a, December). *NF EN 13501-1 - Fire classification of construction products and building elements — Part 1 : Classification using data from reaction to fire tests.*

AFNOR, A. F. d. N. (2018b, December). *NF EN 9053-1 - Acoustique — Détermination de la résistance à l'écoulement de l'air — Partie 1: Méthode statique.*

AFNOR, A. F. d. N. (2022, July). *NF EN 13823 - Reaction to fire tests for building products — Building products excluding floorings exposed to the thermal attack by a single burning item.*

AFNOR, A. F. d. N. (2023, October). *NF EN 10534-2 - Détermination du facteur d'absorption acoustique et de l'impédance des tubes d'impédance Partie 2 : Méthode de la fonction de transfert.*

Allard, J.-F., & Daigle, G. (1994). *Propagation of Sound in Porous Media: Modeling Sound Absorbing Materials. The Journal of the Acoustical Society of America*, *95*(5), 2785–2785. https://doi.org/10.1121/1.409801

Amziane, S., & Collet, F. (Eds.). (2017). *Bio-aggregates Based Building Materials: State-of-the-Art Report of the RILEM Technical Committee 236-BBM* (Vol. 23). Springer Netherlands. https://doi.org/10.1007/978-94-024-1031-0

Antoun, K., Ayadi, M., El Hage, R., Nakhl, M., Sonnier, R., Gardiennet, C., Le Moigne, N., Besserer, A., & Brosse, N. (2022). Renewable phosphorous-based flame retardant for lignocellulosic fibers. *Industrial Crops and Products*, *186*, 115265. https://doi.org/10.1016/j.indcrop.2022.115265

ASTM. (2022). *ASTM D2843 - Standard Test Method for Density of Smoke from the Burning or Decomposition of Plastics.*

Ayadi, M. (2023, December). *Elaboration et caractérisation d'isolants thermiques et acoustiques à base de fibres biosourcées.*

Ayadi, M., Segovia, C., Baffoun, A., Zouari, R., Fierro, V., Celzard, A., Msahli, S., & Brosse, N. (2023). Influence of Anatomy, Microstructure, and Composition of Natural Fibers on the Performance of Thermal Insulation Panels. *ACS Omega*, *8*(51), 48673–48688. https://doi.org/10.1021/acsomega.3c02481

Bankvall, C. (1973). Heat Transfer in Fibrous Materials. *Journal of Testing and Evaluation*, *1*(3), 235–243. https://doi.org/10.1520/JTE10010J

Bautista, M., De Ilarduya, A., Alla, A., & Muñoz-Guerra, S. (2015). Poly(butylene succinate) Ionomers with Enhanced Hydrodegradability. *Polymers*, *7*(7), 1232–1247. https://doi.org/10.3390/polym7071232

Bensoussan, A. (1978). Asymptotic analysis for periodic structures. *North-Holland Publishing Company*, *5*.

Berzin, F., & Vergnes, B. (2021). Thermoplastic natural fiber based composites. In *Fiber Reinforced Composites* (pp. 113–139). Elsevier. https://doi.org/10.1016/B978-0-12-821090-1.00015-6

Biot, M. A. (1956a). Theory of Propagation of Elastic Waves in a Fluid-Saturated Porous Solid. I. Low-Frequency Range. *The Journal of the Acoustical Society of America*, *28*(2), 168–178. https://doi.org/10.1121/1.1908239

Biot, M. A. (1956b). Theory of Propagation of Elastic Waves in a Fluid-Saturated Porous Solid. II. Higher Frequency Range. *The Journal of the Acoustical Society of America*, *28*(2), 179–191. https://doi.org/10.1121/1.1908241

Branciforti, M. C., Marinelli, A. L., Kobayashi, M., Ambrosio, J. D., Monteiro, M. R., & Nobre, A. D. (2009). Wood Polymer Composites Technology Supporting the Recovery and Protection of Tropical Forests: The Amazonian Phoenix Project. *Sustainability*, *1*(4), 1431–1443. https://doi.org/10.3390/su1041431

Bruneau, M. (2006). *Fundamentals of acoustics*. ISTE Ltd.
OCLC: ocm68711955.

Campolina, B., Dauchez, N., Atalla, N., & Doutres, O. (2012). Effect of porous material compression on the sound transmission of a covered single leaf panel. *Applied Acoustics*, *73*(8), 791–797. https://doi.org/10.1016/j.apacoust.2012.02.013

Castagnède, B., Aknine, A., Brouard, B., & Tarnow, V. (2000). Effects of compression on the sound absorption of fibrous materials. *Applied Acoustics*, *61*(2), 173–182. https://doi.org/10.1016/S0003-682X(00)00003-7

Castagnède, B., Moussatov, A., & Tarnow, V. (2001). Parametric study of the influence of compression on the acoustical anisotropy of automotive felts. *Comptes Rendus de l'Académie des Sciences - Series IIB - Mechanics*, *329*(4), 295–301. https://doi.org/10.1016/S1620-7742(01)01322-8

Cérezo, V. (2005). *Propriétés mécaniques, thermiques et acoustiques d'un matériau à base de particules végétales : approche expérimentale et modélisation théorique*.

Chabriac, P., Gourdon, E., Gle, P., Fabbri, A., & Lenormand, H. (2016). Agricultural by-products for building insulation: Acoustical characterization and modeling to predict micro-structural parameters. *Construction and Building Materials*, *112*, 158–167. https://doi.org/10.1016/j.conbuildmat.2016.02.162

Champoux, Y., & Allard, J.-F. (1991). Dynamic tortuosity and bulk modulus in air-saturated porous media. *Journal of Applied Physics*, *70*(4), 1975–1979. https://doi.org/10.1063/1.349482

Chapple, S., & Anandjiwala, R. (2010). Flammability of Natural Fiber-reinforced Composites and Strategies for Fire Retardancy: A Review. *Journal of Thermoplastic Composite Materials*, *23*(6), 871–893. https://doi.org/10.1177/0892705709356338

Chaudhry, A., Mabrouk, A., & Abdala, A. (2020). Thermally enhanced pristine polyolefins: Fundamentals, progress and prospective. *Journal of Materials Research and Technology*, *9*(5), 10796–10806. https://doi.org/10.1016/j.jmrt.2020.07.101

Cheng, K., Winter, W. T., & Stipanovic, A. J. (2012). A modulated-TGA approach to the kinetics of lignocellulosic biomass pyrolysis/combustion. *Polymer Degradation and Stability*, *97*(9), 1606–1615. https://doi.org/10.1016/j.polymdegradstab.2012.06.027

Cheng, X.-W., Guan, J.-P., Tang, R.-C., & Liu, K.-Q. (2016). Phytic acid as a bio-based phosphorus flame retardant for poly(lactic acid) nonwoven fabric. *Journal of Cleaner Production*, *124*, 114–119. https://doi.org/10.1016/j.jclepro.2016.02.113

Collet, F., Achchaq, F., Djellab, K., Marmoret, L., & Beji, H. (2011). Water vapor properties of two hemp wools manufactured with different treatments. *Construction and Building Materials*, *25*(2), 1079–1085. https://doi.org/10.1016/j.conbuildmat.2010.06.069

Colson, V., Bourebrab, M., Dalmais, M., Jadeau, O., & Lanos, C. (2019). Formulation of novel fire retardant additives for biobased insulation material. *37*.

Costes, L., Laoutid, F., Brohez, S., & Dubois, P. (2017). Bio-based flame retardants: When nature meets fire protection. *Materials Science and Engineering: R: Reports*, *117*, 1–25. https://doi.org/10.1016/j.mser.2017.04.001

Danihelová, A., Sčensný, P., Gergeľ, T., Ondrejka, V., Němec, M., Igaz, R., Štefko, J., & Mitterová, I. (2021). Influence of Flame Retardant Impregnation on Acoustic and Thermophysical Properties of Recycled Technical Textiles with the Potential for Use in Wooden Buildings. *Polymers*, *13*(16), 2598. https://doi.org/10.3390/polym13162598

Deacon, J. W., & Deacon, J. W. (2006). *Fungal biology* (4th ed). Blackwell Pub.

Deborde, L. (2025). *L'isolation thermique biosourcée, de la formulation au démonstrateur : performances hygrothermiques, comportement ignifuge et résistance fongique*.

Deborde, L., Sonnier, R., Dumazert, L., Lanos, C., & Colson, V. (2023). Characterization of hemp fiber fire reaction. *Journal of Vinyl and Additive Technology*, vnl.21978. https://doi.org/10.1002/vnl.21978

Deissler, R. G. (1964). Diffusion approximation for thermal radiation in gases with jump boundary condition. *Journal of Heat Transfer*, *86*(2), 240–245.

Delannoy, G. (2018). *Durabilité d'isolants à base de granulats végétaux*.

Deshmukh, G. S. (2022). Advancement in hemp fibre polymer composites: A comprehensive review. *Journal of Polymer Engineering*, *42*(7), 575–598. https://doi.org/10.1515/polyeng-2022-0033

Dorez, G., Ferry, L., Sonnier, R., Taguet, A., & Lopez-Cuesta, J.-M. (2014). Effect of cellulose, hemicellulose and lignin contents on pyrolysis and combustion of natural fibers. *Journal of Analytical and Applied Pyrolysis*, *107*, 323–331. https://doi.org/10.1016/j.jaap.2014.03.017

Dorez, G., Taguet, A., Ferry, L., & Lopez Cuesta, J.-M. (2014). Phosphorous compounds as flame retardants for polybutylene succinate/flax biocomposite: Additive versus reactive route. *Polymer Degradation and Stability*, *102*, 152–159. https://doi.org/10.1016/j.polymdegradstab.2014.01.018

El-Sawalhi, R., Lux, J., & Salagnac, P. (2016). Estimation of the thermal conductivity of hemp based insulation material from 3D tomographic images. *Heat and Mass Transfer*, *52*(8), 1559–1569. https://doi.org/10.1007/s00231-015-1674-4

European Environment Agency. (2020). *Environmental noise in Europe, 2020*. Publications Office. Retrieved August 3, 2023, from https://data.europa.eu/doi/10.2800/686249

Farah, S., Anderson, D. G., & Langer, R. (2016). Physical and mechanical properties of PLA, and their functions in widespread applications — A comprehensive review. *Advanced Drug Delivery Reviews*, *107*, 367–392. https://doi.org/10.1016/j.addr.2016.06.012

Fatima, S., & Mohanty, A. (2011). Acoustical and fire-retardant properties of jute composite materials. *Applied Acoustics*, *72*(2–3), 108–114. https://doi.org/10.1016/j.apacoust.2010.10.005

Freivalde, L., & Kukle, S. (2012). Content of Hemp Fibres and Properties of Nonwovens. *Material Science. Textile and Clothing Technology*, *7*, 84–89.

Freivalde, L., Kukle, S., & Strazds, G. (2011). Hemp Fibres for Nonwoven Insulation Materials. *Material Science. Textile and Clothing Technology*, *6*, 36–41.

Freivalde, L., Kukle, S., Andžs, M., Bukšāns, E., & Grāvītis, J. (2014). Flammability of raw insulation materials made of hemp. *Composites Part B: Engineering*, *67*, 510–514. https://doi.org/10.1016/j.compositesb.2014.08.007

Füchsl, S., Rheude, F., & Röder, H. (2022). Life cycle assessment (LCA) of thermal insulation materials: A critical review. *Cleaner Materials*, *5*, 100119. https://doi.org/10.1016/j.clema.2022.100119

Gaan, S., & Sun, G. (2007a). Effect of phosphorus and nitrogen on flame retardant cellulose: A study of phosphorus compounds. *Journal of Analytical and Applied Pyrolysis*, *78*(2), 371–377. https://doi.org/10.1016/j.jaap.2006.09.010

Gaan, S., & Sun, G. (2007b). Effect of phosphorus flame retardants on thermo-oxidative decomposition of cotton. *Polymer Degradation and Stability*, *92*(6), 968–974. https://doi.org/10.1016/j.polymdegradstab.2007.03.009

Galimshina, A., Moustapha, M., Hollberg, A., Padey, P., Lasvaux, S., Sudret, B., & Habert, G. (2022). Bio-based materials as a robust solution for building renovation: A case study. *Applied Energy*, *316*, 119102. https://doi.org/10.1016/j.apenergy.2022.119102

Glé, P. (2013). *Acoustique des Matériaux du Bâtiment à base de Fibres et Particules Végétales - Outils de Caractérisation, Modélisation et Optimisation*.

Goué, E. L. (2019). *Utilisation de composés biosourcés pour la conception de papiers à haute résistance à l'eau et à propriétés antifongiques*.

Grant, C., Hunter, C., Flannigan, B., & Bravery, A. (1989). The moisture requirements of moulds isolated from domestic dwellings. *International Biodeterioration*, *25*(4), 259–284. https://doi.org/10.1016/0265-3036(89)90002-X

Grazieschi, G., Asdrubali, F., & Thomas, G. (2021). Embodied energy and carbon of building insulating materials: A critical review. *Cleaner Environmental Systems*, *2*, 100032. https://doi.org/10.1016/j.cesys.2021.100032

Gulhane, S., Turukmane, R., Mahajan, C., & Joshi, M. (2018). Hydroentangling process and properties of spunlace nonwovens. *Chemical Fibers International*, *68*, 190–192.

Hajj, R., El Hage, R., Sonnier, R., Otazaghine, B., Gallard, B., Rouif, S., Nakhl, M., & Lopez-Cuesta, J.-M. (2018). Grafting of phosphorus flame retardants on flax fabrics: Comparison between two routes. *Polymer Degradation and Stability*, *147*, 25–34. https://doi.org/10.1016/j.polymdegradstab.2017.11.006

Hajj, R., El Hage, R., Sonnier, R., Otazaghine, B., Rouif, S., Nakhl, M., & Lopez-Cuesta, J.-M. (2020). Influence of lignocellulosic substrate and phosphorus flame retardant type on grafting yield and flame retardancy. *Reactive and Functional Polymers*, *153*, 104612. https://doi.org/10.1016/j.reactfunctpolym.2020.104612

Hempitecture. (2025). Hempitecture - hemp wool data sheet. hempitecture.com

Hou, X., Amais, R. S., Jones, B. T., & Donati, G. L. (2016). Inductively Coupled Plasma Optical Emission Spectrometry. *Encyclopedia of Analytical Chemistry*.

Hull, T. R., Witkowski, A., & Hollingbery, L. (2011). Fire retardant action of mineral fillers. *Polymer Degradation and Stability*, *96*(8), 1462–1469. https://doi.org/10.1016/j.polymdegradstab.2011.05.006

Hussain, A., Samreen, & Fatima, N. (2023). Mineral Fibres in the Textile Industry: A Sustainable Approach. *Current Trends in Fashion Technology & Textile Engineering*, *8*(5), 555749. https://doi.org/10.19080/CTFTTE.2023.08.555749

Hýsek, Š., Wimmer, R., & Böhm, M. (2016). Optimal Processing of Flax and Hemp Fibre Nonwovens. *BioResources*, *11*(4), 8522–8534. https://doi.org/10.15376/biores.11.4.8522-8534

Indiloft. (2025). Indiloft - hemp wool data sheet. indinature.co

Inovia, T. (2020). Guide de Culture Chanvre. *Terres Inovia*.

, I. P. C. C. (2023, July 25). *IPCC, 2023: Climate Change 2023: Synthesis Report. Contribution of Working Groups I, II and III to the Sixth Assessment Report of the Intergovernmental Panel on Climate Change [Core Writing Team, H. Lee and J. Romero (eds.)]. IPCC, Geneva, Switzerland.* (First). Intergovernmental Panel on Climate Change (IPCC). https://doi.org/10.59327/IPCC/AR6-9789291691647

Islam, S., & Hasan, B. (2025). An overview of the effects of water and moisture absorption on the performance of hemp fiber and its composites. *SPE Polymers*, *6*(1), e10167. https://doi.org/10.1002/pls2.10167

ISO. (1991). *ISO 8302 - Thermal insulation — Determination of steady-state thermal resistance and related properties — Guarded hot plate apparatus.*

ISO. (2014). *ISO 17554 - Reaction to fire tests — Mass loss measurement.*

ISO. (2015). *ISO 5660-1 - Reaction-to-fire tests — Heat release, smoke production and mass loss rate — Part 1: Heat release rate (cone calorimeter method) and smoke production rate (dynamic measurement).*

ISO. (2018). *ISO 1716 - Essais de réaction au feu de produits — Détermination du pouvoir calorifique supérieur (valeur calorifique).*

ISO. (2020a). *ISO 1182 - Essais de réaction au feu de produits — Essai d'incombustibilité.*

ISO. (2020b). *ISO 11925-2 - Reaction to fire tests — Ignitability of products subjected to direct impingement of flame — Part 2: Single-flame source test.*

ISO. (2022, June). *ISO 22007-2 - Plastics — Determination of thermal conductivity and thermal diffusivity — Part 2: Transient plane heat source (hot disc) method.*

Iwase, T., Izumi, Y., & Kawabata, R. (1998). A new measuring method for sound propagation constant by using sound tube without any air spaces back of a test material. *Internoise and Noise-Con Congress and Conference Proceedings*, *14*.

Jaouen, L., Bécot, F.-X., & Chevillotte, F. (2025). Characterizations of acoustical porous media: Standardized methods, current trends and challenges. *Frontiers in Acoustics*, *3*, 1543456. https://doi.org/10.3389/facou.2025.1543456

Jaouen, L., Gourdon, E., & Glé, P. (2020). Estimation of all six parameters of Johnson-Champoux-Allard-Lafarge model for acoustical porous materials from impedance tube measurements. *The Journal of the Acoustical Society of America*, *148*(4), 1998–2005. https://doi.org/10.1121/10.0002162

Jerman, M., & Černý, R. (2012). Effect of moisture content on heat and moisture transport and storage properties of thermal insulation materials. *Energy and Buildings*, *53*, 39–46. https://doi.org/10.1016/j.enbuild.2012.07.002

Jian, J., Xiangbin, Z., & Xianbo, H. (2020). An overview on synthesis, properties and applications of poly(butylene-adipate-co-terephthalate)–PBAT. *Advanced Industrial and Engineering Polymer Research*, *3*(1), 19–26. https://doi.org/10.1016/j.aiepr.2020.01.001

Johnson, D. L., Koplik, J., & Dashen, R. (1987). Theory of dynamic permeability and tortuosity in fluid-saturated porous media. *Journal of Fluid Mechanics*, *176*, 379. https://doi.org/10.1017/S0022112087000727

Jompang, L., Thumsorn, S., On, J. W., Surin, P., Apawet, C., Chaichalermwong, T., Kaabbuathong, N., O-Charoen, N., & Srisawat, N. (2013). Poly(Lactic Acid) and Poly(Butylene Succinate) Blend Fibers Prepared by Melt Spinning Technique. *Energy Procedia*, *34*, 493–499. https://doi.org/10.1016/j.egypro.2013.06.777

Kaczmar, J. W., Pach, J., & Burgstaller, C. (2011). The chemically treated hemp fibres to reinforce polymers. *Polimery*, *56*(11/12), 817–822. https://doi.org/10.14314/polimery.2011.817

Kellie, G. (2016, June). *Advances in Technical Nonwovens* (1st ed.). Woodhead Publishing.

Kerdudou, P., Chéné, J. .-., Jacqus, G., Perrot, C., Berger, S., & Leroy, P. (2015). A semi-empirical approach to link macroscopic parameters to microstructure of fibrous materials. *44th International Congress and Exposition on Noise Control Engineering*.

Kim, N., Dutta, S., & Bhattacharyya, D. (2018). A review of flammability of natural fibre reinforced polymeric composites. *Composites Science and Technology*, *162*, 64–78. https://doi.org/10.1016/j.compscitech.2018.04.016

Korjenic, A., Petránek, V., Zach, J., & Hroudová, J. (2011). Development and performance evaluation of natural thermal-insulation materials composed of renewable resources. *Energy and Buildings*, *43*(9), 2518–2523. https://doi.org/10.1016/j.enbuild.2011.06.012

Korjenic, A., Zach, J., & Hroudová, J. (2016). The use of insulating materials based on natural fibers in combination with plant facades in building constructions. *Energy and Buildings*, *116*, 45–58. https://doi.org/10.1016/j.enbuild.2015.12.037

Kozłowski, R., & Władyka-Przybylak, M. (2008). Flammability and fire resistance of composites reinforced by natural fibers. *Polymers for Advanced Technologies*, *19*(6), 446–453. https://doi.org/10.1002/pat.1135

Lafarge, D., Lemarinier, P., Allard, J. F., & Tarnow, V. (1997). Dynamic compressibility of air in porous structures at audible frequencies. *The Journal of the Acoustical Society of America*, *102*(4), 1995–2006. https://doi.org/10.1121/1.419690

Langlais, C., & Klarsfeld, S. (1997). Isolation thermique à température ambiante. Bases physiques.

Langlais, C., & Klarsfeld, S. (2004). Isolation thermique à température ambiante. Propriétés.

Laoutid, F., Bonnaud, L., Alexandre, M., Lopez-Cuesta, J.-M., & Dubois, Ph. (2009). New prospects in flame retardant polymer materials: From fundamentals to nanocomposites. *Materials Science and Engineering: R: Reports*, *63*(3), 100–125. https://doi.org/10.1016/j.mser.2008.09.002

Lecoublet, M., Khennache, M., Leblanc, N., Ragoubi, M., & Poilâne, C. (2021). Physico-mechanical performances of flax fiber biobased composites: Retting and process effects. *Industrial Crops and Products*, *173*, 114110. https://doi.org/10.1016/j.indcrop.2021.114110

Lee, M., Kang, E.-C., & Lee, S.-M. (2023). Effects of different flame-retardant treatments on the sound absorption properties of low-density fiberboard. *BioResources*, *18*(3), 5859–5872. https://doi.org/10.15376/biores.18.3.5859-5872

Lei, L., Dauchez, N., & Chazot, J. (2018). Prediction of the six parameters of an equivalent fluid model for thermocompressed glass wools and melamine foam. *Applied Acoustics*, *139*, 44–56. https://doi.org/10.1016/j.apacoust.2018.04.010

Lekavicius, V., Shipkovs, P., Ivanovs, S., & Rucins, A. (2015). Thermo-Insulation Properties Of Hemp-Based Products. *Latvian Journal of Physics and Technical Sciences*, *52*(1), 38–51. https://doi.org/10.1515/lpts-2015-0004

Li, N., Wu, Y.-X., Zhang, Y.-D., Wang, S.-R., Zhang, G.-C., & Yang, J. (2023). Phytic acid is a new substitutable plant-derived antifungal agent for the seedling blight of Pinus sylvestris var. mongolica caused by Fusarium oxysporum. *Pesticide Biochemistry and Physiology*, *191*, 105341. https://doi.org/10.1016/j.pestbp.2023.105341

Liang, L., Alorbu, C., McDonald, A., & Cai, L. (2024). Phytic acid for dual wood protection against fungi and fire. *Wood and Fiber Science*, *56*(2), 72–82. https://doi.org/10.22382/wfs-2024-07

Liang, Y., Jian, H., Deng, C., Xu, J., Liu, Y., Park, H., Wen, M., & Sun, Y. (2023). Research and Application of Biomass-Based Wood Flame Retardants: A Review. *Polymers*, *15*(4), 950. https://doi.org/10.3390/polym15040950

Liu, B.-w., Zhao, H.-b., & Wang, Y.-Z. (2022). Advanced Flame-Retardant Methods for Polymeric Materials. *Advanced Materials*, *34*, 2107905. https://doi.org/10.1002/adma.202107905

Luu, H. T. (2017). Modélisation multi-échelle de la dissipation acoustique dans des textiles techniques faits de fibres naturelles.

Luu, H. T., Perrot, C., & Panneton, R. (2017). Influence of Porosity, Fiber Radius and Fiber Orientation on the Transport and Acoustic Properties of Random Fiber Structures. *Acta Acustica united with Acustica*, *103*(6), 1050–1063. https://doi.org/10.3813/AAA.919134

Lyon, R. E., & Walters, R. N. (2004). Pyrolysis combustion flow calorimetry. *Journal of Analytical and Applied Pyrolysis*, *71*(1), 27–46. https://doi.org/10.1016/S0165-2370(03)00096-2

Melelli, A., Jamme, F., Beaugrand, J., & Bourmaud, A. (2022). Evolution of the ultrastructure and polysaccharide composition of flax fibres over time: When history meets science. *Carbohydrate Polymers*, *291*, 119584. https://doi.org/10.1016/j.carbpol.2022.119584

Mojtabi, A., Prat, M., Quintard, M., & Taine, J. (2025). Transferts de chaleur dans les milieux poreux - Conduction, convection, rayonnement.

Mokhena, T. C., Sadiku, E. R., Ray, S. S., Mochane, M. J., Matabola, K. P., & Motloung, M. (2022). Flame retardancy efficacy of phytic acid: An overview. *Journal of Applied Polymer Science*, *139*(27). https://doi.org/10.1002/app.52495

Moudood, A., Hall, W., Öchsner, A., Li, H., Rahman, A., & Francucci, G. (2019). Effect of Moisture in Flax Fibres on the Quality of their Composites. *Journal of Natural Fibers*, *16*(2), 209–224. https://doi.org/10.1080/15440478.2017.1414651

Moudood, A., Rahman, A., Öchsner, A., Islam, M., & Francucci, G. (2019). Flax fiber and its composites: An overview of water and moisture absorption impact on their performance. *Journal of Reinforced Plastics and Composites*, *38*(7), 323–339. https://doi.org/10.1177/0731684418818893

Moussa, M., El Hage, R., Sonnier, R., Chrusciel, L., Ziegler-Devin, I., & Brosse, N. (2020). Toward the cottonization of hemp fibers by steam explosion. Flame-retardant fibers. *Industrial Crops and Products*, *151*, 112242. https://doi.org/10.1016/j.indcrop.2020.112242

Moussatov, A., Ayrault, C., & Castagnède, B. (2001). Porous material characterization – ultrasonic method for estimation of tortuosity and characteristic length using a barometric chamber. *Ultrasonics*, *39*(3), 195–202. https://doi.org/10.1016/S0041-624X(00)00062-7

Mulla, M. H., Norizan, M. N., Mohammad Rawi, N. F., Mohamad Kassim, M. H., Abdullah, C. K., Abdullah, N., & Norrrahim, M. N. F. (2025). A review of fire performance of plant-based natural fibre reinforced polymer composites. *International Journal of Biological Macromolecules*, *305*, 141130. https://doi.org/10.1016/j.ijbiomac.2025.141130

Nykter, M. (2006). *Microbial quality of hemp (Cannabis sativa L.) and flax (Linum usitatissimum L.) from plants to thermal insulation*. University of Helsinki, Department of Agrotechnology.
OCLC: 141385680.

Oldham, D. J., Egan, C. A., & Cookson, R. D. (2011). Sustainable acoustic absorbers from the biomass. *Applied Acoustics*, *72*(6), 350–363. https://doi.org/10.1016/j.apacoust.2010.12.009

Palumbo, M., Lacasta, A., Giraldo, M., Haurie, L., & Correal, E. (2018). Bio-based insulation materials and their hygrothermal performance in a building envelope system (ETICS). *Energy and Buildings*, *174*, 147–155. https://doi.org/10.1016/j.enbuild.2018.06.042

Pandey, R., Dayal, R., & Srivastava, R. L. (2014). *Flax Fiber Processing Technology*. University Press.

Pasangulapati, V., Ramachandriya, K. D., Kumar, A., Wilkins, M. R., Jones, C. L., & Huhnke, R. L. (2012). Effects of cellulose, hemicellulose and lignin on thermochemical conversion characteristics of the selected biomass. *Bioresource Technology*, *114*, 663–669. https://doi.org/10.1016/j.biortech.2012.03.036

Patti, A., & Acierno, D. (2020, May 6). Thermal Conductivity of Polypropylene-Based Materials. In W. Wang & Y. Zeng (Eds.), *Polypropylene - Polymerization and Characterization of Mechanical and Thermal Properties*. IntechOpen. https://doi.org/10.5772/intechopen.84477

Paul, P., Ahirwar, M., & Behera, B. (2022). Acoustic behaviour of needle punched nonwoven structures produced from various natural and synthetic fibers. *Applied Acoustics*, *199*, 109043. https://doi.org/10.1016/j.apacoust.2022.109043

Pereira, P. H. F., Rosa, M. d. F., Cioffi, M. O. H., Benini, K. C. C. d. C., Milanese, A. C., Voorwald, H. J. C., & Mulinari, D. R. (2015). Vegetal fibers in polymeric composites: A review. *Polímeros*, *25*(1), 9–22. https://doi.org/10.1590/0104-1428.1722

Perrot, C. (2006). *Microstructure et macro-comportement acoustique : approche par reconstruction d'une cellule élémentaire représentative*.

Piegay, C. (2019). *Approche conjointe acoustique et thermique pour l'optimisation des laines végétales du bâtiment*.

Piégay, C., Glé, P., Gourdon, E., & Gourlay, E. (2020). A cylindrical self-consistent modelling of vegetal wools thermal conductivity. *Construction and Building Materials*, *232*, 117123. https://doi.org/10.1016/j.conbuildmat.2019.117123

Piégay, C., Glé, P., Gourdon, E., Gourlay, E., & Marceau, S. (2018). Acoustical model of vegetal wools including two types of fibers. *Applied Acoustics*, *129*, 36–46. https://doi.org/10.1016/j.apacoust.2017.06.021

Pittau, F., Habert, G., & Iannaccone, G. (2021). The renovation of the building stock in Europe: An essential opportunity to store carbon in buildings. *Rivista Tema*, *05*(02). https://doi.org/10.30682/tema0502l

Programme, U. E. (2020). *2020 Global Status Report for Buildings and Construction: Towards a Zero-emission, Efficient and Resilient Buildings and Construction Sector*. Nairobi.

Programme, U. E. (2022). *2022 Global Status Report for Buildings and Construction: Towards a Zero-emission, Efficient and Resilient Buildings and Construction Sector*. Nairobi.

Roy, M. P. K., Malik, M. T., & Sinha, M. T. K. (2011). Thermal Bonded Nonwoven - An Overview. *Technical textile*, 15.

Rude, T. J., Strait Jr., L. H., & Ruhala, L. A. (2000). Measurement of Fiber Density by Helium Pycnometry. *Journal of Composite Materials*, *34*(22), 1948–1958. https://doi.org/10.1106/NUYP-PARA-RA5R-7NUE

Sá, T. S. W. (2025). Comparison of two flame-retardant treatment methods on bulk hemp fibers: Towards a large-scale viability as a raw material for building insulation. *Industrial Crops and Products*, *228*, 120903. https://doi.org/10.1016/j.indcrop.2025.120903

Salissou, Y., & Panneton, R. (2010). Wideband characterization of the complex wave number and characteristic impedance of sound absorbers. *The Journal of the Acoustical Society of America*, *128*(5), 2868–2876. https://doi.org/10.1121/1.3488307

Sauvageon, T., Lavoie, J.-M., Segovia, C., & Brosse, N. (2018). Toward the cottonization of hemp fibers by steam explosion – Part 1: Defibration and morphological characterization. *Textile Research Journal*, *88*(9), 1047–1055. https://doi.org/10.1177/0040517517697644

Schiavoni, S., DAlessandro, F., Bianchi, F., & Asdrubali, F. (2016). Insulation materials for the building sector: A review and comparative analysis. *Renewable and Sustainable Energy Reviews*, *62*, 988–1011. https://doi.org/10.1016/j.rser.2016.05.045

Signori, F., Coltelli, M.-B., & Bronco, S. (2009). Thermal degradation of poly(lactic acid) (PLA) and poly(butylene adipate-co-terephthalate) (PBAT) and their blends upon melt processing. *Polymer Degradation and Stability*, *94*(1), 74–82. https://doi.org/10.1016/j.polymdegradstab.2008.10.004

Singha, K., Maity, S., Singha, M., Paul, P., & Gon, D. P. (2012). Fiber Diameter, Probability distribution, Log-normal distribution, Fiber size. *International Journal of Textile Science*, *1*(1), 7–14. https://doi.org/10.5923/j.textile.20120101.02

Sonnier, R., Otazaghine, B., Viretto, A., Apolinario, G., & Ienny, P. (2015). Improving the flame retardancy of flax fabrics by radiation grafting of phosphorus compounds. *European Polymer Journal*, *68*, 313–325. https://doi.org/10.1016/j.eurpolymj.2015.05.005

Stamboulis, A. (2000). Environmental Durability of Flax Fibres and their Composites based on Polypropylene Matrix. *Applied Composite Materials*, *7*(5/6), 273–294. https://doi.org/10.1023/A:1026581922221

Stamboulis, A., Baillie, C. A., & Peijs, T. (2001). Effects of environmental conditions on mechanical and physical properties of ¯ax ®bers, 11.

Summerscales, J., Dissanayake, N., Virk, A., & Hall, W. (2010). A review of bast fibres and their composites. Part 2 – Composites. *Composites Part A: Applied Science and Manufacturing*, *41*(10), 1336–1344. https://doi.org/10.1016/j.compositesa.2010.05.020

Szolnoki, B., Toldy, A., Konrád, P., Szebényi, G., & Marosi, G. (2013). Comparison of additive and reactive phosphorus-based flame retardants in epoxy resins. *Periodica Polytechnica Chemical Engineering*, *57*(1–2), 85. https://doi.org/10.3311/PPch.2175

Taib, M. N. A. M., Antov, P., Savov, V., Fatriasari, W., Madyaratri, E. W., Wirawan, R., Osvaldová, L. M., Hua, L. S., Ghani, M. A. A., Edrus, S. S. A. O. A., Chen, L. W., Trache, D., & Hussin, M. H. (2022). Current progress of biopolymer-based flame retardant. *Polymer Degradation and Stability*, *205*, 110153. https://doi.org/10.1016/j.polymdegradstab.2022.110153

Taibi, J., Rouif, S., Clément, J.-L., Ameduri, B., Sonnier, R., & Otazaghine, B. (2022). Flame retardancy of flax fibers by pre-irradiation grafting of a phosphonate monomer. *Industrial Crops and Products*, *176*, 114334. https://doi.org/10.1016/j.indcrop.2021.114334

Tarnow, V. (1996). Airflow resistivity of models of fibrous acoustic materials. *The Journal of the Acoustical Society of America*, *100*(6), 3706–3713. https://doi.org/10.1121/1.417233

Technichanvre. (2025). Technichanvre - Hemp wool data sheet. technichanvre.com

Teixeira, M., Sonnier, R., Otazaghine, B., Ferry, L., Aubert, M., Tirri, T., Wilén, C.-E., & Rouif, S. (2018). Radiation-grafting of flame retardants on flax fabrics – A comparison between different flame retardant structures. *Radiation Physics and Chemistry*, *145*, 135–142. https://doi.org/10.1016/j.radphyschem.2017.10.013

Then, Y. Y., Ibrahim, N. A., Zainuddin, N., Ariffin, H., Chieng, B. W., & Wan Yunus, W. M. Z. (2015). Influence of Fiber Content on Properties of Oil Palm Mesocarp Fiber/Poly(butylene succinate) Biocomposites. *BioResources*, *10*(2), 2949–2968. https://doi.org/10.15376/biores.10.2.2949-2968

Thygesen, A. (2006). *Properties of hemp fibre polymer composites -An optimisation of fibre properties using novel defibration methods and fibre characterisation.*

Tie, T. S., Mo, K. H., Putra, A., Loo, S. C., Alengaram, U. J., & Ling, T.-C. (2020). Sound absorption performance of modified concrete: A review. *Journal of Building Engineering*, *30*, 101219. https://doi.org/10.1016/j.jobe.2020.101219

Tomaszewska, K., Kałużna-Czaplińska, J., & Jóźwiak, W. (2010). Thermal and thermocatalytic degradation of polyolefins as a simple and efficient method of landfill clearing. *PJCT*, *12*(3), 50–57. https://doi.org/10.2478/v10026-010-0034-x

Tupciauskas, R., Orlovskis, Z., Blums, K. T., Liepins, J., Berzins, A., Pavlovics, G., & Andzs, M. (2024). Mold Fungal Resistance of Loose-Fill Thermal Insulation Materials Based on Processed Wheat Straw, Corn Stalk and Reed.

Umnova, O., Tsiklauri, D., & Venegas, R. (2009). Effect of boundary slip on the acoustical properties of microfibrous materials. *The Journal of the Acoustical Society of America*, *126*(4), 1850–1861. https://doi.org/10.1121/1.3204087

van der Werf, H. M. G. (2002). Hemp Production in France. *Journal of Industrial Hemp*, *7*(2), 105–109. https://doi.org/10.1300/J237v07n02_12

Vasiliauskienė, D., Boris, R., Balčiūnas, G., Kairytė, A., & Urbonavičius, J. (2022). Impact of Cellulolytic Fungi on Biodegradation of Hemp Shives and Corn Starch-Based Composites with Different Flame-Retardants. *Microorganisms*, *10*(9), 1830. https://doi.org/10.3390/microorganisms10091830

Volf, M., Diviš, J., & Havlík, F. (2015). Thermal, Moisture and Biological Behaviour of Natural Insulating Materials. *Energy Procedia*, *78*, 1599–1604. https://doi.org/10.1016/j.egypro.2015.11.219

Wang, M., Yin, G.-Z., Yang, Y., Fu, W., Díaz Palencia, J. L., Zhao, J., Wang, N., Jiang, Y., & Wang, D.-Y. (2022). Bio-based flame retardants to polymers: A review. *Advanced Industrial and Engineering Polymer Research*, S2542504822000331. https://doi.org/10.1016/j.aiepr.2022.07.003

WHO. (2018). *Environmental noise guidelines for the European Region*. World Health Organization, Regional Office for Europe.
OCLC: 1129816077.

Xu, J., Manepalli, P. H., Zhu, L., Narayan-Sarathy, S., & Alavi, S. (2019). Morphological, barrier and mechanical properties of films from poly (butylene succinate) reinforced with nanocrystalline cellulose and chitin whiskers using melt extrusion. *Journal of Polymer Research*, *26*(8), 188. https://doi.org/10.1007/s10965-019-1783-8

Yan, L., Chouw, N., & Jayaraman, K. (2014). Flax fibre and its composites – A review. *Composites Part B: Engineering*, *56*, 296–317. https://doi.org/10.1016/j.compositesb.2013.08.014

Yang, H., Yan, R., Chen, H., Lee, D. H., & Zheng, C. (2007). Characteristics of hemicellulose, cellulose and lignin pyrolysis. *Fuel*, *86*(12–13), 1781–1788. https://doi.org/10.1016/j.fuel.2006.12.013

Yu, F., Ba, Z., Gao, Z., Wang, Y., Xie, Y., Wang, H., Qiu, Z., & Xiao, Z. (2024). Modification with lignin-based N-P flame retardant to improve the flame retardancy and smoke suppression of wood. *Chemical Engineering Journal*, *493*, 152827. https://doi.org/10.1016/j.cej.2024.152827

Yu, X., Jin, X., He, Y., Yu, Z., Zhang, R., & Qin, D. (2024). Eco-friendly bamboo pulp foam enabled by chitosan and phytic acid interfacial assembly of halloysite nanotubes: Toward flame retardancy, thermal insulation, and sound absorption. *International Journal of Biological Macromolecules*, *260*, 129393. https://doi.org/10.1016/j.ijbiomac.2024.129393

Zampori, L., Dotelli, G., & Vernelli, V. (2013). Life Cycle Assessment of Hemp Cultivation and Use of Hemp-Based Thermal Insulator Materials in Buildings. *Environmental Science & Technology*, *47*(13), 7413–7420. https://doi.org/10.1021/es401326a

Zhao, J., Xiuwen, W., Hu, J., Liu, Q., Shen, D., & Xiao, R. (2014). Thermal degradation of softwood lignin and hardwood lignin by TG-FTIR and Py-GC/MS. *Polymer Degradation and Stability*, *108*, 133–138. https://doi.org/10.1016/j.polymdegradstab.2014.06.006

Zieger, V., Lecompte, T., & Hellouin De Menibus, A. (2020). Impact of GHGs temporal dynamics on the GWP assessment of building materials: A case study on bio-based and non-bio-based walls. *Building and Environment*, *185*, 107210. https://doi.org/10.1016/j.buildenv.2020.107210